Modelling Mixed Traffic Flow of Autonomous Vehicles and Human-Driven Vehicles

Tang Li

A thesis submitted for the degree of Doctor of Philosophy of
Imperial College London

Centre for Transport Studies
Department of Civil and Environmental Engineering
Imperial College London, United Kingdom

October 2021

Abstract

Autonomous Vehicles (AVs) are bringing revolutionary opportunities and challenges to urban transport systems. They can reduce congestion, improve operational efficiency and liberate drivers from driving. Though AVs might bring attractive potential benefits, most benefits are evaluated at high AV penetration rates or an all-AV scenario. In practice, limited by price barriers, adoption rates and vehicle-renewal periods, AVs may not replace Human-Driven Vehicles (HDVs) to achieve a high penetration rate in a short time. It can be expected that the road network will operate with a mix of AVs and HDVs in the near to medium future. Therefore, there is a strong motivation to analyse the performance of road networks under mixed traffic conditions.

The overall aim of this PhD research is to analyse mixed traffic flows of AVs and HDVs to help traffic managers and Local Authorities (LAs) improve the performance of urban traffic systems by right-of-way reallocation and dynamic traffic management. To achieve this aim, this PhD research is divided into four parts.

Firstly, the impact of heterogeneity between AVs and HDVs on road capacity is investigated. A theoretical model is proposed to calculate the maximum capacity of heterogeneous traffic flow. Based on the theoretical model, it is shown that road capacity increases convexly with AV penetration rates. This finding provides a theoretical basis to support the hypothesis that right-of-way reallocation can increase road capacity under the mixed traffic flow. To cross-validate the above finding, different right-of-way reallocation strategies are evaluated on a two-lane road with SUMO simulation. Compared with a do-nothing scenario, the road capacity can be increased by approximately 11% with a proper RoW reallocation strategy at low or medium AV penetration rates.

Secondly, whether CAVs can be used as mobile traffic controllers by adjusting their speed on a certain link is investigated. It is found that in some circumstances, system efficiency can be improved by CAVs adjusting their speed on a certain link to nudge the network towards the system optimum. According to a numerical analysis on the Braess network, total travel time can be reduced by 9.7% when CAVs actively slow down on a link. To take more realistic circumstances into account, a SUMO simulation

case study is conducted, where HDVs only have partial knowledge about travel costs. The results of the simulation demonstrate that when CAVs are acting as mobile traffic controllers by actively reducing speed on a certain link, total travel time can be reduced by approximately 6.8% compared with the do-nothing scenario.

Thirdly, whether travel efficiency can be improved with only a part of the vehicular flow cooperatively changing their routing under mixed conditions is investigated. It has been found that it is possible to use CAVs to influence HDVs' day-to-day routing and push the network towards the system optimal distribution dynamically on a large network with multiple OD pairs. Taking non-linear cost-flow relationship and signal timing into account, an Optimal Routing and Signal Timing (ORST) control strategy is proposed for CAVs and tested in simulation. Compared with initial user equilibrium, total travel time can be reduced by approximately 7% when a portion of CAVs cooperatively charge their routing with the ORST control strategy at the 75% CAV penetration rate. This opens up possibilities, besides road pricing, to improve system efficiency by controlling routing and signal timing strategy for CAVs.

Fourthly, whether additional travel efficiency can be achieved by jointly optimising routing and signal timing with information from CAVs is further investigated. Specifically, the impact of information levels on routing and signal timing efficiency has been investigated quantitatively. The results demonstrate that different levels of information will lead the road traffic system to reach different equilibrium points. Then the proposed ORST control strategy is compared with existing routing and signal timing strategies. The results present that ORST can reduce approximately 10% of the total travel time compared to user equilibrium. In addition, the proposed model has also been tested on a revised Nguyen-Dupuis network. At 25% CAV penetration rates, the proposed model can successfully reduce approximately 23% of total travel time.

In summary, the mixed flow of AVs and HDVs is investigated in this PhD research. To increase the efficiency of urban traffic systems, novel strategies have been proposed and tested with numerical analysis and simulation, which provides inspirations and quantitative evidence for traffic managers and LAs to manage the mixed traffic flow efficiently.

Declaration of Originality

I hereby certify that all material in this thesis is my own work. Some parts of this thesis (e.g. Chapter 3) are a reproduction of my own published paper. Any quotation from or description of the work of others is acknowledged by reference to the sources, whether published or unpublished.

Tang Li

October 2021

Copyright Declaration

Tang Li

October 2021

Acknowledgements

First and foremost, I would like to give my sincere thank to my supervisors Dr Aruna Sivakumar, Dr Fangce Guo, Dr Rajesh Krishnan and Professor John Polak. Their excellent supervision, patient guidance, extraordinary expertise and kind support raise me up and guide me go through all the challenges. They are not only my supervisors in research but also my mentors in my life. Meanwhile, I would like to give my gratitude to China Scholarship Council. Without the financial support, I would not have enough funding to finish my PhD.

Four years ago, at the new PhD students' welcome event, Professor Washington Yotto Ochieng shared his PhD life. He said there are ups and downs, but it is a good experience, and he learned a lot from it. When I look back to the last four years, I find my PhD is a unique journey and a treasure in my life. Prof. John Polak showed me the beauty of research and how to develop theories from an ordinary assumption. He accepted me and gave me an opportunity to study at the Urban System Lab (USL) and Center for Transport Studies (CTS). Dr Aruna Sivakumar, Dr Fangce Guo and Dr Rajesh Krishnan offered me great help, especially in the most difficult time when John left. They guided me step by step on how to narrow down research questions, how to review literature, how to find ways to solve problems, how to improve writing, how to present my research to peers in the conference, how to supervise students, how to gives lectures, how to write a proposal and identify research directions. I have been lucky to have them in the last four years, and it is my pleasure to continue working with them in the future.

I also want to thank my friends and colleagues at Imperial Dr Neil Hoose, Dr Scott Le Vine, Dr Jacek Pawlak, Dr Nicolo Daina, Dr Ahmadreza Faghih Imani, Dr Jianlin Luan, Dr Yanjie Dong, Dr Sebastian Maier, Dr Zongxiang Wu, Dr Francesco Mance, Dr Chenyang Wu, Dr Lin Zhu, Dr Yuanying Zhao, In-chan Kim, Alessandra Abeille, Huiqiao Hou, Abulfatah Abu, Abhilash Singh, Han Wang and Xuehao Zhai. We go through difficult times together, the leave of John and the outbreak of COIVD. I received lots of suggestions and support from all of you. Thank you very much.

Furthermore, I would like to thank my mentor, Professor Yun Bai. When I was an undergraduate student, you brought me to the world of research and taught me a lot of things in study and life. After my graduation, you still give me lots of supports and encouragement. Your kind support and advice help me go through the tough time. I would like to express my heartfelt thanks to Professor Yun Bai. Meanwhile, I would like to give my gratitude to Professor Baohua Mao. Your lectures and seminars inspired me. I learned a lot from your expertise and wisdom. I am very appreciative of your support in applying PhD.

I also would like to thank my friends and colleagues in China and around the world, Dr Yao Chen, Gehui Liu, Jiaxi Li, Jiajie Li, Yuhe Zhou, Wen Zhou, Ziling Zeng, Hongyu Lu, Lin Yu, Canwen Zhong and Jialei Ding. It is nice to keep in contact with all of you, and I wish you all the best in your studies, works and research.

Most importantly, I would like to dedicate this work to my parents and my wife Yuwei Lin. My thanks to my parents for giving me birth and raise me up. And my thanks to my wife for your accompany, patience and support. Without your love, I would never finish my PhD and this thesis.

Before the end, I recalled the last time I visited John. He said that we are all great people with our own skills and talents. He thanks us for the accompany, but we young people should keep going, and he wishes us to become a star in our field. Hopefully, he will be proud of us when the day comes.

Lastly, my thanks to you who is reading this thesis! Thanks for reading my thesis!

Contents

Abstract 1

Declaration of Originality 3

Copyright Declaration 4

Acknowledgements 5

Contents 7

List of Figures 12

List of Tables 15

Chapter 1 Introduction 17

1.1 Background and motivations 17

1.1.1 Long-term policy decisions 17

1.1.2 Dynamic short-term traffic management 18

1.2 Research aims and objectives 19

1.3 Outline of the thesis 20

1.4 List of publications 23

Chapter 2 Literature review 24

2.1 Structure of the literature review 24

2.2 Modelling AVs and HDVs 26

2.2.1 Development and Classification of AVs 26

2.2.2 Sub-system of existing AVs and their performance 28

2.2.3 Existing models of AVs and HDVs 35

2.2.4 Summary 45

2.3 Heterogeneous traffic flow of AVs and HDVs 45
2.3.1 Classification of heterogeneity in mixed traffic flow 46
2.3.2 Existing models of heterogeneous traffic flow 47
2.3.3 Summary 49
2.4 Traffic control system and controlling traffic with CAVs in mixed condition .. 51
2.4.1 Architecture of Traffic Signal Controller 51
2.4.2 Controlling traffic with CAVs in mixed condition 52
2.4.3 Summary 54
2.5 Seeking system optimal traffic assignment with HDVs and CAVs 55
2.5.1 HDVs' routing behaviour and user equilibrium 55
2.5.2 Seeking system optimal equilibrium in practice 56
2.5.3 Summary 58
2.6 Cooperation between CAVs and signals in routing and signal timing 58
2.6.1 Combine routing and signal control problem 58
2.6.2 Summary 61
2.7 Conclusion 62
Chapter 3 Right-of-way reallocation for mixed flow of AVs and HDVs 66
3.1 Background and research context 66
3.2 Theoretical capacity model for heterogeneous traffic flow 69
3.2.1 Fundamental equations of flow and assumptions 69
3.2.2 Headway and safety constraint 72
3.2.3 Maximum theoretical capacity of heterogeneous flow 74
3.3 Numerical analysis of mixed flow 75
3.3.1 Parameters for AVs and HDVs 75
3.3.2 Comparison between theoretical capacity and capacity reported in the literature 76

3.3.3 Numerical analysis of mixed flow and right-of-way reallocation for mixed flow ... 79

3.4 Case studies for right-of-way reallocation on a two-lane road ... 83

3.4.1 Overview of scenario design ... 83

3.4.2 Simulation framework and the choice of vehicle following model ... 84

3.4.3 Results of right-of-way reallocation strategies ... 85

3.5 Sensitivity analysis ... 90

3.5.1 Sensitivity analysis of the proposed theoretical model ... 91

3.5.2 Sensitivity analysis of the desired time gap ... 93

3.6 Conclusion ... 97

Chapter 4 Managing mixed traffic flow with CAVs as mobile traffic controllers ... 100

4.1 Background and research context ... 100

4.2 Numerical analysis of CAVs acting as mobile traffic controllers in mixed traffic conditions ... 101

4.3 Simulation case study of CAVs acting as mobile traffic controllers ... 104

4.4.1 Overview of the network structure ... 104

4.4.2 Scenarios of case study ... 105

4.4.3 Results of case study ... 106

4.4 Conclusion ... 108

Chapter 5 Dynamic process of routing and signal timing towards system optimal equilibrium in mixed CAVs and HDVs traffic ... 110

5.1 Background and research context ... 110

5.2 Routing behaviour of HDVs and CAVS towards user equilibrium and system optimal distribution ... 112

5.2.1 Notations ... 112

5.2.2 HDVs' routing behaviour towards User equilibrium ... 112

5.2.3 CAVs' routing behaviour towards System optimal distribution 114

5.3 The dynamic process towards system optimal distribution 116

5.3.1 A numerical analysis of a simple network 117

5.3.2 A numerical analysis of a larger network with multiple OD pairs 120

5.4 Simulation studies of the dynamic process of routing and signal timing towards system optimal distribution in mixed conditions 124

5.4.1 Overview of the network structure 125

5.4.2 Initial status toward user equilibrium with PAP...................................... 126

5.4.3 From user equilibrium toward system optimal distribution with ORST ... 128

5.4.4 Dynamic process towards system optimal distribution in mixed CAVs and HDVs flow 131

5.5 Conclusion 132

Chapter 6 An analysis of the value of optimal routing and signal timing control strategy with CAVs 134

6.1 Background and research context 134

6.2 Case study of optimal routing and signal timing strategies under different levels of information on a simple network 136

6.2.1 Overview of the network structure 136

6.2.2 Routing and signal timing under different levels of information 137

6.2.3 Sensitivity analysis of mixed traffic conditions on a simple network 144

6.3 Case study of optimal routing and signal timing strategies on a large network with multiple OD pairs 148

6.4 Conclusion 154

Chapter 7 Conclusion and future work 156

7.1 Summary and contributions 156

7.2 Potential practical applications.. 160

7.3 Future research 161

References 163

Appendix 1: A algebraic analysis of the simple network in Subsection 5.3.1...........182

Appendix 2: Permission document for reproduction...184

Appendix 3: CRediT authorship contribution statement of Right-of-way reallocation for mixed flow of autonomous vehicles and human driven vehicles.........................185

Appendix 4: A heuristic analysis of CAVs acting as mobile controllers in mixed traffic conditions by adjusting the speed on a certain link 186

Appendix 5: Routing and signal timing strategies under different levels of information 189

List of Figures

Figure 1.1 Issue tree of this PhD research 20

Figure 2.1 Structure of literature review 25

Figure 2.2 IBEO 2D LRF system (left)(Scholz et al., 2006) and Velodyne HDL-64 3D LRF system (right)(Velogdyne, 2018) 33

Figure 2.3 Structure of the vehicle guidance system for AVs (left)(Andreas et al., 2000) & the vehicle parameterization (right)(Beji et al., 2003) 40

Figure 2.4 Various heterogeneity on traffic flow 46

Figure 2.5 Architecture of Traffic Signal Controller (Gollop, 2016) 51

Figure 2.6 Structure of rest of thesis 65

Figure 3.1 Safety constraint when the following vehicle approaching a stopped vehicle 73

Figure 3.2 Relative safety constraint 73

Figure 3.3 Comparison between theoretical capacity and capacity reported in the literature 76

Figure 3.4 Theoretical capacity of mixed AVs and HDVs flow 80

Figure 3.5 Capacity comparison between two mixed lanes and an AV and a HDV dedicate lane at a 50% penetration rate 81

Figure 3.6 The two-lane road for case studies 83

Figure 3.7 The general simulation framework of different scenarios 84

Figure 3.8 Do-nothing (two mixed lanes) strategy VS the most proper RoW reallocation strategies 85

Figure 3.9 Results of RoW reallocation strategies when 87

Figure 3.10 Rate of capacity increase with RoW reallocation (3D and heat map) 88

Figure 3.11 Sensitivity of parameters increase and decrease 50% in the theoretical model 92

Figure 3.12 Impacts of AVs reaction time on crucial points of RoW strategies 94

Figure 3.13 Impacts of desired time gap setting on do nothing scenarios 95

Figure 3.14 Impacts of desired time gap setting on RoW reallocation scenarios........96

Figure 4.1 A typical Braess network...102

Figure 4.2 CAVs acting as mobile traffic controllers 103

Figure 4.3 The relationship between Δbc, CAV, total travel time and traffic assignment...103

Figure 4.4 The network for case study..105

Figure 4.5 Scenarios of the simulation case study 106

Figure 4.6 Total travel time of different scenarios 107

Figure 5.1 A simple network with two routes...113

Figure 5.2 User equilibrium for a simple network with two routes..........................114

Figure 5.3 System optimal distribution for a simple network with two routes.........115

Figure 5.4 The model of dynamic process towards system optimal distribution 117

Figure 5.5 Dynamic process towards system optimal distribution (CAVs penetration rate 50%)...118

Figure 5.6 Dynamic process towards system optimal distribution (CAVs penetration rate 75%)...119

Figure 5.7 Nguyen-Dupuis Network (Nguyen & Dupuis, 1984; Xie et al., 2019)....120

Figure 5.8 Dynamic process on the Nguyen-Dupuis network under different penetration rates and iterations 123

Figure 5.9 The structure of the road network 125

Figure 5.10 Proportional-switch Adjustment Process towards user equilibrium 127

Figure 5.11 ORST towards system optimal distribution 130

Figure 5.12 Dynamic process towards system optimal distribution in mixed condition 131

Figure 6.1 The structure of a road network...137

Figure 6.2 An example of shockwaves caused by congestion and queueing 138

Figure 6.3 Total travel time vs iterations (SUE) ... 139

Figure 6.4 Total travel time vs iterations (PAP) ... 140

Figure 6.5 The changes of route flow and travel cost with PAP ... 140

Figure 6.6 Total travel time vs iterations (PAP+P0) ... 141

Figure 6.7 (a) Change of route flow and travel cost; (b) Change of green time and delay ... 142

Figure 6.8 Total travel time vs particles (ORST) ... 142

Figure 6.9 Total travel time of routing and signal timing strategies under different levels of information ... 143

Figure 6.10 Sensitivity analysis for mixed CAV conditions ... 145

Figure 6.11 Total and average travel time under different demands and penetration rates ... 146

Figure 6.12 The reduction rate of average travel time under different demands and penetration rates ... 147

Figure 6.13 Revised Nguyen-Dupuis Network with traffic signals ... 148

Figure 6.14 The performance of the proposed model under different CAV penetration rates ... 152

Figure 7.1 Summary of contributions ... 159

List of Tables

Table 2.1 SAE level of autonomous vehicles 27

Table 2.2 Summary of AVs Sub-system by the level of automation.......................... 29

Table 2.3 Detection and Warning Comparison of LDW systems 30

Table 2.4 Parameter values for algorithms (Bella & Russo, 2011) 30

Table 2.5 Experimental braking data 32

Table 2.6 Performance Specifications of ICC 32

Table 2.7 Performance Specifications of ICC 34

Table 2.8 Parameter of AVs with their subsystem 34

Table 2.9 Summary of the GHR model (Brackstone & McDonald, 1999) 35

Table 2.10 Summary of the vehicle following models for HDVs 37

Table 2.11 Summary of lane changing model for HDVs 39

Table 2.12 Summary of vehicle following, lateral and lane changing model for AVs43

Table 2.13 Summarise of existing research on various heterogeneity........................ 50

Table 2.14 Ilgin Guler et al. (2014) summarised results.. 52

Table 3.1 Notations for theoretical capacity model 70

Table 3.2 Parameters for the numerical analysis and SUMO simulation 75

Table 3.3 Results of Do-nothing and the most proper RoW reallocation strategies (Partial data) 86

Table 3.4 Results of sensitivity analysis for Demand=5000 vehicle/h 97

Table 4.1 User equilibrium and System optimal on Braess network 102

Table 5.1 Notations used in this chapter 112

Table 5.2 Dynamic process towards system optimal distribution (CAVs penetration rate 50%) 118

Table 5.3 Dynamic process towards system optimal distribution (CAVs penetration rate 75%) 119

Table 5.4 Dynamic process on Nguyen-Dupuis network (first three iterations) 121

Table 5.5 Dynamic process on Nguyen-Dupuis network (last three iterations) 123

Table 5.6 Proportional-switch Adjustment Process towards user equilibrium 127

Table 5.7 ORST towards system optimal distribution 129

Table 5.8 Dynamic process towards system optimal distribution in mixed conditions 132

Table 6.1 Results of routing and signal timing strategies under different levels of information 144

Table 6.2 The sensitivity analysis of ORTS under different CAVs penetration rates 145

Table 6.3 The sensitivity analysis of ORTS under different demands and penetration rates 146

Table 6.4 Dynamic process of signal timing on Nguyen-Dupuis network 149

Table 6.5 Dynamic process of routing on Nguyen-Dupuis network (iteration 0,1,2)150

Table 6.6 Dynamic process of routing on Nguyen-Dupuis network (iteration 3,4,5)151

Chapter 1 Introduction

1.1 Background and motivations

Autonomous Vehicles (AVs), which can self-operate and handle various driving tasks with little or without human intervention, are bringing revolutionary opportunities to urban traffic systems. They can reduce congestion, improve operational efficiency and liberate drivers from driving. For example, compared with Human-Driven Vehicles (HDVs), AVs can keep a shorter headway to the leading vehicle with the help of LIDAR or sensors to reduce congestion.

Though AVs might bring attractive potential benefits, most of the benefits are evaluated at high AV penetration rates or an all-AV scenario (Khattak et al., 2020; Liu et al., 2018; Rajamani & Shladover, 2001; Wagner, 2016). In practice, limited by price barriers, adoption rates and vehicle-renewal periods, AVs cannot replace HDVs to achieve a high penetration rate in a short time. In addition, behaviours of AVs might also be different from each other, which is caused by the development of AV technology (Ouster, 2018; Russell et al., 1997) and users' personal settings (Eichelberger & McCartt, 2014). It can be expected that the road network will operate in a mixed condition in the near to medium future.

Therefore, there is a strong motivation to analyse the characteristics of mixed traffic flows, which can help traffic managers and Local Authorities (LAs) to make informed policy decisions and find novel traffic management strategies during the transition period to the future where all vehicles are potentially autonomous.

1.1.1 Long-term policy decisions

Investigating the characteristics of the mixed traffic flow, especially heterogeneity between AVs and HDVs, can help traffic managers identify AVs' impacts on urban traffic systems. As AVs cannot replace HDVs in the short term, long term policies can be proposed to improve the efficiency of urban traffic systems for the transferring period. For example, with the increase of AVs, the utilisation of limited road infrastructures will become a challenge. As the performance of AVs dedicated lane, HDVs dedicated lane and mixed lane are different under different scenarios, right-of-way might need to be re-allocated in a more efficient way to reduce congestion. However, from a practical perspective, changing the right-of-way frequently might confuse drivers and increase operational costs. Therefore, it is necessary to investigate the critical points of right-of-way reallocation to reduce unnecessary changes and help traffic managers identify when different strategies need to be adopted.

1.1.2 Dynamic short-term traffic management

Apart from the long-term policy, the emergence of connected and automated technologies also provides opportunities for dynamic short-term traffic management in mixed conditions. By combining connected and automated technologies, Connected Autonomous Vehicles (CAVs) can self operate or cooperate with other vehicles and signals to achieve different driving tasks with the help of Vehicle to Vehicle (V2V) and Vehicle to Infrastructure(V2I) communication.

With V2I communication, data collected by CAVs can be transferred to the signal controller and ITS servers. These data might further be used for traffic signal control. For instance, equipped with the laser range finder and onboard cameras, CAV can act as a mobile traffic sensor providing traffic state of surrounding vehicles, such as speed, location and trajectory, to complement or replace conventional fixed sensors in the traffic control system.

Not only as a mobile sensor, but CAV can also become a mobile traffic controller. In the mixed flow, human drivers prefer to increase personal utility. Though some of HDV's driving behaviour, such as choosing the shortest route, can increase personal utility, these behaviours might reduce system efficiency because the System Optimal (SO) might be different from User Equilibrium (UE). As CAV can receive information about the surrounding environment and signal timing, based on these data, CAV can actively change its speed on the lane to influence the behaviour of other vehicles. Therefore, there is a motivation to investigate whether system travel efficiency can be improved with a few AVs acting as mobile traffic controllers by actively changing their speed on a road section.

With V2V communication, CAVs can cooperate with other vehicles. Ideally, in a fully connected and automated environment, all the CAVs can behave cooperatively in routing with traffic signals to achieve a System Optimal (SO) assignment. However, in the mixed flow, HDVs might not be connected, which means they might not cooperate with other vehicles actively and make their own routing decisions to maximise personal utility even when connected or guided by a system. This raises a crucial question as to whether travel efficiency can still be improved with only a part of the vehicular flow cooperatively changing its routing in the mixed condition.

V2V and V2I communication also open up an opportunity to jointly optimise routing and signal timing with information from CAVs such as the prior travel time and signal green time. As human drivers only have partial knowledge about travel costs and traffic status on the road network, most existing research related to HDVs assignment has not taken signal timing into account. However, in practice, route travel cost and vehicle's route choice might also be influenced by the signal timing. Therefore it is necessary to investigate whether additional travel efficiency can be achieved by jointly optimising routing and signal timing with information from CAVs.

1.2 Research aims and objectives

The overall aim of this PhD research is to analyse the mixed flows of AVs and HDVs to help traffic managers and Local Authorities (LAs) to improve the performance of urban traffic systems by right-of-way re-allocation and dynamic traffic management. To achieve this aim, the following are the four research objectives of this PhD research:

- RO1: Explore the impact of heterogeneity between AVs and HDVs on road capacity and propose appropriate right-of-way reallocation strategies to improve road capacity.
- RO2: Develop driving strategies for CAVs to interact with HDVs under mixed traffic conditions and explore whether CAVs can be used as mobile traffic controllers.
- RO3: Develop models to improve system travel efficiency with a few CAVs cooperatively changing their routing in the mixed conditions.
- RO4: Explore whether additional travel efficiency can be achieved by jointly optimising routing and signal timing with information from CAVs.

In summary, an issue tree is used to elaborate the relationship between motivation, challenges, opportunities, gaps and research objectives. These details are shown in Figure 1.1.

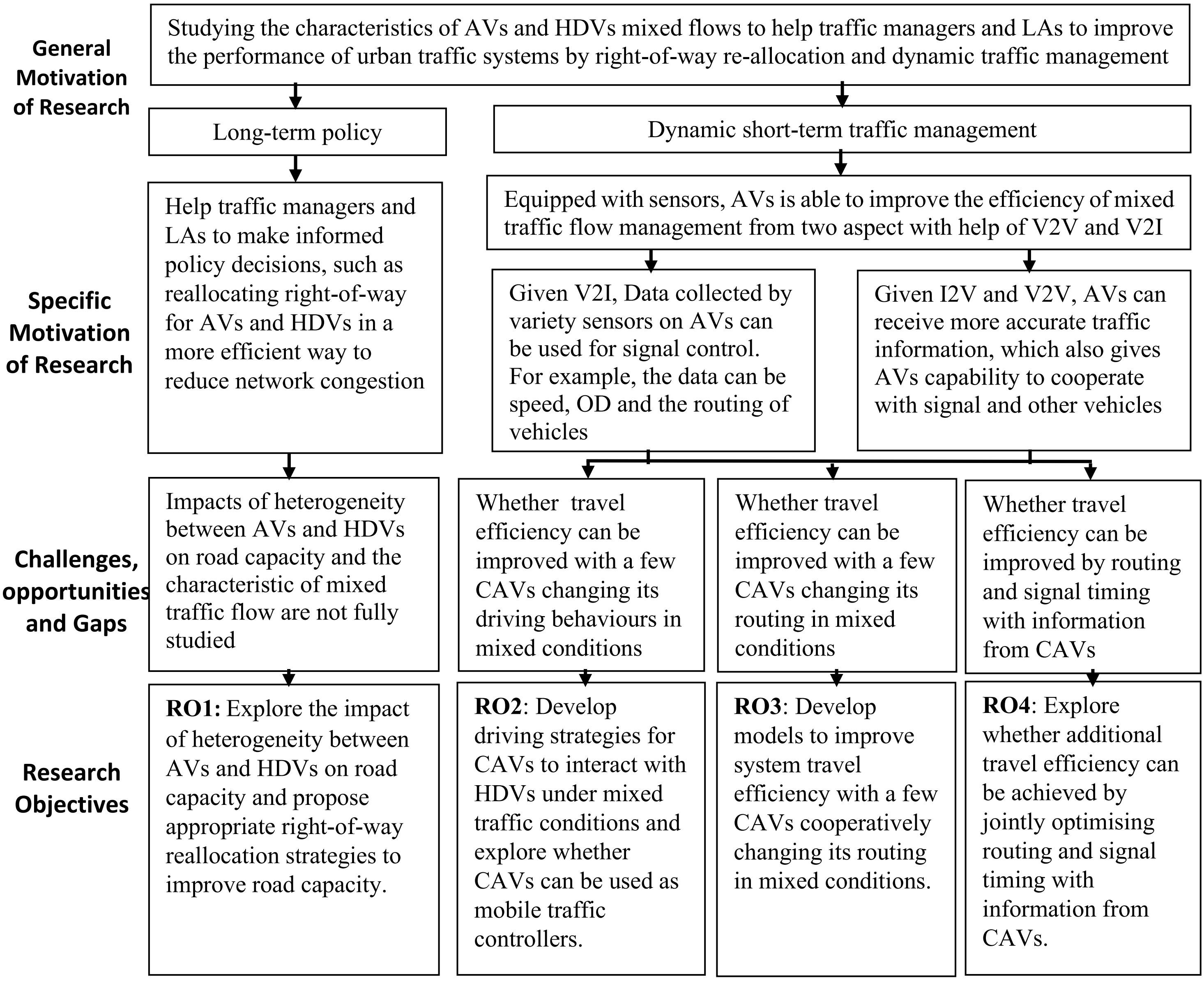

Figure 1.1 Issue tree of this PhD research

1.3 Outline of the thesis

This PhD thesis consists of seven chapters and is organised as follows (Part of the chapters are adapted from my peer-reviewed and published journal or conference papers, as listed in the next section):

Chapter 1: The background and motivations for this research are discussed in the first chapter. Based on the overall aim of the PhD research, four specific research objectives are proposed and summarised in the issue tree.

Chapter 2: According to the research objectives and the issue tree, the structure of the literature review is introduced in Section 2.1. In Section 2.2, the literature related to the modelling of AVs and HDVs is first reviewed to provide a foundation to investigate the characteristics of the mixed traffic flow. Then corresponding to four specific research objectives, the rest of the literature review is divided into four sections: the heterogeneous flow of AVs and HDVs, traffic control system and controlling traffic with CAVs, seeking system optimal equilibrium with HDVs and CAVs, and cooperation between AVs and signals in routing and signal timing. Finally, a summary and conclusion are given in Section 2.6.

Chapter 3 (adapted from Li et al. (2020)): To address RO1, the impacts of heterogeneity between AVs and HDVs on road capacity are investigated in this chapter. A theoretical model has been proposed to calculate the maximum capacity of heterogeneous saturated traffic flow. It has been proved that the theoretical maximum capacity of heterogeneous saturated flow increases convexly with AV penetration rates. The properties of the convex function further demonstrate that the road capacity can be increased with RoW reallocation in mixed traffic conditions. Then four different RoW reallocation strategies are proposed and evaluated by using the Simulation of Urban Mobility (SUMO) (Lopez et al., 2018) microsimulation tool. The results of the simulation demonstrate that the road capacity can be significantly improved with appropriate RoW reallocation strategies at low and medium AV penetration rates.

Chapter 4: According to RO2, whether CAVs can be used as mobile traffic controllers are investigated in this chapter. A numerical analysis on the Braess network (Braess et al., 2005) demonstrated that it is possible to increase system-level efficiency when CAVs adjust their speed on a certain link. As CAV can receive information about the surrounding environment and its behaviour change can influence the behaviour of other vehicles, a novel control strategy for CAVs acting as mobile traffic controller are proposed to improve system travel efficiency and evaluated using SUMO.

Chapter 5: Focused on RO3, whether travel efficiency can be improved with only a part of the vehicular flow cooperatively changing its routing in the mixed condition are investigated in this chapter. In the mixed flow of CAVs and HDVs, HDVs might not be connected and make their own routing decisions to maximise personal utility even when connected. To improve system efficiency, a dynamic process of routing and signal timing towards SO assignment in the mixed condition has been proposed. The results of the analytical model demonstrate that it is possible to influence HDVs' day-to-day routing using the CAVs and thus push the system towards SO assignment dynamically.

Chapter 6: To explore RO4, whether additional travel efficiency can be achieved by routing and signal timing with information from CAVs are investigated in this chapter. The impact of information levels on routing and signal timing efficiency has been investigated quantitatively. Then an Optimal Routing and Signal Timing (ORST) control strategy has been proposed. Compared with existing routing and signal timing strategies, the proposed ORST can successfully reduce the total travel time in the network.

Chapter 7: The contributions and potential practical implementations of this PhD research are summarised in this chapter. Moreover, as AV is a rapidly growing research field, the potential future research that builds upon this PhD is also discussed.

1.4 List of publications

Part of my PhD research works presented in this dissertation has been published in journals or conferences and listed as follow:

Journal papers:

J1) Li, T., Guo, F., Krishnan, R., Sivakumar, A., Polak, J., 2020. Right-of-way reallocation for mixed flow of autonomous vehicles and human driven vehicles. *Transportation Research Part C: Emerging Technologies* 115, 102630.

Conference papers:

C1) Li, T., Guo, F., Krishnan, R., Sivakumar, A., 2019. Right-of-way reallocation for mixed flow of autonomous vehicles and human driven vehicles. *University Transport Study Group 51st Annual Conference.*

C2) Li, T., Guo, F., Krishnan, R., Sivakumar, A., 2021. An analysis of the value of optimal routing and signal timing control strategy with CAVs. *Transportation Research Board 100th Annual Meeting.*

C3) Li, T., 2021. Generalised model to reduce total travel time dynamically with CAVs in mixed traffic of CAVs and HDVs. *University Transport Study Group 53rd Annual Conference.*

Other related journal and conference papers published during my PhD study are:

C4) Zhong, C., Li, T., Guo, F., Sivakumar, A., Krishnan, R., 2021. Heterogeneous flows of autonomous and human driven vehicles: an analysis of the impacts of vehicle size on road and passenger capacity. *Transportation Research Board 100th Annual Meeting*.

Journal papers currently under review:

J2) Li, T., Guo, F., Krishnan, R., Sivakumar, A., 2021. Dynamic process of routing and signal timing towards reducing total travel cost in mixed CAVs and HDVs traffic. (under review at *Transportation Research Part C*)

J3) Li, T., Guo, F., Krishnan, R., Sivakumar, A., 2021. An analysis of the value of optimal routing and signal timing control strategy with connected autonomous vehicles. (under review at *Journal of Intelligent Transportation Systems*)

Chapter 2 Literature review

2.1 Structure of the literature review

Based on the research objectives and issue tree discussed in Chapter 1, the structure of the literature review is shown in Figure 2.1. In Section 2.2 (corresponding to overall aims), to provide a foundation to investigate the characteristics of AVs and HDVs mixed flows, the literature related to modelling AVs and HDVs is reviewed. Firstly, in Subsection 2.2.1, the development and classification of AVs are reviewed to clarify the levels of automation. For each level of automation, various driving tasks are achieved by different sub-systems. Therefore to support parameters identification, existing AVs' sub-systems and their performance are reviewed in Subsection 2.2.2. Then different forms of the vehicle following model for AVs and HDVs, including micro-models and macro-models, are reviewed in Subsection 2.2.3, and a summary is given in Subsection 2.2.4.

In Section 2.3 (corresponding to RO1), to explore the impacts of heterogeneity on road capacity, the literature related to heterogeneity on traffic flow are reviewed. In Subsection 2.3.1, the classification of heterogeneity in mixed traffic flow are discussed. Then existing research on various heterogeneity is reviewed in Subsection 2.3.2 and summarised in Subsection 2.3.3.

In Section 2.4 (corresponding to RO2), to explore whether CAVs can be used as mobile traffic controllers, the literature related to the traffic control system and controlling traffic with CAVs are reviewed in Subsections 2.4.1 and 2.4.2. Then a summary is given in Subsection 2.4.3.

In Section 2.5 (corresponding to RO3), to improve system efficiency with a few CAVs cooperatively changing its routing in the mixed condition, the literature related to seeking system optimal traffic assignment with CAVs and HDVs are reviewed. In Subsection 2.5.1, HDV's routing behaviour and development of user equilibrium are discussed. Then to improve system efficiency, existing research on seeking system optimal equilibrium in practice are reviewed in Subsection 2.5.2, and a summary is given in Subsection 2.5.3.

In Section 2.6 (corresponding to RO4), to explore whether additional travel efficiency can be achieved by jointly optimising routing and signal timing with information from CAVs, the literature related to cooperation between CAVs and signals in routing and signal timing are reviewed. The combined routing and signal control problem are reviewed in Subsection 2.6.1 and summarised in Subsection 2.6.2. Finally, all of this literature reviews chapter is concluded in Section 2.7.

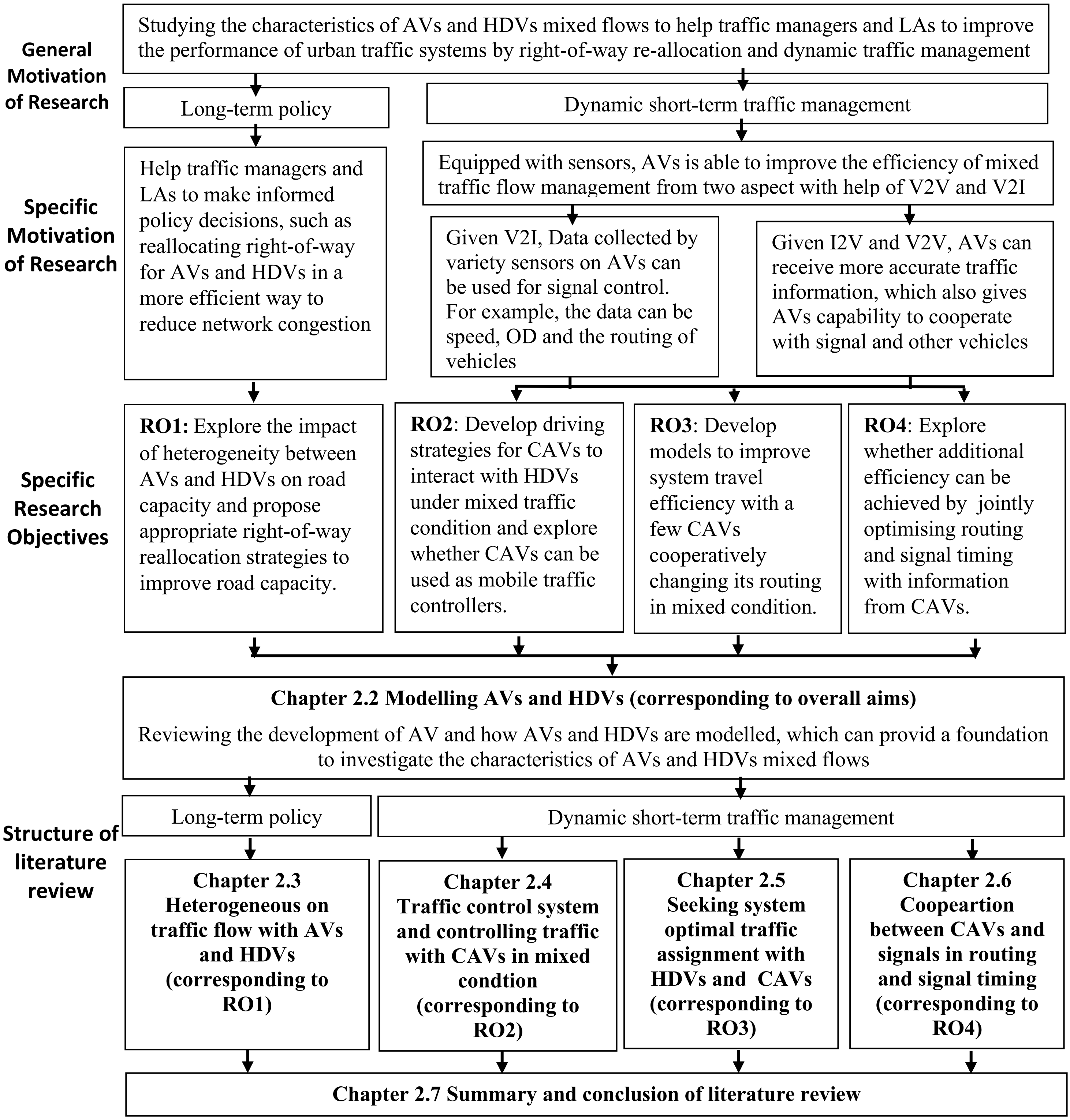

Figure 2.1 Structure of literature review

2.2 Modelling AVs and HDVs

Modelling AVs and HDVs is a powerful tool to help scholars to study the characteristics of traffic flow. For any model, parameters and model formulation are two key aspects. Therefore, in this section, the development and classification of AVs will be first reviewed as a general background. After that, the performance of key sub-systems of different levels of AVs will be reviewed to support parameter identification. Then the different forms of the vehicle following model for AVs and HDVs in existing literature will be reviewed to provide a foundation to investigate the characteristics of mixed flow.

2.2.1 Development and Classification of AVs

The history of Autonomous Vehicles can go back to 1926. The Milwaukee Sentinel (1926) reported a trial of a driverless car. However, the initial driverless car is not real driverless. The vehicle is controlled by radio. Not until the late 20th century, the autonomous prototype cars were developed by different research groups, such as Japan's Mechanical Engineering, Bundeswehr University Munich (Schmidhuber, 2011) and Mercedes-Benz (Bohrer et al., 1995)

However, limited by the available technology, for example, computing power, sensor technologies and localisation technology, AVs were still not capable of sensing the complex reality road traffic. In 2004, DARPA held a Grand Challenge 150 miles driverless car competition, where vehicles needed to deal with complex circumstances and rules. Unfortunately, the best team just travelled 7.4 miles (DARPA, 2004)

With the development of AVs technology, one year late in 2005, five teams completed the competition, which showed that AVs could deal with more complex situations (DARPA, 2005). Recently, many companies such as Google, Uber, Baidu and DiDi invested lots of capital on AVs research and development. The road testing of AVs is also permitted in some locations in the USA and the UK.

With the development of AVs, levels of automation are increasing. To identify the different levels of automation, SAE published a classification of AVs where AVs are divided from level 0 to level 5 (SAE 2014), shown in Table 2.1.

Table 2.1 SAE level of autonomous vehicles

SAE level	Name	Execution of Steering and Acceleration/ Deceleration	Monitoring of Driving Environment	Fallback Performance of Dynamic Driving Task	System Capability (Driving Modes)
Human Driver monitors the driving environment					
0	No Automation	Human driver	Human driver	Human driver	n/a
1	Driver Assistance	Human driver and system	Human driver	Human driver	Some driving modes
2	Partial Automation	system	Human driver	Human driver	Some driving modes
Automated driving system("system") monitors the driving environment					
3	Conditional Automation	system	system	Human driver	Some driving modes
4	High Automation	system	system	system	Some driving modes
5	Full Automation	system	system	system	all driving modes

With the increasing automation levels, the system or AVs can complete more complex driving tasks. In SAE classification, Level 0 is no automation, which is HDVs. Level 1 is human-driven vehicles equipped with some assistance systems, such as Anti-lock Braking System (ABS), Lane Departure Warning System (LDWS) and Lane Keeping Assistance (LKA). In these two levels, a human driver will execute all driving activities. When it comes to Level 2 partial automation, the system will control the vehicle's steering and acceleration/deceleration. In level 3 conditional automation. AVs start to monitor the environment around them. For level 4 high automation and level 5 full automation, which have not been achieved so far, AVs will achieve dynamic driving tasks and have various driving modes.

For each level of automation, there are different sub-systems designed to achieve parts of the driving function, such as steering, braking and monitoring the environment. In the next section, the sub-system of AVs and their performance will be discussed.

2.2.2 Sub-system of existing AVs and their performance

Driving is a skill, which consists of different tasks such as steering, monitoring the environment, and path planning. For human drivers, driving courses and licence tests are designed to ensure drivers can handle different driving tasks. When it comes to AVs, different sub-systems are developed to achieve these tasks for driving. In this section, the function of each sub-system is summarised in the following Table 2.2. After that, each sub-system's performance will be discussed, and their parameters are summarised in Table 2.8.

1) Rear View Cameras

The Rear View Cameras (RVC) are level 0 automation systems (NHTSA, 2013), which can monitor the area behind the rear bumper. The primary purpose of this system is to avoid collisions happen in the back area, which was associated with a 28% reduction in crashes (Mazzae et al., 2008). The key performance parameter of RVC is response times to the objective. According to an NHTSA's test, the response times for the eight tested sensor systems varied from 0.18 to 1 second, and only three of them met the ISO response time limit, which is 0.35 seconds (NHTSA, 2009).

2) Lane Departure Warning

Once a danger occurs, such as a vehicle closing the edges of the lane, the warning will be sent by Lane Departure Warning (LDW) system (Lo et al., 2013). In an ideal condition, the Volvo LDW system is estimated to benefit from a 47% reduction in lane departure crashes (Gordon et al., 2010). Narote et al. (2018) reviewed various LDW systems from 1998 to 2017. They find that different techniques can achieve good results from a detection rate point of view so far. However, the system should be robust and quick enough to meet real-time criteria. Meanwhile, the false alarm should be minimum. A detection and warning comparison of LDW systems are showed in Table 2.3.

Table 2.2 Summary of AVs Sub-system by the level of automation

level	Sub-system	Main Function	Key Performance parameters
0	Rear View Cameras	Rear View Cameras (RVC) can help the driver to view an image of the area behind the rear bumper during parking. Meanwhile, the rear parking sensor will detect the objective and alarm.	Response times: 0.18~1s (tested) 0.35s (recommend) (NHTSA, 2009)
0	Lane Departure Warning	Lane Departure Warning (LDW) system can detect lane marks and provide alerts when the vehicle is too close to the edges of the lane.	Dictation rates: 87% ~100% (Bhujbal & Narote, 2015) (Gaikwad & Lokhande, 2015)
0	Forward Collision Warning	Forward Collision Warning (FCW) system can warn drivers of possible hazards in front of the vehicle so that drivers can react to avoid crashes or reduce damages from unavoidable crashes.	PATH (Wilson et al., 1997) Mazda (Ararat et al., 2006) SDA (Jamson et al., 2008)
1	Forward Collision Mitigation	Forward Collision Mitigation (FCM) system is a development of FCW. The system will detect objects' distances and closing speeds and automatically decelerate or stop if the driver does not respond to the alarm.	Emergency braking: $5\ m/s^2$ (Coelingh et al., 2006) $10\ m/s^2$ (Coelingh et al., 2010)
1	Electronic Stability Control	Electronic Stability Control (ESC) system can continuously monitor the actual motion of the vehicle and apply brakes independently to each wheel, which allows ESC to help the driver maintain control of the vehicle, especially in difficult situations, such as icy roads	Dwell test: 1s after COS: yaw rate≤ 35% peak 1.75s after COS: yaw rate≤ 20% peak (British Standards Institution, 2016)
1	Anti-lock Braking Systems	Anti-lock Braking Systems (ABS) can release and re-applying the brakes multiple times in a short time to reduce braking distance by using the principle that static friction is larger than sliding friction	Experimental braking data. Table 2.5 (Wu & Shih, 2003)
1	Cruise Control	Cruise Control (CC) can help the driver to maintain their set speed without manual acceleration or deceleration constantly.	Range: 3-100 m Range Accuracy <0.5 m Relative Speed <±160 km/h Accuracy < 1.5 km/h (Russell et al., 1997)
2	Adaptive Cruise Control	Adaptive Cruise Control (ACC) system uses distance sensing technology to automatically maintain a constant distance between the vehicle and the vehicle directly ahead.	Headway or time gap： the Mercedes DISTRONIC system: 1s ~ 2s (Richardson, 1999) Volvo: 1s ~2.5s (Eichelberger & McCartt, 2014)
2&3	Laser Range Finder System	Laser Range Finder (LRF) is commonly used in level 3, or higher-level AVs, which takes distance scans more than 10 times a second to monitor vehicles and pedestrians around the AVs	Range: 0.2- 200m Accuracy: ± 2-3cm(typical) (Ouster, 2018; Robosense, 2018a; Robosense, 2018b; Velogdyne, 2018)

Table 2.3 Detection and Warning Comparison of LDW systems

	LDW (Bhujbal & Narote, 2015)		LDW(Gaikwad & Lokhande, 2015)	
	Day	**Night**	**Day**	**Night**
True Lane Detection	97.80%	100%	87.88%	94.13%
False Lane Detection	3.28%	0.00%	18.75%	5.87%
True Warning	93.56%	98.46%	90.50%	96.43%
False Warning	6.44%	1.54%	9.50%	3.57%

3) Forward Collision Warning

The Forward Collision Warning (FCW) system, a level 0 vehicle automation system (NHTSA, 2013), is designed to warn drivers of possible hazards in front of the vehicle. Then the driver can brake or steer to avoid crashes or minimise injuries. The performance of FCW relies on the parameter setting, algorithm of warming distance calculation and error of speed and distance measurement. There are three kinds of warming distance calculation algorithms, and their parameters are shown in Table 2.4

a) The PATH Algorithm (Wilson et al., 1997)

$$R_{warning} = 0.5\left[(V_f^2/\alpha_f) - (V_l^2/\alpha_l)\right] + V_f\tau + R_{min}$$

b) The Mazda algorithm(Ararat et al., 2006)

$$R_{warning} = 0.5\left[(V_f^2/\alpha_f) - (V_l^2/\alpha_l)\right] + V_f\tau_1 + V_l\tau_2 + R_{min}$$

c) The Stop Distance Algorithm(SDA) (Jamson et al., 2008)

$$R_{warning} = 0.5\left[(V_f^2/\alpha_f) - (V_l^2/\alpha_l)\right] + V_f\tau_{driver}$$

Table 2.4 Parameter values for algorithms (Bella & Russo, 2011)

	PATH	Mazda	SDA
α_f: accelerated of following vehicle(m/s^2)	6	6	5
α_l: accelerated of lead vehicle (m/s^2)	6	8	5
τ : brake reaction time (s)	1.2	n/a	n/a
τ_1: brake reaction time of following vehicle(s)	n/a	0.1	n/a
τ_2: brake reaction time of lead vehicle(s)	n/a	0.6	n/a
τ : driver's reaction time (s)	n/a	n/a	1.5
R_{min}: Minimum range	5	5	n/a

*V_f *and* V_l are speed of following and leading vehicle

4) Forward Collision Mitigation

The Forward Collision Mitigation (FCM) system, also known as collision imminent braking or auto-brake, is a development of the FCW. The system will detect objects' distances and closing speed and will automatically decelerate, steer or stop if the driver does not respond to the alarm. Because FCM is function-specific automation, it is a level 1 automation (NHTSA, 2013). When it comes to the performance of the system, the second generation Volvo Collision Warning with Full Auto Brake and Pedestrian Detection (CWAB-PD) can provide warning, brake and partial automatic emergency breaking of 5 m/s^2 (Coelingh et al., 2006). The third generation can achieve full automatic emergency braking up to 10 m/s^2 (Coelingh et al., 2010).

5) Electronic Stability Control

The Electronic Stability Control (ESC) system is designed to help drivers maintain control of their vehicle on high-speed, sudden turning or icy roads. ESC can continuously monitor the actual motion of the vehicle and apply brakes independently to each wheel to avoid oversteer and understeer. It has been recognized as a level 1 vehicle automation system(NHTSA, 2013). According to the ISO 19365:2016, a dwelling test is required for the ESC system, where a sine wave at a frequency of 0.7 Hz with a delay of 500 ms beginning at the second peak amplitude is used as test input. There are two requirements of tested output. First, at 1 second after the completion of steer (COS) time, the value of yaw rate shall not exceed 35% of the first peak value recorded after the steering-wheel angle changes sign. After that, at 1.75 seconds after the COS time, the yaw rate value shall not exceed 20% of the first peak value (British Standards Institution, 2016).

6) Anti-lock Braking Systems

Anti-lock Braking Systems (ABS) can release and re-apply the brakes multiple times in a short time to reduce braking distance by using the principle that static friction is larger than sliding friction. The relationship between longitudinal coefficient, lateral coefficient and slip are not linear. Zanten et al. (1990) found that the breaking distance can be reduced if the slip is kept between 8% and 30%. An experimental test researched the performance of different ABS control models, where the vehicle started braking at 64 km/h on the dry and wet state. Results are shown in Table 2.5.

Table 2.5 Experimental braking data

Control type	Road state	Braking time (s)	Stopping distance (m)	Average acceleration (m/s^2)
Sliding-mode switching control	Dry	2.15	23.76	−8.27
Sliding-mode PWM control	Dry	2.18	23.82	−8.16
Electric control unit	Dry	2.09	23.60	−8.51
Sliding-mode switching control	Wet	2.60	28.20	−6.84
Sliding-mode PWM control	Wet	2.66	28.47	−6.69
Electric control unit	Wet	5.45	48.43	−3.26

7) Cruise Control

Cruise Control (CC) can help the driver maintain their set speed without constant manual acceleration or deceleration. Teetor (1950) invented vehicle fittings for automatically controlling, which can prevent speed from exceeding an arbitrary velocity or maintain speed at a set velocity. However, this set velocity means the vehicle cannot automatically decelerate when approaching a lead vehicle or barrier. To improve CC, sensors, such as millimetre-wave radar, are used for Intelligent Cruise Control (ICC). Some performance parameters of ICC are shown in Table 2.6 (Russell et al., 1997).

Table 2.6 Performance Specifications of ICC

Characteristic	Value
Operating Frequency	76-77 GHz
Waveform	FM-CW
Range	3-100 metres
Range Accuracy	< 0.5 metres
Relative Speed	< ± 160 km/h
Relative Speed Accuracy	< 1.5 km/h
Update Rate	20 Hz
Max Targets Under Track	40

*FM-CW is Frequency-Modulated Continuous-Wave

8) Adaptive Cruise Control

Adaptive Cruise Control (ACC) system uses distance sensing technology to automatically maintain a constant distance between the vehicle and the vehicle directly ahead, which is an improvement of Cruise Control. ACC will operate at a set speed when there are no other vehicles in front of the vehicle. If ACC senses a vehicle, it can maintain a set time headway to the forward vehicle.

In practice, the DISTRONIC system allows time gaps between 1 and 2 s to be selected by the driver (Richardson, 1999). A test-track study did by Rudin-Brown and Parker (2004) assessed in three counterbalanced conditions: No ACC (self-maintained average headway of 2 s), ACC-Short (headway of 1.4 s) and ACC-Long (headway of 2.4 s). The results demonstrate that ACC can induce behavioural adaptation in drivers.

An interview survey of Volvo Drivers who own 2010-2012 model Volvo vehicles with several vehicle automation technologies found that Among 315 owners who responded to questions about adaptive cruise control, 80% (252 owners) reported that they had used it at some point. In these 252 owners, 33% of users adjusted the time gap to 1or 2 bars (corresponding to 1s or 1.5s time gap); 22% of users adjusted the time gap to 4 or 5 bars (corresponding to 2s or 2.5s time gap). Whereas 36% of users only use default setting 3bars (1.5s time gap), others do not know their setting (Eichelberger & McCartt, 2014).

9) Laser Range Finder (LRF) System

Laser-range finder is commonly used in level 3 or higher-level AVs, taking distance scans more than ten times a second to monitor vehicles and pedestrians around the AVs. In the 1980s, the NASA applied LRF system on their Robert Cuningham. (Lewis & Johnston, 1977). In 1994, a concept design of scanning LRF for AVs was proposed by Kelly at Carnegie Mellon University (Kelly, 1994). In the 2006 DARPA urban challenge, one of the participators used the range-finders designed by IBEO (Cacciola, 2007). The IBEO can achieve a two-dimensional (2D) scan view, as shown in Figure 2.2. The object can be tracked when the object is tracked longer than 0.5s, and A small object must be closer than 10 m (Scholz et al., 2006).

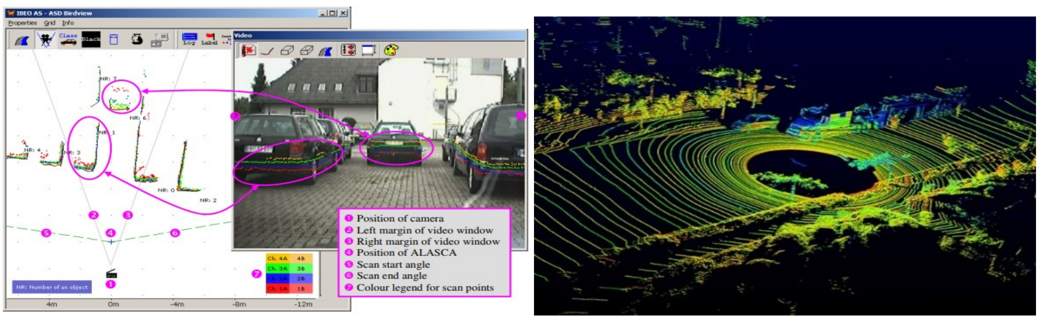

Figure 2.2 IBEO 2D LRF system (left)(Scholz et al., 2006) and Velodyne HDL-64 3D LRF system (right)(Velogdyne, 2018)

In recent years, with the development of the LRF system. Multi-channel 3D scanning can be achieved. For example, Velodyne HDL-64 can achieve 3D scanning in the 120m range, as shown in Figure 2.2. Further detailed performance parameters are shown as in Table 2.7:

Table 2.7 Performance Specifications of ICC

Characteristic	RS-LiDAR 16	RS-LiDAR 32	HDL-64	OS-2
Channels/beams	16 beams	32 beams	64 beams	64 beams
Accuracy	± 2cm(typical)	± 2cm(typical)	± 2cm(typical)	± 3 cm
Range	0.2-150 metres	0.2-200 metres	120 metres	>200 metres
Angular resolution				
(Vertical)	30°	40°	0.4°	0.26°
(Horizontal)	0.09°~ 0.36°	0.09°~ 0.36°	0.08°~ 0.35°	0.18°
Field of view				
(Vertical)	2°	+1.66°~ -4.66°	26.9°	+7.9°~ -7.9°
(Horizontal)	360°	360°	360°	360°
Price	$4,588	$27,350	$75,000	$24,000
Citation	(Robosense, 2018a)	(Robosense, 2018b)	(Velogdyne, 2018)	(Ouster, 2018)

In summary, nine different AVs Sub-systems were reviewed in this section. Each of these systems can achieve portion function of driving, for example, cruising, emergency braking and environment perception. It can be observed that automated technologies are developing rapidly. Though AVs are still developing and data about AVs' performance are not easy to access, the performance of these sub-systems in practice can still help scholars identify parameters of AVs modelling, which can be summarised in Table 2.8.

Table 2.8 Parameter of AVs with their subsystem

Driving tasks	Name of parameter	L1 &2 AVs	Reference
Steering	Acceleration speed	Depends on vehicle	
	Deceleration speed	6 m/s^2	(Bella & Russo, 2011)
	Emergency brake	5 m/s^2	(Coelingh et al., 2006)
		10 m/s^2	(Coelingh et al., 2010)
Monitoring of Driving Environment	Detection range	3-100 m	(Russell et al., 1997)
		0.2-200 m	(Robosense, 2018b)
	Speed detection error	< 1.5 km/h	(Russell et al., 1997)
	range detection error	±0.5 m	(Russell et al., 1997)
		±2-3cm(static)	(Robosense, 2018b)
Driving safety	Time headway	1-2 s	(Richardson, 1999)
		1-2.5 s	(Eichelberger & McCartt, 2014)
	Reaction time	0.7-1.5 s	(Bella & Russo, 2011)

2.2.3 Existing models of AVs and HDVs

Vehicle following and lane changing are two primary driving tasks for drivers, leading to the development of the vehicle following model and lane changing model. In this sub-section, existing research on the vehicle following model and lane changing mode for HDVs and AVs will be reviewed.

1) Vehicle Following Model for HDVs

Vehicle following model (FVM) is used to describe the longitudinal interaction between the leading and following vehicle. The research of drivers' following behaviour started in the 1950s (Pipes, 1953; Reuschel, 1950). After that, many scholars proposed different forms of the vehicle following model. However, the general form of the vehicle following model can be described as Response = Sensitivity × Stimulus, where response represents the reaction of the following driver. Stimulus and sensitivity are elements that lead to the driver's response and the degree of this response.

The Gazis–Herman–Rothery (GHR) model (Gazis et al., 1959; Gazis et al., 1961; Herman & Potts, 1959), or named as General Motors (GM) model shown in Equation (2.1), may be the most classical vehicle following model, where the stimulus is the relative speed and distance between the leading and the following vehicle. Summary of optimal parameter combinations for the GHR model by different scholars is shown in Table 2.9.

Table 2.9 Summary of the GHR model (Brackstone & McDonald, 1999)

Research	*m*	*l*	Scale
Chandler et al. (1958)	0	0	Micro
Gazis et al. (1959)	0	1	Macro
Herman and Potts (1959)	0	1	Micro
Helly (1959)	1	1	Macro
Gazis et al. (1961)	0-2	1-2	Macro
May and Keller (1967)	0.8	2.8	Macro
Heyes and Ashworth (1972)	-0.8	1.2	Marco
Treiterer and Myers (1974) (dcn/acn)	0.7/0.2	2.5/1.6	Micro
Ceder and May (1976) (Single regime)	0.6	2.4	Macro
Ceder and May (1976) (uncgd/cgd)	0/0	3/0-1	Macro
Aron (1988) (dcn/ss/acn)	2.5/2.7/2.5	0.7/0.3/0.1	Micro
Ozaki (1993) (dcn/acn)	0.9/-0.2	1/0.2	Micro

*dcn/acn: deceleration/acceleration; uncgd/cgd: uncongested/congested; ss: steady state.

$$a_n(t) = cv_n^m(t)\frac{\Delta v(t-T)}{\Delta x^l(t-T)} \tag{2.1}$$

Though the GHR model can successfully model traffic flow and link the micro behaviour of vehicles to form macro characteristic of flow-speed-density by integral, for two vehicles travelling at the same speed, any value of spacing between them is acceptable for the GHR model. To address this problem, Helly (1959) proposed that driver has a desired following distance, and the driver seeks to minimise both the speed difference and the difference between the actual space headway and the desired headway.

With the disadvantage that the safety distance has not been considered in the GHR model, Gipps (1981) proposed a relative safety constraint $x_n^* \leq x_{n-1}^* - s_{n-1}$, where x_n^* is location of vehicle n after braking; s_n is the size of vehicle n. Krauss (1998) inspired by Gipps model and further proposed maximum safe velocity as a new constraint.

To model macro characteristics, Bando et al. (1995) proposed the Optimal Velocity (OV) model to analyse the stability of traffic flow. Using numerical simulation, Bando found that when $f < \frac{\alpha}{2}$ the state is stable, $f = \frac{\alpha}{2}$ the state is marginal and $f > \frac{\alpha}{2}$ the state is unstable. Where f is the derivative of V at b; V is the legal velocity of the vehicle; b is the constant spacing of two successive vehicles.

Treiber et al. (2000) proposed that the model proposed by Gipps, Krauss did not show traffic instabilities or hysteresis effects for vanishing fluctuations. Therefore the Intelligent Driver Model(IDM), which considers both the desired speed and the desired space headway, was proposed to formulating the theoretical phase diagram for bottlenecks.

Considering elaborate rules of the car-following model have been proposed over 50 years, Newell (2002) proposed an ingenious simplified car-following model, which assumed that an nth vehicle is following an $(n-1)$th vehicle on a homogeneous way. Newell model only have two parameters distance d_n and to, time τ_n, which can be further represent by the wave speed $\vec{w}_n$ (Chiabaut et al., 2010). Though the Newell model is relatively simple, it can model the macro traffic flow with a few parameters.

All of these vehicle following models have a numerical formula to describe the relationship between acceleration, relative speed and relative distance. Their mathematical form of model and parameters used are summarised in Table 2.10.

Table 2.10 Summary of the vehicle following models for HDVs

Reference	Main model	Used parameters
Gazis et al. (1959)	$a_n(t) = c\frac{\Delta v(t-T)}{\Delta x(t-T)}$	$c = 0.6s^{-1}$ $T = 1.5s$
Gazis et al. (1961)	$a_n(t) = cv_n^m(t)\frac{\Delta v(t-T)}{\Delta x^l(t-T)}$	$c = 0.31{\sim}0.937$ $m = -1{\sim}2$ $l = 0-2$
Helly (1959)	$a_n(t) = \alpha_1\Delta V_n(t-T) + \alpha_2[\Delta X_n(t-T) - \Delta\widetilde{X_n}(t)]$ $\Delta\widetilde{X_n}(t) = \beta_1 + \beta_2 V_n(t-\tau_n) + \beta_3 a_n(t-\tau_n)$	$T = 0.5{\sim}2.2s$ $\alpha_1 = 0{,}17{\sim}1.3$ $\alpha_2 = 0{,}17{\sim}1.3$
Gipps (1981)	$v_n(t+T) = \min\{v_n(t) + 2.5a_n\tau\left(1-\frac{v_n(t)}{V_n}\right) * \sqrt{0.025+\frac{v_n(t)}{V_n}},$ $b_nT + \sqrt{b_n^2T^2 - b_n(2[x_{n-1}(t) - s_{n-1} - x_n(t)]) - v_n(t) * T - \frac{v_{n-1}(t)^2}{2\hat{b}}}\}$	$a_n = N(1.7, 0.3^2)m/s^2$ $b_n = -0.2a_n$ $s_n = N(6.5, 0.3^2)m$ $V_n = N(20, 3.2^2)\ m/s$ $T = 2/3\ s$ $\hat{b} = Min(-3, \frac{b_n-3}{2})\ m/s^2$
Bando et al. (1995)	$a_n(t) = \alpha(V(\Delta x_n) - V_n(t))$ $\Delta x_n = x_{n+1} - x_n$ $V(\Delta x_n) = \tanh(\Delta x)$ or $V(\Delta x_n) = \tanh(\Delta x - 2) + tanh2$	$\alpha = 1$
Krauss (1998)	$v_{des} = Min(v_{max}, v + a, v_{saft}(t))$ $v = \max[0, rand[v_{des} - \epsilon a, v_{des}]]$ $v_{saft} = v_l(t) + \frac{g(t) - v_l(t)T}{\frac{\bar{v}}{b(\bar{v})} + T}$	$T \approx 1s$ $l \approx 7.5s$ $v_{max} \approx 7.5s$ $a \approx 0.8m/s^2$ $b \approx 0.6m/s^2$
Treiber et al. (2000)	$a_n(t) = a^{(n)}\left[1 - \left(\frac{v_n(t)}{v_0^{(n)}(t)}\right)^\beta - \left(\frac{s_n^*(t)}{s_n(t)}\right)^2\right]$ (IDM model) $s_n^*(t) = s_0^{(n)} + s_1^{(n)}\sqrt{\frac{V}{v_0^{(n)}}} + T^n v + \frac{v\Delta v}{2\sqrt{a^{(n)}b^{(n)}}}$	$v_0^{(n)} = 120km/h$ $T^n = 1.6s$ $a^{(n)} = 0.73\ m/s^2$ $b^{(n)} = 1.67\ m/s^2$ $\beta = 4$ $s_0 = 2m$ $s_1 = 0m$ Vehicle length $l = 5m$
Newell (2002)	$x_n(t+\tau_n) = x_{n-1}(t) - d_n$ $d_n + v\tau_n = s_n$	Not applied

Though the above models have a continuous mathematic form, which can be integrated to analyse the macro characteristic of traffic flow, some vehicle following models do not have a continuous mathematic form. For instance, Cellular Automata (CA), which was proposed in the 1950s (Von Neumann, 1951), reproduced the macroscopic behaviour of a complex system using minimal microscopic descriptions. The CA model constitutes four key components: the physical environment, the cells' states, the cells' neighbourhoods, and local transition rules. Nagel and Schreckenberg (1992) introduced a stochastic discrete CA model for freeway traffic. At each time step, the model updates four consecutive steps performed in parallel for all vehicles.

Wiedemann and Reiter (1992) proposed a psychophysical model used in VISSIM to simulate driver behaviour. There were four driving regimes: free flow, approaching, following and decelerating, where relative speed was defined as an action point to divide different driving regimes.

To model the indeterminacy of human behaviour, fuzzy logic has been used, where numbers of overlapping fuzzy sets will be defined to describe relative speed or distance. Kikuchi and Chakroborty (1992) used $\Delta x, \Delta v$ and a as inputs to fuzzy traditional GHR models. McDonald et al. (1997) used fuzzy modelling to modelling behaviour of 3 lane motorways.

2) Lane Changing Model for HDVs

Different from the vehicle following model, Lane Changing Model (LCM) is used to describe the lateral movement of the vehicle. Though the general purpose of lane change is to get a better driving environment, the lane change model is more complex and harder to be concluded in a general form because it involves a decision making process and influence from surrounding traffic.

The general decision process of lane changing decision is that whether it is possible, necessary and desirable to change lane (Gipps, 1986a). More specifically, factors that influence the lane changing decision process include safety, location of permanent obstructions, the pressure of transit lanes, driver's intention, the pressure of heavy vehicles and speed. Gipps' framework can simulate the lane changing behaviour. However, it is a deterministic model.

After Gipps' pioneering work, Yang and Koutsopoulos (1996) developed a similar lane changing model in the microscopic traffic simulator, MITSIM, where a probability function is used to model the probability of lane change. The errors and change of gap acceptance have also been considered in the model.

Following Yang and Koutsopoulos, Ahmed (1999) pointed that a gap is considered acceptable only when both the lead and lag gaps are acceptable. To minimising negative induced by lane change, Kesting et al. (2007) proposed minimising overall braking induced by lane change (MOBIL). The MOBIL rules are applied, and multilane traffic is simulated in combination with the Intelligent Driver Model (IDM).

Though the whole decision framework is hard to be concluded in a single table, a summary of lane changing models is shown in Table 2.11.

Table 2.11 Summary of lane changing model for HDVs

Reference	Main model	Used parameter
Gipps (1986a)	Feasibility: $v_n(t+T) = b_nT + \sqrt{b_n^2T^2 - b_n(2[x_{n-1}(t) - s_{n-1} - x_n(t)]) - v_n(t) * T - \frac{v_{n-1}(t)^2}{2\hat{b}}}\}$ For follower $\frac{v_n(t+T)-v_n(t)}{T} > b_{willing}$ Urgency: $b_n = [2 - (D_n - x_n(t)/10\, V_n]b_n^*$	$b_{willing} = -4\, m/s^2$
Yang and Koutsopoulos (1996)	$p_n = \begin{cases} \exp\,[(x_n - x_0)^2/\sigma_n^2] & x_n > x_0 \\ 1 & x_n \le x_0 \end{cases}$ $g_n^i = \varepsilon_n^i + \begin{cases} g_{max}^i & x_n \ge x_{max} \\ g_{min}^i + (g_{max}^i - g_{min}^i)\frac{x_n - x_{min}}{x_{max} - x_{min}} & x_{min} < x_n < x_{max} \\ g_{min}^i & x_n \le x_{min} \end{cases}$	Not reported
Ahmed (1999)	$G_n^{cr,lead}(t) = exp[a - bv_b + \varepsilon_n^{lead}(t)]$ $G_n^{cr,lag}(t) = \exp[-9.32 + 0.117\min(\Delta v_n^{lag}(t), 10) + 0.1174\max(\Delta v_n^{lag}(t) - 10{,}0) + 1.57\delta_n^{lag}(t) + 1.88\ln(L_n^{rem}(t) + 1.90v_n + \varepsilon_n^{lag}(t))]$ $p_n = \frac{1}{1 + \exp(1.90 - 0.52delay(t))}$	$a = 2.72$ $b = 0.055$
Kesting et al. (2007)	$\tilde{a}_c - a_c + p(\tilde{a}_n - a_n + \tilde{a}_o - a_o) > \Delta a_{th} + \Delta a_{bias}$ $\tilde{a}_n \ge -b_{safe}$ $a_\alpha = \frac{dv_\alpha}{dt} = a(s_\alpha, v_\alpha, \Delta v_\alpha)$ (IDM model)	$p = 0\sim1$ $\Delta a_{th} = 0.1\, m/s^2$ $\Delta a_{bias} = 0.3 m/s^2$

3) Vehicle Following Model, Lateral Model and Lane Changing Model for AVs

With the development of autonomous prototype cars in the late 20th century, such as Japan's Mechanical Engineering, Bundeswehr University Munich (Schmidhuber, 2011) and Mercedes-Benz (Bohrer et al., 1995), many scholars paid their attention to the research of AVs.

At the early stage, scholars focused on how to control the longitudinal and lateral movement of AVs. Andreas et al. (2000) proposed the structure of vehicle guidance system for AVs, which is shown in Figure 2.3 left. In this structure, the Linear–Quadratic–Gaussian (LQG) was chosen for the controller because it rejects disturbances better than the Proportional–Integral–Derivative (PID) controller and reacts faster than a H_∞-optimal controller. Kato and Tsugawa (2001) used Proportional–Derivative (PD) control for cooperative driving of AVs. In this research, the localisation data collected by Differential Global Positioning System (DGPS) were exchanged through inter-vehicle communication and the speed command u_i is given as: $u_i = v_p + K_1(v_p - v_i) + K_2(L_i - L_r)$. Where $K_1 = M_1 \cdot |L_r - L_i|/|L_r|$, $K_2 = M_2 \cdot |L_r - L_i|/|L_r|$. Considering stabilisation of AVs control is a problem, Beji et al. (2003) proposed time-varying controller for longitudinal and steering stabilisation. The elaborate kinematics parameterization of the vehicle is shown in Figure 2.3 right. These automatic control algorithms were successfully applied on AVs prototype cars and promoted the development of AVs prototype cars.

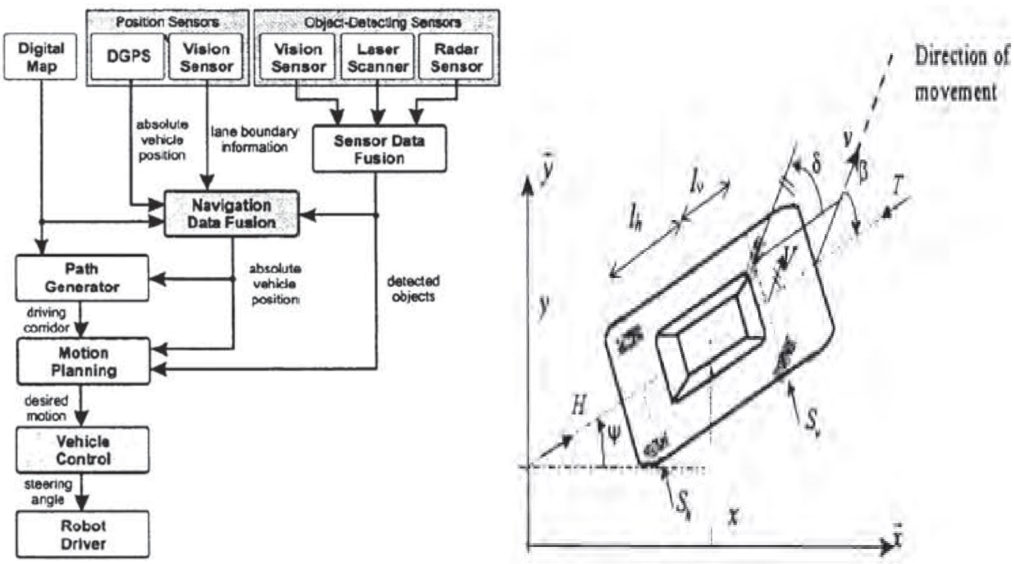

Figure 2.3 Structure of the vehicle guidance system for AVs (left)(Andreas et al., 2000) & the vehicle parameterization (right)(Beji et al., 2003)

When it comes to modelling AVs on road traffic, considering Autonomous Intelligent Cruise Control (AICC) can maintain constant time headway with the leading vehicle, Girault and Yovine (1999) proposed a non-linear controller model for longitudinal behaviour of AVs. Different from the GHR model and IDM model, the constant time headway was used instead of desired speed or distance.

Following this research, Girault (2004) proposed a hybrid controller model for the lateral behaviour of AVs. There are eight different phases in this model, which are accelerating, merge, drop-out, cruise, yield, exit, end and collision. For each phase, the velocity acceleration law and follow acceleration law will be applied with the leading vehicle and side leading vehicle depending on the phase, which could be used to model automated highways.

For the similar reason that adaptive cruise control (ACC) system can maintain desired speed and distance with the leading vehicle, Kesting et al. (2008) used the IDM model to represent AVs. An improvement of this research is that, above operation level, a driving strategy matrix, which describes AVs' driving strategy at different traffic states such as free traffic, congested traffic and bottleneck, has been used for strategic level. Meanwhile, the AVs and truck mixed traffic was modelled in this research.

With the development of vehicle-to-vehicle(V2V) communication and connected autonomous vehicle(CAVs), in the trial (Kato & Tsugawa, 2001), the constant-time-gap control systems and cooperative control system proposed by Rajamani and Shladover (2001) for automated highway systems(AHS). This control model can maintain 6.5m inter-vehicle spacing with the accuracy of $\pm\ 20cm$.

With the development of research on AHS, the Safety Spacing Policy integrated longitudinal and lateral control for AVs proposed (Zhao & Kamel, 2009). This idea is similar to the Gipps model, where the following vehicle should maintain a safe distance to the front vehicle.

Another significant research on CAVs did by Milanés and Shladover (2014). The recorded experimental data of ACC and Cooperative ACC (CACC) have been used to test the speed profile of IDM controller, ACC controller and CACC controller. Their AVs testing results show that ACC controller and CACC controller can model vehicle's speed profile more accurately than IDM controller. Moreover, compared to the ACC controller, the CACC controller can overcome the limitations that the group of consecutive ACC vehicles are unstable.

Le Vine et al. (2016) researched the queue discharge phenomenon of AVs with V2V communications. In this study, Assured-Clear-Distance-Ahead (ACDA) driving strategy was used for AVs, which requires that the following vehicle maintain a minimum longitudinal distance between the leading vehicle. However, from the mathematical point of view, the ACDA strategy is similar to the Gipps model, which requires that $x_n^* \leq x_{n-1}^* - s_{n-1}$.

Recently, some scholars have started to pay attention to mixed traffic flow. Wagner (2016) did a SUMO simulation of a city with AVs, where Krauss (1998) model was used for AVs and HDVs. The simulation showed that AVs could reduce delays between 5 and 80%. However, the difference between AVs and HDVs simply distinguished by the preferred time gap, which may reduce the convincing of this simulation.

Le Vine et al. (2017) studied freeway 'pipeline' capacity to support legal standards. In this research, the Assured Clear Distance Ahead (ACDA) model was used to represent AVs and Wiedemann's model was used to represent HDVs. Nine different scenarios with different maximum capacities are discussed in this research, which showed that the pipeline capacity would change when the acceleration and deceleration of the vehicle change.

Liu et al. (2018) modelled CACC vehicles mixed with HDVs in the traffic stream. The HDVs are modelled with combination of Newell (2002) model, Gipps (1981) model and IDM Treiber et al. (2000). And AVs model as CACC controller (Milanés & Shladover, 2014). Though different penetration rates are considered in this study, simply choosing a minimum value of acceleration from the Newell, Gipps and IDM model may not be sufficient to represent the behaviour of HDVs. Because these vehicle following models were developed from different assumptions, for example, the first constraints of engine torque in Gipps model has been ignored in this combination.

The summary of the vehicle following model, lateral model and lane changing models are shown in Table 2.12

Table 2.12 Summary of vehicle following, lateral and lane changing model for AVs

Reference	Main model	Used parameter
Girault and Yovine (1999)	**Vehicle following model :** $a_n(t) = \frac{v_{n-1}(t) - v_n(t)}{h} + \lambda\frac{x_{n-1}(t) - x_n(t)}{hv_n(t)} - \lambda$	$a_{min} = -0.5g = -4.905\ m/s^2$ $a_{max} = 0.2g = 1.926\ m/s^2$ $h = 0.6s$ $\lambda\ from\ 3\ to\ 17\ m/s^2$
Kato and Tsugawa (2001)	**Vehicle following model:** $u_i = v_p + K_1(v_p - v_i) + K_2(L_i - L_r).$ **Lateral model** $\delta = \arctan\ [2/(3y_1 - x_1\tan\theta_1)/x_1^2]$	$K_1 = M_1 \cdot \lvert L_r - L_i\rvert/\lvert L_r\rvert$ $K_2 = M_2 \cdot \lvert L_r - L_i\rvert/\lvert L_r\rvert$ $M_1 and\ M_2$ are control gains have not been report
Rajamani and Shladover (2001)	**Vehicle following model:** $a_{i\_des} = (1 - C_1)a_{i-1} + C_1a_l - \left(2\xi - C_1\left(\xi + \sqrt{\xi^2 - 1}\right)\right)\omega_n\dot{\varepsilon}_i - \left(\xi + \sqrt{\xi^2 - 1}\right)\omega_nC_1(v_i - v_l) - \omega_n^2\varepsilon_i$	C_1 is the relative weighting ξ control gain of damping coefficient $\omega_n$control gain of bandwidth $C_1, \xi\ and\ \omega_n$ not reported
Girault (2004)	**Vehicle following model** : "follow" law $a_n(t) = \frac{v_{n-1}(t) - v_n(t)}{h} + \lambda\frac{x_{n-1}(t) - x_n(t)}{hv_n(t)} - \lambda$ **Lane Changing model:**:"velocity" law $a_n(t) = \mu(v_{max} - v_n(t))$	$a_{min} = -0.5g = -4.905\ m/s^2$ $a_{max} = 0.2g = 1.926\ m/s^2$ $h = 0.6s$ $\lambda =\ 7\ m/s^2$ $\mu =\ 7m/s^2$
Kesting et al. (2008)	**Vehicle following model: IDM** $a_n(t) = a^{(n)}\left[1 - \left(\frac{v_n(t)}{v_0^{(n)}(t)}\right)^4 - \left(\frac{s_n^*(t)}{s_n(t)}\right)^2\right]$ $s_n^*(t) = s_0^{(n)} + T^nv + \frac{v\Delta v}{2\sqrt{a^{(n)}b^{(n)}}}$ **Lane Changing model: MOBIL** $\tilde{a}_c - a_c + p(\tilde{a}_n - a_n + \tilde{a}_o - a_o) > \Delta a_{th} + \Delta a_{bias}$ $\tilde{a}_n \geq -b_{safe}$ $a_\alpha = \frac{dv_\alpha}{dt} = a(s_\alpha, v_\alpha, \Delta v_\alpha)$ (IDM model)	Car: Truck: $v_0^{(n)} = 120km/h$ $85km/h$ $T^n = 1.5s$ $2.0s$ $a^{(n)} = 1.4\ m/s^2$ $0.7\ m/s^2$ $b^{(n)} = 2\ \ m/s^2$ $2\ \ m/s^2$ $s_0 = 2m$ $2m$ $p = 0{\sim}1$ $\Delta a_{th} = 0.1\ m/s^2$ $\Delta a_{bias} = 0.3m/s^2$
Zhao and Kamel (2009)	**Vehicle following model + Lateral model** $a_{i\_des} = \tau\dot{a}_i + a_i = \frac{-(\lambda\delta_i + x_i - x_{i-1})}{\mathrm{t} - \frac{\gamma}{j_i}v_i}$	δ_i: steering angle $\lambda, \gamma = 0.4$ $\tau = 0.1s$ $t = 0.1s$ $j = -7.32\ m/s^2$
Milanés and Shladover (2014)	**Vehicle following model (a): IDM**	**IDM:** $v_0^{(n)} = 33.3\ m/s$ $T^n = 1.1s$ $a^{(n)} = 1\ m/s^2$ $b^{(n)} = 2\ m/s^2$

	$a_n(t) = a^{(n)}\left[1-\left(\frac{v_n(t)}{v_0^{(n)}(t)}\right)^4 - \left(\frac{s_0 + \quad {}^{n}v + \frac{v\Delta v}{2\sqrt{a^{(n)}b^{(n)}}}}{s_n(t)}\right)^2\right]$ **Vehicle following model (b):ACC controller** $a_k = k_1(x_{k-1} - x_k - t_{hw}v_k) + k_2(v_{k-1} - v_k)$ **Vehicle following model (b):CACC controller** $e_k = x_{k-1} - x_k - t_{hw}v_k$ $v_k = v_{k_{prev}} + k_p e_k + k_d \dot{e}_k$	$s_0 = 0\ m$ **ACC:** t_{hw}:current time-gap $k_1 = 0.23s^{-2}$ $k_2 = 0.07s^{-1}$ **CACC:** e_k : gap error of k-th consecutive vehicle $k_p = 0.45$ $k_d = 0.25$
Le Vine et al. (2016)	**Vehicle following model: ACDA** $x_{min} = v_f^0 * t_{lag.f}^- + \frac{1}{2}\frac{\left(v_f^0\right)^2}{a_f^-} - \frac{1}{2}\frac{(v_l^0)^2}{a_l^-} + x_{veh}$	$a_f^- = 9.2 - 28.3ft/s^2$ $a_l^- = 9.2 - 41.6ft/s^2$ $t_{lag.f}^- = 0.05 - 0.5s$ $x_{veh} = 14.25 - 23.75\ ft$
Wagner (2016)	**Vehicle following model: Karuss (Taylor expansion)** $a = \frac{V^2 - v^2 + 2b(T\Delta v + g - v\tau)}{T(2b\tau + bT + 2v)}$	**AVs:** $\tau = 0.5s$ **HDVs:** $\tau = 1s$ σ = 0.5 noise parameter in SUMO
Le Vine et al. (2017)	**Vehicle following model for HDVs:** Wiedemann **Vehicle following model for AVs:** ACDA	$a_f^- = 5.0$ m$/s^2$(variate on scenarios) $a_l^- = 8.6$ m$/s^2$ (variate on scenarios) $t_{lag,f} = 0.4s$
Liu et al. (2018)	**Vehicle following model for HDVs:** $a = \min\left(a_N, a_{free}, a_{seft}\right)$ $a_n(t) = \frac{(d(t) - d_{jam})/\tau_h - v(t)}{\tau_h/2}$ $(Newell's\ part)$ $a_{free}(t) = a_{max}[1 - \left(\frac{v(t)}{v_{free}}\right)^{\alpha}]$ $(IDM\ part)$ $a_{safe}(t) = \frac{v_{saft}(t + \tau_r) - v(t)}{\tau_r}(Gipps\ part)$ **Lane change model:** **anticipatory lane change (AlC) criteria** $a_{ALC} = \min\left(a_{safe}, a_{comfort}, a_{target}\right)$ **Vehicle following model for AVs:** $a_{sv} = k_1(d - t_{sw}v_{sv} - L) + k_2(v_l - v_{sv})$ **Vehicle following model for CAVs:** $a_{sv} = k_3(v_{free} - v_{sv})$ $v_{sv} = v_{sv}(t - \Delta t) + k_p e_k(t) + k_d \dot{e}_k(t)$ $e_k = d(t - \Delta t) - T v_{sv} - L$	Mean(Std) $\tau_h = 1.4s$(0.2s) $d_{jam} = 1.5m$(0.2m) $a_{max} = 2.0\ m/s^2$(0.5) $v_{free} = 110km/h$(10km/h) $\tau_r = 0.8s$ (0.2s) $b_f = 4.0m/s^2$ $(0.5m/s^2)$ $\hat{b} = 4.0\ m/s^2(0.5m/s^2)$ $\varphi_h(0), \varphi_j(0), \varphi_r(0) = 0.5$ $I_s = 10s$ $k_1 = 0.23s^{-2}$ $k_2 = 0.07s^{-1}$ $k_p = 0.45\ s^{-1}$ $k_3 = 0.4s^{-1}$ $k_d = 0.0125/\Delta t$ L = 4.5m(0.5m) t_{sw}: 31.1% at 2.2 s, 18.5% at 1.6 s; and 50.4% at 1.1 s (Nowakowski et al., 2010)

2.2.4 Summary

To provide a foundation to investigate the characteristics of mixed flow, the literature related to modelling AVs and HDVs has been reviewed in this Section 2.2. Considering parameters and models are two critical aspects to modelling AVs and HDVs, the development and classification of AVs are first reviewed to introduce different levels of automation in Subsection 2.2.1. The level of AVs has been divided into five different levels, where levels 1,2 & 3 automation has already been achieved in practice. For each level of automation, there are sub-systems designed to achieve part of driving functions. Therefore in Subsection 2.2.2, sub-systems of existing AVs and their performance are reviewed and summarised in Table 2.8, which can provide a reference for parameter identification. Then different forms of the vehicle following model and parameters used for AVs and HDVs in the existing literature are reviewed and summarised in Table 2.10, Table 2.11 and Table 2.12. To further identify appropriate parameters and models used in this PhD research, different vehicle following models for AVs and HDVs will be compared and discussed in Section 3.3 in detail.

2.3 Heterogeneous traffic flow of AVs and HDVs

In Section 2.2, existing models to describe the behaviour of AVs and HDVs are reviewed. Ideally, in a pure AVs or HDVs scenario, if all the vehicles following the same behaviour pattern, the traffic flow will be homogeneous. However, in practice, it is not easy to observe homogenous traffic flow because the behaviour of a vehicle is different from others. This behaviour difference will influence the characteristics of traffic flow, such as wave speed (Chiabaut et al., 2010) and capacity (Yang et al., 2015). Notwithstanding many studies on the modelling of traffic flow, it is rather surprising that only a few studies have paid attention to the impact of heterogeneity on traffic flow. With the emergence of AVs, the heterogeneity between AVs and HDVs will be more crucial for traffic managers and local authorities.

In practice, the heterogeneity between AVs and HDVs is complex because it is caused by many factors, such as vehicle types, driver's driving styles, internal fluctuation and level of automation. In some circumstances, it is hard to distinguish these factors from one to another. Therefore, in this section, different heterogeneity will be identified first. After that, existing research on different heterogeneity will be reviewed. Then research gaps will be identified.

2.3.1 Classification of heterogeneity in mixed traffic flow

Vehicle and drivers are two mains components of traffic flow. In general, the heterogeneity on traffic flow consists of vehicle heterogeneity and driver heterogeneity, which can be further divided into internal and cross heterogeneity. From the driving behaviour point of view, all the complex driving behaviours consist of two fundamental processes, sensing and motion. During the sensing process, vehicle's states and surrounding environments, such as the speed and distance of vehicles, will be perceived by humans or sensors. When it comes to the motion, the reaction will be taken based on collected information and specific control strategy. Therefore, different types of heterogeneity are presented in Figure 2.4.

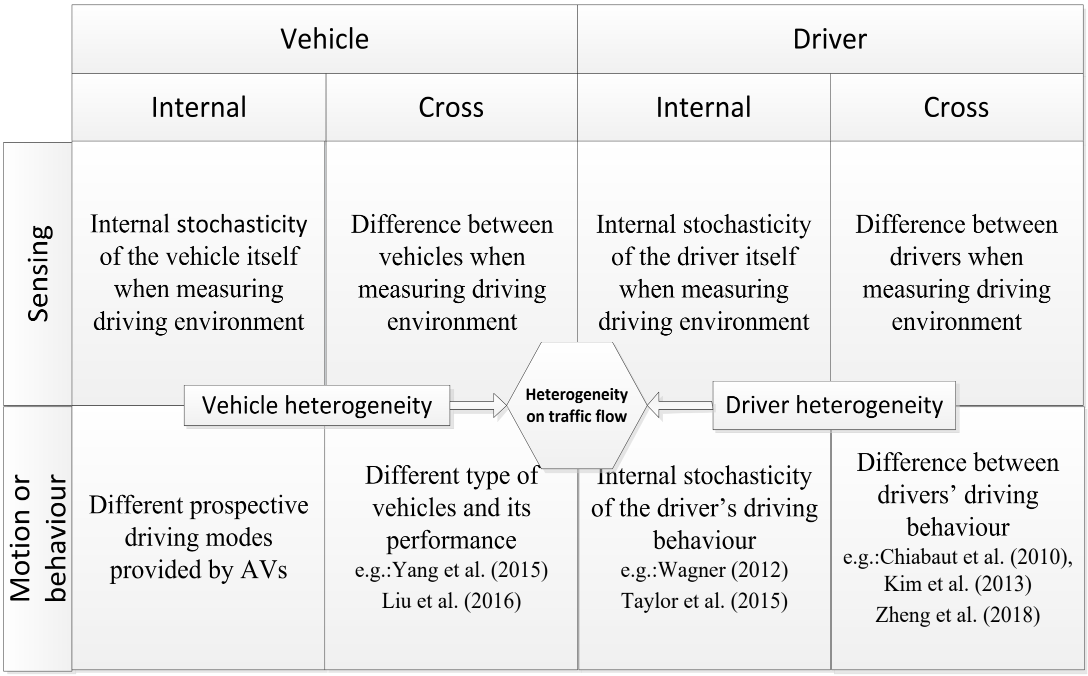

*Part of cited paper discussed in sub-section 2.3.2

Figure 2.4 Various heterogeneity on traffic flow

The internal-driver-sensing heterogeneity is caused by the internal stochasticity of the driver itself when measuring driving environments, for example, inconsistent cognition of fast and safety distance at different psychological states. Similarly, internal-driver-motion heterogeneity is caused by the internal stochasticity of the driver's driving behaviour. For example, in a similar situation, the driver may be aggressive one time and not another time.

Different from internal heterogeneity, cross-driver-sensing and cross-driver-motion heterogeneity are mainly caused by the difference between drivers during sensing and motion.

For example, the sensing of desired speed and distance are different from driver to driver. Similarly, the motion of the driver or the driver's driving style is influenced by the driver's personality. For instance, an aggressive driver might prefer to keep a shorter distance to the leading vehicle.

For the vehicle heterogeneity, internal-sensing, internal-motion, cross-sensing, and cross-motion heterogeneity also exist. However, different from the driver variated from person to person, vehicle heterogeneity is more stable to some extent because the performance of a machine depends on its design, which has less randomness.

For example, for the internal-vehicle-sensing heterogeneity, the internal stochasticity of a vehicle when measuring driving environments mainly depends on the accuracy of sensors under different operating conditions, such as rain or high temperature. Similarly, though the same type of AVs and HDVs will have the same mechanical performance, the internal-vehicle-motion heterogeneity can be caused by different driving modes provide by AVs.

For the cross-vehicle-sensing and cross-vehicle-motion heterogeneity, different types of sensors and vehicles will have different accuracy and mechanical performance, which will directly influence the accuracy of sensors and motion of a vehicle.

In summary, different sources of heterogeneity are identified in Figure 2.4. In the following subsection, existing research on different heterogeneity will be reviewed to explore the impacts of heterogeneity between AVs and HDVs on road capacity and level of service.

2.3.2 Existing models of heterogeneous traffic flow

At an early stage, research of heterogeneity started on cross drivers' heterogeneity. Chiabaut et al. (2010) did significant work of calibrating Newell's car-following model from individual observations. Though Newell's car-following model is a simplified vehicle following model, which assumes that two consecutive vehicles are related by a shift $-\vec{w}(s_x/w, s_x)$, this simplified model can successfully link micro driver heterogeneity to macro traffic flow. For example, the macro shift $-\vec{W_n} = -\vec{w}_1 - \vec{w}_2 \dots - \vec{w}_n$.

Kim et al. (2013) used a different angle to describe cross driver heterogeneity. A rigorous methodology is proposed to calibrate a GM-type car-following model with random coefficients to describe heterogeneity cross drivers. Similarly, Zheng et al. (2018) proposed a stochastic model in Lagrangian coordinates to describe heterogeneity in driving behaviour.

Though cross-driver heterogeneity is modelled in the above studies, using observations to calibrate the model is based on the assumption that the cross-driver heterogeneity is all or at least the primary heterogeneity in these observed data. However, in practice, a human may have some inconsistent behaviour, in other words, intra-driver heterogeneity. This internal heterogeneity of drivers also attracted some scholars. Wagner (2012) used the IDM vehicle following model with an acceleration noise term to analyse the internal stochasticity of the driver itself. Taylor et al. (2015) extended Newell's car-following model to incorporate time-dependent parameters calibrated by the Dynamic Time Warping (DTW) algorithm to present the internal heterogeneity of the driver.

When it comes to vehicle heterogeneity, different from the driver variated from person to person, vehicle heterogeneity is more stable to some extent because the heterogeneity comes from different kinds of vehicles and their engineering performance. For example, the behaviour of private cars and heavy vehicles is different. Yang et al. (2015) proposed a cellular automata model for car-truck heterogeneous, which assume that there are four types of the following combination, car-following-car (CC), car-following-truck, truck-following-car (TC) and truck-following-truck (TT). Similarly, Liu et al. (2016) used a nonlinear IDM vehicle following model to describe car-truck heterogeneous.

When it comes to AVs, Chen et al. (2017) formulated four different spacing levels, which are (1) s_0 for a HDVs following HDVs, (2) $\beta^A s_0$ for lead AV in platoon with HDVs, (3) γs_0 for other AVs in the platoon, (4) $\beta^b s_0$ for first HDVs following AVs platoon. Though no specific value of s_0 is given in this research, these four spacing levels have been used to formulate the baseline capacity C_0. After that a theoretical framework to study how the macroscopic capacity in equilibrium traffic will change with the introduction of AVs.

The behaviour difference of AVs following HDVs, HDVs following HDVs, AVs following AVs and HDVs following AVs also attracted other scholars' attention. Ghiasi et al. (2017)

used the Markov chain model to model headway of HDVs and CAVs in different following circumstances, which can further be used to calculate the capacity. The results of this theoretical research indicated that CAVs might increase highway capacity.

For the CAVs platoon, Gong and Du (2018) proposed one-step Model Predictive Control (MPC) and p-step MPC for the CAVs platoon in mixed traffic flow with AVs. Vehicle trajectory data from NGSIM are used to compare traffic systems with and without platoon and AVs.

From the microsimulation point of view, Liu et al. (2018) modelled CVS in heterogeneous traffic flow. In this research, the HDVs are modelled with a combination of the Newell (2002) model, Gipps (1981) model and IDM Treiber et al. (2000). And AVs model as CACC controller (Milanés and Shladover, 2014). According to the case study, Pipeline capacity is roughly 90% higher at 100% penetration. But insignificant under low and medium penetrations (20%-60%). The summary of existing research on different heterogeneity is shown in Table 2.13.

2.3.3 Summary

To investigate the impacts of heterogeneity between AVs and HDVs on road capacity, the literature related to heterogeneity on traffic flow are reviewed in Section 2.3. Though heterogeneous flow has been studied in these research works, there are two gaps that still deserved to be investigated.

Firstly, as Ghiasi et al. (2017) argued, the actual headway settings of AVs are crucial for the qualitative conclusion. However, most of the existing research has weak support for their parameter. To solve this problem, a sensitivity analysis should be conducted to demonstrate the potential influences of AV behaviour changes on heterogeneity.

Secondly, most of the existing models are simulation-based, which means the theoretical foundation is not solid enough. Solving these gaps can build stronger theoretical support for the impacts of heterogeneity on traffic flow and level of service. Moreover, the theoretical model can be used to analyse AVs dedicated lane, mixed lane or other right-of-way allocation policy, which can help traffic managers and local authorities to better understand and manage mixed traffic flow.

Table 2.13 Summarise of existing research on various heterogeneity

Studies	Discussed heterogeneity	HDVs	AVs	V2V	Field Data	Model	Comments and highlights
Chiabaut et al. (2010)	Cross-driver-motion	Yes	No	No	I-80 NGSIM data	Stochastic Newell's car-following	Proves that the mean wave speed is the harmonic mean of individual wave speed
Wagner (2012)	Internal-driver-motion Cross-driver-motion	Yes	No	No	German freeway A3	IDM with acceleration noise term	Found that preferred headway is not constant, which causing observable randomness in traffic flow
Kim et al. (2013)	Cross-driver-motion	Yes	No	No	NGSIM database	GHR model with random coefficients	Confirmed that random coefficients of the model fluctuated across drivers
Taylor et al. (2015)	Internal-driver-motion	Yes	No	No	NGSIM database	Newell's model + DTW	The cost matrix is applied to model internal fluctuates of headway in DTW
Yang et al. (2015)	Cross-vehicle-motion	Yes	No	No	NGSIM database	Cellular automata model	Traffic congestion can be effectively reduced up to 6.3% by increasing the proportion of TC or CT combination
Liu et al. (2016)	Cross-vehicle-motion	Yes	No	No	NGSIM database	IDM with four different following combinations	Genetic Algorithm(GA) used to calibrate the model
Chen et al. (2017)	Cross-vehicle-motion	Yes	Yes	Yes	-	Numerical Capacity formulation	Analysed capacity functions under different lane policies
Ghiasi et al. (2017)	Cross-vehicle-motion	Yes	Yes	Yes	-	Markov chain	Caution scholars to quantitatively analyse the actual headway settings before drawing any qualitative conclusion
Zheng et al. (2018)	Cross-driver-motion (speed spacing relations)	Yes	No	No	Numerical test +NGSIM	Stochastic dynamical model	Proposed new Stochastic dynamical model in Lagrangian coordinates
Gong and Du (2018)	Cross-vehicle-motion	Yes	Yes	Yes	NGSIM for HDVs	One step MPC+ P step MPC+ Newell's model	Developed a cooperative platoon control for mixed CAVs and HDVs
Liu et al. (2018)	Cross-vehicle-motion	Yes	Yes	Yes	-	Newell+Gipps+IDM ACC+CACC controler	Pipeline capacity is roughly 90% higher at 100% penetration. But insignificant under low and medium penetrations

2.4 Traffic control system and controlling traffic with CAVs in mixed condition

In Section 2.4, to explore whether CAVs can be used as mobile traffic controllers, the literature related to the existing traffic control system and potential to control traffic with CAVs are reviewed in Subsection 2.4.1 and Subsection 2.4.2.

2.4.1 Architecture of Traffic Signal Controller

In the UK, a typical traffic signal controller is connected to a series of sensors to detect vehicles, traffic lights, an electrical supply and communications. A typical architecture of the Traffic Signal Controller (TSC) is shown in Figure 2.5.

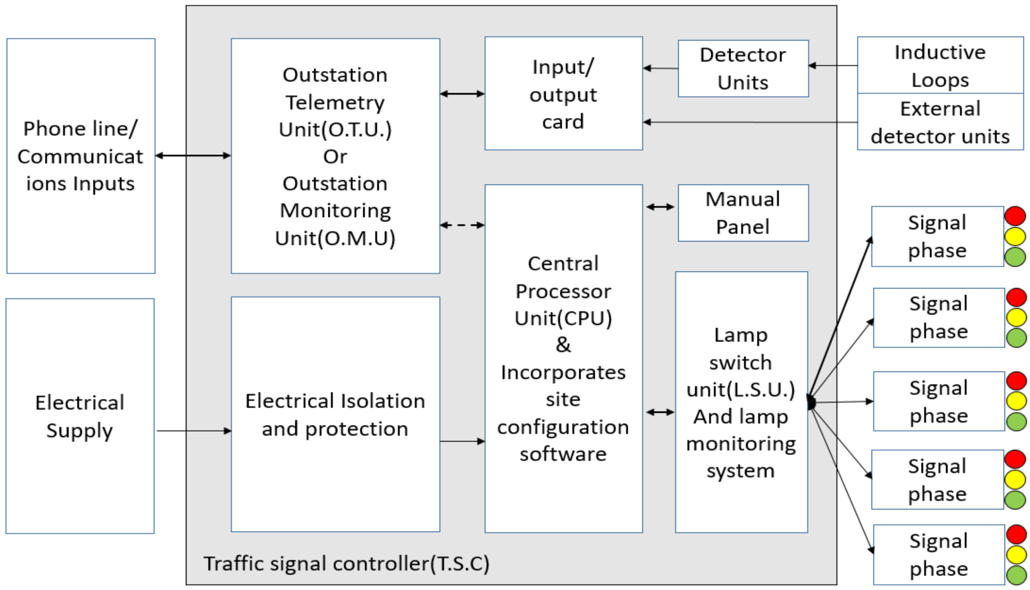

Figure 2.5 Architecture of Traffic Signal Controller (Gollop, 2016)

There are three different control modes for the traffic signal: manual mode, fixed time mode, and vehicle actuated mode. Manual mode is the simplest control mode, which allows engineers or police officers to manually control the TSC in exceptional circumstances, such as during an incident. In the fixed time mode, the signal will run stages in a fixed order. Each stage will have a pre-defined green time and cycle time. The third control mode is Vehicle Actuated (VA) mode, which allows the TSC to respond to a vehicle. When a vehicle is approaching the junction, it will be detected by sensors, and the demand will be transferred to TSC for signal control.

However, all of the above control modes are local-level control. With Outstation Telemetry Unit(OTU) or Outstation Monitoring Unit (OMU), TSC can be connected to other entities, such as another TSC or control centre. This architecture also provides potential channels for V2I and I2V communication. With the development of connected and automated technologies, TSC may receive data from sensors on AVs, which can provide additional information, such as speed, OD and surrounding vehicle's state. In addition, not only providing data, but CAVs might also become mobile traffic controllers to manage traffic flow by responding to instructions from the TSC. Related research works are reviewed in the following subsection.

2.4.2 Controlling traffic with CAVs in mixed condition

With the development of connected and automatic technologies, controlling traffic efficiently with CAVs attracted scholars' attention. Ilgin Guler et al. (2014) investigated using the connected vehicle to improve intersection efficiency for two one-way streets without turning. The optimisation process can be summarised as follows. When the next vehicle arrives at the intersection, all possible combinations of departures will be identified to form set k. After that, for any k, the departure time will be identified. Then the value of the objective will be calculated, and the minimised combination will be selected for discharge. A MATLAB simulated with an assumed parameter was used to evaluate the value of connected vehicle technology. The delay minimisation algorithm is compared with the First-In-First-Out (FIFO) strategy to evaluate the value of connected vehicle technology. The results are shown in Table 2.14, where '+' is existent, and '++' is significant.

Table 2.14 Ilgin Guler et al. (2014) summarised results

	Low demand		High demand	
	Unbalanced	Balanced	Unbalanced	Balanced
Value of platooning	+	++	++	++
Value of flexibility			+	+
Value of autonomous vehicle control	+	+		
Value of information from connected vehicles	++	++	+	+

For the same two one-way streets without turning, Li et al. (2014) pointed out that additional efficiency can be achieved by reducing the loss of green time of the first vehicle. An optimisation algorithm was developed with communication between AVs and signal controllers, which assumes that vehicle trajectories can be fully optimised. Compared to traditional actuated signal control, this algorithm could reduce the average travel time delay by 16.2-36.9%.

Mirheli et al. (2018) proposed a signal-head-free intersection control logic in a fully CAVs environment, which can near-optimal trajectories for CAVs to cross intersections without any movement conflict. However, these CAVs require very accurate sensors and motion cooperation, which may not be achieved until level 5 automation for all the vehicles.

It should be noted that Ilgin Guler et al. (2014), Li et al. (2014) and Mirheli et al. (2018) all assumed that all the vehicles in the system are connected, which mean their control strategies might not be applied in mixed condition.

To take mixed conditions into account, Yang et al. (2016) extended Ilgin Guler et al. (2014) works, which researched isolated signal control with various levels of vehicles, including conventional, connected and automated vehicles. A bi-level optimisation problem was built in this study where the upper level is a penalty function, and the Lower level is the Newell vehicle following model.

Recently, an interesting field experiment was carried by Stern et al. (2018) to use AVs to control stop-and-go waves. A fleet of 21 HDVs and 1 Arizona self-driving capable Cognitive and Autonomous Test (CAT) vehicle was operating in a circle to modelling traffic flow. At the beginning of the experiment, all the vehicles kept the same distance to the leading vehicle. When all vehicles were under human control, with the operation of vehicles, stop-and-go waves appeared dynamically. Then when the AV activated its automation mode, the fluctuation of velocity in the flow successfully decreased, which indicated that it is possible to control traffic by adjusting CAV's behaviour in mixed conditions.

Inspired by Stern et al. (2018)'s works, Kreidieh et al. (2018) investigated dissipating stop-and-go waves with deep reinforcement learning, which can achieve near-complete wave dissipation with 10% autonomous penetration. The frequency and magnitude of formed waves can also be reduced when the penetration rate is 2.5%. Similarly, Giammarino et al. (2020) extended the field test with simulation to investigate the stability of dissipating stop-and-go waves.

All of Stern et al. (2018), Kreidieh et al. (2018), and Giammarino et al. (2020)'s research works indicated a possibility that is using CAVs to manage mixed traffic flow or transport system, which has not been fully studied and will be further investigated in this PhD research.

2.4.3 Summary

In summary, to explore whether CAVs can be used as mobile traffic controllers, the literature related to the existing traffic control system and controlling traffic with CAVs are reviewed in Section 2.4.

According to the architecture of the traffic signal controller in the UK, the outstation telemetry unit provides a channel for communication between CAVs and signals. With V2X communication, TSC can receive data from sensors on AVs. On the opposite, CAVs might also receive more precise instruction from the traffic controller.

Existing literature demonstrated that with an appropriate strategy to adjust CAV's speed in the mixed traffic flow, CAVs could be used to reduce the fluctuation of speed or dissipate stop-and-go waves. These studies indicated that it is possible to use CAVs as a mobile traffic controller. However, most of the existing research only considered using CAV to influence the speed of the following vehicle. Signal timing and routing have not been taken into account. Therefore, in this PhD research, whether CAVs can be used as mobile traffic controllers to influence the routing of HDVs or cooperate with traffic signals will be further investigated.

2.5 Seeking system optimal traffic assignment with HDVs and CAVs

To explore whether system efficiency can be improved with a few CAVs cooperatively changing its routing in the mixed condition, the literature related to seeking system optimal traffic assignment with CAVs and HDVs are reviewed in this section. In Subsection 2.5.1, HDV's routing behaviour and development of user equilibrium are discussed. Then existing research on seeking system optimal equilibrium in practice are reviewed in Subsection 2.5.2, and a summary is given in Subsection 2.5.3.

2.5.1 HDVs' routing behaviour and user equilibrium

Modelling the assignment of traffic on a road network is a fundamental but crucial challenge for scholars and traffic managers. It provides an insight into the operation of the road traffic system, which can help traffic managers to manage the system more effectively. As the assignment of traffic depends on drivers' routing, vehicle routing behaviour has been studied by many researchers. The simplest route choice model assumes that drivers will use the shortest route on the network (Dantzig & Ramser, 1959; Ramming, 2001), which leads to the development of the shortest path problem (signal destination) (Ahuja et al., 1988; Dijkstra, 1959; Faro & Giordano, 2016; Heywood et al., 2019; Nazemi & Omidi, 2013) and vehicle routing problem (multiple destinations) (Laporte, 2009; Mancini, 2017; Schermer et al., 2019; Taniguchi & Shimamoto, 2004).

Both shortest path problem and vehicle routing problem are focused on individual utility. Their impacts on a road traffic system as a whole attracted some researchers attention. As route travel costs are related to the link flow and network topological structure, when drivers do not have knowledge about traffic status, travel costs can only be estimated by the topological structure of the network. In this circumstance, the distribution of vehicles on the network is an all-or-nothing assignment (Dial, 1971; Spiess & Florian, 1989), where only a few routes on the network is used. On the opposite, when drivers have full knowledge about traffic status and travel cost on the network, the distribution of vehicles on the network is a user equilibrium (Beckmann et al., 1956; Wardrop, 1952), where the travel cost on used routes is equal or less than that the travel cost on unused routes.

However, in practice, drivers neither have full nor zero knowledge about traffic status, but instead fall somewhere in between. Therefore, to allow drivers to have different levels of information and knowledge about travel conditions, discrete route choice models have been proposed, such as logit model (Daganzo & Sheffi, 1977; Fisk, 1980), multinomial logit model (Dial, 1971), path size logit (Ben-Akiva & Bierlaire, 1999) and C-logit (Cascetta et al., 2002). Discrete route choice models assume that drivers' knowledge about travel cost is inaccurate and the error term in the latent utility function follows a certain distribution, such as type I extreme value distribution (Ramming, 2001). At the individual level, a driver believes they used the shortest route to the destination. However, at the system level, not all believed shortest routes are really the shortest route, which makes the total travel cost of stochastic user equilibrium achieved by discrete route choice models higher than user equilibrium (Yang, 1999).

Though drivers' knowledge about the travel cost is inaccurate, they can accumulate and improve their knowledge about travel cost and traffic status on the network by day-to-day routing to achieve user equilibrium (Smith, 1979a; Smith, 1984). Yang and Zhang (2009) pointed out that day-to-day traffic dynamics models of routing demonstrated driver's learning and behaviour adjustment process, which provided an insight into the evolution of the traffic pattern over time. Based on the analytical asymptotic convergence properties, they classified adjustment processes into five categories: 1) simplex gravity flow dynamics (Smith, 1983); 2) the Proportional-switch Adjustment Process (PAP) (Huang & Lam, 2002; Peeta & Yang, 2003; Smith, 1984; Smith & Wisten, 1995); 3) the network tatonnement process (Friesz et al., 1994); 4) the projected dynamical system (Nagurney & Zhang, 1997; Zhang & Nagurney, 1996); 5) evolutionary traffic dynamics (Sandholm, 2001; Yang, 2005). They further studied a general class of drivers' dynamic route choice, named rational behaviour adjustment process, and found it is consistent with the assignment process of Smith (1979a), in which the stationarity of link flows is equivalent to user equilibrium.

2.5.2 Seeking system optimal equilibrium in practice

It should be noted that though drivers can achieve UE by accumulating knowledge about the network via day-to-day re-routing without any cooperation, UE might not be the optimal solution from the system point of view. To improve system efficiency, Wardrop (1952) proposed a second principle that total travel costs are minimised. A traffic distribution satisfying Wardrop's second principle is called a system optimal traffic distribution. To achieve this distribution, drivers must be well-informed and co-operate in choosing routes.

However, Prashker and Bekhor (2000) pointed out that the SO traffic distribution is achieved by assuming a non-realistic behavioural assumption. To make the SO traffic distribution more realistic in practice, route guidance systems and corresponding algorithms have been developed to influence HDVs' routing (Hajiahmadi et al., 2013; Lentzakis et al., 2018; Yildirimoglu et al., 2015). The route guidance systems can provide useful information to drivers, such as expected travel times and best routes (Boyce, 1988) and also lead to system-wide near-optimal performance (Lentzakis et al., 2018).

Road pricing is another method to push the system towards the SO traffic distribution. As some drivers might not following the suggestion of route guidance systems, road pricing can be used to adjust generalised travel cost and demand on the network (Brownstone & Small, 2005; Geroliminis & Levinson, 2009; Yang & Bell, 1997; Zheng et al., 2012). In practice, the road pricing system has been adopted in many cities, such as Singapore City (Olszewski & Xie, 2005) and Hong Kong (Dawson & Catling, 1986).

Recently, with the emergence of connected and automatic technology, whether controlling a portion of cooperative AVs can improve system efficiency has begun to attract scholars' attention. Li et al. (2018) investigated how a central agent may bring a mixed traffic system to an equilibrium that both maximises efficiency and stability. Similarly, Chen et al. (2020) investigated to which level the CAVs can push the system to SO in mixed traffic environments. However, the interaction dynamic and signal timing have not been fully studied, which might ignore some circumstances that even when the penetration rate of CAVs is not enough to push the system to the SO point, changing the behaviour of a portion of system users can still achieve system-level improvements, for example, reducing total travel time by push the system approaching SO distribution.

2.5.3 Summary

In summary, modelling the assignment of traffic on the network to provide an insight into the operation of the road traffic system and developing management strategies to improve travel efficiency has been studied by many researchers over the last 60 years. Most of these models and management strategies are designed for HDVs and have to face the fact that human drivers only have partial knowledge about traffic conditions and might not cooperate with other vehicles actively.

The emergence of CAVs opens up opportunities and challenges to achieve the system optimal distribution. As CAVs can share information about traffic status and behave cooperatively in routing, the non-realistic behavioural assumption of the SO distribution becomes realistic in a fully connected and automated environment. However, CAVs cannot replace HDVs in a short time. In the mixed flow of CAVs and HDVs, HDVs might not cooperate with other vehicles actively and make their own routing decisions to maximise personal utility. This raises a crucial question as to whether travel efficiency can still be improved with only a part of the vehicular flow cooperatively changing its routing in the mixed flow conditions, which will be investigated in this PhD research in Chapter 5.

2.6 Cooperation between CAVs and signals in routing and signal timing

To explore whether additional travel efficiency can be achieved by routing and signal timing with information from CAVs, the literature related to cooperation between CAVs and signals in routing and signal timing are reviewed in Section 2.6. The combined routing and signal control problem are reviewed in Subsection 2.6.1 and summarised in Subsection 2.6.2.

2.6.1 Combine routing and signal control problem

As routing and signal timing interact with each other, the opportunities to combine route choice and signal control has been explored by many researchers. Allsop (1974) discussed the possibilities of using traffic control to influence the route choice to achieve different UE. A few years later, Allsop and Charlesworth (1977) developed an iterative procedure where the TRANSYT software was used to calculate signal setting and estimate the relationship between link travel time and traffic flow. With the iterations of routing and signal setting, two different combinations of signal setting and traffic assignment were derived from the same OD matrix, which demonstrated that it is possible to influence route choice by signal setting.

Based on this idea of using traffic control to influence route choice, Smith (1979b) developed a theoretical model for the combined route choice and signal control problem. In this research, a simple network with two routes and a signal-controlled junction was used to demonstrate that the Webster (1958) method of signal setting did not maximise network capacity, because both Webster (1958) and TRANSYT (Robertson, 1969) ignored the influence of signal setting on route-choice. To maximise network capacity, Smith (1979b) proposed the P0 policy where the saturation flow multiplying delay on one route should equal to the saturation flow multiplying delay another route. However, it should be noted that Smith assumed the travel time on both routes is the same. In other words, travel time on the route is not influenced by the flow on the link, which is unreasonable to some extent, because the total travel time on the network may not be minimised when the influence of flow on travel time is ignored.

Later, Smith (1981) extended the theoretical model to demonstrate that if the junction cost-flow function is continuous and the function tends to positive infinity when flow tends to link capacity, the problem of route choice and traffic signal control will have an equilibrium. However, Smith (1981) also pointed out that this condition might not be satisfied in practice and the practical implications for realistic networks need further study. Heydecker (1983) also found if the cost function increases strictly monotonically with the flow on the link, the equilibrium will have a unique solution. At a T-junction or signal-controlled junction, however, this condition is not always satisfied.

Taale and van Zuylen (2001) reviewed research on the combined route choice and signal control problem. They found that the iterative approach (Cantarella et al., 1991; Meneguzzer, 1995; Smith & Ghali, 1990), the global optimisation approach (Chiou, 1999; Maher et al., 2001; Yang & Yagar, 1994) and the game-theoretic approach (Chen, 1998) are three main approaches that have been proposed to solve the combined route choice and signal control problem. Taale and van Zuylen (2001) also pointed out that although most of the research optimised route choice and green time simultaneously, the setting of cycle time and offset has not been fully studied.

To take offset and cycle time into account, Chiou (1999) proposed a bi-level programming approach where the signal setting was controlled by standard cycle time, starts and green time. A mixed search procedure, including the locally optimal search and global search heuristics, was used to found better Karush–Kuhn–Tucker points with reasonable computation effort. The system performance index was the sum of a weighted linear combination of the rate of delay and the number of stops per unit time for all traffic streams. The results of the case study demonstrated that the heuristic mixed search optimisation procedure could achieve better results than the non-optimising computation of mutually consistent signal timings and link flows.

Similarly, Ceylan and Bell (2004) proposed a Genetic Algorithm (GA) approach to solve signal control and stochastic user equilibrium assignment problem on an Allsop and Charlesworth (1977) network. The results showed that the GA approach was efficient and much simpler than the previous heuristic algorithm. To test GA on a real network, Chester's network was used, and the results of the case study showed that compared to a SATURN-based signal optimisation procedure, the GA approach achieved lower total travel time (Teklu et al., 2007). The improvement of total travel time was more significant with a congested network, whereas the improvement was not very clear under relatively mild congestion conditions. Though the GA approach can find an optimised result, as a heuristic algorithm, it cannot guarantee that the calculated result is a globally optimum result.

When it is hard to find a globally optimum result, distributed traffic control strategies for local traffic has been the focus of some researchers. Inspired by the backpressure routing algorithm on communication and power networks, a distributed algorithm to control traffic signals was proposed (Wongpiromsarn et al., 2012), which is better than the Sydney Coordinated Adaptive Traffic System (SCATS) according to the simulation results. Taale et al. (2015) combined signal control and route guidance based on the backpressure routing principles and found that using back-pressure for both signal control and route guidance has promising results, although the difference with optimised local control was small. Zaidi et al. (2016) combined backpressure signal control with adaptive routing. The results demonstrated that multi-commodity and adaptive routing algorithms provide significant improvement compared with a fixed schedule controller and a single-commodity back-pressure controller.

Recently, Smith (2015) extended his early theoretical research and formulated a theoretical dynamic system. Three dynamic relationships, including the relationship between route choice & route costs, route costs & bottleneck delay, and costs-bottleneck delay & green-time have been described mathematically. Then this triple dynamic relationship can be combined into a Lyapunov function for the whole system, which is guaranteed to converge to a convex set of equilibria with suitable variable step lengths.

With the emergence of connected technologies, Chai et al. (2017) investigated traveller's route choice as affected by traffic signal control strategies. A VANET (Vehicular Ad hoc NETwork) was considered for route choice, where travellers have access to the real-time traffic information through V2V/V2I and make route choice decisions at each intersection using hyper-path trees. Six different traffic control strategies and three routing methods were simulated in OmNet++ and SUMO. The results showed that the proposed dynamic routing method could reduce overall travel cost and the proposed adaptive signal control reduces the average delay effectively.

2.6.2 Summary

In summary, elaborate models for the combined route choice and signal control problem have been proposed in the last 45 years. Most of these models are designed for HDVs and have to face the fact that human drivers only have partial knowledge about travel costs and traffic status on the road network. The increasing availability of information through V2V and V2I is accounted by Chai et al (2017). However, the link travel time for the hyper-path trees is estimated by probabilities and the impacts of driver information levels on travel efficiency with different routing and signal timing strategies has not been fully studied in their paper. In Chapter 6, the levels of information about traffic conditions and their improvement with CAVs will be discussed. Then, an ORST control strategy for CAVs will be proposed and compared with four widely-used routing and signal timing strategies under different levels of information.

2.7 Conclusion

In conclusion, based on the research objectives and issue tree presented in Chapter 1, the literature review is organised as Figure 2.1 to summarise existing research and identify research gaps.

According to the overall aim of this PhD research, the literature related to modelling AVs and HDVs is first reviewed in Section 2.2 to provide a foundation to investigate the characteristics of mixed flow. Then corresponding to four specific research objectives, literature related to the heterogeneous flow of AVs and HDVs; traffic control system and controlling traffic with CAVs; seeking system optimal equilibrium with HDVs and CAVs; cooperation between AVs and signals in routing and signal timing have been reviewed separately.

According to RO1, to investigate the impact of heterogeneity on road capacity, the literature related to heterogeneity on traffic flow is reviewed in Section 2.3. Though heterogeneous flow has been studied by scholars, there are two gaps that still deserve to be investigated. Firstly, as Ghiasi et al. (2017) argued, the actual headway settings of AVs are crucial for the qualitative conclusion. However, most of the existing research overlook this aspect. To address this problem, a sensitivity analysis should be conducted to understand the potential influences of AV behaviour changers on heterogeneity. Secondly, most of the existing models are simulation-based, and the theoretical foundation is not well developed. Solving is gaps can build stronger theoretical support for understanding the impact of heterogeneous flow on road capacity, which can help traffic managers and local authorities manage mixed traffic flow more effectively. Therefore theoretical model will be proposed to calculate the maximum capacity of heterogeneous traffic flow in Chapter 3.

According to RO2, to explore whether CAVs can be used as mobile traffic controllers, the literature related to the existing traffic control system and controlling traffic with CAVs are reviewed in Section 2.4. Existing literature demonstrated that with an appropriate strategy to adjust speed, CAVs could be used to reduce the fluctuation of velocity in the mixed flow and dissipating stop-and-go waves, which indicated it is possible to use CAVs as a mobile traffic controller. However, most of the existing research only considered using CAV to influence the speed of the following vehicle. Using CAV to influence HDVs' routing have not been taken into account. Therefore, in this PhD research, whether CAVs can be used as mobile traffic controllers by adjusting the speed on a link will be further investigated in Chapter 4.

According to RO3, To explore whether system efficiency can be improved with a few CAVs cooperatively changing its routing in the mixed condition, the literature related to seeking system optimal traffic assignment with CAVs and HDVs are reviewed in Section 2.5. In summary, the emergence of CAVs opens up opportunities and challenges to achieve the system optimal distribution. As CAVs can share information about traffic status and behave cooperatively in routing, the non-realistic behavioural assumption of the SO distribution for HDVs becomes realistic in a fully connected and automated environment. However, in the mixed flow of CAVs and HDVs, HDVs might not cooperate with other vehicles actively and make their own routing decisions to maximise personal utility. As the interaction between CAVs and HDVs is not fully studied, whether travel efficiency can still be improved with only a part of the vehicular flow cooperatively changing its routing in the mixed condition will be investigated in this PhD research in Chapter 5.

According to RO4, to explore whether additional travel efficiency can be achieved by routing and signal timing with information from CAVs, the literature related to cooperation between CAVs and signals in routing and signal timing are reviewed. In summary, elaborate models for the combined route choice and signal control problem have been proposed in the last 45 years. However, most of these models are designed for HDVs and have to face the fact that human drivers only have partial knowledge about travel costs and traffic status on the road network. The increasing availability of information through V2V and V2I start to attract scholars' attention, such as Chai et al (2017). However, in Chai et al (2017)'s study the link travel time for the hyper-path trees is estimated by probabilities, and the impacts of driver information levels on travel efficiency with different routing and signal timing strategies have not been fully studied. Therefore, in Chapter 6, the levels of information about traffic conditions and their improvement with CAVs will be discussed. Then, an ORST control strategy for CAVs will be proposed and compared with existing routing and signal timing strategies under different levels of information.

To sum up, the overall aim of this PhD research is to analyse the mixed flows of AVs and HDVs to help traffic managers and Local Authorities (LAs) to improve the performance of urban traffic systems by right-of-way re-allocation and dynamic traffic management. To achieve this aim, four specific research objective has been proposed, and their relevant literature has been reviewed in Chapter 2 to summarise existing research and identify research gaps. The rest of PhD thesis will be organised as Figure 2.6. In the next chapter, the impacts of heterogeneity between AVs and HDVs on road capacity will be investigated.

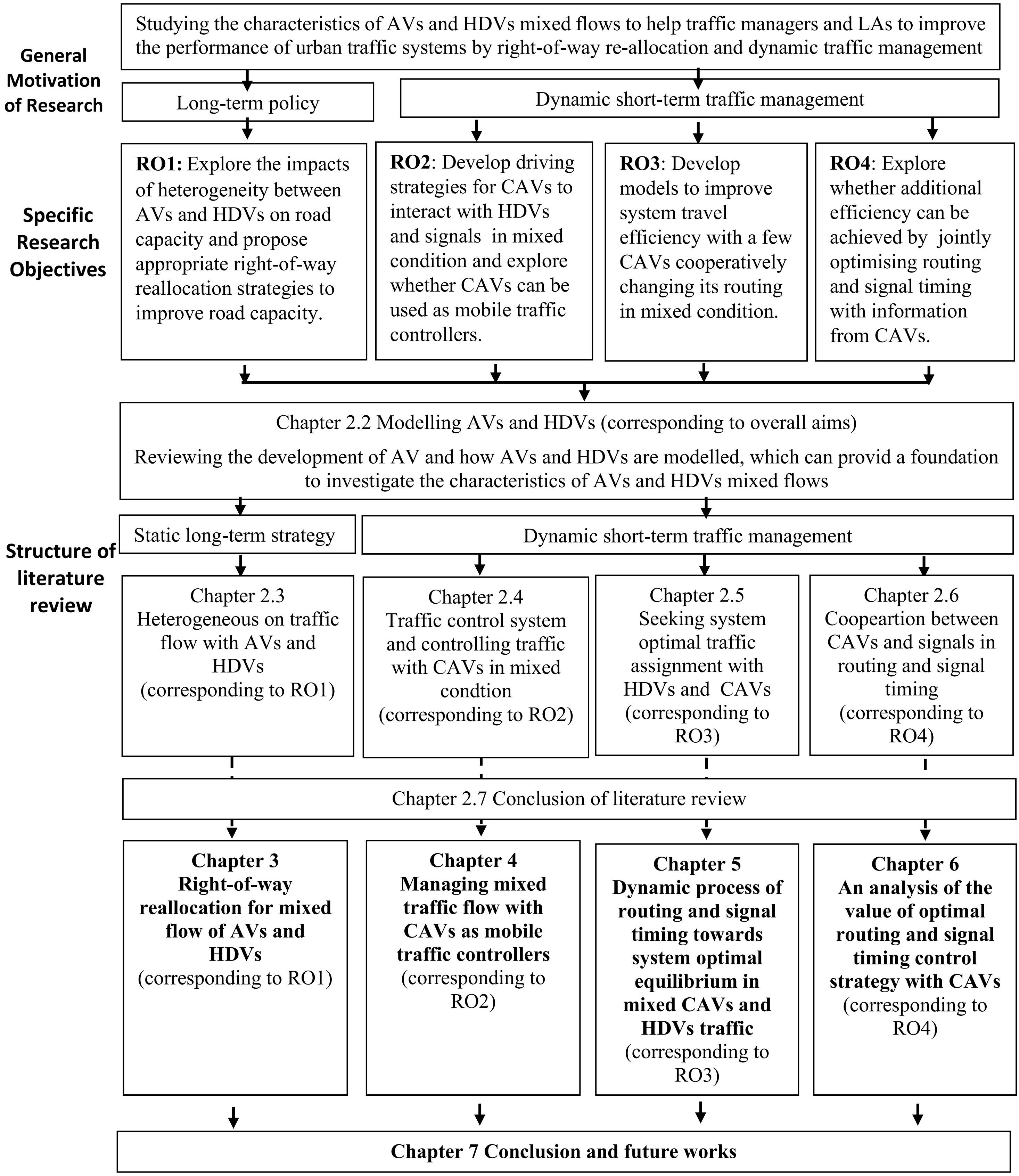

Figure 2.6 Structure of rest of thesis

Chapter 3 Right-of-way reallocation for mixed flow of AVs and HDVs

In this chapter (adapted from J1 listed in Section 1.4 and the author statement attached in Appendix 3), the impact of heterogeneity between AVs and HDVs on road capacity is investigated, which can help traffic managers and local authorities to understand the nonlinear changes in road capacity with increasing AV penetration rate and to efficiently reallocate the Right-of-Way (RoW) for the mixed flow of AVs and HDVs.

3.1 Background and research context

Efficiently reallocating the RoW for AVs and HDVs is a crucial challenges for traffic managers and local authorities in mixed traffic conditions. Ideally, at high AV penetration rates or an all-AV scenario, road capacity will significantly increase if AVs can keep a shorter headway to the leading vehicle with the help of lidar or sensors. Most of the existing research has focused on the impact of these 'ideal' situations on road capacity (Khattak et al., 2020; Liu et al., 2018; Rajamani & Shladover, 2001; Wagner, 2016). However, the change of road capacity in mixed flow is not significant at low AV penetration rates (Amirgholy et al., 2020; Chang & Lai, 1997; Liu et al., 2018; Ye & Yamamoto, 2018b) and the network delay could increase due to the heterogeneity between AVs and HDVs (Department for Transport, 2016).

This nonlinear capacity change caused by heterogeneity provides an opportunity to further improve road capacity with appropriate RoW reallocation strategies, because conflicts between AVs and HDVs can be relieved with explicit RoW. For example, Ghiasi et al. (2017) used the Markov chain to model mixed HDVs and CAVs flow and found that lane management (dedicated lane for CAVs) can improve traffic throughput with certain CAV technologies. Based on the average speed and spacing characteristics of AVs, Chen et al. (2017) proposed a theoretical model and demonstrated that compared with sticking to dedicated lanes for AVs and HDVs, mixed policies could achieve higher capacity on a two-lane highway. Recently, Ye and Yamamoto (2018a) used a cellular automaton model to model CAVs and found that the benefit of CAV dedicated lanes can only be obtained with medium density vehicular flow. Mohajerpoor and Ramezani (2019) proposed an analytical delay model of mixed CAV and HDV flow and pointed out that lane allocation management strategies, such as assigning a dedicated lane for AVs, can reduce delay. Similarly, Amirgholy et al. (2020) found that experienced delay can be reduced with optimal lane management strategies and dynamically controlling the platoon size of CAVs.

Though it is possible to increase road capacity with RoW reallocation strategies, the critical points of capacity increase under different demand and AV penetration rates have not been fully studied, because the nature of RoW reallocation and capacity change with AV penetration rate are complex from four perspectives.

Firstly, the road utilisation rates might decrease when a lane is allocated to AVs or HDVs. Although the dedicated lane is exclusive to one vehicle type to reduce conflicts, which leads to a theoretical capacity increase of that lane, the practical service level might still decrease due to the imbalance between supply and demand. Therefore, the trade-off between avoiding conflicts with dedicated lanes and increasing road utilisation rates with mixed-use lanes should be considered.

Secondly, there is no consensus among scholars regarding the impact of mixed AVs and HDVs flow on road capacity. Some studies found that in ideal situations, road capacity increases at high AV penetration rates. For example, Rajamani and Shladover (2001) demonstrated that the smallest gap that can be used by the upper controller of constant-time-gap autonomous control systems is 1s, which means the theoretical maximum traffic flow of approximately 3000 vehicle/h per lane can be achieved in an all AV scenario. Wagner (2016) believed that a 0.5s time gap could be safely achieved with the improvement of AV technologies. Based on a SUMO simulation study, network delays can be reduced with this 0.5s time gap. However, compared with the 1.4s time gap for human drivers on average, 0.5s time gap was only observed during aggressive driving in practice. Recently, Liu et al. (2018) modelled CAVs in mixed traffic flow and pointed out that the pipeline capacity increases by 90% with an all-AV scenario compared with the all-HDV scenario. Zheng et al. (2020) found mean spacing variance and mean speed variance can be reduced with the increase of AV penetration rate, which means less congestion duration and higher traffic throughput.

However, road capacity is not always expected to increase with AV penetration rate. Le Vine et al. (2015) demonstrated that there is a tension between the intersection capacity and the in-vehicle experience of drivers. When AVs are operated with a lower acceleration speed to improve the occupants' in-vehicle experience for reading and working, road capacity may decrease by 14%. According to a VISSIM based simulation by the Department for Transport (2016), the average delay slightly increases at low AV penetration rates compared with a zero AV penetration rate. Amirgholy et al. (2020) also found that low penetration rates of AVs and CAVs have no significant impacts on the performance of the traffic system. Considering there is not a consensus about the impacts of mixed flow on road capacity. It is worthwhile to further investigate the relationship between road capacity and AV penetration rate.

Thirdly, the spatial and temporal distribution of traffic demand is varied. For example, peak times demand is higher than off-peak demand. This variated demand increases the complexity of the RoW reallocation problem because the imbalance between supply and demand is amplified with the fluctuating demand. Ideally, this problem can be addressed by adopting different RoW reallocation strategies at different times and places. However, from a practical perspective, changing RoW frequently might increase operation costs and confuse drivers. Therefore, the critical points of RoW reallocation should be identified to minimise frequent reallocation.

Last but not least, AV behaviour might be changed by the development of AV technology, such as increased sensor accuracy (Ouster, 2018; Russell et al., 1997), or users' personal settings, such as the setting up of personalised time intervals on the AV (Eichelberger & McCartt, 2014). This means the degree of heterogeneity between AVs and HDVs might also vary, which can further strengthen or weaken the impacts of RoW reallocation. Hence, to investigate the potential influences of AV behaviour changes on RoW reallocation, a sensitivity analysis should be conducted.

Against this background, to address RO1, the impacts of heterogeneity between AVs and HDVs on road capacity is investigated in this chapter. Then appropriate right-of-way reallocation strategies are proposed to improve road capacity. More specific objectives based on RO1 are as follows:

1) To investigate the impacts of AV and HDV mixed flow conditions on road capacity with both theoretical and numerical analysis.
2) To investigate whether road capacity can be improved with different RoW reallocation strategies.
3) To identify critical points of capacity increase with proper RoW reallocation strategies under different traffic demand and AV penetration rates, which can help traffic managers and local authorities better understand and manage mixed traffic flow in a dynamic manner.
4) To analyse the impacts of AV behaviour changes on RoW reallocation through appropriate sensitivity analysis.

3.2 Theoretical capacity model for heterogeneous traffic flow

To investigate the impact of AVs and HDVs mixed flows on road capacity, a theoretical model based on the relative safety constraint has been proposed in this section to calculate the maximum capacity of the heterogeneous traffic flow. Firstly, the fundamental equations and assumptions are introduced in Section 3.2.1. Meanwhile, notations used in the theoretical capacity model are listed in Table 3.1. Then headway and safety constraints of the theoretical model are discussed in Section 3.2.2. Finally, the theoretical model is presented in Section 3.2.3.

3.2.1 Fundamental equations of flow and assumptions

When the flow is saturated, the demand is equal to or slightly larger than the supply. Therefore, the observed flow can be used to evaluate road capacity. Based on the fundamental definition of traffic flow, with a given observation time period T, the flow q can be calculated by the total number of vehicles observed at a point on the road using Equation (3.1).

$$q = \frac{N}{T} \tag{3.1}$$

The observation time period T should also satisfy Equation (3.2), which demonstrates that observation time period T is equal to the sum of vehicles' gross time headway t_i.

$$T = \sum_{i=1}^{N} t_i \tag{3.2}$$

As the average of gross time headway of flow can be calculated by Equation (3.3), Equation (3.1) can be rewritten as Equation (3.4), which indicates that flow q is an inverse of the average headway of flow.

$$\bar{t} = \frac{T}{N} = \frac{\sum_{i=1}^{N} t_i}{\sum_{i=1}^{N} 1} \tag{3.3}$$

$$q = \frac{N}{T} = \frac{1}{\frac{T}{N}} = \frac{1}{\frac{\sum_{i=1}^{N} t_i}{N}} = \frac{1}{\bar{t}} \tag{3.4}$$

Table 3.1 Notations for theoretical capacity model

Notation	Unites	Definitions
i	n/a	index of individual vehicle
j	n/a	index of a set of vehicles with the same behaviour, which is mutually exclusive to other sets
N	veh	total numbers of observed vehicles
n	n/a	total numbers of mutually exclusive vehicle sets
T	h	the time period for observation
q	veh/h	observed flow
t_i	s	gross time headway of vehicle i
$\bar{t}$	s	average of gross time headway
w_j	n/a	weight of j set of vehicles ($\sum_{j=1}^{n} w_j = 1$)
$t^{(j)}$	s	gross time headway of j set of vehicles
$t_i^{(j)}$	s	gross time headway of vehicle i in j set of vehicles
v_i	m/s	speed of vehicle i
l_{lead}	m	length of the leading vehicle
l_{follow}	m	length of the following vehicle
v_{lead}	m/s	speed of the leading vehicle
v_{follow}	m/s	speed of the following vehicle
b_{lead}	m/s^2	deceleration speed of the leading vehicle
b_{follow}	m/s^2	deceleration speed of the following vehicle
$l_{i,headway}^{(j)}$	m	gross distance headway of vehicle i in j set of vehicles
$l_{safety\ gap}^{(j)}$	m	safety gap for j set of vehicles
$l_{buffer}^{(j)}$	m	distance vehicle keep to the tail of leading vehicle when stopped in j set of vehicles
$l_{error}^{(j)}$	m	maximum error of distance measurement in j set of vehicles (by drivers or sensors including the measurement precision margin)
$\tau^{(j)}$	s	reaction time of j set of vehicles (by drivers or controllers)

Firstly, assuming the observed flow is a homogenous flow. It means that the behaviour of all the vehicles in the system is the same, which leads to the average gross time headway $\bar{t}$ equals to the individual gross time headway t_i as Equation (3.5).

$$\bar{t} = t_i \tag{3.5}$$

Based on Equation (3.5), Equation (3.4) can be further rewritten as Equation (3.6), which demonstrates that the maximum capacity of homogeneous flow is related to the individual gross time headway t_i.

$$q = \frac{1}{\bar{t}} = \frac{1}{t_i} \tag{3.6}$$

However, the assumption of homogenous flow is a critical assumption, which is rarely observed in practice. Caused by many factors, such as drivers' personality (Chiabaut et al., 2010; Kim et al., 2013), control algorithms (Liu et al., 2018; Yang et al., 2015), vehicle physical performance (Yang et al., 2015) and imprecise control (Wagner, 2012), behaviours of vehicles are different, which means that the flow is heterogeneous.

Therefore, the first assumption can be extended to the second assumption that observed flow is a heterogeneous flow with n sets of mutually exclusive vehicle behaviours. These n sets of mutually exclusive vehicle behaviours will have n sets of mutually exclusive gross time headway $t^{(j)}$. With this assumption, the relationship between $\bar{t}$ and t_i is formulated by Equation (3.7).

$$\bar{t} = \frac{T}{N} = \frac{\sum_{i=1}^{N} t_i}{N} = w_1 t^{(1)} + \cdots w_n t^{(n)} \tag{3.7}$$

Hence, Equation (3.4) can be rewritten as Equation (3.8).

$$q = \frac{1}{\bar{t}} = \frac{1}{\sum_{j=1}^{n} w_j t^{(j)}} \tag{3.8}$$

It should be noted that when n sets of mutually exclusive vehicles behaviours are the same, i.e. $t^{(1)} = t^{(2)} \ldots = t^{(n)}$ and the flow is equal to a homogenous flow. Equation (3.8) is mathematically equivalent to Equation (3.6), because the weighted average headway is equal to individual gross time headway t_i. Moreover, when n is equal to N, i.e. all the vehicles in the system behave differently, Equation (3.8) can represent the fully heterogeneous flow. These two situations can demonstrate that Equation (3.8) with the second assumption can successfully model both homogeneous and fully heterogeneous flow. Meanwhile, the key factor of capacity calculation has been transferred to the time headway of the j set of vehicles ($t^{(j)}$) and the weight w_j .

3.2.2 Headway and safety constraint

As discussed in Section 3.2.1, the key factor of capacity calculation has been transferred to gross time headway a set of vehicles ($t^{(j)}$) and their weight w_j. As the weight w_j is determined by the penetration rate of j set of vehicles, the calculation of $t^{(j)}$ is focused in this section.

Based on the fundamental kinetics equations, $t^{(j)}$ can be formulated by Equation (3.9).

$$t^{(j)} = l^{(j)}_{i,headway}/v_i \tag{3.9}$$

For a saturated flow, v_i is determined by the speed, and the gross distance headway $l^{(j)}_{i,headway}$ can be formulated by Equation (3.10)

$$l^{(j)}_{i,headway} = l^{(j)}_{safety\,gap} + l^{(j)}_{buffer} + l^{(j)}_{error} + l_{lead} \tag{3.10}$$

Where $l^{(j)}_{i,headway}$ is the gross distance from the head of following vehicle i to the head of leading vehicle $i-1$; $l^{(j)}_{safety\_gap}$ is the braking distance of the j set of the following vehicle. $l^{(j)}_{buffer}$ is the distance driver would keep to the leading vehicle after braking as the safety buffer distance, which can be observed at the stop line; $l^{(j)}_{error}$ is the error of position measurement, which is caused by drivers' preception or sensors' accuracy; l_{lead} is the length of the leading vehicle.

As shown in Figure 3.1, when the following vehicle is approaching a stopped vehicle, to avoid a collision, the following vehicle should start braking at the gross distance $l^{(j)}_{i,headway}$, which is consisted of the braking distance $l^{(j)}_{safety\_gap}$, buffer distance $l^{(j)}_{buffer}$, potential localisation error $l^{(j)}_{error}$ and the length of the leading vehicle l_{lead}.

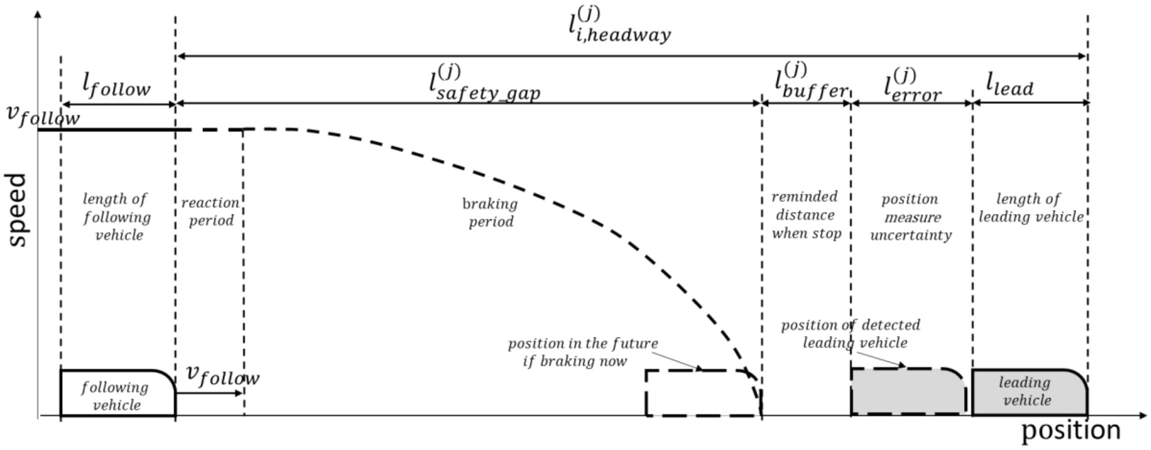

Figure 3.1 Safety constraint when the following vehicle approaching a stopped vehicle

When the leading vehicle is moving, relative safety constraint or its relaxation and derivation have been used in most of the vehicle following models, such as the Gipps (1986b) and Krauss (1998) for HDVs and ACC model (Milanés & Shladover, 2014) and ACDA model (Le Vine et al., 2016) for AVs.

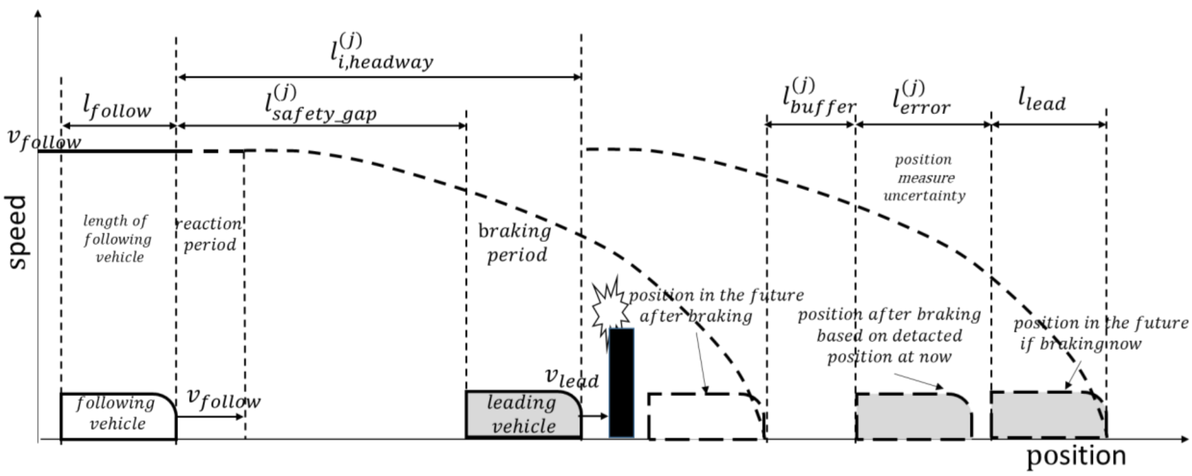

Figure 3.2 Relative safety constraint

As shown in Figure 3.2, to keep a relative safe distance and avoid rear-end collision, the braking distance of the following vehicle should not exceed the tail of the leading vehicle after braking. According to the kinetic equations, the gross distance headway $l_{i,headway}^{(j)}$ should satisfy Equation (3.11).

$$l_{i,headway}^{(j)} + \frac{v_{lead}^2}{2b_{lead}} \geq l_{buffer}^{(j)} + l_{error}^{(j)} + l_{lead} + \frac{v_{follow}^2}{2b_{follow}} + v_{follow}\tau^{(j)} \quad (3.11)$$

In the boundary condition, to maximise road capacity, the gross distance headway $l_{i,headway}^{(j)}$ can be formulated by Equation (3.12)

$$l_{i,headway}^{(j)} = \frac{v_{follow}^2}{2b_{follow}} + v_{follow}\tau^{(j)} - \frac{v_{lead}^2}{2b_{lead}} + l_{buffer}^{(j)} + l_{error}^{(j)} + l_{lead} \quad (3.12)$$

3.2.3 Maximum theoretical capacity of heterogeneous flow

Based on the equations and assumptions discussed in Section 3.2.1 and Section 3.2.2, the theoretical model for both homogeneous and fully heterogeneous flow can be formulated to calculate the maximum theoretical capacity of heterogeneous flow as Equation (3.13).

$$q = \frac{1}{\bar{t}} = \frac{1}{\sum_{j=1}^{n} w_j \frac{l_{i,headway}^{(j)}}{v_j}} \quad (3.13)$$

As discussed in Section 3.2.2, v_j is determined by the speed limit or expected speed in a road section. The gross distance headway $l_{i,headway}^{(j)}$ is formulated by Equation (3.12) based on relative safety constrain. Therefore, Equation (3.13) can be further rewritten into Equation (3.14).

$$q = \frac{1}{\sum_{j=1}^{n} w_j \frac{\frac{v_{follow}^2}{2b_{lead}} + v_{follow}\tau^{(j)} - \frac{v_{lead}^2}{2b_{follow}} + l_{buff}^{(j)} + l_{error}^{(j)} + l_{lead}}{v_j}} \quad (3.14)$$

Considering in practice, it is not easy to know the length of the leading vehicle l_{lead}, the reference point to calculate road capacity can be shifted from the head of the vehicle to the rear bumper of the vehicle. Then, Equation (3.14) can be further rewritten into Equation (3.15)

$$q = \frac{1}{\sum_{j=1}^{n} w_j \frac{\frac{v_{follow}^2}{2b_{lead}} + v_{follow}\tau^{(j)} - \frac{v_{lead}^2}{2b_{follow}} + l_{buff}^{(j)} + l_{error}^{(j)} + l_{follow}}{v_j}} \quad (3.15)$$

In summary, the theoretical model to calculate the maximum theoretical capacity of heterogeneous flow has been proposed and shown in Equation (3.15). In order to evaluate the proposed model, in Section 3.3, a numerical analysis with the literature-based parameters will be adopted, and the results of the proposed theoretical model will be compared with the results reported in the existing literature.

3.3 Numerical analysis of mixed flow

To evaluate the proposed theoretical model, a numerical analysis is adopted in this section. Based on the existing literature, key parameters are identified in Section 3.3.1. Then the proposed model is compared with the existing vehicle following models in Section 3.3.2, which indicates that the proposed model can successfully formulate the upper boundary of theoretical capacity. Finally, in Section 3.3.3, the results of the theoretical capacity of mixed flow and its mathematical property are discussed, which provide theoretical support to improve road capacity with RoW reallocation strategies.

3.3.1 Parameters for AVs and HDVs

To adopt vehicle following models in practice, parameters should be calibrated based on traffic conditions. However, a common challenge in this area is that, limited by traffic volume and penetration rate, it is hard to find suitable mixed AVs and HDVs flow for calibration. Therefore, to identify the reasonable value of parameters for AVs and HDVs, parameters used in the existing literature (reviewed in Section 2.2) have been taken as a reference and the key parameters used in the numerical analysis and simulation are shown in Table 3.2.

Table 3.2 Parameters for the numerical analysis and SUMO simulation

Theoretical model for HDVs	Theoretical model for AVs	Krauss model for HDVs simulation	ACC controller for AVs simulation
$l_{lead} = 4.5m$	$l_{lead} = 4.5m$	$a_{max} = 2.6\ m/s^2$	$a_{max} = 2.6\ m/s^2$
$l_{follow} = 4.5m$	$l_{follow} = 4.5m$	$b = 4.0\ m/s^2$	$b = 5.0\ m/s^2$
$l_{buff} = 0.9m$	$l_{buff} = 0.9m$	$\tau = 1.5\ s$	$t_{sw} = 0.8\ s$
$l_{error} = 0.1m$	$l_{error} = 0.1m$	$\sigma = 0.5$	$\sigma = 0$
$b_{follow} = 4.0\ m/s^2$	$b_{follow} = 4.0\ m/s^2$		$k_1 = 0.23s^{-2}$
$b_{lead} = 4.0\ m/s^2$	$b_{lead} = 4.0\ m/s^2$		$k_2 = 0.07s^{-1}$
$\tau = 1.5$	$\tau = 0.8$		

3.3.2 Comparison between theoretical capacity and capacity reported in the literature

In Section 3.2, a theoretical model has been proposed to calculate the maximum capacity of heterogeneous flow. Although the proposed theoretical model can be used to model fully heterogeneous flow with n sets of mutually exclusive vehicle behaviours, for concision and concentration, only heterogeneity between AVs and HDVs are focused in this numerical analysis.

Based on the key parameters identified in Table 3.2, the maximum theoretical capacity of all-AV flows and all HDVs flows under different speeds are calculated by Equation (3.15) and shown as the orange and blue lines in Figure 3.3. Meanwhile, results of capacity reported in the existing literature at different speeds are shown as points in Figure 3.3.

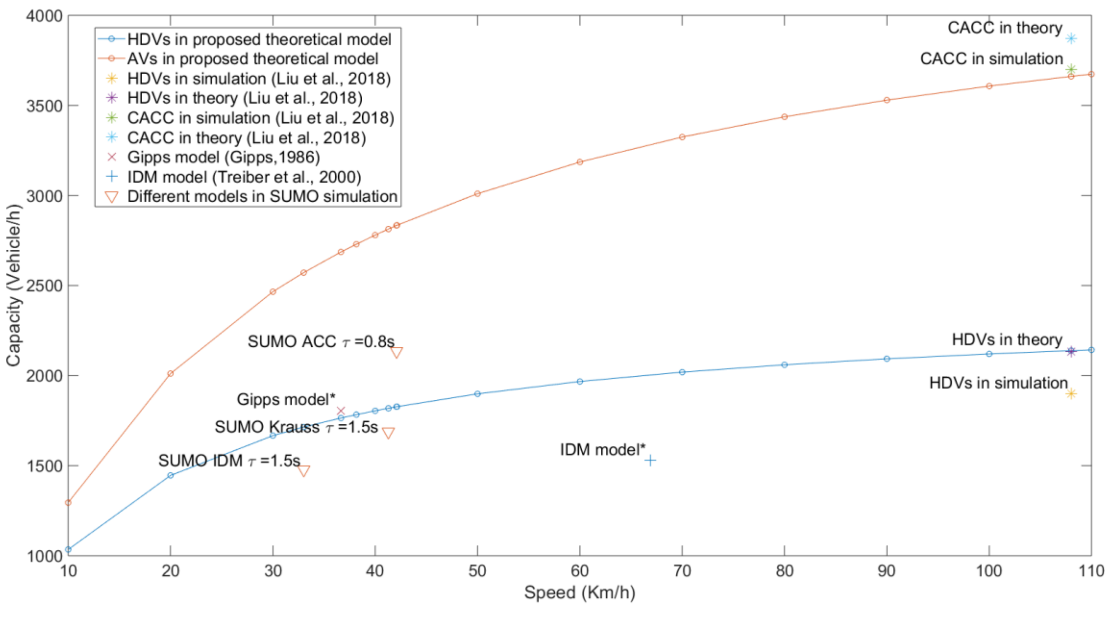

'' means that the point is an estimated value from the figures in the literature.*

Figure 3.3 Comparison between theoretical capacity and capacity reported in the literature

It can be observed from Figure 3.3 that the results calculated by the proposed theoretical model are slightly larger than the results reported in the existing literature. This is caused by the factor that though relative safety constrain has been adopted in many vehicle following models, to avoid driver driving on a boundary condition where drivers might need to brake frequently when external disturbance or noises exist, these models relaxed or derivated the relative safety strategy to some extent.

For example, in Gipps (1981) model shown as Equation (3.16), the driver of vehicle n must ensure that $x_{n-1}^* - s_{n-1} \geq x_n^*$, which is the relative safety before relaxation.

$$x_{n-1}(t) - \frac{v_{n-1}(t)^2}{2b_{n-1}} - s_{n-1} \geq x_n(t) + \frac{\big(v_n(t) + v_n(t+\tau)\big) * \tau}{2} - \frac{v_n(t+\tau)^2}{2b_n} \tag{3.16}$$

However, Gipps (1981) proposed that without the introduction of the parameter θ, a single vehicle approaching a stationary object or stop line would travel at its desired speed until it had to commence maximum braking. Therefore, a relaxed reaction time $\tau + \theta$ was introduced to formuate Equation (3.17) in the Gipps model.

$$x_{n-1}(t) - \frac{v_{n-1}(t)^2}{2b_{n-1}} - s_{n-1} \geq x_n(t) + \frac{\big(v_n(t) + v_n(t+\tau)\big) * \tau}{2} + v_n(t+\tau)\theta - \frac{v_n(t+\tau)^2}{2b_n} \tag{3.17}$$

where θ was set to $\tau/2$ and the estimated $\hat{b}$ was used to replace b_{n-1} because the deceleration speed of the leading vehicle can not be known directly. Combining these with the quadratic formula, the final safety constraint in Gipps model can be solved as Equation (3.18).

$$v_n(t+\tau) \leq \; b_n\tau + \sqrt{b_n^2\tau^2 - b_n(2[x_{n-1}(t) - s_{n-1} - x_n(t)]) - v_n(t) * \tau - \frac{v_{n-1}(t)^2}{2\hat{b}}} \tag{3.18}$$

Similarly, in the Krauss (1998) model, un-relaxed relative safety constraints formulated as Equation (3.19). This equation has been derivated by Taylor series expansion, where higher-order terms have been removed to get Equation (3.20). Meanwhile, the desired gap was chosen to be $g_{der} = \tau v$, where τ is the reaction time of drivers. Krauss proposed that the true reaction time should smaller than or equal to the reaction time that each driver assumes in the model to ensure safety.

$$d(v_f) + v_f\tau \leq \mathrm{d}(v_l) + x_l - x_f - l \tag{3.19}$$

$$d'(\bar{v})v_f + v_f\tau \leq d'(\bar{v})v_l + x_l - x_f - l \tag{3.20}$$

In the IDM model, a vehicle will adjust its acceleration if the speed or distance deviates from the desired value as Equation (3.21). The desired gap $s_n^*(t)$ is calculated by Equation (3.22), which is a derivated safey constraint. This desired gap $s_n^*(t)$ is relevant to $t_{sth}v$, where t_{sth} is defined as safe time headway. As discussed in the Krauss model, the safe time headway should not be smaller than the true reaction time. Otherwise, the safe time headway is unsafe. From another perspective, t_{sth} is a form of relaxed reaction time τ.

$$a_n(t) = a^{(n)}\left[1 - \left(\frac{v_n(t)}{v_0^{(n)}(t)}\right)^4 - \left(\frac{s_n^*(t)}{s_n(t)}\right)^2\right] \tag{3.21}$$

$$s_n^*(t) = s_0^{(n)} + t_{sth}v + \frac{v\Delta v}{2\sqrt{a^{(n)}b^{(n)}}} \tag{3.22}$$

In the ACC controller, which is developed from automatic control algorithms, the current time gap setting t_{hw} has been used, which means that the desired time gap can be specified by the user. According to Equation (3.23), the desired gap specified by users is equal to $t_{hw}v_k$, which is similar to the desired gap in the Krauss model $g_{der} = \tau v$. The similarity of these two equations of desired gap and the inherence of t_{hw} and τ demonstrate that the time headway parameter is relaxation or derivation of the reaction time parameter.

$$a_k = k_1\,(x_{k-1} - x_k - t_{hw}v_k) + k_2(v_{k-1} - v_k) \tag{3.23}$$

Though the inherent relationship of safety constraints indicates that the results calculated by the proposed theoretical model should be larger than results reported in the existing literature, there are three points which are Gipps model, CACC in theory and CACC in simulation larger than the proposed theoretical model. With further investigation, these are caused by the parameter difference and the object difference.

In the Gipps model, the safety constraint has been relaxed by set θ as $\tau/2$, which is mathematically equal to double the reaction time τ. However, the parameter τ is $2/3\ s$ in the Gipps model for HDVs, which is much less than 1.5s in the proposed theoretical model for HDVs. Even when τ is doubled, it is still less than 1.5s. Therefore, the reported capacity in the Gipps model is slightly larger than the maximum theoretical capacity of all HDVs flow with the proposed theoretical model.

When it comes to CACC in theory and CACC in simulation, the research object of this research is CAVs, which is expected to have a higher capacity than AVs. Liu et al. (2018) also used the headway to calculate theoretical pipeline capacity for mixed CAVs using Equation (3.23), which is similar to the proposed Equation (3.8). However, the headway was given directly as a fixed parameter, which is a limitation of Liu's research.

$$C_{mix} = \frac{3600}{P_{leader}HW_{leader} + P_{follower}HW_{follower} + P_{human}HW_{human}} \quad (3.23)$$

Where $HW_{leader} = 2.0s$, $HW_{follower} = 0.71s$, $HW_{human} = 1.5s$. And P_{leader}, $P_{follower}$, P_{human} are the probability of any vehicle being a CACC platoon leader, platoon follower, and manually driven vehicle, which can be calculated by CACC market penetration.

In summary, the comparison between relative safety constraints in the proposed theoretical model and formulations of the different vehicle following models indicates that the proposed theoretical model can identify the maximum road capacity of heterogeneous traffic flow. As only the capacity of all-HDV flow and all-AV flow has been investigated in Section 3.3.2, numerical analysis of mixed flow and right-of-way reallocation will be discussed in the next section.

3.3.3 Numerical analysis of mixed flow and right-of-way reallocation for mixed flow

The discussion of all-AV flow and all-HDV flow in Section 3.3.1 demonstrates that the proposed theoretical model can successfully formulate the upper boundary of theoretical capacity. With Equation (3.15) and identified parameters in Table 3.2, the maximum theoretical capacity of mixed flow can be further calculated as Figure 3.4(a) and also shown are Figure 3.4 (b) with two cuts on 0.5 AV penetration rate (Figure 3.4(c)) and 50km/h speed (Figure 3.4(d)).

As shown in Figure 3.4(c), theoretical capacity increase concave with speed. On the opposite, Figure 3.4(d) demonstrates that theoretical capacity increase convex with penetration rates. This convex increase of road capacity with AV penetration rates can be further proved by Equation (3.24).

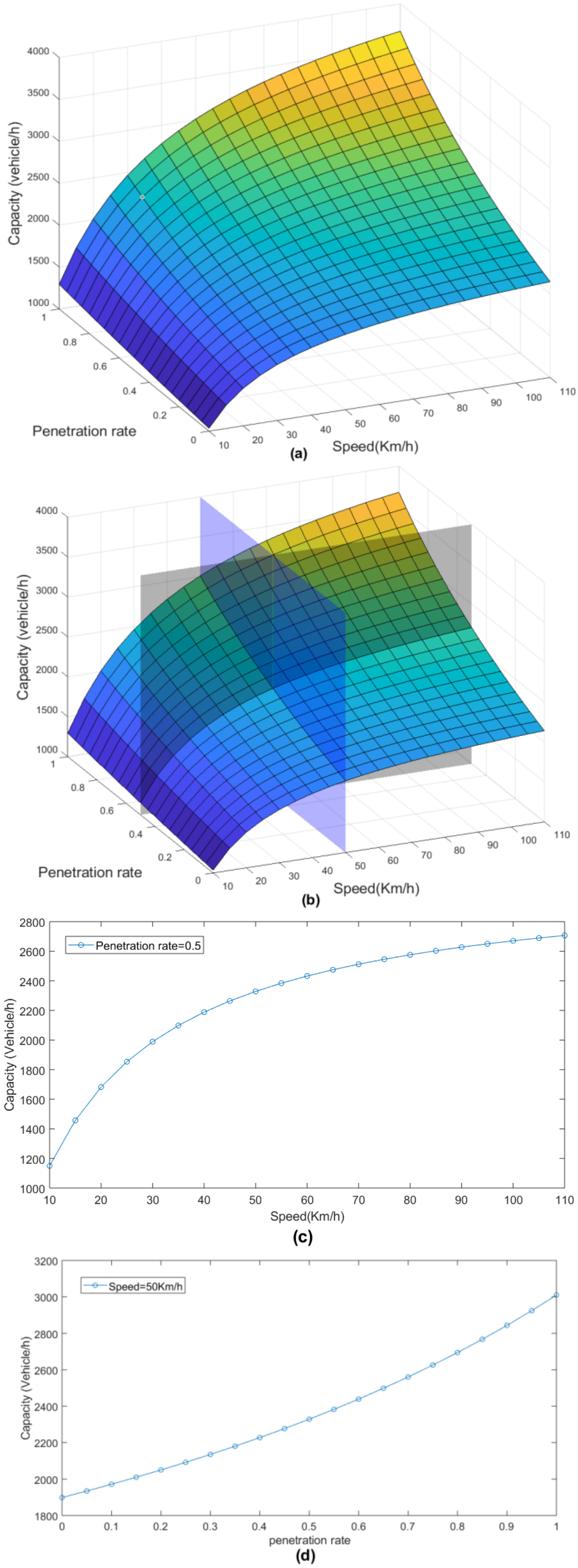

Figure 3.4 Theoretical capacity of mixed AVs and HDVs flow

$$\frac{\partial^2 q}{\partial w_{AVs}^2} = 2 * \left(\frac{1}{(1 - w_{AVs}) * \frac{l_{headway}^{HDVs}}{v_{HDVs}} + w_{AVs} * \frac{l_{headway}^{AVs}}{v_{AVs}}} \right)^{-3} * \left(\frac{l_{headway}^{AVs}}{v_{AVs}} - \frac{l_{headway}^{HDVs}}{v_{HDVs}} \right)^2 \geq 0 \quad (3.24)$$

For any convex function, Equation (3.25) is always satisfied due to the properties of a convex function:

$$f\left(\frac{x_1 + x_2}{2}\right) \leq \frac{f(x_1) + f(x_2)}{2} \qquad \forall x_1, x_2 \qquad (3.25)$$

This property of convex function provides theoretical support to increase road capacity with RoW reallocation. For example, on a two-lane road, when the penetration rate of AV is 50%, the theoretical capacity of the two mixed lanes (do nothing) can be calculated by Equation (3.15) and shown as the blue line in Figure 3.5. Meanwhile, when this two-lane road is reallocated to an AV dedicated lane and a HDV dedicated lane, the theoretical capacity of this two-lane road can be calculated by the sum of the dedicated lanes' capacity calculated by Equation (3.15), which are shown as the orange line in Figure 3.5. Comparing these two lines, the results demonstrate that by avoiding conflicts between HDVs and AVs, road capacity can be increased with RoW reallocation at a 50% AVs penetration rate.

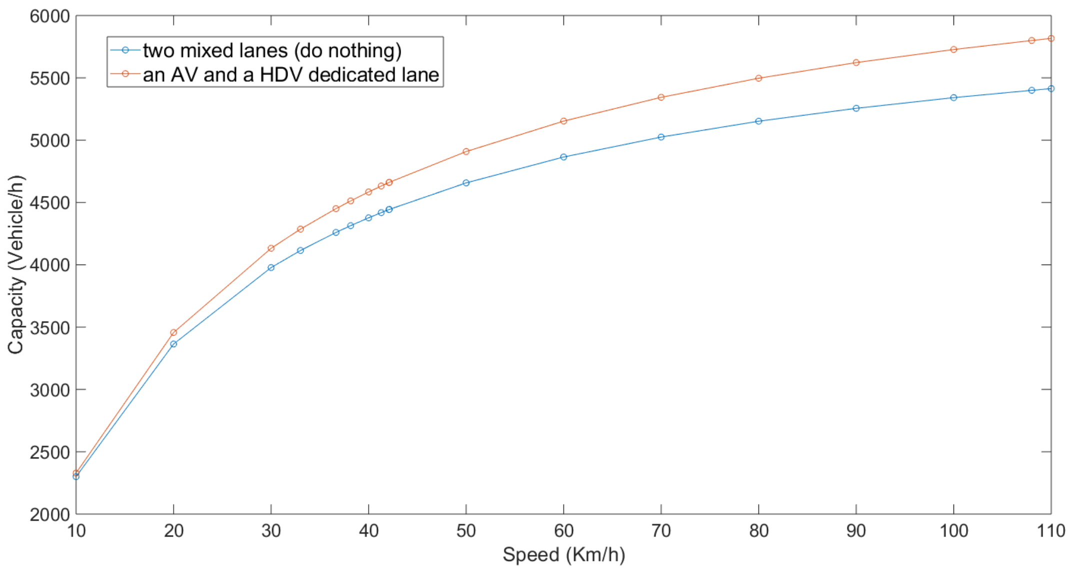

Figure 3.5 Capacity comparison between two mixed lanes and an AV and a HDV dedicate lane at a 50% penetration rate

In summary, the numerical analysis in Section 3.3 demonstrates that the proposed theoretical model can successfully fill the gap that a precise relationship between road capacity and AVs penetration rates has not been adequately modelled in the current studies. With the proposed theoretical model, the maximum capacity of mixed AVs and HDVs flow can be calculated as Figure 3.4(a) with Equation (3.15).

In addition, the property of the proposed theoretical model has been investigated. According to Figure 3.4(d) and Equation (3.25), theoretical capacity has been proved increasing convexly with penetration rates. This convex property provides theoretical support to increase road capacity with RoW reallocation. For example, as shown in Figure 3.5, by avoiding conflicts between HDVs and AVs, the road capacity of a two-lane road can be increased with RoW reallocation at 50% AVs penetration rates.

Though the numerical analysis demonstrates that theoretical capacity can be increased with RoW reallocation at 50% AVs penetration rates, as discussed in Section 3.1, this problem is more complex in practice. First of all, the road utilisation rates might decrease when AVs and HDVs are reallocated to a dedicated lane. As the practical level of service might decrease due to imbalanced demands and supplies, the trade-off between avoiding conflicts with dedicated lanes and increasing road utilisation rates with mixed lanes should be taken into account. Secondly, the spatial and temporal distribution of traffic demand is varied, which further enhances the imbalance between supplies and demands. In addition, different RoW reallocation strategies might need to be applied under different mixed traffic conditions. However, limited by the weakness of the proposed theoretical model that demands and various RoW reallocation strategies are not easy to be taken into account, only an AV and a HDV dedicated lane at 50% penetration rate has been investigated in Section 3.3. Therefore, in the following Section 3.4, different RoW reallocation strategies will be proposed and evaluated by SUMO simulation under different demands and penetration rates, which can overcome the weakness of the proposed theoretical model and cross-validate the results of numerical analysis.

3.4 Case studies for right-of-way reallocation on a two-lane road

To building upon the theoretical model, different RoW reallocation strategies will be proposed and evaluated with SUMO simulation under different demands and AV penetration rates. Firstly, an overview of scenario design is introduced in Section 3.4.1. Then the SUMO simulation framework and the choice of the vehicle following model will be discussed in Section 3.4.2. Finally, results will be presented in Section 3.4.3.

3.4.1 Overview of scenario design

A two-lane road is formulated in Figure 3.6, which has been divided into three sections with 50km/h speed limits. All the vehicles will enter the system from section one and run through section two to leave the system at the end of section three.

Figure 3.6 The two-lane road for case studies

For this two-lane road, the prospective RoW reallocation strategies are:

#1 Two mixed lanes (do nothing policy).

#2 One mixed lane and one AV dedicated lane.

#3 One mixed lane and one HDV dedicated lane.

#4 One AV dedicated lane and one HDV dedicated lane.

Considering that the speed limit for a specific road is usually a fixed constant, all of these RoW reallocation strategies will be evaluated under two key variables. The first variable is the AV penetration rate. According to the numerical analysis of the proposed theoretical model, theoretical capacity increases convexly with penetration rates. For testing and verification, a similar phenomenon should be observed in the SUMO simulation for the two mixed lanes strategy. When it comes to other RoW reallocation strategies, it is also necessary to evaluate their performance under different AV penetration rates. Therefore, AV penetration rates will be chosen as a variable, which increases from 0% to 100%, with a 5% interval (21 levels), to investigate the performance of RoW reallocation strategies under different mixed conditions.

The second variable is traffic demand. As discussed earlier, the imbalance between supply and demand can lead to a decrease in the level of service. This imbalance might be further aggravated by time-varying demand. Therefore, traffic demand is another variable that needs to be taken into account. In this case study, demand is varied from 1000 vehicle/h to 10000 vehicle/h, with 100 vehicle/h intervals (91 levels), to investigate the performance of RoW reallocation strategies from off-peak to peak hours.

Combining these two variables, i.e. AV penetration rates and traffic demands, the four different RoW reallocation strategies will be evaluated under 1911 different scenarios (21 x 91). Based on these scenarios, the efficiency improvement of the RoW reallocation strategies under different scenarios will be evaluated.

3.4.2 Simulation framework and the choice of vehicle following model

SUMO, also known as Simulation of Urban Mobility (Lopez et al., 2018), is an open-source microscopic simulation package, which can handle large scale simulation. The main reason that SUMO has been used in this study is that SUMO supports XML and Python, which means that a large number of scenarios can be formulated and executed for experiments by secondary development in python. The simulation framework is shown in Figure 3.7.

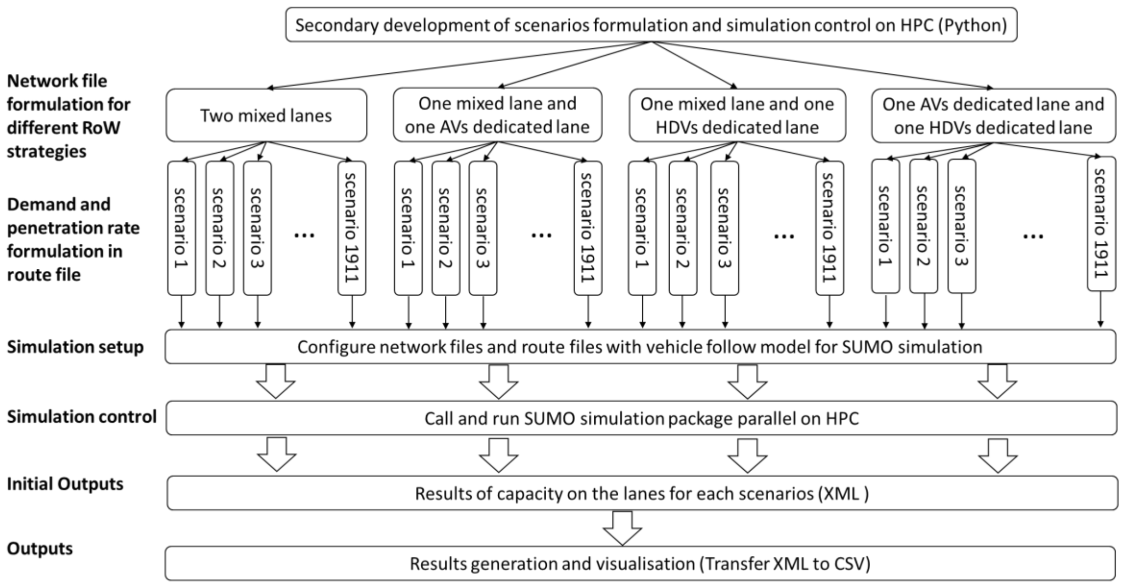

Figure 3.7 The general simulation framework of different scenarios

In this simulation framework, the choice of proper vehicle following models for AVs and HDVs is one of the most important elements. As the ACC model has been tested with experimental data, the ACC model will be used to model the behaviour of AVs with parameters given in Table 3.2. When it comes to HDVs, as discussed in Section 3.3.2, compared with the proposed theoretical model, vehicle following models for HDVs relax the safety constraints to some extent. Based on the comparison between the theoretical model and performance of different vehicle following models in SUMO in Figure 3.3, the Krauss model will be used to model the behaviour of HDVs because the result is closer to the theoretical model.

3.4.3 Results of right-of-way reallocation strategies

Based on the proposed framework, the simulation results are shown in Figure 3.8 and Table 3.3. The surface shown in Figure 3.8(a) illustrates the results of the do-nothing (two mixed lanes) RoW strategy when the local authority and traffic managers do not intervene in the system and agree that both AVs and HDVs can access all the lanes equally. On the other hand, Figure 3.8(b) and Table 3.3 illustrate the maximum value of the other three RoW reallocation strategies, where the local authority and traffic managers are assumed to adopt the most appropriate RoW reallocation strategy under each scenario.

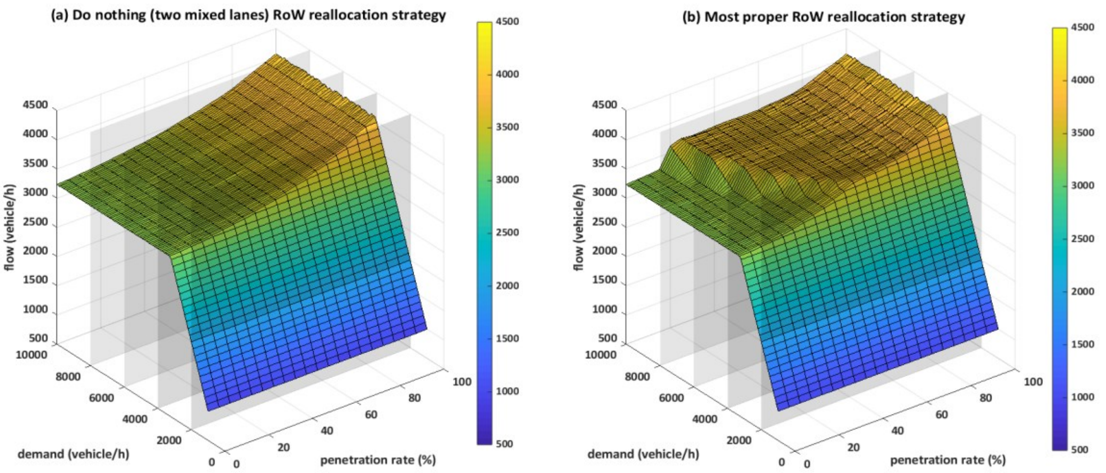

Figure 3.8 Do-nothing (two mixed lanes) strategy VS the most proper RoW reallocation strategies

Table 3.3 Results of Do-nothing and the most proper RoW reallocation strategies (Partial data)

demand	flow strategies	Penetration rate (%) 0	10	20	30	40	50	60	70	80	90	100
1000	Do nothing	1001	999	1000	1002	998	999	999	1000	1000	997	1000
	Proper RoW	1002	1001	1002	1001	1001	1002	1000	1000	1000	1000	1001
2000	Do nothing	2006	2005	2001	2005	2005	2003	2003	2002	2001	2000	2000
	Proper RoW	2006	2004	2002	2001	2006	2006	2002	2000	2002	2001	2000
3000	Do nothing	2998	3000	2996	2999	2997	2995	2997	2996	2996	2997	2996
	Proper RoW	2998	2999	2998	2999	2997	2994	2996	2993	2996	2994	2996
4000	Do nothing	3236	3259	3293	3341	3400	3469	3552	3643	3744	3910	3992
	Proper RoW	3236	3260	3307	3379	3467	3610	3676	3700	3774	3892	3992
5000	Do nothing	3238	3261	3291	3344	3399	3462	3543	3638	3747	3894	4087
	Proper RoW	3238	3263	3305	3368	3601	3664	3677	3723	3789	3906	4087
6000	Do nothing	3233	3266	3294	3342	3395	3462	3549	3637	3756	3901	4027
	Proper RoW	3233	3267	3309	3417	3667	3667	3672	3709	3782	3927	4027
7000	Do nothing	3239	3261	3295	3342	3398	3468	3548	3643	3751	3905	4061
	Proper RoW	3239	3267	3301	3668	3670	3665	3667	3699	3778	3914	4061
8000	Do nothing	3234	3260	3299	3346	3391	3465	3549	3642	3750	3906	4084
	Proper RoW	3234	3261	3302	3656	3667	3666	3670	3727	3790	3882	4084
9000	Do nothing	3238	3264	3296	3342	3398	3461	3548	3640	3748	3906	4069
	Proper RoW	3238	3267	3413	3669	3675	3667	3667	3718	3779	3912	4069
10000	Do nothing	3237	3263	3299	3343	3395	3462	3548	3641	3747	3907	4067
	Proper RoW	3237	3261	3612	3649	3667	3667	3668	3699	3767	3922	4067

*Colour classifications linked with five areas identified in Figure 3.10(b) are based on the Rate of Capacity Increase (RoCI), the relationship between supply and demand, and the best RoW reallocation strategies (#1,#2#,#3 or #4).
*Grey is area 'I' (RoCI=0, demand ≤ supply, #1); Blue is area'II' (RoCI ≤ 0.1%,#3); Light Bule is area 'III' (0.1%<RoCI<5%,#3); Yellow is area 'IV' (RoCI≥5%, #2 or #4); Green is area 'V' (RoCI<5%, #2, penetration rate =100% is included as special areas);

To further analyse the performance of the different RoW reallocation strategies, four slides have been cut at the demand of 2000, 4000, 6000 and 8000 from Figure 3.8, which is shown in Figure 3.9.

It can be observed from Figure 3.9 (a), the four different RoW reallocation strategies have similar performance when the AV penetration rate is higher than 25%. This is because the traffic demand is lower than maximum road capacity and all the demand can be satisfied in these scenarios. However, when the penetration rate is lower than 25%, reallocating a lane to be an AV dedicated lane reduces the real level of service. This is because although conflicts between AVs and HDVs has been reduced by the dedicated lane, the exclusiveness of the dedicated lane reduces the road utilisation rate since HDVs cannot use the AV dedicated lane.

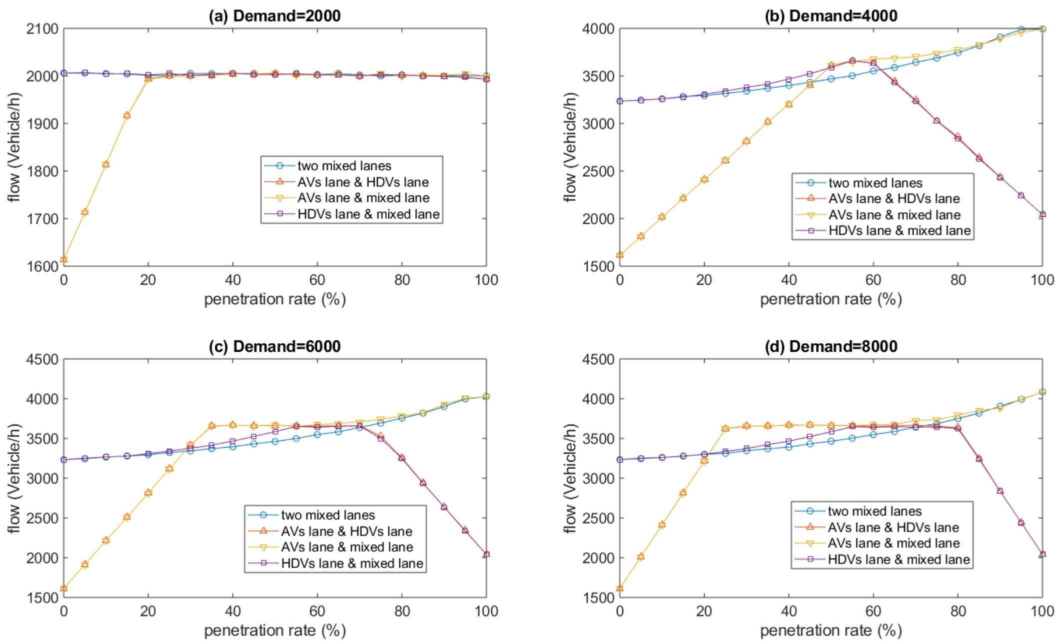

Figure 3.9 Results of RoW reallocation strategies when demand = 2000, 4000, 6000 and 8000 (vehicle/h)

It can be seen in Figure 3.9 (b), that maximum capacity increases convexly with penetration rate for the two mixed lanes strategy, which cross-validates the mathematical proof of Equation (3.24) and numerical analysis in Section 3.3.3. Although the road capacity increases convexly with AV penetration rate, road capacity can be further increased with proper RoW reallocation strategies. For example, road capacity can be further increased with one mixed lane and one HDV dedicated lane compared with the two mixed lanes strategy, as shown by the purple line, when AV penetration rate is in the range of 0% to 60%. From 45% to 60% of AV penetration rate, road capacity can be further increased with the one mixed lane and one AV dedicated lane strategy, as shown by the orange line. From 45% to 100% of penetration rates, road capacity can also be increased with one mixed lane and one AV dedicated lane, as shown by the yellow line.

In Figure 3.9 (c) and (d), it can be observed that the crucial point of the different RoW reallocation strategies is shifted with the increase in traffic demand. In summary, the following characteristics for RoW reallocation strategies can be identified and concluded: 1) when demand is lower than road capacity, observed flow is equal to demand; 2) for the two mixed lanes strategy, the road capacity only increases convexly with AV penetration rate; 3) compared to the two mixed lanes strategy, the other three

RoW reallocation strategies can further increase road capacity. However, this increase is influenced by demand and AV penetration rate, because the trade-off between avoiding conflicts with dedicated lanes and increasing road utilisation rates with mixed lanes should be taken into account; 4) in general, reallocating a lane to be an AV dedicated lane at low AV penetration rate and reallocating a lane to be an HDV dedicated lane at high AV penetration rate are both unreasonable strategies. Moreover, the threshold points of these unreasonable strategies will shift from the middle point (50% penetration rate) to external points with the increase of traffic demand.

To further identify the improvement of road capacity and crucial points of RoW reallocation strategies, the Rate of Capacity Increase (RoCI) with RoW reallocation strategies compared with do-nothing is shown in Figure 3.10.

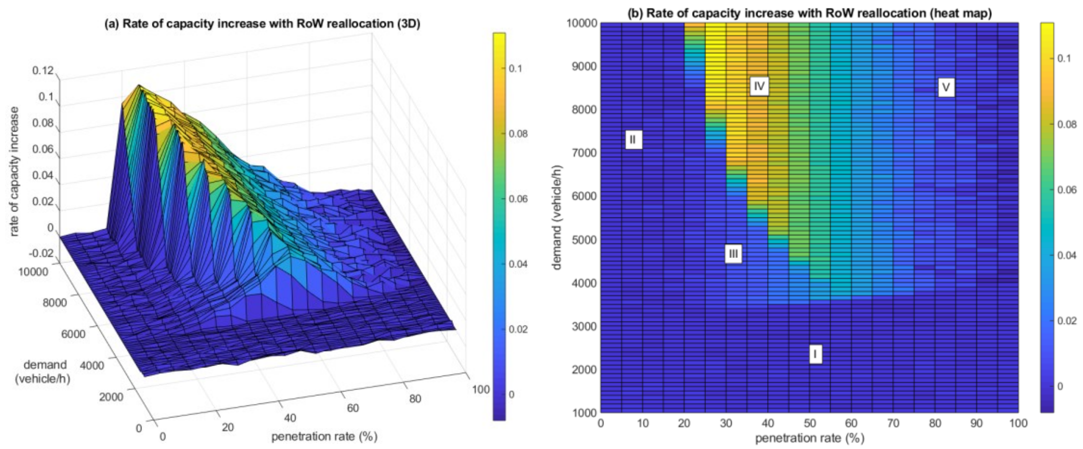

Figure 3.10 Rate of capacity increase with RoW reallocation (3D and heat map)

Intuitively, it can be observed from Figure 3.10(a) that the road capacity is significantly increased at low or medium AV penetration rates and the maximum RoCI is about 11%. To further identify the crucial points of RoW reallocation strategies, five areas can be identified in Figure 3.10(b) based on the RoCI, the relationship between supply and demand, and the best RoW reallocation strategies (#1,#2,#3 and #4).

In the first area 'I' (RoCI=0%, demand≤supply, #1), it is not necessary to adopt RoW reallocation strategies. This is because demand is lower than road capacity in this area, and the observed flow is always equal to demand. In this situation, the rate of increase is always zero from 0% to 100% penetration rate, despite the theoretical road capacity increasing convexly with penetration rate, which formulates the boundary of area 'I' in Figure 3.10(b).

In the second area 'II' (RoCI≤0.1%, #3), RoW reallocation strategies do not yield significant benefits. Though as shown in Figure 3.9 (b) (c) (d) and Figure 3.10, road capacity can be slightly increased with one mixed lane and one HDV dedicated lane, due to the low penetration rate of AVs, conflicts between AVs and HDVs is not prominent, which makes the capacity increase not significant.

In the third area 'III' (0.1%<RoCI<5%, #3), RoW reallocation strategies yield benefits. With the increase of AVs penetration rate, as shown in Figure 3.9 (b) and Figure 3.10, reallocating two lanes to one mixed lane and one HDV dedicated lane can successfully increase the road capacity because the conflicts between AVs and HDVs will be reduced.

In the fourth area 'IV' (5%≤RoCI, #2 or #4), RoW reallocation strategies will yield significant benefit, when the demand for AVs is high. As shown in Figure 3.9 (c) (d) and Figure 3.10, reallocating two lanes to one mixed lane and one AV dedicated lane can significantly increase the road capacity at low or medium penetration, and the maximum improvement is 11%.

In the fifth area 'V' (RoCI<5%, #2), it is still significant to adopt RoW reallocation strategies. However, the rate of increase will gradually decrease with the increase of AV penetration rates. This is because when the penetration rate is higher than 50%, with the increase of penetration rate, the degree of heterogeneity of mixed flow will decrease; meanwhile, the road capacity also gradually increases in the do nothing (two mixed lanes) RoW strategy. When the penetration rate is 100%, specially included in the area 'V', the rate of increase is zero, because do nothing RoW strategy and most proper RoW reallocation strategies reach the same point in an All-AV scenario.

In summary, the case studies for right-of-way reallocation on a two-lane road demonstrate that the road capacity can be significantly increased with proper RoW reallocation strategies at low or medium AV penetration rates. Five different areas have been further identified to demonstrate the crucial points of RoW reallocation strategies, which can help traffic managers and local authorities better understand and manage mixed traffic flow. In addition, the convex increase of road capacity with penetration rate has been cross-validated in the SUMO simulation, compared with the theoretical proof and numerical analysis. In the next section, a sensitivity analysis is conducted to further analyse the influence of AV behaviour changes on RoW reallocation.

3.5 Sensitivity analysis

It should be noted that with the parameters identified in Table 3.2, only specific kinds of AVs and HDVs have been evaluated by the theoretical model and SUMO simulation. However, as discussed in Section 3.1, AVs are emerging technologies and the behaviour of AVs might change with further development of the AV technologies such as control algorithms, LiDAR, high precision maps and computing power. For example, l_{error}^{j} can be reduced with the improvement of sensors. Russell et al. (1997) developed a forward-looking automotive radar sensor for AVs, which has a 0.5 m range accuracy and 1.5 km/h speed accuracy from 3 m to 100 m. More recently, Ouster (2018) achieved a 0.1 m range accuracy from 0 m to 250 m.

In addition, the user's parameter setting is another factor that influences the behaviour of AVs. Ideally, an AV is able to maintain a smaller time gap to the leading vehicle with the help of quicker reaction time and more accurate sensors. However, the user can still select a longer time gap based on personal preference. For example, Eichelberger and McCartt (2014) surveyed the drivers of Volvo vehicles that have advanced crash avoidance and related technologies (Level 2 or Level 3 AVs). The settings of the system are shown as 1 to 5 bars, which represent the time interval to the leading vehicle from 1s to 2.5s. 33% of the users adjusted the time gap to 1 or 2 bars; 22% of the users adjusted the time gap to 4 or 5 bars, whereas the rest of the users only used the default setting of 3 bars.

Therefore, in subsection 3.5.1, the sensitivity analysis of parameters in the theoretical model is presented to demonstrate the impacts of the development of AV technologies on road capacity. Then in subsection 3.5.2, the influence of the user-preferred time gap on the performance of RoW reallocation strategies is investigated with simulation.

3.5.1 Sensitivity analysis of the proposed theoretical model

In order to evaluate the impacts of the development of AV technologies on road capacity, the values of the different parameters in the second column of Table 3.2 are increased and decreased by 50% for sensitivity analysis. The changes in road capacity are calculated by the theoretical model and the rate of changes compared to the baseline (parameters in Table 3.2) are shown in Figure 3.11.

It can be observed from Figure 3.11 that when τ^{AVs}, l_{follow}^{AVs}, l_{buffer}^{AVs} and l_{error}^{AVs} decrease by 50%, the rate of capacity change is positive. This demonstrates that the theoretical road capacity will increase if the development of AV technologies supports a shorter reaction time, vehicle length and buffer distance to the leading vehicle or if AVs have more accurate sensors. The differences between Figure 3.11 (a)(b)(c)(d) and (e)(f)(g)(h) further indicates that AV reaction time τ^{AVs} has the highest sensitivity, followed by the AV vehicle length l_{follow}^{AVs}. Though the change of l_{buffer}^{AVs} and l_{error}^{AVs} have some influence on theoretical road capacity, their sensitivity is not as high as τ^{AVs} and l_{follow}^{AVs}.

The sensitivity of parameters is also influenced by the AV penetration rate and speed. When AV penetration rate increases, there will be more AVs in the system, which leads to a sensitivity increase of all the AV parameters. On the other hand, the impact of speed on sensitivity is not universal. When speed increases, the sensitivity of l_{error}^{AVs}, l_{follow}^{AVs} and l_{follow}^{AVs} gradually decrease, but the sensitivity of τ^{AVs} gradually increases.

In summary, the sensitivity analysis of the proposed theoretical model demonstrates that the sensitivity of $\tau^{AVs} > l_{follow}^{AVs} > l_{buffer}^{AVs} > l_{error}^{AVs}$, moreover, AV penetration rate and speed of vehicle can influence the sensitivity of the parameters. Although AV reaction time τ^{AVs} has the highest sensitivity, as discussed in Section 5, users may still prefer (and therefore select) a longer time gap. This means that AV reaction time τ^{AVs} has been relaxed to the desired time gap t_{hw} as specified by users, which will be further investigated in Section 3.5.2.

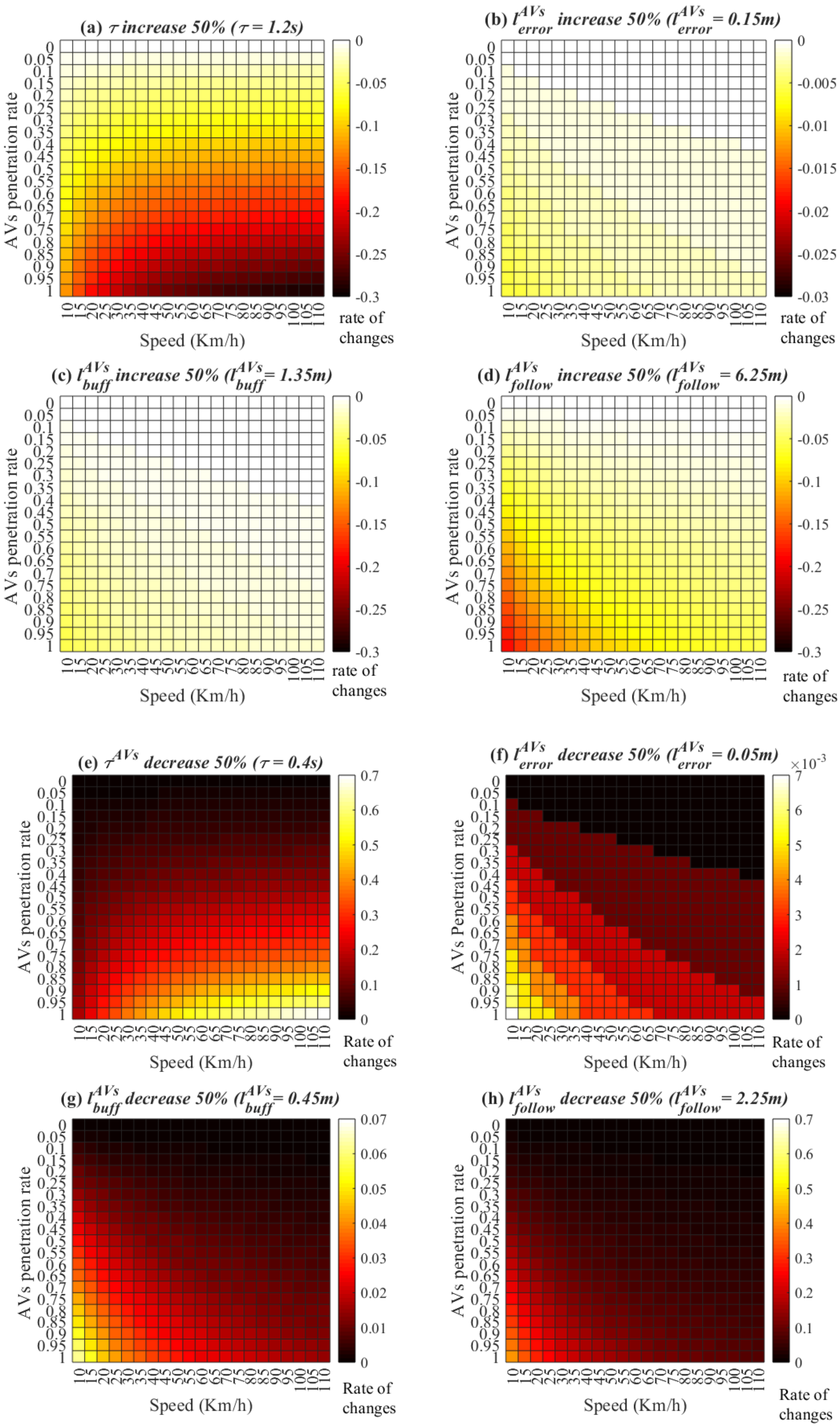

Figure 3.11 Sensitivity of parameters increase and decrease 50% in the theoretical model

3.5.2 Sensitivity analysis of the desired time gap

As discussed above, the change of AV settings for the desired time gap can strengthen or weaken the heterogeneity between AVs and HDVs, which further influences the RoCI with RoW reallocation strategies. Therefore, the impacts of desired time gap setting on the performance of RoW reallocation strategies will be investigated in this section through the SUMO simulation.

Although most sensors can detect stimuli very quickly, AVs need time to react to the stimulus. Also, just as the reaction time of human behaviours is relative to the reflex arc, the reaction time of AVs should also be linked to the reaction loop of AVs to a stimulus. However, in practice, there is not a universal reaction loop for AVs, because the control of AVs involves communication between different modules such as detection module (Bohrer et al., 1995), High Definition (HD) map (Wolcott & Eustice, 2014), and path planning module (Likhachev & Ferguson, 2009). Therefore, in order to identify a reasonable reaction time range for AVs, a similar system has been taken as the reference. For example, in the Automatic Train Operation (ATO) system, the train-borne Communication-Based Train Control (CBTC) equipment reaction time guided by IEEE standards ranges from 0.07s to 0.75s (Schifers & Hans, 2000), where the upper boundary is close to the reaction time (0.8s) used in this study.

Considering that the user desired time gap setting should be larger than the reaction time (e.g. longest reaction time in the ATO system is 0.75s), while the largest available time gap for users is 2.5s (Eichelberger & McCartt, 2014), the time gap setting t_{hw} is varied from 0.8 s to 2.5s in the sensitivity analysis. The results of the SUMO simulation with different reaction times are shown in Figures 3.12, 3.13, 3.14 and Table 3.4. It can be observed from Figure 3.12, Figure 3.13 and Table 3.4 that with increasing reaction time, the road capacity for the all-AV scenarios (demand=5000 vehicle/h) is almost halved from 4087 vehicle/h at 0.8s to 2113 vehicle/h at 2.5s.

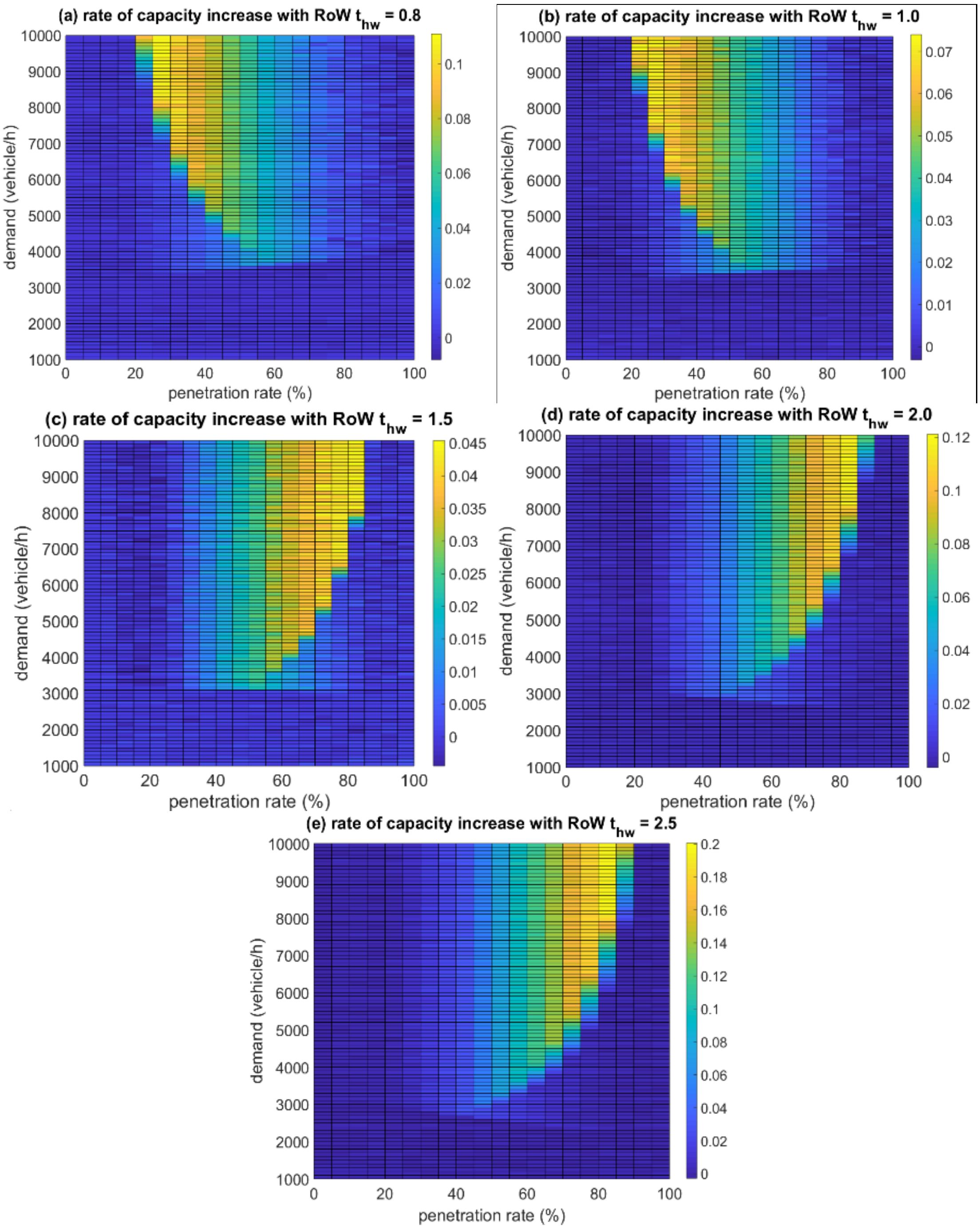

Figure 3.12 Impacts of AVs reaction time on crucial points of RoW strategies

It can be seen that the main difference between Figure 3.12 (a) (b) and Figure 3.12 (c) (d) (e) is the inversion of RoCI with RoW reallocation strategies. With the increase of user desired time gap setting, this phenomenon will be observed when the behaviour of AVs is ‘ worse ’ than the HDVs. However, even in this case, RoW strategies can still increase road capacity compared with the do nothing policy. Meanwhile, as shown in Figure 3.12, the boundaries of the five areas also shift with the change of user-desired time gap setting, because the RoCI is related to the difference in behaviours between the AVs and HDVs. If heterogeneity between AVs and HDVs is significant, the rate of capacity increase will become larger.

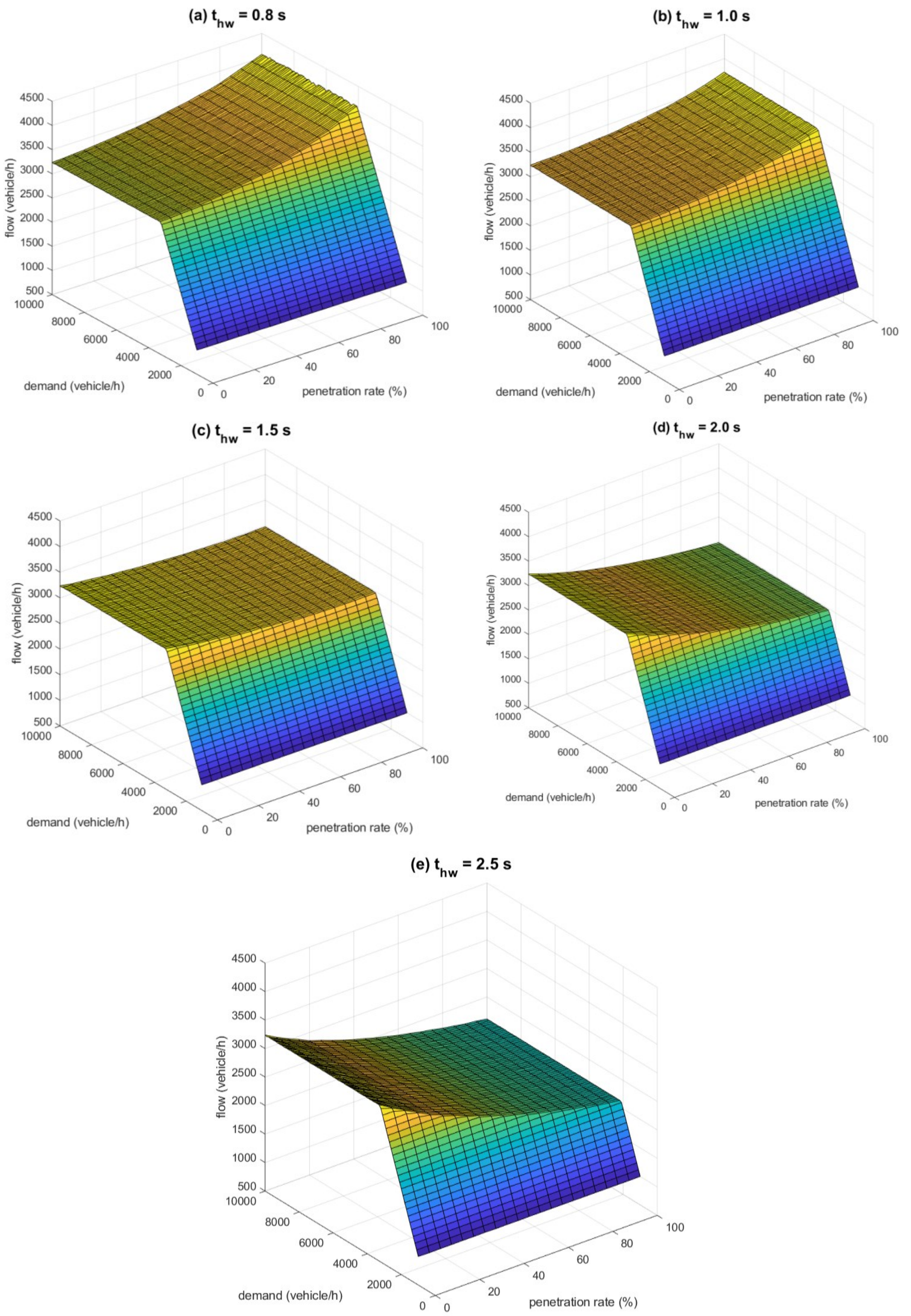

Figure 3.13 Impacts of desired time gap setting on do nothing scenarios

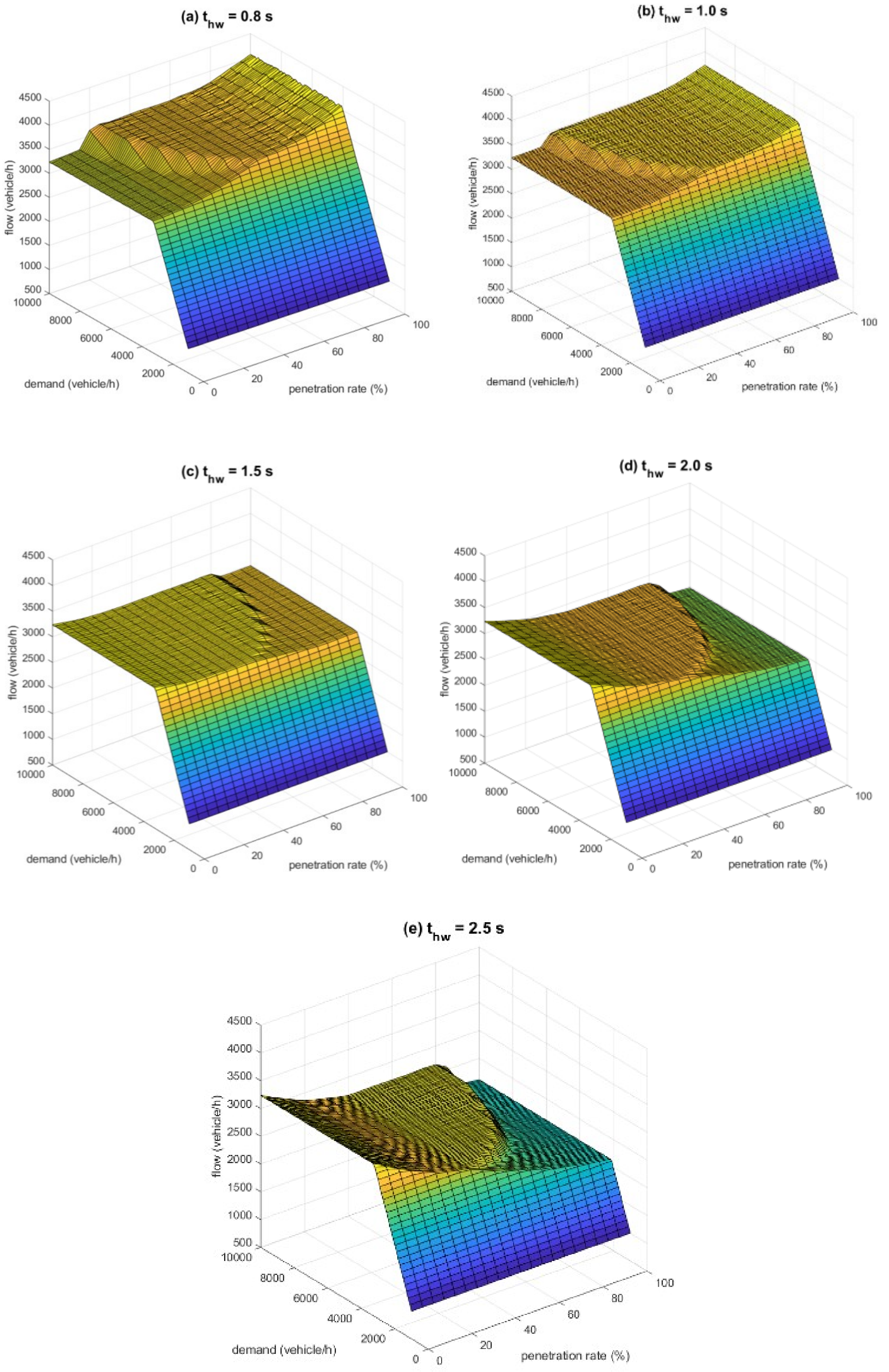

Figure 3.14 Impacts of desired time gap setting on RoW reallocation scenarios

Table 3.4 Results of sensitivity analysis for Demand=5000 vehicle/h

t_{hw}	flow / strategies	Penetration rate (%) 0	10	20	30	40	50	60	70	80	90	100
0.8s	Do nothing	3238	3261	3291	3344	3399	3462	3543	3638	3747	3894	4087
	Proper RoW	3238	3263	3305	3368	3601	3664	3677	3723	3789	3906	4087
1s	Do nothing	3238	3238	3251	3271	3289	3337	3377	3436	3509	3601	3728
	Proper RoW	3238	3239	3253	3295	3474	3468	3470	3485	3524	3602	3728
1.5s	Do nothing	3238	3176	3129	3090	3054	3031	2998	2982	2972	2967	2977
	Proper RoW	3238	3168	3122	3105	3103	3101	3103	3006	2978	2970	2977
2s	Do nothing	3238	3102	2993	2890	2800	2729	2658	2602	2547	2511	2471
	Proper RoW	3238	3105	2988	2917	2862	2858	2845	2734	2555	2508	2471
2.5s	Do nothing	3238	3038	2862	2724	2600	2490	2395	2302	2235	2166	2113
	Proper RoW	3238	3043	2868	2765	2670	2675	2666	2557	2238	2168	2113

3.6 Conclusion

The primary contributions are two-fold. Firstly, a theoretical model based on relative safety constraint, rather than a theoretical model based on average speed and spacing characteristics pre-assumed, is proposed to calculate the maximum capacity of heterogeneous traffic flow. The relative safety constraint and its derivation has been widely used in many vehicle following models, which is a reasonable method to ensure road safety and makes the theoretical model become comparable to the existing vehicle following models.

Further numerical analyses of the theoretical model demonstrate that road capacity increases convexly with AV penetration rates, which has been proved in theory with Equation (3.24). The properties of convex functions provide the theoretical support for RoW reallocation, which is tested numerically in Section 3.3.3 and demonstrates that by avoiding conflicts between HDVs and AVs, road capacity can be increased with RoW reallocation at a 50% AV penetration rate.

Although the numerical analysis of the theoretical model found that road capacity can be increased at 50% AV penetration rates by a dedicated AV and a dedicated HDV lane, the RoW reallocation strategy is more complex in practice. Specifically, since traffic demand is time varied, the trade-off between avoiding conflicts by using dedicated lanes and increasing road utilisation with mixed lanes should be taken into account.

Secondly, to take different demand, AV penetration rate and RoW reallocation strategies into account, SUMO simulation was used for large scale case study. This leads to the second contribution of this research, viz. crucial points of different RoW strategies on a two-lane road have been identified, which provides quantitative evidence for traffic managers and LAs for policymaking. The results demonstrate that road capacity on a two-lane road can be significantly increased by up to 11% at low or medium penetration rates with appropriated RoW reallocation strategies. Based on the rate of capacity increase, five different areas have been further identified to demonstrate the crucial points of RoW reallocation strategies, which can help traffic managers and local authorities better understand and manage mixed traffic flow. In addition, the convex increasing of road capacity with AV penetration rate has been cross-validated in the SUMO simulation.

Moreover, the impacts of AVs behaviours changes caused by the development of technologies and users' personal settings on road capacity and RoW reallocation strategies have been investigated. The sensitivity analysis of the theoretical model has been conducted, which demonstrates that the sensitivity of $\tau^{AVs} > l_{follow}^{AVs} > l_{buffer}^{AVs} > l_{error}^{AVs}$. As τ^{AVs} has the highest sensitivity, the change of AV reaction time with the improvement of AV technology will have significant impacts on road capacity. However, Not only AV technologies' development but also user's parameter setting can influence the behaviour of AV, which further effects the performance of RoW reallocation strategies. The results of SUMO simulation demonstrate that the rate of capacity increase with proper RoW reallocation strategies is related to the behaviours difference between AVs and HDVs. If heterogeneity between AVs and HDVs is significant, the rate of capacity increase will become remarkable. Last but not least, even when behaviours of AVs 'worsen' compared to HDVs, RoW strategies can still increase road capacity compared with do-nothing policy.

In conclusion, in Chapter 3, the impact of heterogeneity between AVs and HDVs on road capacity are investigated. The properties of convex functions provide the theoretical support for RoW re-allocation, and it has been found that road capacity can be increased with proper RoW re-allocation strategies. As the overall aim of this PhD research is to analyse the mixed flows of AVs and HDVs to help traffic managers and

Local Authorities (LAs) to improve the performance of urban traffic systems by right-of-way re-allocation and dynamic traffic management, in the next following Chapters (Chapter 4, 5 and 6), the opportunities for dynamic short-term traffic management in mixed conditions with the emergence of connected and automated technologies will be investigated.

Chapter 4 Managing mixed traffic flow with CAVs as mobile traffic controllers

With the emergence of connected and automated technologies, whether CAVs can be used as mobile traffic controllers are investigated in this chapter. In Section 4.1, the background and research context are introduced. Then in Section 4.2 a numerical analysis of the Braess network (Braess et al., 2005) demonstrated that it is possible to increase system-level efficiency when CAVs adjust their speed on a certain link. To further investigate the feasibility of using CAVs as mobile traffic controllers, a microscope simulation is conducted in Section 4.3. Finally, the conclusion is given in Section 4.4.

4.1 Background and research context

Equipped with sensors, Connected Autonomous Vehicles (CAVs) can perceive and collect data from the surrounding environment then communicate and interact with other vehicles and signal controllers. This provides an opportunity for CAV to become a mobile sensor or even a mobile traffic controller. In the mixed flow of CAVs and Human Driven Vehicles (HDVs), HDV prefer to driver for a better driver environment. Though some of HDV's driving behaviour, such as following a leading vehicle closely, choosing the shortest route or changing to a better lane, can increase its personal utility, these behaviours might reduce system efficiency.

For example, a typical traffic jam can be triggered by lane changing (Laval & Daganzo, 2006). In some circumstances, a small perturbation can also grow to a stop-and-go wave, also known as phantom traffic jams, when vehicle density exceeds the critical value (Flynn et al., 2009; Sugiyama et al., 2008; Tadaki et al., 2013).

According to a field experiment with 21 HDVs and 1 AVs, Stern et al. (2018) found that the stop-and-go wave generated by HDVs can be dissipated via the control of the autonomous vehicle in the mixed flow, which indicated that it is possible to control or engage traffic flow with a few mobile controllers (less than 5%).

Inspired by Stern et al. (2018)'s works, Kreidieh et al. (2018) investigated dissipating stop-and-go waves with deep reinforcement learning, which can achieve near-complete wave dissipation with 10% autonomous penetration. Similarly, Giammarino et al. (2020) extended the field test with simulation to investigate the stability of dissipating stop-and-go waves.

Though existing research demonstrated that with an appropriate strategy to adjust speed, CAVs can be used to reduce the fluctuation of velocity in the mixed flow and dissipate stop-and-go waves, most of the existing research only considered using CAV to influence the speed of the following vehicle. The influences of CAVs' speed adjustment on HDV's routing behaviour and using CAVs as an extension of the signal controller have not been fully studied.

Against this background, the main aim of this chapter is to develop driving strategies for CAVs to interact with HDVs and signals in the mixed condition and explore whether CAVs can be used as mobile traffic controllers. The specific objectives of this chapter can be summarised as follows:

(1) To investigate whether system travel efficiency can be increased when CAVs act as mobile traffic controllers by adjusting the speed on a certain link.

(2) To develop driving strategies for CAVs to interact with HDVs and signal control in mixed conditions to reduce total travel time.

4.2 Numerical analysis of CAVs acting as mobile traffic controllers in mixed traffic conditions

Whether system efficiency can be improved with CAVs acting as mobile traffic controllers actively adjusting the speed on a certain link is investigated heuristically in Appendix 4. However, it is hard to evaluate whether the optimisation problem is solvable or not without an expression of the function. In this section 4.2, a numerical analysis of CAVs acting as mobile traffic controllers on the Braess network (Braess et al., 2005) is conducted to demonstrate the possibility.

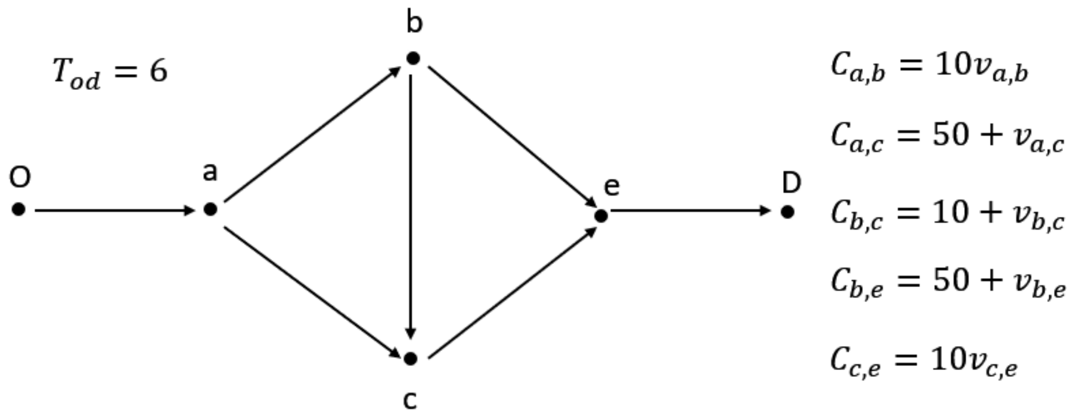

Figure 4.1 A typical Braess network

As shown in Figure 4.1, a typical Braess network consists of six nodes and seven links. Vehicles are travelling from the origin point O to the destination point D and demand T_{od} equal to six. For any vehicle travelling from O to D, there are three routes noted as follows:

- Route 1: O→a→b →e→D
- Route 2: O→a→b→c→e→D
- Route 3: O→a→c →e→D

According to Wardrop's first and second principal, user equilibrium and system optimal traffic distribution can be calculated and shown in Table 4.1

Table 4.1 User equilibrium and System optimal on Braess network

	Route 1 flow	Route 2 flow	Route 3 flow	Total travel time
User equilibrium	2	2	2	552
System optimal	3	0	3	498

In the mixed traffic condition, when CAVs can act as mobile traffic controllers actively adjusting the speed on a certain link, $\Delta_{a,CAV}$ can be added on any link, which is shown in Figure 4.2.

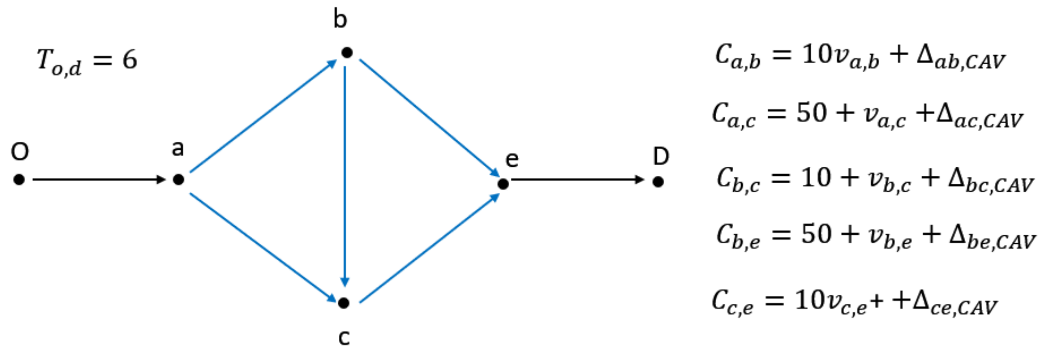

Figure 4.2 CAVs acting as mobile traffic controllers

Set Δ_{min} equal to zero, which indicated that all the CAVs already travel at the allowed speed, and it is not possible to increase speed to reduce link travel cost. Meanwhile Set Δ_{max} equal to fifteen, which indicated that CAVs could reduce their speed on a certain link within the boundary.

On the Braess network, the relationship between max $\Delta_{bc,\,CAV}$, total travel time and traffic assignment are shown in Figure 4.3.

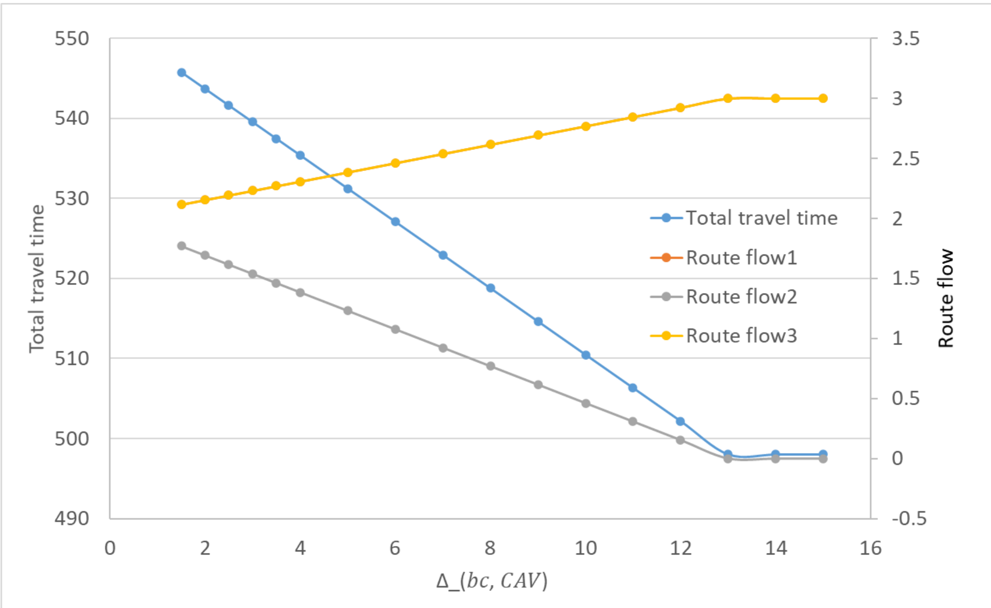

Figure 4.3 The relationship between $\Delta_{bc,\,CAV}$, total travel time and traffic assignment

It can be observed from Figure 4.3 that for this Braess network, when CAVs actively reduce speed to increase travel cost on link bc, total travel time can be gradually reduced. When $\Delta_{bc,\,CAV}$ equal to 13, Total travel time can be reduced from 552 to 498.

In summary, the numerical analysis on the Braess network demonstrated that not only CAVs could influence the speed of the following vehicle to dissipate stop-and-go waves, on the network, CAVs can also act as mobile traffic controllers actively adjusting the speed on a certain link to reduce total travel time. However, it should be noted that the Braess network is a simple network with an idealised cost-flow relationship (static and macroscopic). Meanwhile, when solving Equation (A4.1) and Equation (A4,4) (attached in appendix 4), there is an underlying assumption that both HDVs and CAVs have full knowledge about travel cost and traffic state on the network, which might not be realistic in practice. Therefore to take more realistic circumstances into account, a SUMO simulation case study is conducted, where the cost-flow relationship is based on simulation; HDVs have only a partial knowledge about travel cost; CAVs can receive information about signal timing to become an extension of the signal controller.

4.3 Simulation case study of CAVs acting as mobile traffic controllers

According to the theoretical model in Section 4.2 and the numerical analysis in Section 4.3, it has been found that in some circumstances, it is possible to reduce total travel time with CAVs actively adjusting the speed on a certain link. To take more realistic circumstances into account, a SUMO simulation case study is conducted in this section.

4.3.1 Overview of the network structure

As shown in Figure 4.4, The network $G(N = 5, L = 6)$ has five nodes, including a signal-controlled node (Node 3), six links and 10 edges. The length of each edges shown in Figure 4.4 is 500 meters. The yellow time between phases is set as 3s, and the initial green time for edge 4 and edge 5 are 30s and 70s. Travel demand is 2000 vehicle/h from the origin point to the destination point, and two available routes can be identified as follow:

- Route 1 = edge_1 edge_2 edge_4 edge_7 edge_9 edge_10
- Route 2 = edge_1 edge_3 edge_5 edge_6 edge_8 edge_10

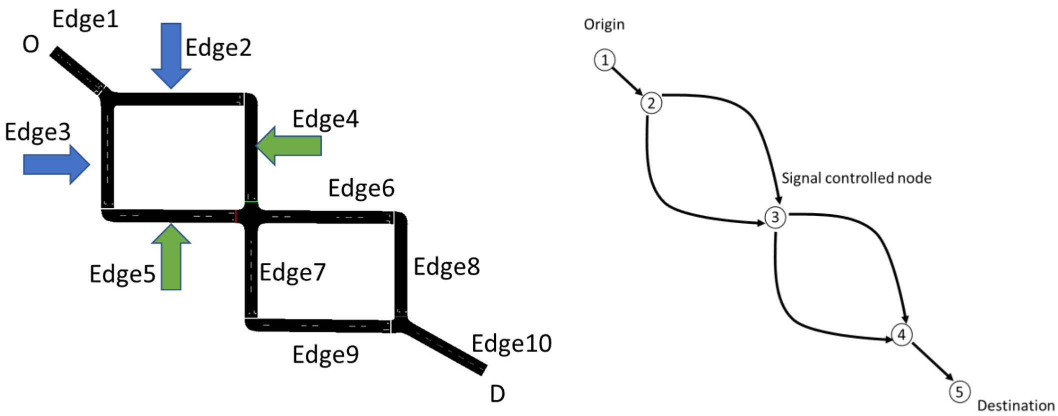

Figure 4.4 The network for case study

4.3.2 Scenarios of case study

As discussed in the summary of Section 4.3, in practice, HDVs only have partial knowledge about travel costs on the network. When it comes to CAVs, CAV can communicate with other CAVs and traffic signals to get information about the traffic state. This communication capability makes CAVs might become an extension of the signal controller to act as a mobile traffic controller.

To take these two factors into account, the Traffic Control Interface (TraCI) in SUMO is used to building up different control strategies for HDVs and CAVs under different scenarios, which can be summarised as follow and shown in Figure 4.5:

- #S1: CAVs penetration rate is 0%. The default routing of SUMO is used.
- #S2: CAVs penetration rate is 50%. The default routing of SUMO is used.
- #S3: CAVs penetration rate is 0%. HDVs have partial knowledge about travel costs on the forward links. When HDVs approaching node 2, HDVs can observe the traffic state on edge 2 and edge 3 (traffic state on edge 4 and edge 5 are unknown). As HDVs prefer to driving or a better environment, when travel cost on edge 2 is higher than edge 3, HDVs will choose the route via edge 3. Otherwise, chose the route via edge 2.
- #S4: CAVs penetration rate is 50%. HDVs have the same information and behaviour pattern as #S3. CAVs have complete knowledge about travel costs on the forward links but still following default routing and do nothing.
- #S5: CAVs penetration rate is 50%. HDVs have the same information and behaviour pattern as #S3. CAVs have complete knowledge about travel costs

on the forward links. Similar to HDVs, CAVs will also drive for a better environment. When travel cost on edge 2 plus edge 4 is higher than edge 3 plus edge 5, HDVs will choose the route via edge 3. Otherwise, chose the route via edge 2.

- #S6: CAVs penetration rate is 50%. HDVs and CAVs' information and behaviour patterns are the same as #S5. In addition, based on the information from the traffic signal, CAVs act as a mobile traffic controller, which will reduce the speed on edge 2 or edge 3 to influence the behaviour of HDVs.

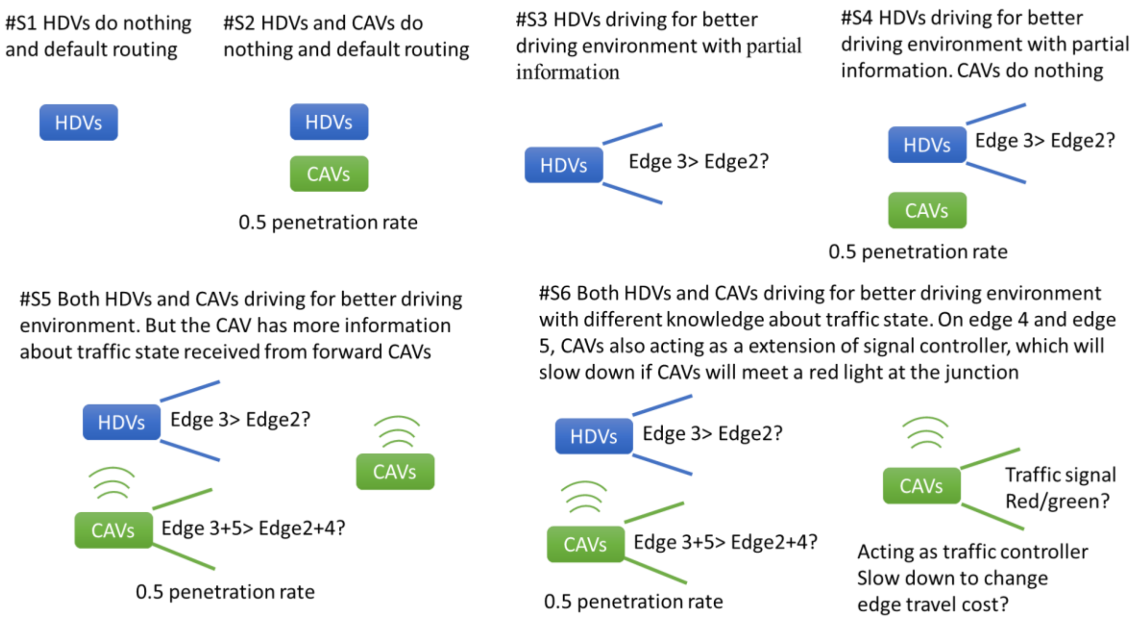

Figure 4.5 Scenarios of the simulation case study

4.3.3 Results of case study

As discussed in Subsection 4.4.1 and Subsection 4.4.2, different scenarios are simulated in SUMO, and the results are shown in Figure 4.6.

Comparing #S2 with #S1 (or #S4 with #S3), it can be found that when CAVs penetration rate increased from 0% to 50%, total travel time reduced from 690278s in #S1 to 674036s in #S2 (or from 674036s in #S3 to 652371s in #S4), which is consistent with the results in Chapter 3 that road capacity increase with penetration rates when AVs are able to drive with smaller headways to the leading vehicle. (Li et al., 2020).

Comparing #S3 with #S1 (or #S4 with #S2), it can be found that compared with do nothing (default routing), even when HDVs only have partial knowledge about travel costs on the network. Total travel time can be reduced when HDVs drive for a better driving environment.

Comparing #S5 with #S4 and #S3, when both CAVs and HDVs are driving for a better driving environment, more accurate knowledge about travel costs on the network can further reduce total travel time.

Comparing #S6 with all other scenarios, even when both CAVs and HDVs are driving for a better driving environment. System travel efficiency can be further improved (total travel time reduce to 628045s), when CAVs act as a mobile traffic controller actively reducing speed on edge 2 and edge 3.

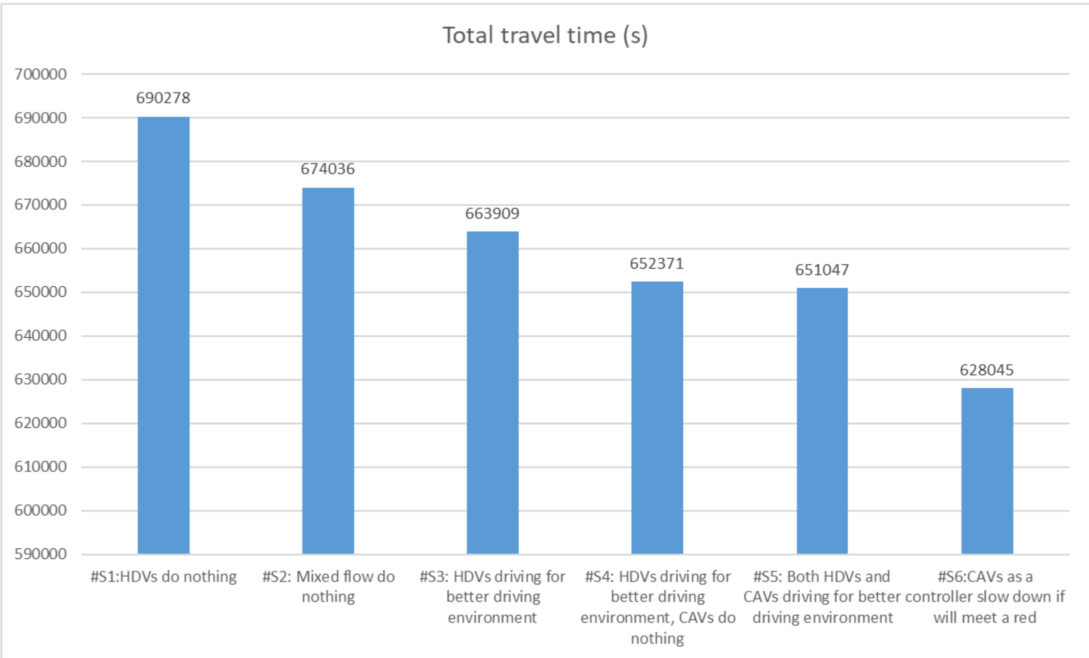

Figure 4.6 Total travel time of different scenarios

In summary, to take more realistic circumstances into account, a SUMO simulation case study is conducted in Section 4.4, where different scenarios are designed to take the following factors into account: 1) the cost-flow relationship is based on simulation; 2) HDVs only have partial knowledge about travel cost on the network; 3) CAVs can receive information about signal timing and act as mobile traffic controller actively adjusting speed on certain links. According to the results of the simulation, when CAVs acting as mobile traffic controllers, total travel time can be reduced by about 6.8% compared with do nothing (#S2) and about 3.5% compared CAVs not acting as controllers (#S5)

4.4 Conclusion

In conclusion, based on RO2, whether CAVs can be used as mobile traffic controllers are investigated in this chapter. According to the existing studies, CAVs can be used to reduce the fluctuation of velocity in the mixed flow and dissipate stop-and-go waves. However, most of the existing research only considered using CAV to influence the speed of the following vehicle. The influences of CAVs' speed adjustment on HDV's routing behaviour have not been fully studied, which also leads to two contributions of this Chapter.

Firstly, to investigate the influences of CAVs' speed adjustment on HDV's routing behaviour, a numerical analysis of CAVs acting as mobile traffic controllers on the Braess network was conducted and found that total travel time can be reduced by 9.7%, when CAVs actively slow down on Link bc.

Secondly, considering Braess network is a simple network with an idealised cost-flow relationship, and in practice, HDVs only have partial knowledge about travel costs. a SUMO simulation case study is conducted in Section 4.5 where TraCI is used to build up different control strategies for HDVs and CAVs under different scenarios. According to the results of the simulation, when CAVs acting as mobile traffic controllers actively reduce speed on the link, total travel time can be reduced by about 6.8% compared with do nothing (#S2) and about 3.5% compared CAVs not acting as controllers (#S5).

Compared with conventional approaches such as road pricing and speed limit, controlling CAVs as mobile traffic controllers provides a new approach to solving the problem novelly. In practice, conventional road pricing and the speed limit are adopted in certain areas or certain time periods. The benefit of road pricing or speed limits might be reduced when demand and OD are changed frequently during the day. Because for the same network, when demand changes, User Equilibrium (UE) assignment and

System Optimal (SO) assignment might change correspondingly. Deploying CAVs as mobile traffic controllers adjusting the speed on a certain link can be more elaborate, flexible and less painful to drivers. With the help of V2V and V2I communication, CAVs can quickly react to the change of traffic state and demand. Then the necessary speed adjustment can be conducted on a specific link or a specific road section for a short period. As the finely tuned speed adjustment is less noticeable and would not cost drivers additional money, it might be less painful and easier to be accepted.

Given that using CAVs as mobile traffic controllers is a novel idea, the analysis in this chapter is just a starting point and raises additional questions. For example, whether CAV actively changing their routing along with signal timing can achieve system optimal traffic assignment, which will be investigated in the subsequent chapters.

Chapter 5 Dynamic process of routing and signal timing towards system optimal equilibrium in mixed CAVs and HDVs traffic

The emergence of Connected Autonomous Vehicles (CAVs) opens up an opportunity to achieve a System Optimal (SO) traffic distribution. Ideally, in a fully connected and automated environment, all the CAVs can behave cooperatively in routing with traffic signals to reduce total travel time. However, in a mixed flow of CAVs and Human Driven Vehicles (HDVs), HDVs might not be connected, which means they might not cooperate with other vehicles actively and make their own routing decisions to maximise personal utility even when connected.

In this chapter (adapted from J2 listed in Section 1.4), whether travel efficiency can be improved with only a part of the CAV cooperatively changing its routing in mixed conditions will be investigated. Firstly, the background and research context are introduced in Section 5.1. Then in Section 5.2, the routing behaviour of HDVs toward user equilibrium and the cooperative routing behaviour of CAVs towards system optimal distribution are discussed independently. As both routing behaviours exist in the mixed flow, the interaction between these two kinds of routing behaviour and the dynamic process towards system optimal distribution are investigated by the numerical analysis at macroscopic in Section 5.3. Then in Section 5.4, an Optimal Routing and Signal Timing (ORST) control strategy is proposed to take non-linear cost-flow relationship and signal timing into account and tested with microscopic SUMO simulation. Finally, conclusions are given in Section 5.5.

5.1 Background and research context

Improving travel efficiency is a challenge for both travellers and traffic managers. To reduce individual travel time, drivers prefer to use a route with less journey time. When the journey time on all used routes is equal to or less than the journey time on unused routes, Wardrop equilibrium, also known as User Equilibrium (UE), is achieved (Wardrop, 1952). However, for traffic managers, user equilibrium might not be the optimal solution for the whole system. Wardrop (1952) also discussed a traffic distribution to minimise total travel time, which is called a system optimal distribution.

This system optimal distribution, or an approximation to it, is often sought by traffic managers seeking to reduce total travel time.

To achieve the system optimal distribution, drivers should have full knowledge about travel cost and traffic status on the road network, and cooperate with all other vehicles when they choose routes. However, in practice, it is not easy for all drivers to obtain full knowledge about traffic status and behave cooperatively in routing with other vehicles actively. Therefore, route guidance systems (Boyce, 1988; Lentzakis et al., 2018; Taale et al., 2015) and road pricing (Brownstone & Small, 2005; Yang & Bell, 1997) has been adopted by traffic managers to push the system towards the system optimal distribution.

Though drivers can be guided or induced by route guidance systems and road pricing, the decision making is still in the hands of a human driver. With the emergence of connected and automatic technologies, Connected Autonomous Vehicles (CAVs) provide opportunities to achieve the system optimal distribution. Ideally, in a fully connected and automated environment, CAVs can share information about traffic status and behave cooperatively in routing with traffic signals to reduce total travel time. However, limited by the price, ethical worries and vehicle-renewal periods, CAVs cannot replace Human-Driven Vehicles (HDVs) to achieve a high penetration rate in a short time, which means the system will operate in the mixed condition. As HDVs might not be connected, they might not cooperate with other vehicles actively and make their own routing decisions to maximise personal utility, even when connected. This raises a crucial question as to whether travel efficiency can still be improved with only a part of the vehicular flow cooperatively changing its routing in the mixed flow.

Against this background, the main aim of this chapter is to investigate whether travel efficiency can be improved with a part of the vehicular flow cooperatively changing its routing and identify a strategy for CAVs to push the system towards the system optimal distribution dynamically. The specific objectives of this chapter are as follows:

(1) To investigate the dynamic process of routing and signal timing in the mixed flow of CAVs and HDVs.

(2) To explore whether travel efficiency can be improved with a part of the vehicular flow cooperatively changing its routing in the mixed flow conditions.

(3) To identify a strategy for CAVs to push the system towards system optimal distribution dynamically.

5.2 Routing behaviour of HDVs and CAVS towards user equilibrium and system optimal distribution

5.2.1 Notations

Some notations used in this chapter are listed in Table 5.1.

Table 5.1 Notations used in this chapter

Notations	Definitions
$G(N, L)$	A network including N nodes, and L links
od	Index of OD
a	Index of link
p	Index of route
n	Index of node
s	Index of signal phases
v_a	Total flow on link a
v_{a_CAVs}	CAVs flow on link a
v_{a_HDVs}	HDVs flow on link a
$C_a(\boldsymbol{v}, \boldsymbol{\psi})$	Travel cost on link a
$n^{(s)}$	Nodes n controlled by a signal with has s^{th} phases
$\psi_a^{n^{(s)}}(\xi_a^{n^{(s)}}, \sigma_a^{n^{(s)}})$	Signal setting of s^{th} phase at signal-controlled nodes n for link a
ξ	Cycle time
σ	Durations of green as proportions of cycle time
$T_a(\boldsymbol{v})$	Travel time on link a, when is not controlled by signal
$D_a^{(s)}(\boldsymbol{v}, \psi_a^{n^{(s)}}(\xi_a^{n^{(s)}}, \sigma_a^{n^{(s)}}))$	Delay on link a
Q_a	Saturation flow on link a

5.2.2 HDVs' routing behaviour towards User equilibrium

As discussed in section 2.5, drivers can achieve UE by accumulating knowledge about the network via day-to-day re-routing without any cooperation. In order to find the shortest route to achieve UE, drivers should have knowledge about the link travel cost $C_a(\boldsymbol{v}, \boldsymbol{\psi})$, which is related to the link a, link flow $\boldsymbol{v}$ and signal setting $\boldsymbol{\psi}$ (Bifulco et al., 2016; Chiou, 2003; Yang & Yagar, 1995).

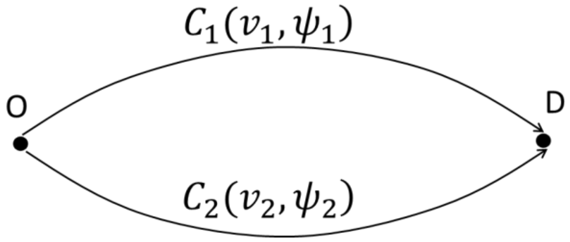

Figure 5.1 A simple network with two routes

Taking a simple network with two routes shown in Figure 5.1 as an example, to achieve UE, the journey time on all used routes should equal and less than any unused route. Based on Beckmann et al. (1956)'s formulation shown in Equation (5.1), UE can be transferred into an equivalent mathematical optimisation problem, where unique equilibrium assignments can be calculated by solving the constrained optimisation.

$$\underset{\boldsymbol{v},\boldsymbol{r}}{\text{Minimise}}\, Z(\boldsymbol{v}) = \sum_{a\in L} \int_{v=0}^{v_a} C_a\,(v) dv \tag{5.1}$$

Subject to

$$\left.\begin{array}{l} r_p \geq 0 \quad \forall p \in P_{od} \\ \sum_{p\in P_{od}} r_p = R_{od} \end{array}\right\} \quad \forall od$$

$$v_a = \sum_{od} \sum_{p\in P_{od}} r_p\, \delta_a^p \quad \forall\, a\epsilon L$$

According to the nature of calculus, the objective $Z(\boldsymbol{v})$ is equal to the area between the cost-flow function and axis, which is the sum of blue and orange areas in Figure 5.2. When the signal setting ψ is given, the travel cost function is a determinate function related to the flow v on this route, and the UE can be achieved when travel cost on two routes are the same.

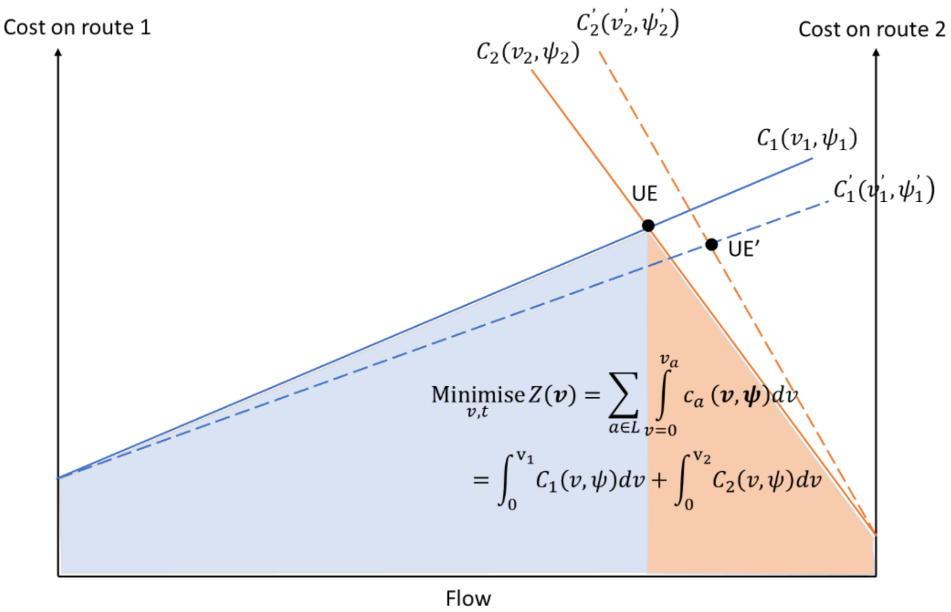

* the link travel cost function is simplified to a linear equation in the plot and analytical model, but it is non-linear in the simulation and practice.

Figure 5.2 User equilibrium for a simple network with two routes

However, when signal timing is changed, the cost-flow function will change correspondingly, which means the travel cost on route 1 become different from the travel cost on route 2. In this case, some drivers will shift from the higher-cost route to the lower-cost route. A different UE can be achieved with this re-routing process, which demonstrates to some extent drivers' route choices can be influenced by signal timing.

5.2.3 CAVs' routing behaviour towards System optimal distribution

Different from UE, the system optimal distribution aims to reduce total travel time to improve system efficiency. It can be calculated by solving the constrained optimisation problem as Equation (5.2):

$$\underset{\boldsymbol{v},\boldsymbol{r}}{\text{Minimise}}\, W(\boldsymbol{v}) = \sum_{a \in L} v_a\, C_a(\boldsymbol{v}, \boldsymbol{\psi}) \tag{5.2}$$

Subject to

$$\left.\begin{array}{l} r_p \geq 0 \quad \forall p \in P_{od} \\ \sum_{p \in P_{od}} r_p = R_{od} \end{array}\right\} \quad \forall od$$

$$v_a = \sum_{od} \sum_{p \in P_{od}} r_p\, \delta_a^p \quad \forall\, a \epsilon L$$

As shown in Figure 5.3, when the signal timing is given and the system reached a UE, total travel time $W(\boldsymbol{v})$ equal to the area of the red rectangle. However, as discussed in section 5.1, user equilibrium might not be the optimal solution for the whole system. If vehicles can behaviours cooperatively in routing, for example, some CAVs shifting from route 2 to route 1, the new total travel time $W(\boldsymbol{v})$ becomes the sum of two blue rectangle areas. When the sum of two blue rectangle areas smaller than the red rectangle area (i.e. blue areas smaller than red areas in Figure 5.3), the total travel time is reduced compared with UE.

Though system efficiency can be improved with CAVs behaviour cooperatively in routing to achieve SO, it should be noted that this status might not be stable in the mixed condition. As HDVs might not be connected, they might not cooperate with other vehicles actively. When travel cost on route 1 higher than route 2, some HDVs might shift from route 1 to route 2, which will push the system back to a user equilibrium. To investigate this dynamic process, an analytical model will be proposed and discussed in the next section.

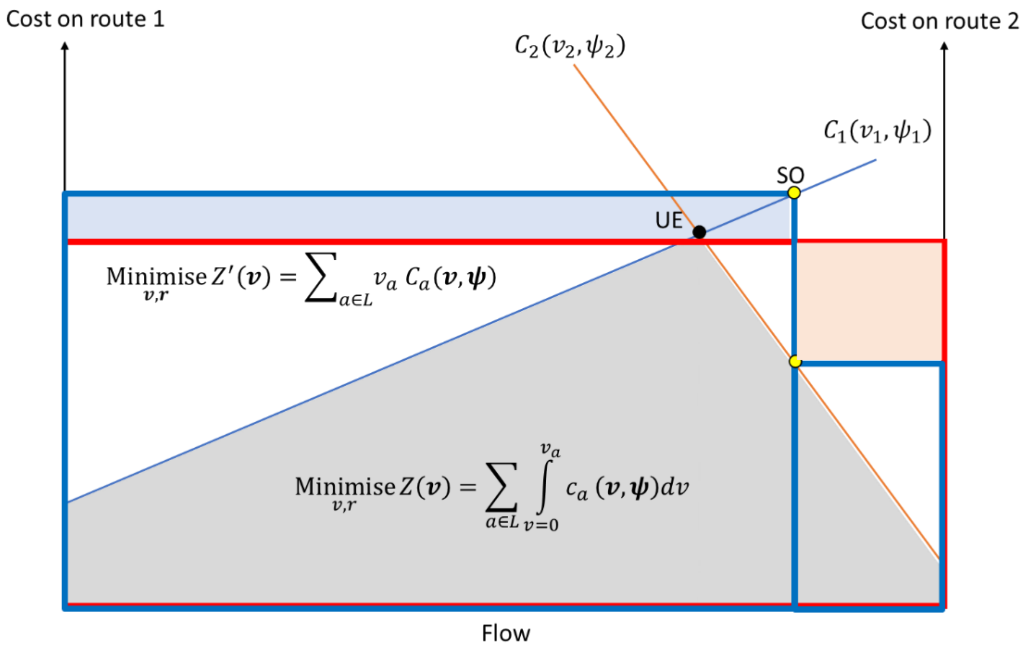

* the link travel cost function is simplified to a linear equation in the plot and analytical model, but it is non-linear in the simulation and practice.

Figure 5.3 System optimal distribution for a simple network with two routes

5.3 The dynamic process towards system optimal distribution

As discussed in Section 5.2.3 above, though total travel time can be reduced with CAVs behaviour cooperatively in routing to push the system towards SO distribution, HDVs might push the system back to the user equilibrium. A model has been proposed to demonstrate this dynamic process shown in Figure 5.4, and the behaviour pattern of CAVs and HDVs can be summarised as follow:

- **HDVs' routing behaviour**
  In the mixed flow, HDVs will seek the shortest route to maximise personal utility. In other words, minimise private cost.

$$e_p \begin{Bmatrix} > 0 \;\Rightarrow\; C_p = C_{od}^{*} \\ = 0 \;\Rightarrow\; C_p \geq C_{od}^{*} \end{Bmatrix} \quad \forall p \epsilon P_{od}, \forall od$$

  For any individual HDV, if the travel cost on the route to the destination is higher than the shortest route, that route will not be used by HDV. When all HDVs seek the shortest route, at the macroscopic level, the following objective should be satisfied.

$$\underset{v_{HDVs}, r_{HDVs}}{\text{Minimise}}\; Z(\boldsymbol{v}) = \sum_{a \in L} \int_{v=0}^{v_a} c_a\,(\boldsymbol{v}, \boldsymbol{\psi}) dv$$

- **CAVs' routing behaviour**
  In the mixed flow, CAV can routing cooperatively (can be achieved by behaviour regulation, cooperation with centralised control or cooperation with compensation) to reduce total travel time. In other words, minimise public cost.

$$e_p \begin{Bmatrix} > 0 \;\Rightarrow\; C_p + \sum_{\forall a} \delta_p^a v_a \dfrac{\partial c_a(v_a, \boldsymbol{\psi})}{\partial v_a} = C_{od}^{*} \\ = 0 \;\Rightarrow\; C_p + \sum_{\forall a} \delta_p^a v_a \dfrac{\partial c_a(v_a, \boldsymbol{\psi})}{\partial v_a} \geq C_{od}^{*} \end{Bmatrix} \quad \forall p \epsilon P_{od}, \forall od$$

  As CAVs will routing cooperatively to minimise public cost, at the macroscopic level, the following objective should be satisfied.

$$\underset{v_{CAVs}, r_{CAVs}}{\text{Minimise}}\; \boldsymbol{W}(\boldsymbol{v}) = \sum\nolimits_{a \in L} v_a\, C_a(\boldsymbol{v}, \boldsymbol{\psi})$$

Departure from initial status, drivers (including HDVs and CAVs) can achieve user equilibrium by accumulating knowledge about the network via day-to-day routing without any cooperation. As CAVs can share information about traffic status and behave cooperatively in routing, solving the optimisation problem $W(\boldsymbol{v})$ can help CAVs identify how many vehicles should re-routing cooperatively to achieve system optimal distribution. When the system reaches SO, the change in route travel cost will be experienced by HDVs. Then to reduce individual travel time, HDVs will choose a route with less journey time. These two processes will interact with each other dynamically until the system reaching a stable status.

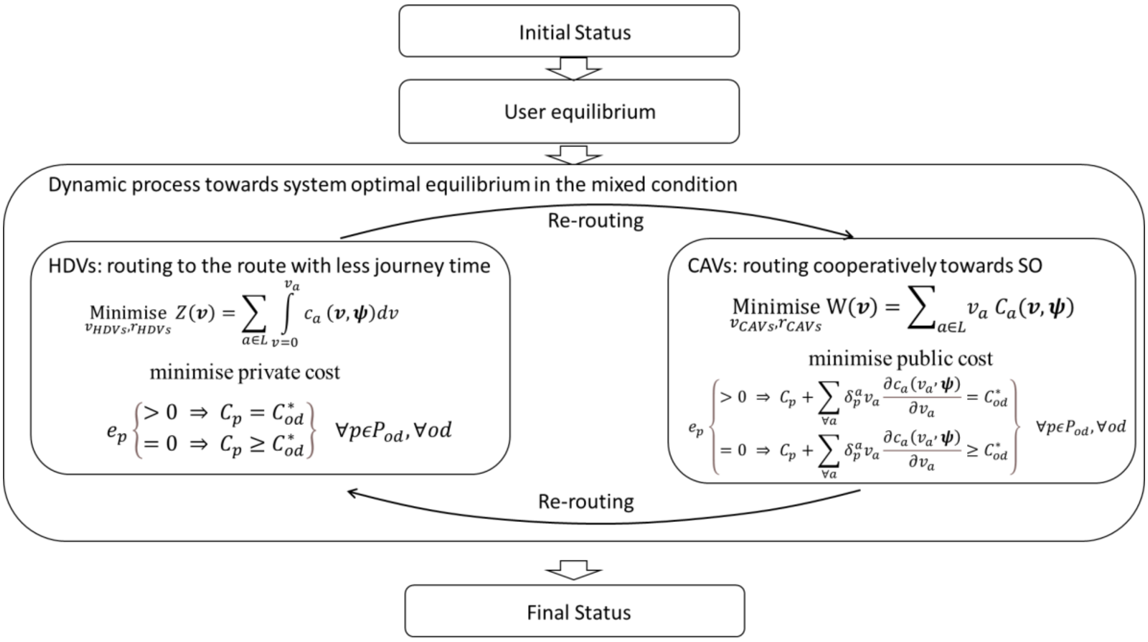

Figure 5.4 The model of dynamic process towards system optimal distribution

5.3.1 A numerical analysis of a simple network

Taking a simple network with two routes shown in Figure 5.1 as an example, assuming signal timing is given; demand from O to D is R; CAVs penetration rate is α; the cost-flow functions are $C(v_1) = av_1 + b$ on the upper route and $C(v_2) = cv_2 + d$ on the lower route (an algebraic analysis of this simple network is attached in appendix 1.

Arbitrarily setting $\alpha = 50\%$; $a = 1$; $b = 20$; $c = 5$; $b = 4$, the numerical example of the dynamic process is shown in Table 5.2 and Figure 5.5. It can be observed that total travel time fluctuates between UE and SO during the dynamic process. When CAVs behave cooperatively shifting from route 2 to route 1, total travel time can be reduced. However, the travel cost difference on the two routes makes HDVs re-routing from route 1 to route 2. Eventually, all the CAVs on route 2 will shift to route 1 and the system will reach a stable status (UE), as $\frac{cR-b+d}{a+c} - \frac{2cR-b+d}{2(a+c)} = 14 - 15.3 < 0$; $\alpha\frac{aR+b-d}{2a+c} - (1-\alpha)\frac{cR-b+d}{2a+c} = 3 - 7 < 0$.

For the same network, when the CAV penetration rate is increased to 75%, a different stable status can be achieved, and the results are shown in Table 5.3 and Figure 5.6.

Table 5.2 Dynamic process towards system optimal distribution (CAVs penetration rate 50%)

	Flow				Cost		
	R1flow (HDVs)	R2 flow (HDVs)	R1 flow (CAVS)	R2 flow (CAVs)	R1 cost	R2 cost	Total travel time
Status 1(50%)	7	3	7	3	34	34	680
Status 2(50%)	7	3	8.3	1.7	35.3	27.5	669.34
Status 3(50%)	5.7	4.3	8.3	1.7	34	34	680
Status 4(50%)	5.7	4.3	9.6	0.4	35.3	27.5	669.34
Status 5(50%)	4.4	5.6	9.6	0.4	34	34	680
Status 6(50%)	4.4	5.6	10	0	34.4	32	674.56
Status 7(50%)	4	6	10	0	34	34	680

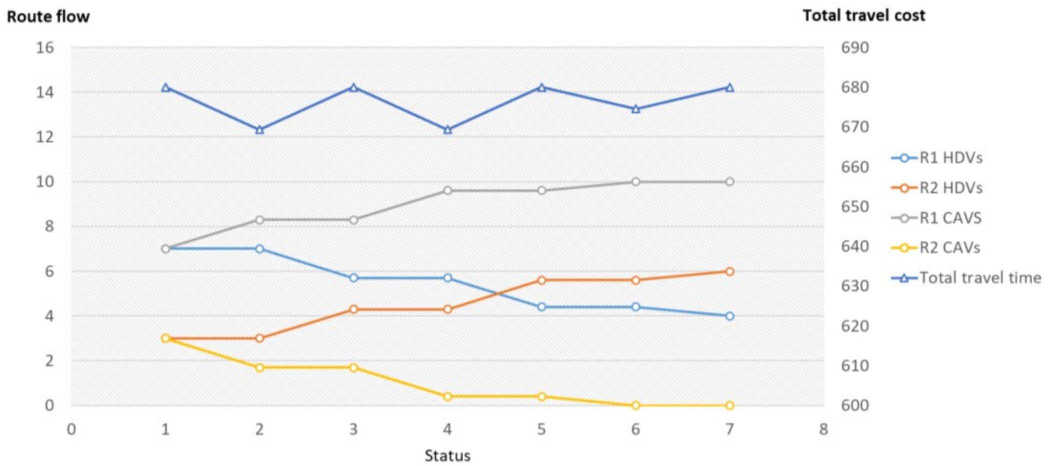

Figure 5.5 Dynamic process towards system optimal distribution (CAVs penetration rate 50%)

According to Table 5.3 and Figure 5.6, the total travel time is still fluctuating between UE and SO during the dynamic process. Eventually, the system reaches a near system optimal distribution status. This is because after status 7, though travel cost on route 1 is higher than route 2, all the HDVs already have shifted from route 1 to route 2. The remaining CAVs on route 1 can behave cooperatively with CAVs on route 2 to push the system towards a near system optimal distribution status, as $\frac{cR-b+d}{a+c} - \frac{2cR-b+d}{2(a+c)} = 14 - 15.3 < 0; 0 < \alpha\frac{aR+b-d}{2a+c} - (1-\alpha)\frac{cR-b+d}{2a+c} = 4.5 - 3.5 < 1.3.$

Table 5.3 Dynamic process towards system optimal distribution (CAVs penetration rate 75%)

	Flow				Cost		
	R1flow (HDVs)	R2 flow (HDVs)	R1 flow (CAVS)	R2 flow (CAVs)	R1 cost	R2 cost	Total travel time
Status 1(75%)	3.5	1.5	10.5	4.5	34	34	680
Status 2(75%)	3.5	1.5	11.8	3.2	35.3	27.5	669.34
Status 3(75%)	2.2	2.8	11.8	3.2	34	34	680
Status 4(75%)	2.2	2.8	13.1	1.9	35.3	27.5	669.34
Status 5(75%)	0.9	4.1	13.1	1.9	34	34	680
Status 6(75%)	0.9	4.1	14.4	0.6	35.3	27.5	669.34
Status 7(75%)	0	5	14.4	0.6	34.4	32	674.56
Status 8(75%)	0	5	15	0	35	29	670

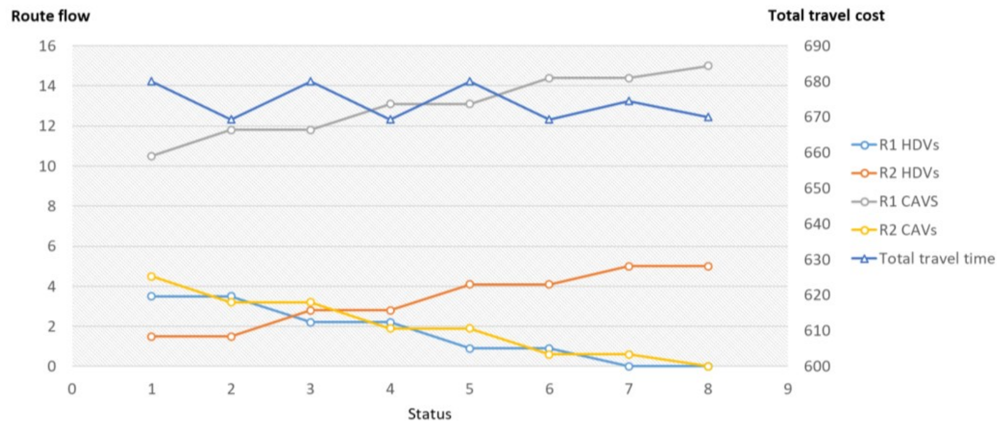

Figure 5.6 Dynamic process towards system optimal distribution (CAVs penetration rate 75%)

Though the numerical analysis on the simple network demonstrated that it is possible to use CAVs to influence HDVs' day to day routing, the assumption of the cost-flow relationship and parameters are arbitrary, which might affect the results for real-life context. In addition, the simple network only has two routes with one OD pair. To address these limitations, a numerical analysis of the Nguyen-Dupuis network with multiple OD pairs and the Bureau of Public Roads (BPR) cost-flow function will be conducted in Subsection 5.3.2. Then a simulation case study will be conducted in Section 5.4.

5.3.2 A numerical analysis of a larger network with multiple OD pairs

It has been demonstrated in Section 5.3.1 that CAVs can influence HDVs' day-to-day routing and push the system towards system optimal distribution dynamically. To investigate whether the proposed approach can be applied on a larger network with multiple OD pairs, the Nguyen-Dupuis Network (Nguyen & Dupuis, 1984) with multiple OD pairs are used in the numerical analysis.

The Nguyen-Dupuis Network includes 13 nodes, 19 links and 4 OD pairs. For these 4 OD pairs, there are 24 different routes, which present as $r(i, j, k)$ where i is the origin node; j is the destination node and k is the k^{th} route from i to j. Assuming the link travel cost under given signal timing is calculated by the Bureau of Public Roads (BPR) function that $C_a(v_a) = t_a^0[1 + \alpha(\frac{v_a}{Q_a})^\beta]$, where t_a^0 is the free-flow travel time on the link a and Q_a is the capacity on the link a. The parameter of α and β are set as 0.15 and 4, which are commonly used in the existing literature.

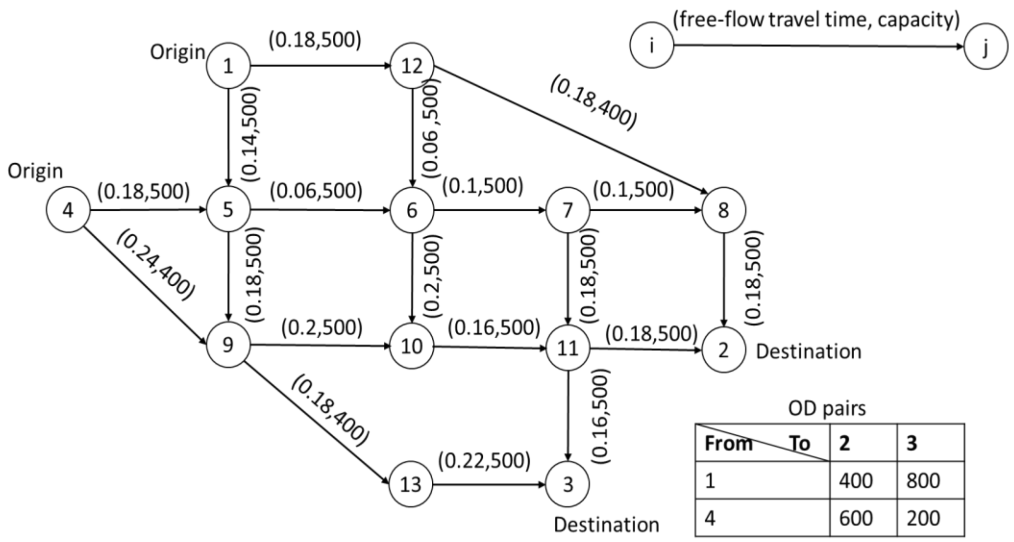

Figure 5.7 Nguyen-Dupuis Network (Nguyen & Dupuis, 1984; Xie et al., 2019)

To get the initial user equilibrium, Equation (5.1) based on the Nguyen-Dupuis Network is solved by the GRG nonlinear solver. When the penetration rate of CAVs is set to 50%, the distribution of CAVs and HDVs flow on the initial user equilibrium point are shown in Table 5.4 iteration 0, where the journey time on all used routes is equal to or less than the journey time on unused routes (Wardrop first principle satisfied) and the Total Travel Time (TTT) is 1584.59.

To push the system towards SO distribution, CAVs can re-route cooperatively by solving Equation (5.3), where HDVs still use the same routes, but CAVs will re-route cooperatively to reduce total travel time. The results are solved by GRG nonlinear solver and shown in Table 5.4 iteration 1 and the total travel time is reduced to 1552.91.

$$\underset{v_{CAVs}, r_{CAVs}}{\text{Minimise}}\ \boldsymbol{W}(\boldsymbol{v}) = \sum\nolimits_{a\in L} v_a\, C_a(\boldsymbol{v}, \boldsymbol{\psi}) \tag{5.3}$$

Subject to

$$\left.\begin{matrix} r_p \geq 0 \quad \forall p \in P_{od} \\ \sum_{p\in P_{od}} r_p = R_{od} \end{matrix}\right\} \quad \forall od$$

$$v_a = \sum_{od} \sum_{p\in P_{od}} r_p\, \delta_a^p \quad \forall\, a\epsilon L$$

Table 5.4 Dynamic process on Nguyen-Dupuis network (first three iterations)

	Iteration 0				Iteration 1				Iteration 2			
	CAVs		HDVs		CAVs		HDVs		CAVs		HDVs	
	flow	cost	flow	cost	flow	cost	flow	cost	flow	cost	flow	cost
r(1,2,1)	0.00	0.81	0.00	0.81	0.00	0.72	0.00	0.72	0.00	0.79	0.00	0.79
r(1,2,2)	0.00	0.81	0.00	0.81	0.00	0.78	0.00	0.78	0.00	0.82	0.00	0.82
r(1,2,3)	0.00	0.81	0.00	0.81	0.00	0.81	0.00	0.81	0.00	0.82	0.00	0.82
r(1,2,4)	0.00	0.89	0.00	0.89	0.00	0.91	0.00	0.91	0.00	0.90	0.00	0.90
r(1,2,5)	0.00	0.81	0.00	0.81	0.00	0.75	0.00	0.75	0.00	0.79	0.00	0.79
r(1,2,6)	0.00	0.81	0.00	0.81	0.00	0.81	0.00	0.81	0.00	0.82	0.00	0.82
r(1,2,7)	0.00	0.81	0.00	0.81	0.00	0.85	0.00	0.85	0.00	0.82	0.00	0.82
r(1,2,8)	200.00	0.71	200.00	0.71	200.00	0.67	200.00	0.67	200.00	0.69	200.00	0.69
r(1,3,1)	119.83	0.83	119.83	0.83	49.01	0.78	119.83	0.78	49.01	0.83	168.99	0.83
r(1,3,2)	68.15	0.83	68.15	0.83	45.13	0.81	68.15	0.81	45.13	0.83	71.50	0.83
r(1,3,3)	0.00	0.91	0.00	0.91	11.63	0.91	0.00	0.91	11.63	0.91	0.00	0.91
r(1,3,4)	119.23	0.83	119.23	0.83	176.90	0.84	119.23	0.84	176.90	0.83	90.15	0.83
r(1,3,5)	53.22	0.83	53.22	0.83	64.09	0.81	53.22	0.81	64.09	0.83	39.84	0.83
r(1,3,6)	39.56	0.83	39.56	0.83	53.23	0.84	39.56	0.84	53.23	0.83	29.52	0.83
r(4,2,1)	140.44	0.81	140.44	0.81	24.07	0.73	140.44	0.73	24.07	0.80	212.28	0.80
r(4,2,2)	22.00	0.81	22.00	0.81	83.32	0.79	22.00	0.79	83.32	0.83	0.00	0.83
r(4,2,3)	19.31	0.81	19.31	0.81	67.94	0.82	19.31	0.82	67.94	0.83	0.00	0.83
r(4,2,4)	0.00	0.95	0.00	0.95	7.18	0.92	0.00	0.92	7.18	0.90	0.00	0.90
r(4,2,5)	118.25	0.81	118.25	0.81	117.50	0.82	118.25	0.82	117.50	0.80	87.72	0.80
r(4,3,1)	0.00	0.83	0.00	0.83	20.41	0.79	0.00	0.79	20.41	0.84	0.00	0.84
r(4,3,2)	0.00	0.83	0.00	0.83	0.04	0.82	0.00	0.82	0.04	0.84	0.00	0.84
r(4,3,3)	0.00	0.91	0.00	0.91	7.40	0.92	0.00	0.92	7.40	0.91	0.00	0.91
r(4,3,4)	0.00	0.83	0.00	0.83	0.00	0.82	0.00	0.82	0.00	0.81	0.00	0.81
r(4,3,5)	100.00	0.75	100.00	0.75	72.14	0.76	100.00	0.76	72.14	0.73	100.00	0.73
TTT	1584.59				1552.91				1571.80			

Comparing route travel cost on iteration 0 and iteration 1, it can be found that when CAVs re-route cooperatively to push the system towards SO distribution. For example, 69.99 CAVs actively re-route from $r(1,3,1)$ to other routes. The re-routeing of CAVs will influence travel cost among the routes. For example, HDVs using $r(1,3,1)$ will enjoy travel cost reduction from 0.83 to 0.78. However, HDVs using $r(1,3,4)$ will suffer a travel cost increase from 0.83 to 0.84. This change of route travel cost will be experienced by HDVs and leads to further re-route of HDVs to seek the shortest route.

As HDVs is seeking the shortest route to maximise personal utility, according to the Wardrop first principle, the journey time on all used routes by HDVs should equal or less than the journey time on unused routes. This distribution can be solved by Equation (5.4), where CAVs still use the same route, but HDVs will re-route to maximise personal utility. The results are solved by the GRG nonlinear solver and shown in Table 5.4 iteration 2. It can be found that the re-route of HDVs leads to an increase of total travel time from 1552.91 to 1571.80, but the journey time on all used routes by HDVs is equal to or less than the journey time on unused routes (i.e., HDVs maximised personal utility).

$$\underset{v_{HDVs}, r_{HDVs}}{\text{Minimise}}\ W(\boldsymbol{v}) = \sum_{a \in L} \int_{v=0}^{v_a} c_a\,(\boldsymbol{v}, \boldsymbol{\psi})dv \tag{5.4}$$

Subject to

$$\left.\begin{array}{l} r_p \geq 0 \quad \forall p \in P_{od} \\ \sum_{p \in P_{od}} r_p = R_{od} \end{array}\right\} \quad \forall od$$

$$v_a = \sum_{od} \sum_{p \in P_{od}} r_p\, \delta_a^p \quad \forall\, a \epsilon L$$

These two processes (HDVs seeking the shortest route and CAVs routing cooperatively to reduce total travel time) interact with each other dynamically. As shown in Table 5.5, for the given Nguyen-Dupuis network with 50% CAVs penetration rate, on the iteration15, though CAVs re-routed to reduce total travel time (from 1580.97 on iteration14 to 1580.96 on iter15), HDVs will not experience the change of route travel cost. Meanwhile, CAVs cannot further reduce total travel time without the active cooperation of HDVs. In this case, the system is converted to a stable status. Comparing to the initial user equilibrium, CAVs successfully reduce total travel time from 1584.59 to 1580.96 dynamically.

Table 5.5 Dynamic process on Nguyen-Dupuis network (last three iterations)

	Iteration 13				Iteration14				Iteration 15			
	CAVs		HDVs		CAVs		HDVs		CAVs		HDVs	
	flow	cost	flow	cost	flow	cost	flow	cost	flow	cost	flow	cost
r(1,2,1)	0.00	0.79	0.00	0.79	0.00	0.79	0.00	0.79	0.00	0.79	0.00	0.79
r(1,2,2)	0.00	0.82	0.00	0.82	0.00	0.82	0.00	0.82	0.00	0.82	0.00	0.82
r(1,2,3)	0.00	0.82	0.00	0.82	0.00	0.82	0.00	0.82	0.00	0.82	0.00	0.82
r(1,2,4)	0.00	0.92	0.00	0.92	0.00	0.92	0.00	0.92	0.00	0.92	0.00	0.92
r(1,2,5)	0.00	0.79	0.00	0.79	0.00	0.79	0.00	0.79	0.00	0.79	0.00	0.79
r(1,2,6)	0.00	0.82	0.00	0.82	0.00	0.82	0.00	0.82	0.00	0.82	0.00	0.82
r(1,2,7)	75.98	0.82	0.00	0.82	75.98	0.82	0.00	0.82	76.47	0.82	0.00	0.82
r(1,2,8)	124.02	0.66	200.00	0.66	124.02	0.66	200.00	0.66	123.53	0.66	200.00	0.66
r(1,3,1)	0.00	0.83	391.62	0.83	0.00	0.83	395.40	0.83	0.00	0.83	395.40	0.83
r(1,3,2)	0.00	0.83	0.00	0.83	0.00	0.83	0.00	0.83	0.00	0.83	0.00	0.83
r(1,3,3)	0.00	0.93	0.00	0.93	0.00	0.93	0.00	0.93	0.00	0.93	0.00	0.93
r(1,3,4)	227.94	0.83	7.67	0.83	227.94	0.83	4.60	0.83	229.16	0.83	4.60	0.83
r(1,3,5)	0.00	0.83	0.02	0.83	0.00	0.83	0.00	0.83	0.00	0.83	0.00	0.83
r(1,3,6)	172.06	0.83	0.68	0.83	172.06	0.83	0.00	0.83	170.84	0.83	0.00	0.83
r(4,2,1)	0.00	0.79	300.00	0.79	0.00	0.79	300.00	0.79	0.00	0.79	300.00	0.79
r(4,2,2)	0.00	0.82	0.00	0.82	0.00	0.82	0.00	0.82	0.00	0.82	0.00	0.82
r(4,2,3)	0.00	0.82	0.00	0.82	0.00	0.82	0.00	0.82	0.00	0.82	0.00	0.82
r(4,2,4)	91.65	0.91	0.00	0.91	91.65	0.91	0.00	0.91	91.82	0.91	0.00	0.91
r(4,2,5)	208.35	0.82	0.00	0.82	208.35	0.82	0.00	0.82	208.18	0.82	0.00	0.82
r(4,3,1)	0.00	0.83	0.00	0.83	0.00	0.83	0.00	0.83	0.00	0.83	0.00	0.83
r(4,3,2)	0.00	0.83	0.00	0.83	0.00	0.83	0.00	0.83	0.00	0.83	0.00	0.83
r(4,3,3)	0.00	0.92	0.00	0.92	0.00	0.92	0.00	0.92	0.00	0.92	0.00	0.92
r(4,3,4)	0.00	0.83	0.00	0.83	0.00	0.83	0.00	0.83	0.00	0.83	0.00	0.83
r(4,3,5)	100.00	0.74	100.00	0.74	100.00	0.73	100.00	0.73	100.00	0.74	100.00	0.74
TTT	1579.81				1580.97				1580.96			

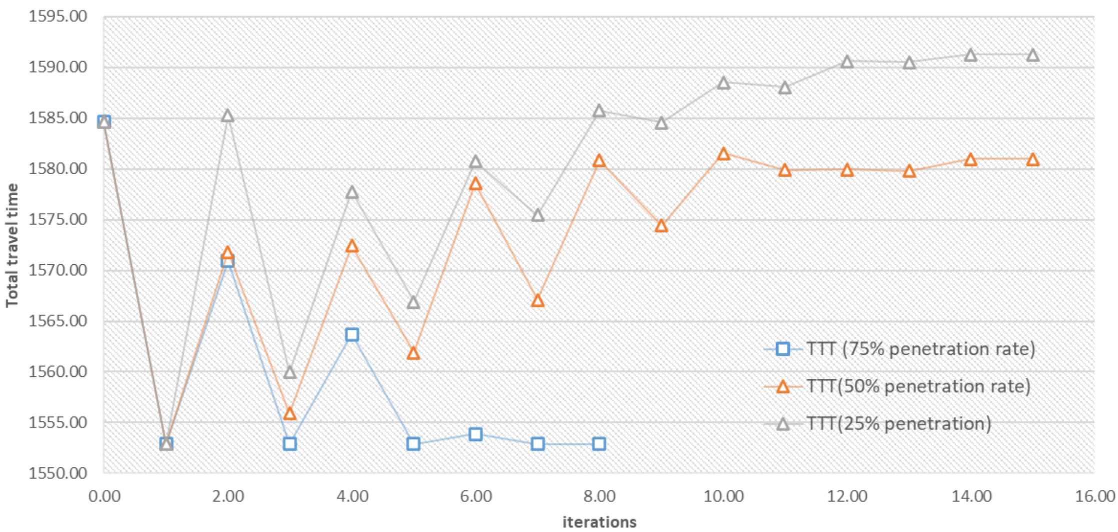

Figure 5.8 Dynamic process on the Nguyen-Dupuis network under different penetration rates and iterations

It can be observed from the iteration details shown in Figure 5.8 that when CAVs re-route cooperatively to reduce total travel time on the network, the re-routeing of CAVs will influence the travel cost on the network. If the change of travel cost is negative to HDVs, HDVs will re-route to maximise personal utility, which might increase total travel time. These two processes interact with each other dynamically, when the CAVs penetration rate is 50%, this dynamic process can push the system from UE towards (or approaching) SO. If there are more CAVs on the system (75% penetration rate), the behaviour of HDVs can be further influenced by CAVs and this dynamic process can push the system from UE to SO. It also should be noted that the stable states of the dynamic process are related to the network structure, demand and CAVs penetration rate. When the CAVs penetration rate is relatively low (such as 25% on this Nguyen-Dupuis network), though total travel time can be reduced at the beginning, the system might evolve to a point with a higher total travel time compared with initial UE.

In summary, this section has demonstrated that it is possible to influence HDVs' day-to-day routing using the CAVs and push the system towards system optimal distribution dynamically. Though individual travel time of CAVs might increase, the system total travel time can be significantly reduced. As the positive externality exists, in practice, it might be reasonable to give CAVs some form of compensation to push the system towards SO. It also should be noted that the cost-flow relationship has been simplified to a linear function or BPR in the model. However, in the real world, influenced by route length, numbers of lanes, route flow and signal timing, the cost-flow relationship is much more complex and might not be linear. Therefore, in Section 5.4, to take the non-linear cost-flow relationship and signal timing into account the link travel cost function will be calculated by SUMO (Lopez et al., 2018) simulation where CAVs are controlled by Cooperative Adaptive Cruising Control (CACC) (Milanés & Shladover, 2014).

5.4 Simulation studies of the dynamic process of routing and signal timing towards system optimal distribution in mixed conditions

The proposed analytical model in Section 5.3 demonstrates the possibility to influence HDVs' day-to-day routing using the CAVs to achieve system optimal distribution dynamically. However, the simplified linear cost-flow function and unchanged signal timing might not be satisfied in practice. Therefore, in Section 5.4, an Optimal Routing and Signal Timing (ORST) control strategy is adopted to take non-linear cost-flow relationship and signal timing into account, which can help CAVs identify how many vehicles should re-route cooperatively with other vehicles and signal controller to achieve system optimal distribution. For HDVs Proportional-switch Adjustment Process (PAP) is adopted to help HDVs accumulate knowledge about the network to achieve UE. The iterations between CAVs and HDVs are simulated in SUMO to investigate the dynamic process of routing and signal timing towards system optimal distribution in mixed conditions and cross-validate the results of the analytical model.

5.4.1 Overview of the network structure

As shown in Figure 5.9, a network $G(N = 5, L = 6)$ with five nodes, including a signal-controlled node and six links will be used for the case study. The length of each edge is set as 500 meters. For the signal timing, the yellow time between phases set as 3s and the initial green time for edge 4 and edge 5 are 30s and 70s. Drivers are not allowed to turn and travel demand from the origin point to the destination point is 2000 vehicles/h. Two available routes can be identified as follow:

- Route 1 = edge_1 edge_2 edge_4 edge_7 edge_9 edge_10
- Route 2 = edge_1 edge_3 edge_5 edge_6 edge_8 edge_10

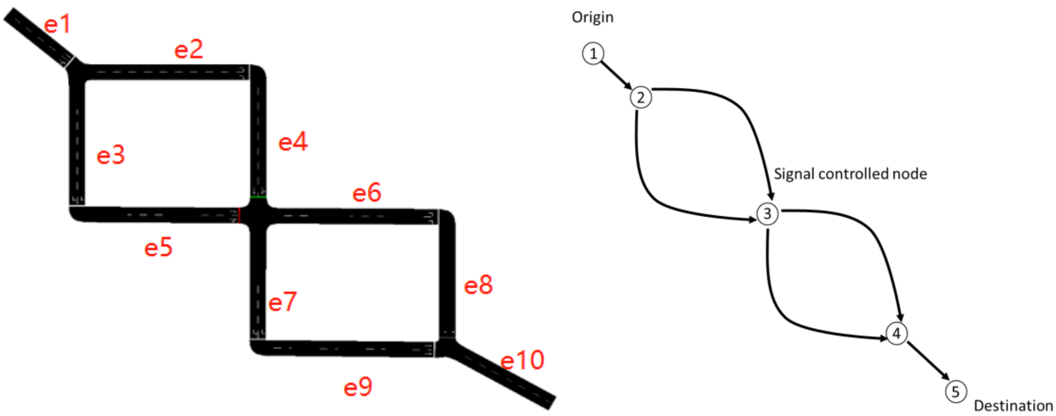

Figure 5.9 The structure of the road network

5.4.2 Initial status toward user equilibrium with PAP

Departure from a non-equilibrium initial status, assuming 50% CAVs and 75% of HDVs use route 1, meanwhile, another 50% CAVs and 25% HDVs use route 2. As the system has not reached a user equilibrium point, the difference of travel cost between two routes will be experienced by HDVs.

Based on the discussion in Section 2.5, though HDVs might not have full knowledge about travel cost and traffic status on the network, they can accumulate knowledge by day-to-day routing. The Proportional-switch Adjustment Process (PAP) (Smith, 2015; Smith, 1979a) is adopted to model the day-to-day dynamic routing process of HDVs towards user equilibrium.

Taking the network shown in Figure 5.9 as an example, on a specific day t, the travel cost via Route 1 $C_1(v_1(t))$ is lower than the travel cost using Route 2 $C_2(v_2(t))$. Some drivers will shift from Route 2 to Route 1 at day $t+1$, which is an increasing function of Route 2 flow $v_2(t)$ and the difference of travel cost on two routes. Therefore, the flow vector $\boldsymbol{v(t)} = [v_1(t), v_2(t)]$; travel cost vector $\boldsymbol{C}(\boldsymbol{v(t)}) = [C_1(\boldsymbol{v}(t)), C_2(\boldsymbol{v}(t))]$ and the changes $\Delta_1(\boldsymbol{v(t)}), \Delta_2(\boldsymbol{v(t)})$ should satisfy Equation (5.5) and Equation (5.6).

$$\Delta_1(\boldsymbol{v(t)}) = -wv_2(t)\left[C_2(\boldsymbol{v}(t)) - C_1(\boldsymbol{v}(t))\right] \tag{5.5}$$

$$\Delta_2(\boldsymbol{v(t)}) = \quad wv_2(t)\left[C_2(\boldsymbol{v}(t)) - C_1(\boldsymbol{v}(t))\right] \tag{5.6}$$

This PAP has been further extended by Smith (2015) to a general road network as Equation (5.7).

$$\Delta_{ODq}(\boldsymbol{v}) = \sum_{(r,s):r<s} w\{v_{qr}[C_{qr}(\boldsymbol{v}(t)) - C_{qs}(\boldsymbol{v}(t))]_{+}\Delta_{qrs} + v_{qs}[C_{qs}(\boldsymbol{v}(t)) - C_{qr}(\boldsymbol{v}(t))]_{+}\Delta_{qrs}\} \tag{5.7}$$

where $x_{+} = \max\{x, 0\}$; Δ_{qrs} is the swap vector from Route r to s for OD pair q.

The results of HDVs proportional-switch adjustment process towards user equilibrium in SUMO simulation are shown in Table 5.6 and Figure 5.10.

Table 5.6 Proportional-switch Adjustment Process towards user equilibrium

CAV penetration rate	Iteration	HDVs Flow (veh)		CAVs Flow (veh)		Green time (s)		Travel Cost (s)		
		r1	r2	r1	r2	r1	r2	r1	r2	total travel time
25%	500	338	1162	250	250	30	70	280	277	555592
50%	500	136	864	500	500	30	70	279	273	550452
75%	500	35	465	750	750	30	70	283	266	544475

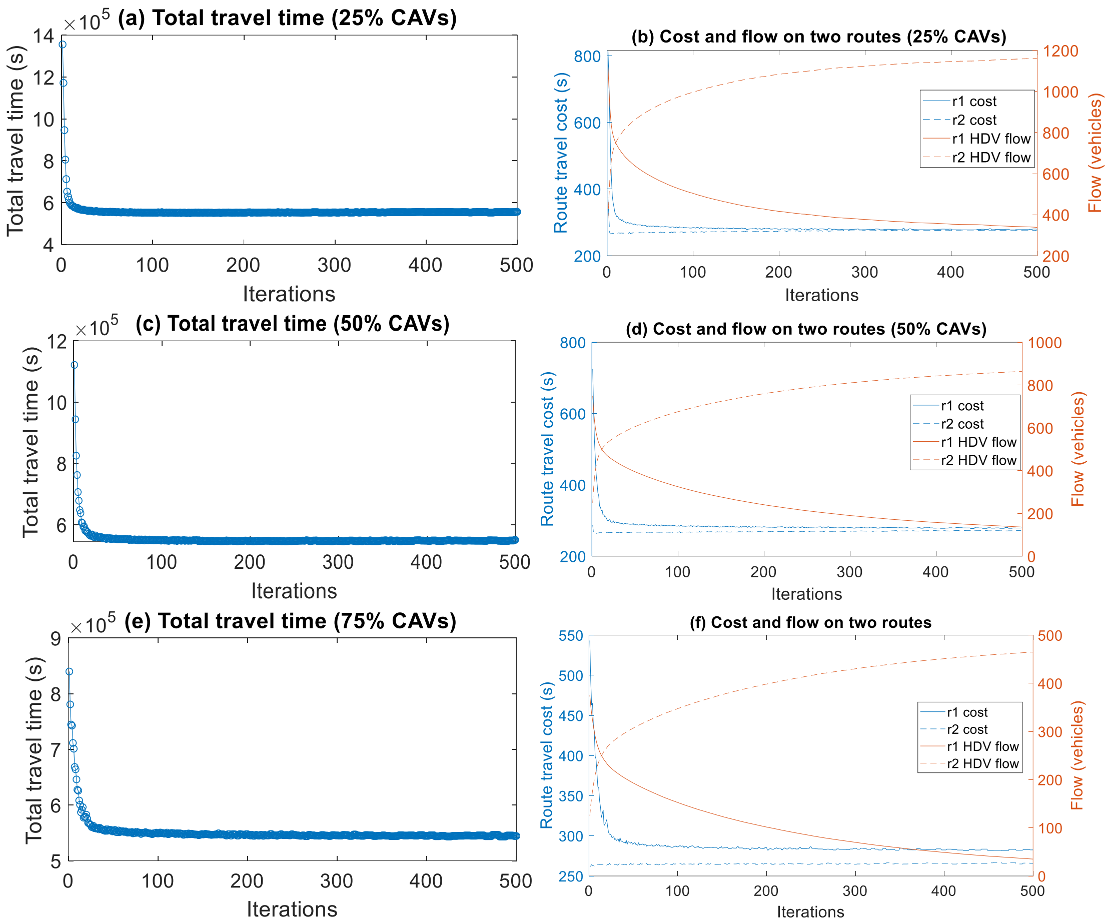

Figure 5.10 Proportional-switch Adjustment Process towards user equilibrium

It can be observed from Figure 5.10 that the decrease of route travel cost is not proportional to the route flow, which indicates that the cost-flow relationship is much more complex and not linear in the simulation or even practice. At the initial status, travel cost on the two routes is different. This difference is experienced by HDVs and leads to the shifting of HDVs from route 1 to route 2. Eventually, the system reached or approaching UE. An interesting phenomenon can also be observed in Table 5.6 that for the same network, when signal timing and demand do not change, total travel time at UE decrease with the increase of CAVs penetration rate, which indicated that congestion is alleviated with CAVs. This phenomenon is consistent with Li et al. (2020) that road capacity increase with AV penetration rate.

5.4.3 From user equilibrium toward system optimal distribution with ORST

Based on the proposed analytical model, when user equilibrium is achieved with HDVs' day-to-day routing, CAVs can behave cooperatively in routing to further push the system towards system optimal distribution. To minimise total travel time and help CAVs identify the routing strategies towards system optimal distribution, the Optimal Routing and Signal Timing (ORST) is adopted to take the non-linear cost-flow relationship and signal timing into account, which is shown as Equation (5.8).

$$\underset{v_{CAVs}, r_{CAVs}, \boldsymbol{\psi}(\gamma,\boldsymbol{\lambda})}{\text{Minimise}} W(\boldsymbol{v}, \boldsymbol{\psi}(\gamma, \boldsymbol{\lambda})) = \sum_{a\in L} v_a\, C_a(\boldsymbol{v}, \boldsymbol{\psi}) = \sum_{a\in L} v_a [T_a(\boldsymbol{v}) + \delta_a^{n^{(s)}} D_a^{n^{(s)}}(\boldsymbol{v}, \boldsymbol{\psi})] \tag{5.8}$$

Subject to

$$\left.\begin{matrix} r_p \geq 0 \quad \forall p \in P_{od} \\ \sum_{p\in P_{od}} r_p = R_{od} \end{matrix}\right\} \quad \forall od \qquad \text{(Demand constraint)}$$

$$v_a = \sum_{od} \sum_{p\in P_{od}} r_p\, \delta_a^p \quad \forall\, a \epsilon L \qquad \text{(Link flow − route flow constraint)}$$

$$\sum_{a\in L} \sum_{s\in S} \lambda_a^{n^{(s)}} \delta_a^{n^{(s)}} = 1 \ \forall\, n \epsilon N^{(\boldsymbol{S})} \qquad \text{(signal timing constraint)}$$

$$\delta_a^{n^{(s)}} = \begin{cases} 1 & if\ link\ a\ is\ controlled\ by\ s\ th\ phase\ at\ nodes\ n \\ 0 & otherwise \end{cases}$$

$$v_a \leq \sum_{s\in S} \lambda_a^{n^{(s)}} Q_a \qquad \text{(Link capacity constraint)}$$

According to Equation (5.8), link travel cost $C_a(\boldsymbol{v}, \boldsymbol{\psi})$ consist of link travel time $T_a(\boldsymbol{v})$ and delay on the link $D_a^{n^{(s)}}(\boldsymbol{v}, \boldsymbol{\psi})$. To minimise total travel time, the following constraints should be satisfied.

1) Demand constraint: For any route p, route flow r_p should be equal or greater than zero, meanwhile, the sum of all routes from the origin to the destination should equal to demand of this od pair R_{od}.

2) Link flow-route flow constraint: For any link a, the link flow v_a equal to the sum of route flows passing this link.

3) Signal timing constraint: For any signal-controlled nodes, the sum of proportional green time at different phases should equal one.

4) Link capacity constraint: the link flow v_a should not exceed the link capacity, which is related to proportional green and the saturation flow on link a.

At this stage, the lack of real-world CAVs data in the mixed condition make it is hard to calibrate the link travel cost function $C_a(\boldsymbol{v}, \boldsymbol{\psi})$ for CAVs. For replacement, CAVs are controlled by Cooperative Adaptive Cruising Control (CACC) model (Milanés & Shladover, 2014) and the link travel cost function will be calculated by SUMO simulation. Considering the link travel cost function $C_a(\boldsymbol{v}, \boldsymbol{\psi})$ calculated by simulation is nonlinear, Particle Swarm Optimisation (PSO) approach proposed by Kennedy and Eberhart (1995) where particles are designed to search nonlinear optimisation problem as a stylised representation of bird flocking or fish schooling movements, will be adopted to solve the nonlinear optimisation problem, and the results are shown in Table 5.7 and Figure 5.11.

As the PSO is used to estimate SO during a certain time slice, the population of PSO has been set as 40. Green time and flow of CAV on route1 are control variables. The value of the objective function (total travel time) is calculated by microscopic SUMO simulation. According to Figure 5.11 and Table 5.7, a system optimal distribution point can be calculated successfully with the proposed ORST within 50 iterations, which can help CAVs re-routing cooperatively to reduce total travel time by pushing the system towards system optimal distribution.

Table 5.7 ORST towards system optimal distribution

CAV penetration rate	Iteration	HDVs Flow (veh)		CAVs Flow (veh)		Green time (s)		Travel Cost (s)		
		r1	r2	r1	r2	r1	r2	r1	r2	total travel time
25%	50	338	1162	232	268	22	78	284	272	550752
50%	50	136	864	407	593	22	78	283	269	545139
75%	50	35	465	1498	2	77	23	254	298	529169

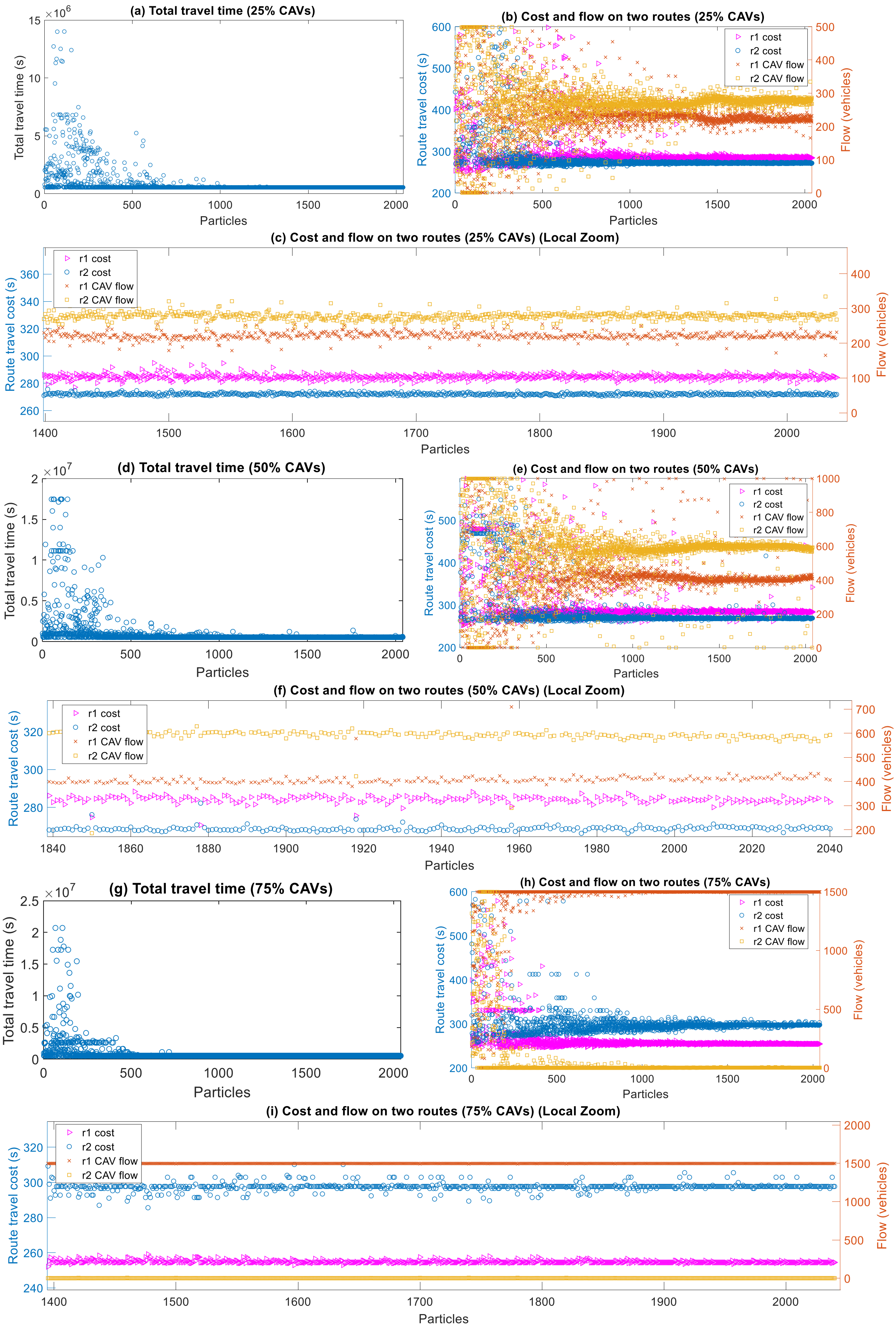

Figure 5.11 ORST towards system optimal distribution

5.4.4 Dynamic process towards system optimal distribution in mixed CAVs and HDVs flow

Based on the discussion in Section 5.3, when the system reaches UE point, to reduce total travel time, CAVs can behave cooperatively to push the system towards SO point. On the opposite, when the system reaches SO point, the change in route travel cost will be experienced by HDVs. To reduce individual travel cost, HDVs will use the route with less journey time, which might push the system back to UE point. The interaction between these two processes has been investigated with SUMO simulation and the results are shown in Table 5.8 and Figure 5.12.

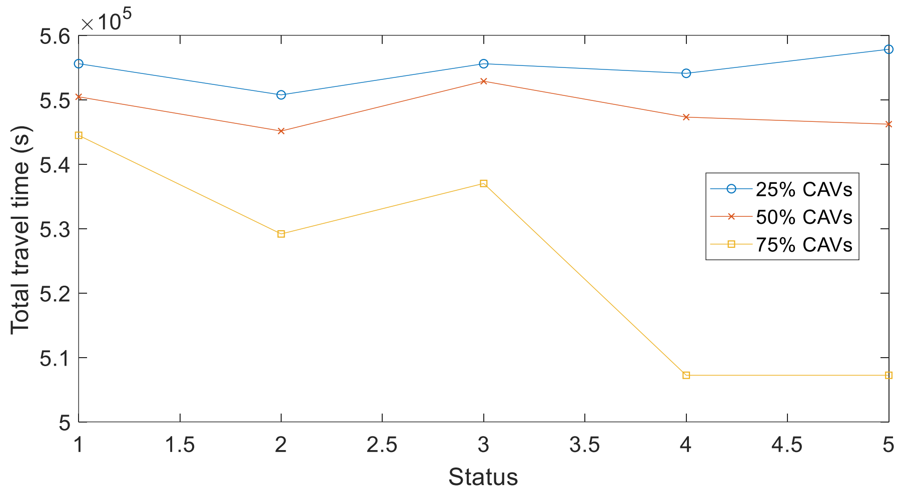

Figure 5.12 Dynamic process towards system optimal distribution in mixed condition

As shown in Table 5.8 and Figure 5.12, the results of the dynamic process with ORST in SUMO simulation, cross-validate the results in the analytical model. At a low CAVs penetration rate, the system is fluctuating between UE and SO. Though total travel time can be reduced with CAVs routing cooperatively, HDVs' re-routing will alleviate this improvement and push the system back to UE. At a middle CAVs penetration rate, the system can be pushed towards SO and reach a relatively stable status between UE and SO to reduce total travel time. At a high CAVs penetration rate, even when not all vehicles behave cooperatively with other vehicles, a part of CAVs cooperatively changing its routing can still push the system to the system optimal distribution.

Table 5.8 Dynamic process towards system optimal distribution in mixed conditions

Status	CAV penetration rate	iteration	HDVs Flow		CAVs Flow		Green time		Cost		
			r1	r2	r1	r2	r1	r2	r1	r2	TTT*
1	25%	500	338	1162	250	250	30	70	280	277	555592
	50%	500	136	864	500	500	30	70	279	273	550452
	75%	500	35	465	750	750	30	70	283	266	544475
2	25%	50	338	1162	232	268	22	78	284	272	550752
	50%	50	136	864	407	593	22	78	283	269	545139
	75%	50	35	465	1498	2	77	23	254	298	529169
3	25%	500	208	1292	232	268	22	78	278	278	555586
	50%	600	17	983	407	593	22	78	276	277	552872
	75%	800	500	0	1498	2	77	23	268	314	537003
4	25%	50	208	1292	370	130	23	77	285	274	554098
	50%	50	17	983	539	461	19	81	286	269	547297
	75%	50	500	0	1475	25	95	5	253	283	507233
5	25%	800	89	1411	370	130	23	77	281	278	557827
	50%	800	0	1000	539	460	19	81	285	269	546204
	75%	800	500	0	1475	25	95	5	253	283	507233

* TTT is total travel time

5.5 Conclusion

This chapter focuses on investigating the dynamic process of routing and signal timing in the mixed condition and whether travel efficiency can be improved with a part of the vehicular flow cooperatively changing its routing in the mixed flow of CAVs and HDVs.

The primary contributions of this chapter are two-fold. Firstly, a model has been proposed to provide an insight into the dynamic process towards system optimal distribution. As CAVs can share information about traffic status and behave cooperatively in routing, solving the optimisation problem $W(\boldsymbol{v})$ can help CAVs identify how many vehicles should re-route cooperatively to achieve system optimal distribution. However, when the system reaches SO point, the differences in route travel cost leads to the re-routing of HDVs, which alleviates the improvement of CAVs' cooperation. These two interacted processes have been investigated with the proposed analytical model, which has demonstrated that it is possible to influence HDVs' day-to-day routing using the CAVs and push the system towards system optimal distribution dynamically on a large network with multiple OD pairs.

Secondly, an Optimal Routing and Signal Timing (ORST) control strategy is adopted for CAVs to take the non-linear cost-flow relationship and signal timing into account. The results of the SUMO simulation cross-validate the results in the numerical analysis. It was shown that at middle or high CAVs penetration rate, a part of CAVs cooperatively changing its routing can push the system towards the system optimal distribution point to reduce total travel time by up to approximately 7%. This opens up other possibilities, besides road pricing, to improve system efficiency with proper routing and signal timing strategy for CAVs.

The nature of the dynamic process comes from the interaction between CAVs' routing behaviour and HDVs' routing behaviour. In the mixed flow, HDVs prefer to use the shortest route to minimise private cost, which leads the system to user equilibrium. However, user equilibrium might not be optimal at the system level, as the behaviour of minimising private cost might increase the public cost. When part of CAV re-routing to minimise public cost (for example, following the proposed ORST strategies), total travel time can be reduced. However, it should be noticed that re-routing of CAV will influence travel costs on the network. When HDVs experience the change of travel cost, HDVs will react to the CAVs' re-routing behaviour to minimise private cost. Ultimately, a static point can be researched through the dynamic process when HDVs can not minimise private cost through unilateral action.

Chapter 6 An analysis of the value of optimal routing and signal timing control strategy with CAVs

With the emergence of connected and automated technologies, Connected Autonomous Vehicles (CAVs) are able to communicate and interact with other vehicles and signal controllers. Vehicle to Vehicle (V2V) and Vehicle to Infrastructure (V2I) communications open up an opportunity to improve routing and signal timing efficiency with additional information from CAVs, such as prior travel time and signal green time. Most of the existing research on routing and signal timing for Human Driven Vehicles (HDVs) has to face the fact that human drivers only have partial knowledge about travel cost and traffic status on the road network, which typically reduces the system efficiency.

In this chapter (adapted from J3 and C3 listed in Section 1.4), the impacts of additional information from CAVs on routing and signal timing efficiency in terms of total travel time has been investigated. Firstly, the background and research context are introduced in Section 6.1. Then in Section 6.2, the proposed Optimal Routing and Signal Timing (ORST) control strategy are compared with four existing routing and signal timing strategies where drivers have different levels of information (discussed in Appendix 5). In Section 6.3, the proposed ORST control strategy is tested with a numerical case study on a larger network with multiple OD pairs. Finally, the conclusion is given in Section 6.4.

6.1 Background and research context

Efficiently assigning traffic flow and green time on a road network to reduce total travel time is a challenge to both drivers (including Human Driven Vehicles (HDVs) and Connected Autonomous Vehicles (CAVs)) and traffic managers. For an individual traveller, the shortest route, influenced by the route length, traffic flow and green time, should be identified to reduce individual travel time. For traffic managers, signal timing should be designed to reduce delay at junctions based on the demand at different phases.

Ideally, when drivers have full knowledge of the travel cost and traffic status on a road network, Wardrop's first equilibrium (WP1), also known as User Equilibrium (UE) when journey time on all routes used by vehicles is equal and less than journey time on unused routes, will be reached (Wardrop, 1952). However, in practice, it is not easy for all drivers to obtain full information about the network, which leads to the extension of Wardrop's first equilibrium by scholars. For example, Daganzo and Sheffi (1977) proposed a revised behavioural principle that "no driver believes he can improve his travel time by unilaterally changing routes". This principle allows drivers to have different levels of information about travel conditions, leading to the development of the Stochastic User Equilibrium (SUE) (Dial, 1971; Fisk, 1980).

Smith (1979a) proposed another version of revised WP1 "Consider a single driver who has travelled at least once today. He may use the same routes tomorrow. However, if he does change a route then he must change to a route which today was cheaper than the one he actually used today". The revised principle proposed by Smith (1984) makes routing become a day to day re-routing process, where drivers can accumulate knowledge about the network by day to day re-routing and will reach equilibrium eventually.

Both of these extensions demonstrated that, in practice, human drivers do not have full knowledge of traffic conditions and their routing behaviours change corresponding to the different levels of information. With the emergence of connected and automated technologies, additional information such as vehicle trajectory (Hu & Sun, 2019; Wang et al., 2020), mixed traffic conditions (Li et al., 2020) and signal timing (Mirheli et al., 2018) can be collected by sensors on CAVs, which provides an opportunity for CAVs and signal controllers to reduce total travel time cooperatively. This leads to Wardrop's second equilibrium (WP2), known as system optimal equilibrium, which states that average travel costs are minimised when all users behave cooperatively in routing (Wardrop, 1952).

Against this background, the main aim of this paper is to investigate the impacts of driver information levels on travel efficiency and propose a novel routing and signal timing control strategy to reduce total travel time when additional information from CAVs become available. The specific objectives of this chapter are as follows:

(1) To quantitatively investigate the impacts of driver information levels on travel efficiency with different routing and signal timing strategies.
(2) To explore whether travel efficiency can be improved with additional information from CAVs.
(3) To evaluate routing and signal timing control strategies to optimise total travel time with additional information from CAVs.

6.2 Case study of optimal routing and signal timing strategies under different levels of information on a simple network

6.2.1 Overview of the network structure

To investigate the impacts of information levels on routing and signal timing efficiency and whether travel efficiency can be improved with information from CAVs. Four existing routing and signal timing strategies under different levels of information and a proposed ORST control strategy for CAVs will be compared in the network $G(N = 5, L = 6)$ shown as Figure 6.1.

The network $G(N = 5, L = 6)$ has five nodes, including a signal-controlled node (Node 3) and six links. The length of each edges shown in Figure 6.1 is 500 meters. The yellow time between phases set as 3s and the initial green time for edge 4 and edge 5 are 30s and 70s. Travel demand is 2000 vehicle/h from the origin point to the destination point and four available routes can be identified as follow:

- Route 1 (Main)= edge_1 edge_2 edge_4 edge_7 edge_9 edge_10
- Route 2 (Main)= edge_1 edge_3 edge_5 edge_6 edge_8 edge_10
- Route 3= edge_1 edge_2 edge_4 edge_6 edge_8 edge_10
- Route 4= edge_1 edge_3 edge_5 edge_7 edge_9 edge_10

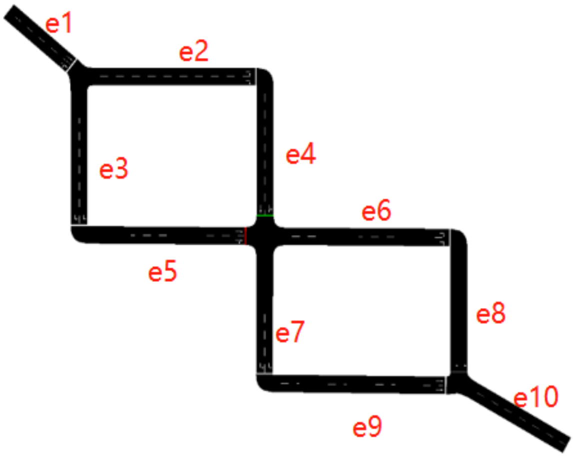

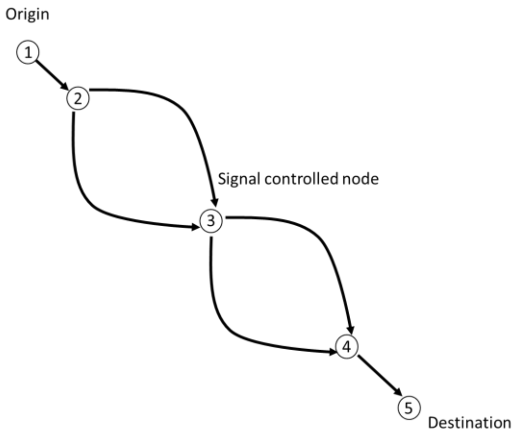

Figure 6.1 The structure of a road network

6.2.2 Routing and signal timing under different levels of information

Strategy 1: Shortest route

As discussed in Section 6.2, when the information about traffic flow and the signal timing is not available or not reliable, identifying the shortest route based on the topological structure is a reasonable strategy for drivers to minimise total travel time. The marouter, which uses a hard-coded capacity-constraint function based on the speed limit, lane number and edge priority to compute travel time in SUMO, has been applied to estimate travel cost.

As the network is symmetrical, the travel cost on each route is the same when the information about signal timing is not available. Marouter assigns 1000 vehicles to Route 3 and another 1000 vehicles to Route 4. However, the actual green timing for these two routes is different, which means that the real travel time on Route 3 and Route 4 might also be different. Based on the results of the simulation, the actual average travel cost on Route 3 and Route 4 are 2009.1s and 569.6s.

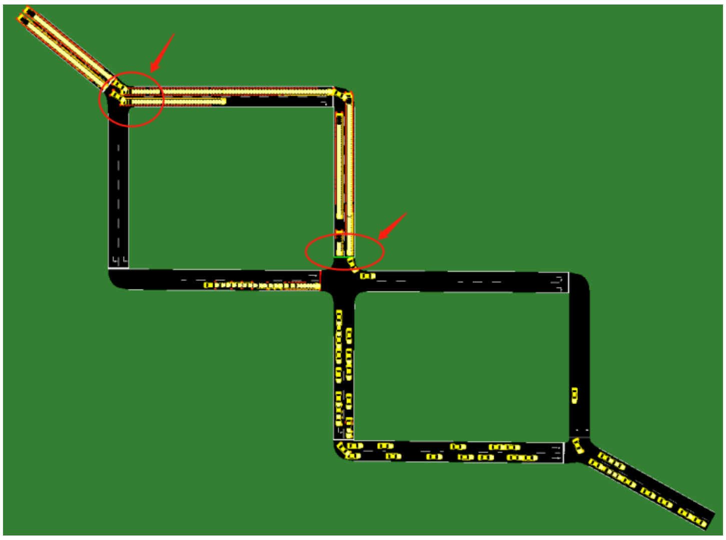

Figure 6.2 An example of shockwaves caused by congestion and queueing

The results demonstrate that though drivers can identify the shortest route based on the topological structure when the information about traffic flow and the signal timing is not available or not reliable, it is not reasonable in some circumstance. Congestion might occur when the information about flow and signal timing has been ignored. As shown in Figure 6.2, unreasonable routings cause congestion on edge 4 and the shockwaves caused by congestion and queueing further affect vehicles at Node 2.

Strategy 2: Stochastic routing

In practice, not only do drivers have information about the network topological structure, but also they have some knowledge about traffic conditions based on their driving experience, which means a stochastic user equilibrium can be achieved under this circumstance. The duarouter, based on Equation (A5.3) for SUE, in SUMO has been applied for routing, where route cost C_p is calculated from the last simulation and θ is scaled by the sum of all routes.

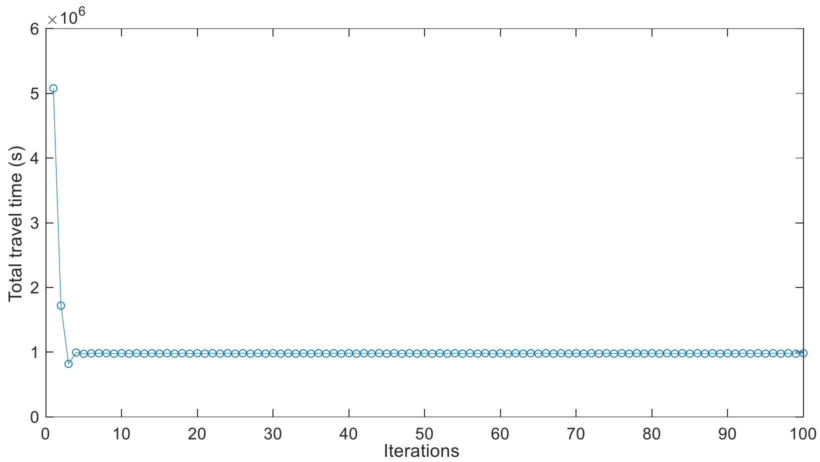

Figure 6.3 Total travel time vs iterations (SUE)

As shown in Figure 6.3, the system iteratively converges to an equilibrium point. Based on the results of the simulation, at the stochastic user equilibrium, 723 vehicles chose Route 2; 537 vehicles chose Route 3; 740 chose Route 4; the travel cost on each used route is 311s and total travel time is 984098s.

Strategy 3: PAP

As discussed in Section 1, though drivers might not have perfect information about traffic conditions, they can accumulate knowledge by day-to-day travelling. When drivers have information about yesterday's travel time, based on the proportional-switch adjustment process, some vehicles might shift from a high-cost route to a low-cost route today.

Considering the structure of the network, going straight does not need to reduce speed for turning. Route 1 and Route 2 have been set as two main routes for the proportional-switch adjustment process and the results are shown in Figure 6.4, in which the PAP strategy makes the system converge to a different equilibrium point where total travel time is 558041s.

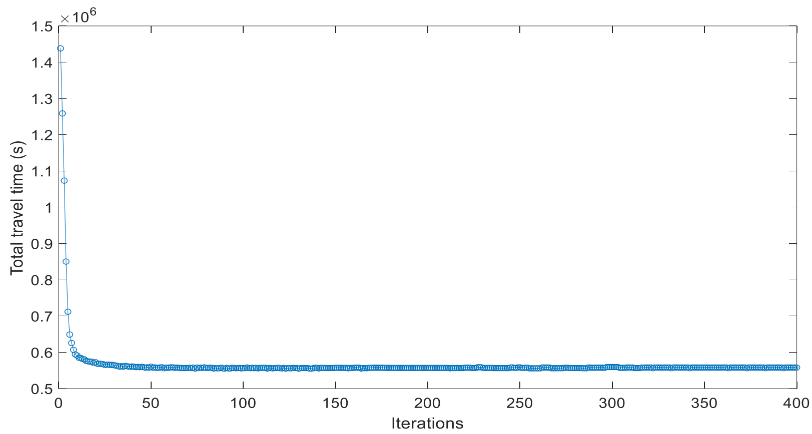

Figure 6.4 Total travel time vs iterations (PAP)

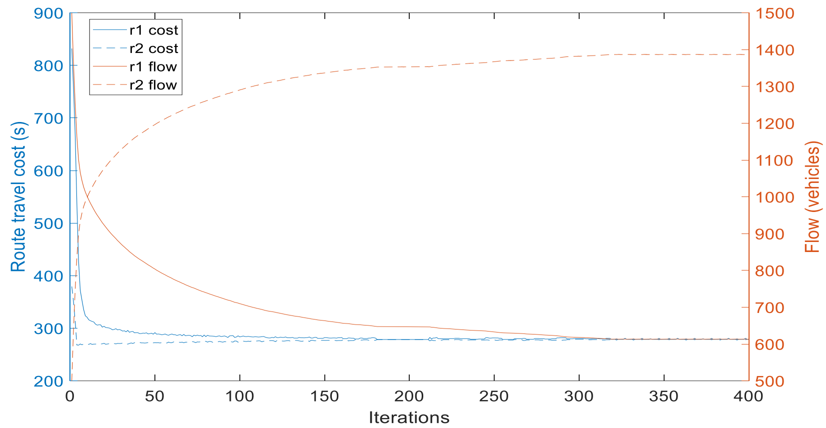

Figure 6.5 The changes of route flow and travel cost with PAP

The changes in route flow and travel cost are shown in Figure 6.5. At the beginning stage, travel cost on Route 1 $C_1(\boldsymbol{v}(t))$ is higher than travel cost on Route 2 $C_2(\boldsymbol{v}(t))$. Though drivers do not have information about signal timing and current link flow, historical travel time helps them move to a user equilibrium point. When historical travel time on Route 1 $C_1(\boldsymbol{v}(t))$ is higher than historical travel time on Route 2 $C_2(\boldsymbol{v}(t))$, a part of the flow will shift from Route 1 to Route 2. Eventually, the system approaches an equilibrium state, where 613 vehicles choose Route 1 with 278.8s average travel time and 1387 vehicles choose Route 2 with the average travel time of 279.1s.

Strategy 4: PAP+P0

Though proportional-switch adjustment process leads to an equilibrium state, the influence of signal control on routing has been ignored. To take signal control into account, PAP has been combined with P0 policy in this scenario, which tries to reduce delay at the junction and maximise road capacity. When the bottleneck delay multiplied by saturated flow on Route 1 is higher than Route 2, i.e. $s_1 b_1 > s_2 b_2$, green timing will be swapped from Route 2 to Route 1.

According to the results of the simulation shown in Figure 6.6 and Figure 6.7, the combined PAP and P0 policy makes the system converge to a new equilibrium point where total travel time is 552985s. To reduce junction delay, the green time on Route 1 increases from 30s to 43s; meanwhile, the green time on Route 2 decreases from 70s to 57s.

At the equilibrium point, where drivers cannot improve their travel time by unilaterally changing routes, 47.25% of the total flow choose Route 1 with 276.6s average travel time and 4.8s average delay, while 52.75% of the total flow choose Route 2 with 276.3s average travel time and 4.7s average delay.

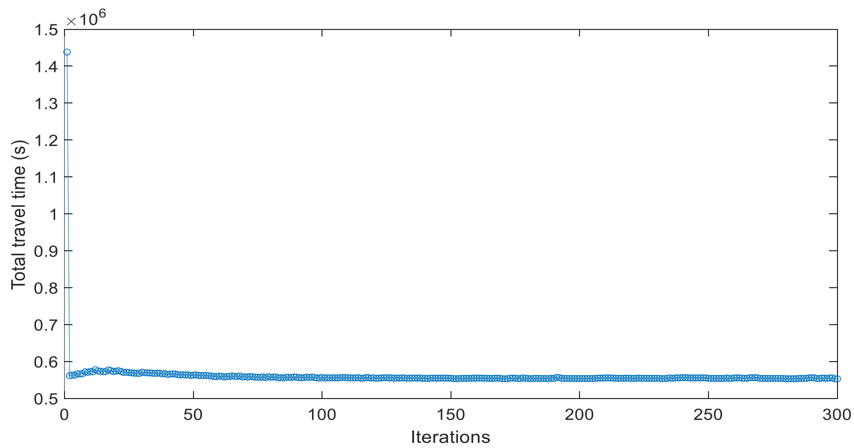

Figure 6.6 Total travel time vs iterations (PAP+P0)

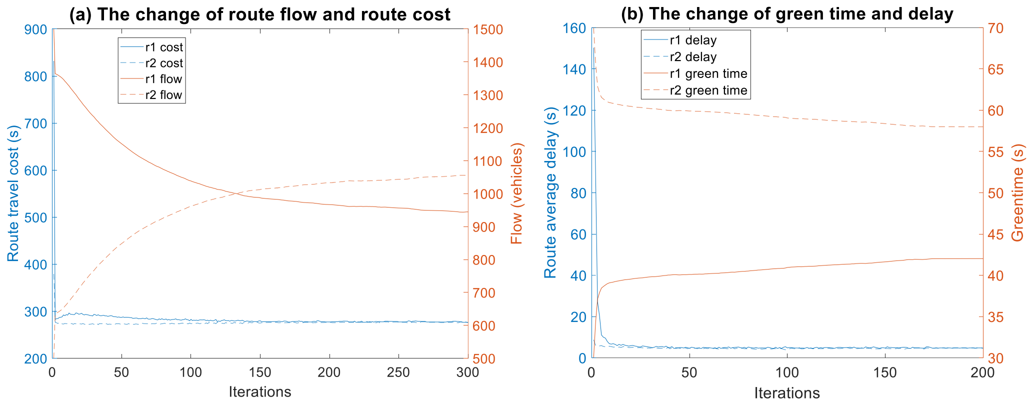

Figure 6.7 (a) Change of route flow and travel cost; (b) Change of green time and delay

Strategy 5: ORST

As discussed in Section 1 and Section 3, with the emergence of connected and automated technologies, CAVs provided an opportunity to improve travel efficiency with additional information from CAVs and signal controller. Considering that CAVs and signal controllers can interact with each other, an optimisation problem can be formulated as shown in Equation (A5.9). To solve this optimisation problem, the Particle Swarm Optimisation (PSO) has been adopted, because of the nonlinear feature of the link travel cost $C_a(\boldsymbol{v}, \boldsymbol{\psi})$ calculated by simulation.

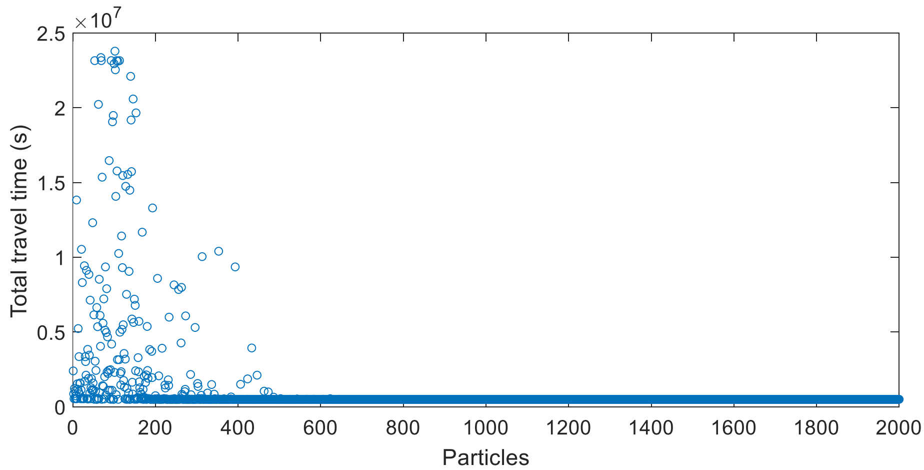

Figure 6.8 Total travel time vs particles (ORST)

The population of the particles is pre-set as 40 and the results of 50 iteration runs is shown in Figure 6.8. A converged optimal solution has been calculated with the total travel time of 501659s. At the converged point, 1999 vehicles use Route 1 with 95s green time and 250.8s average travel time. Only 1 vehicle uses Route 2 with 5s green time and 328s average travel time.

In summary, the proposed ORST control strategy for CAVs has been compared against four existing routing and signal timing strategies under different levels of information to investigate the impacts of information levels on routing and signal timing efficiency. The results are summarised in Table 6.1 and Figure 6.9, which demonstrate that with additional information from CAVs, ORST can reduce approximately 49% of the total travel time compared with SUE and approximately 10% of the total travel time compared with UE.

The impacts of information levels on routing and signal timing efficiency can be concluded as follows. Firstly, comparing the shortest route strategy with stochastic routing or PAP strategies, partial information about traffic flow can help the road traffic system reach a stochastic user equilibrium or user equilibrium point, which can reduce congestion caused by unreasonable routing. Secondly, with information from signal timing, a better user equilibrium can be achieved with PAP+P0 policy to reduce total travel time by adjusting signal timing. Thirdly, when additional information from CAVs becomes available via V2V and V2X communications, ORST can make CAVs behave cooperatively to achieve WP2, where total travel time can be further reduced.

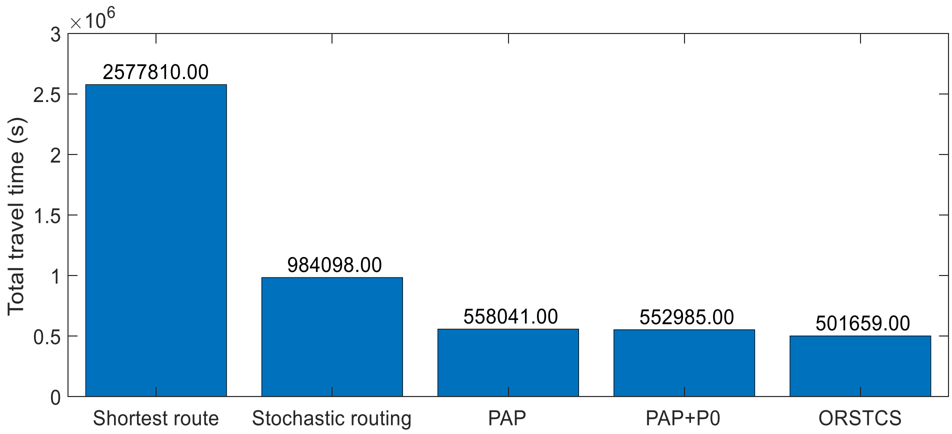

Figure 6.9 Total travel time of routing and signal timing strategies under different levels of information

Table 6.1 Results of routing and signal timing strategies under different levels of information

Results \ Strategies	Shortest route	Stochastic routing	PAP	PAP+P0	ORST
route 1 flow (vehicle/h)	na	na	613	945	1999
route 2 flow (vehicle/h)	na	723	1387	1055	1
route 3 flow (vehicle/h)	1000	537	na	na	na
route 4 flow (vehicle/h)	1000	740	na	na	na
route 1 cost(s)	na	na	278.8	276.6	250.8
route 2 cost(s)	na	311*	279.1	276.3	328
route 3 cost(s)	2009.1	311*	na	na	na
route 4 cost(s)	569.6	311*	na	na	na
edge 4 greentime (s)	30	30	30	43	95
edge 5 greentime (s)	70	70	70	57	5
total traveltime (s)	2577810	984098	558041	552985	501659

* Edge based travel time is estimated by the mean speed in SUMO

6.2.3 Sensitivity analysis of mixed traffic conditions on a simple network

The case studies in Section 6.3 have demonstrated that total travel time can be significantly reduced with the proposed ORST control strategy in a pure CAV scenario. However, in practice, CAVs cannot replace HDVs to achieve a fully connected and automatic environment in the short term. Hence, this section will investigate whether travel efficiency can still be improved by the ORST control strategy in mixed traffic conditions of CAVs and HDVs.

The sensitivity analysis is conducted to evaluate the performance of the ORST control strategy under different CAV penetration rates and demands. The population of the PSO particles is pre-set as 40 and the results of total travel time of 50 iterations are shown in Figure 6.10 (a-c). It can be observed from Table 6.2 and Figure 6.10(d) that when the demand is 2000 vehicle/h, the total travel time decreases with the increase of CAV penetration rate. As expected, the reduction is mild at a low penetration rate and more significant at a high penetration rate when more CAVs are able to cooperate with other vehicles and signals.

Table 6.2 The sensitivity analysis of ORTS under different CAVs penetration rates

Results \ Penetration	0%	25%	50%	75%	100%
route 1 HDVs flow (vehicle/h)	613	460	307	153	0
route 2 HDVs flow (vehicle/h)	1387	1040	693	347	0
route 1 CAVs flow (vehicle/h)	0	213	999	1494	1999
route 2 CAVs flow (vehicle/h)	0	287	1	6	1
route 1 cost (s)	278.8	282.0	260.6	285.9	250.8
route 2 cost (s)	279.1	271.5	292.3	264.8	328.0
edge 4 greentime (s)	30	28	67	81	95
edge 5 greentime (s)	70	72	32	80	5
Total traveltime (s)	558041	550098	543153	523142	501659

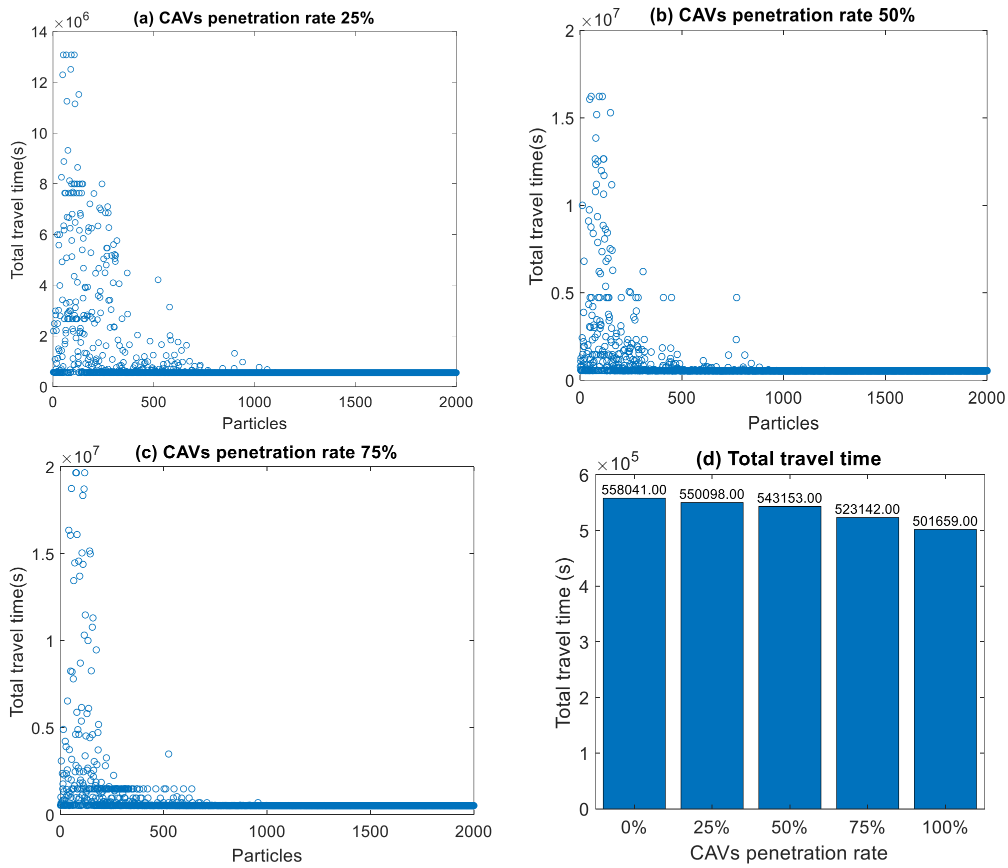

Figure 6.10 Sensitivity analysis for mixed CAV conditions

To further evaluate the performance of ORTS under different congestion levels, the demand varies from 1000 vehicle/h to 3000 vehicle/h. As shown in Table 6.3 and Figure 6.11, both the total and average travel time climb with increasing demand, which indicates that the system performance of a road network will drop with the increase of users in a congestion condition.

Table 6.3 The sensitivity analysis of ORTS under different demands and penetration rates

Penetration / Demand (veh/h)	Total travel time(s)					Average travel time(s)				
	0%	25%	50%	75%	100%	0%	25%	50%	75%	100%
1000	256835	248197	246895	245025	239314	256.8	248.2	246.9	245.0	239.3
1500	401611	391439	386480	376240	366960	267.7	261.0	257.7	250.8	244.6
2000	558041	550098	543153	523142	501659	279.0	275.0	271.6	261.6	250.8
2500	804412	766581	740211	695596	666005	321.8	306.6	296.1	278.2	266.4
3000	1286706	1259283	1260353	1298728	1175031	428.9	419.8	420.1	432.9	391.7

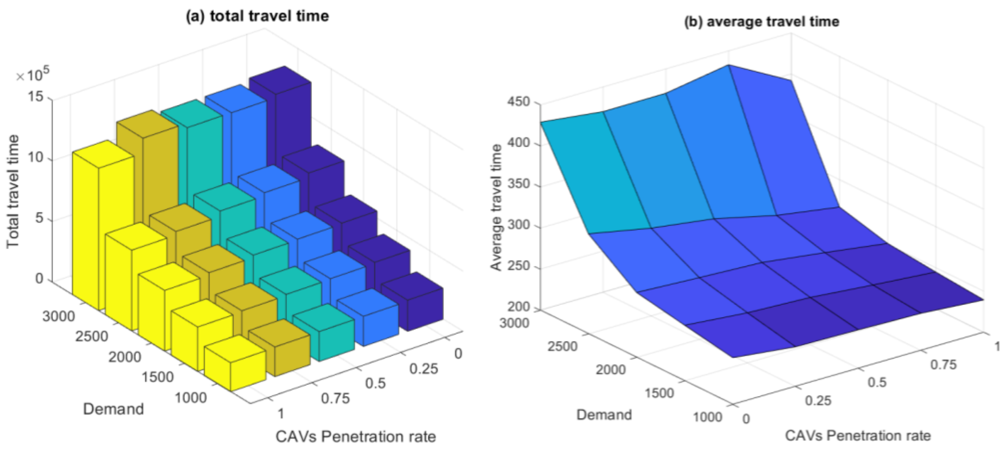

Figure 6.11 Total and average travel time under different demands and penetration rates

In order to quantitatively evaluate the performance of ORTS under different demands, the reduction rate of the average travel time is shown in Figure 6.12, which illustrates that with ORTS control strategy, the improvement of system efficiency is more significant at a mild congestion level. For example, when demand is around 2500 vehicle/h, the system is about to congest. In this state, the further increase in demand will significantly increase average travel time, meanwhile, optimisation space is limited when congestion happens.

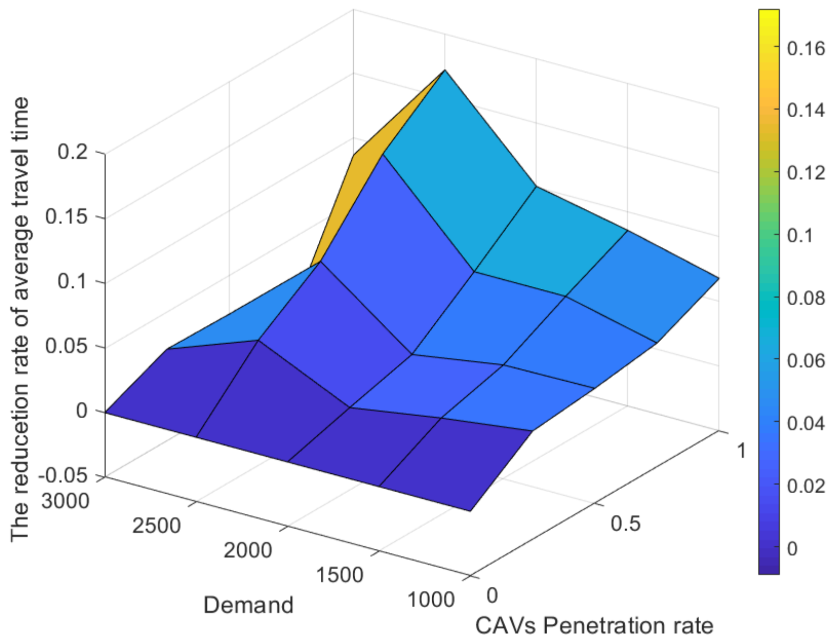

Figure 6.12 The reduction rate of average travel time under different demands and penetration rates

In summary, the results of the sensitivity analysis have demonstrated that system efficiency can still be improved by the ORST control strategy in mixed traffic conditions. The improvement is more significant at a high penetration rate of CAVs and a mild congestion level. This phenomenon is mainly caused by three factors. Firstly, when more CAVs are able to cooperate with other vehicles and signal controllers, the benefits of ORST control strategies are more significant. Secondly, when the road traffic system is highly congested, the improvement of optimisation is limited by road capacity. Thirdly, when both CAVs and HDVs can travel in a free-flow condition, the improvement of ORST control strategies is not significant and is limited by the macroscopic fundamental diagram (MFD).

6.3 Case study of optimal routing and signal timing strategies on a large network with multiple OD pairs

To test the proposed model on a large network, a revised Nguyen-Dupuis network $G(13{,}19)$ is used for the case study (Nguyen & Dupuis, 1984), which includes 13 nodes, 19 links, 3 signal-controlled junctions and 4 OD pairs. The routes are noted as $r(i,j,k)$ where i is the origin node; j is the destination node and k is the k^{th} route from i to j. The green time is noted as $\lambda(i,j)$ where i is inbourd node; j is the signal controlled node.

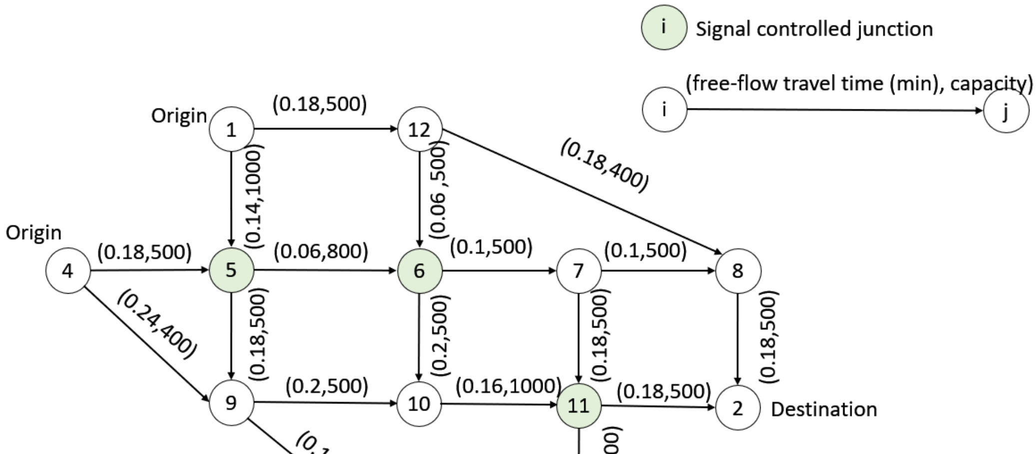

OD pairs

From \ To	2	3
1	200	600
4	400	200

Figure 6.13 Revised Nguyen-Dupuis Network with traffic signals

Assuming the link travel cost $T_a(\boldsymbol{v})$ is calculated by the Bureau of Public Roads (BPR) function that $T_a(v_a) = t_a^0[1 + \alpha(\frac{v_a}{Q_a})^\beta]$, where t_a^0 is the free-flow travel time on the link a; Q_a is the capacity on the link a; α and β are set as 0.15 and 4. The junction delay $D_a^{n^{(s)}}(\boldsymbol{v},\boldsymbol{\psi})$ is calculated by two terms webster equation as Equation (6.1) (Webster, 1958).

$$D_a^{n^{(s)}}(\boldsymbol{v},\boldsymbol{\psi}) = \frac{\xi_a^n(1-\frac{\lambda_a^{n^{(s)}}}{\xi_a^n})}{2(1-\frac{v_a}{Q_a})} + \frac{(\frac{v_a\xi_a^n}{Q_a\lambda_a^{n^{(s)}}})^2}{2v_a(1-\frac{v_a\xi_a^n}{Q_a\lambda_a^{n^{(s)}}})} \quad (s) \tag{6.1}$$

The results of the dynamic process with demand in Figure 6.13 and 25% CAV penetration rate are solved by GRG nonlinear solver and shown in Table 6.4, Table 6.5 and Table 6.6. At the initial state, signal timing is equally assigned to different phases. When all HDVs and CAVs using the shortest routing, a user equilibrium can be achieved with 1506.13 min Total Travel Time (TTT) shown as iteration 0 in Table 6.5.

As user equilibrium is not an optimal assignment at the system level, CAVs can re-route cooperatively with traffic signals to reduce total travel time by solving Equation (A5.9). It can be observed from red rectangles in Table 6.5 that when a subset of the CAVs via r(1,3,4), r(1,3,5), r(4,2,1) and r(4,3,5) change their route cooperatively with traffic signals shown in Iteration 1 Table 6.4. Total travel time can be reduced from 1506.13 min to 1321.26 min.

Though total travel time has been reduced by CAV re-routing cooperatively with traffic signals, the travel cost on the network is changed simultaneously. For HDVs in blue rectangles in Table 6.5, their previous shortest route cannot maximise their personal utility, therefore these HDVs will change their route to maximise their personal utility by solving equation (A5.1). It should be noted that the reason why r(4,2,1) is not used in iteration 2 is that when a few vehicles using r(4,2,1), the route travel cost on r(4,2,1) will increase significantly. Meanwhile, for HDVs in green rectangles, such as r(4,3,5) and r(1,2,8), though their route travel cost changed, their personal utility cannot be improved by changing their route independently.

Table 6.4 Dynamic process of signal timing on Nguyen-Dupuis network

	Iteration 0	Iteration 1	Iteration 2	Iteration3	Iteration4	Iteration5
λ (1,5)	45.00	72.94	72.94	85.00	85.00	85.00
λ (4,5)	45.00	17.06	17.06	5.00	5.00	5.00
λ (5,6)	45.00	11.32	11.32	5.00	5.00	5.00
λ (12,6)	45.00	78.68	78.68	85.00	85.00	85.00
λ (7,11)	45.00	25.64	25.64	5.00	5.00	5.00
λ (10,11)	45.00	64.36	64.36	85.00	85.00	85.00
Cycle time (s)	90.00	90.00	90.00	90.00	90.00	90.00

* λ_{min} is set as 5s

Table 6.5 Dynamic process of routing on Nguyen-Dupuis network (iteration 0,1,2)

	Iteration 0				Iteration 1				Iteration 2			
	CAVs		HDVs		**CAVs**		HDVs		CAVs		**HDVs**	
	flow	cost	flow	cost	flow	cost	flow	cost	flow	cost	flow	cost
r(1,2,1)	0.00	1.13	0.00	1.13	0.00	1.27	0.00	1.27	0.00	0.63	0.00	0.63
r(1,2,2)	0.00	1.50	0.00	1.50	0.00	1.88	0.00	1.88	0.00	1.10	0.00	1.10
r(1,2,3)	0.00	1.51	0.00	1.51	0.00	1.51	0.00	1.51	0.00	0.93	0.00	0.93
r(1,2,4)	0.00	1.42	0.00	1.42	0.00	1.00	0.00	1.00	0.00	1.08	0.00	1.08
r(1,2,5)	0.00	0.93	0.00	0.93	0.00	0.68	0.00	0.68	0.00	0.65	0.00	0.65
r(1,2,6)	0.00	1.31	0.00	1.31	0.00	1.29	0.00	1.29	0.00	1.13	0.00	1.13
r(1,2,7)	0.00	1.31	0.00	1.31	0.00	0.92	0.00	0.92	0.00	0.96	0.00	0.96
r(1,2,8)	50.00	0.56	150.00	0.56	50.00	0.57	150.00	0.57	50.00	0.55	150.00	0.55
r(1,3,1)	0.00	1.48	0.00	1.48	0.00	1.86	0.00	1.86	0.00	1.07	0.00	1.07
r(1,3,2)	0.00	1.48	0.00	1.48	0.00	1.49	0.00	1.49	0.00	0.90	0.00	0.90
r(1,3,3)	0.00	1.40	0.00	1.40	0.00	0.98	0.00	0.98	0.00	1.05	0.00	1.05
r(1,3,4)	104.18	1.28	312.55	1.28	0.00	0.84	312.55	0.84	0.00	0.93	397.14	0.93
r(1,3,5)	45.82	1.28	137.45	1.28	0.00	1.27	137.45	1.27	0.00	1.10	0.00	1.10
r(1,3,6)	0.00	1.29	0.00	1.29	150.00	0.90	0.00	0.90	150.00	0.93	52.86	0.93
r(4,2,1)	28.45	1.09	85.34	1.09	0.00	1.86	85.34	1.86	0.00	0.62	0.00	0.62
r(4,2,2)	0.00	1.46	0.00	1.46	0.00	2.47	0.00	2.47	0.00	1.09	0.00	1.09
r(4,2,3)	0.00	1.47	0.00	1.47	0.00	2.11	0.00	2.11	0.00	0.93	0.00	0.93
r(4,2,4)	0.00	1.38	0.00	1.38	0.00	1.60	0.00	1.60	0.00	1.07	0.00	1.07
r(4,2,5)	71.55	1.09	214.66	1.09	100.00	0.97	214.66	0.97	100.00	1.13	300.00	1.13
r(4,3,1)	0.00	1.44	0.00	1.44	0.00	2.45	0.00	2.45	0.00	1.06	0.00	1.06
r(4,3,2)	0.00	1.44	0.00	1.44	0.00	2.09	0.00	2.09	0.00	0.90	0.00	0.90
r(4,3,3)	0.00	1.36	0.00	1.36	0.00	1.58	0.00	1.58	0.00	1.04	0.00	1.04
r(4,3,4)	0.00	1.07	0.00	1.07	40.68	0.96	0.00	0.96	40.68	1.10	0.00	1.10
r(4,3,5)	50.00	0.95	150.00	0.95	9.32	0.82	150.00	0.82	9.32	0.97	150.00	0.97
TTT (min)	1506.13				1321.26				1317.28			

Table 6.6 Dynamic process of routing on Nguyen-Dupuis network (iteration 3,4,5)

	Iteration 3				Iteration 4				Iteration 5			
	CAVs		HDVs		CAVs		**HDVs**		**CAVs**		HDVs	
	flow	cost	flow	cost	flow	cost	flow	cost	flow	cost	flow	cost
r(1,2,1)	0.00	0.59	0.00	0.59	0.00	0.58	0.00	0.58	0.00	0.58	0.00	0.58
r(1,2,2)	0.00	1.34	0.00	1.34	0.00	1.34	0.00	1.34	0.00	1.34	0.00	1.34
r(1,2,3)	0.00	0.73	0.00	0.73	0.00	0.73	0.00	0.73	0.00	0.73	0.00	0.73
r(1,2,4)	0.00	0.88	0.00	0.88	0.00	0.87	0.00	0.87	0.00	0.87	0.00	0.87
r(1,2,5)	0.00	0.64	0.00	0.64	0.00	0.66	0.00	0.66	0.00	0.66	0.00	0.66
r(1,2,6)	0.00	1.40	0.00	1.40	0.00	1.42	0.00	1.42	0.00	1.42	0.00	1.42
r(1,2,7)	0.00	0.78	0.00	0.78	0.00	0.81	0.00	0.81	0.00	0.81	0.00	0.81
r(1,2,8)	50.00	0.55	150.00	0.55	50.00	0.57	150.00	0.57	50.00	0.57	150.00	0.57
r(1,3,1)	0.00	1.31	0.00	1.31	0.00	1.86	0.00	1.86	0.00	1.32	0.00	1.32
r(1,3,2)	0.00	0.70	0.00	0.70	0.00	1.49	0.00	1.49	0.00	0.71	0.00	0.71
r(1,3,3)	0.00	0.85	0.00	0.85	0.00	0.98	0.00	0.98	0.00	0.85	0.00	0.85
r(1,3,4)	0.00	0.88	397.14	0.88	0.00	0.84	287.33	0.84	0.00	0.78	287.33	0.78
r(1,3,5)	0.00	1.37	0.00	1.37	0.00	1.27	0.00	1.27	0.00	1.39	0.00	1.39
r(1,3,6)	150.00	0.75	52.86	0.75	150.00	0.90	162.67	0.90	150.00	0.78	162.67	0.78
r(4,2,1)	0.00	1.30	0.00	1.30	0.00	1.30	0.00	1.30	0.00	1.31	0.00	1.31
r(4,2,2)	0.00	2.06	0.00	2.06	0.00	2.06	0.00	2.06	0.00	2.07	0.00	2.07
r(4,2,3)	0.00	1.44	0.00	1.44	0.00	1.45	0.00	1.45	0.00	1.46	0.00	1.46
r(4,2,4)	3.69	1.59	0.00	1.59	3.69	1.59	0.00	1.59	6.014	1.60	0.00	1.60
r(4,2,5)	96.31	0.95	300.00	0.95	96.31	0.96	300.00	0.96	93.99	0.95	300.00	0.95
r(4,3,1)	0.00	2.03	0.00	2.03	0.00	2.03	0.00	2.03	0.00	2.04	0.00	2.04
r(4,3,2)	0.00	1.41	0.00	1.41	0.00	1.43	0.00	1.43	0.00	1.43	0.00	1.43
r(4,3,3)	3.69	1.56	0.00	1.56	3.69	1.56	0.00	1.56	6.01	1.57	0.00	1.57
r(4,3,4)	46.31	0.92	0.00	0.92	46.31	0.94	0.00	0.94	43.99	0.93	0.00	0.93
r(4,3,5)	0.00	0.96	150.00	0.96	0.00	0.87	150.00	0.87	0.00	0.87	150.00	0.87
TTT (min)	1186.95				1151.33				1151.23			

According to Table 6.5, when HDVs re-routing passively with CAVs and signals to maximise personal utility. Total travel time is reduced from 1321.26 min to 1317.28 min. As passively re-routing of HDVs also changed travel cost on the network, a portion of CAVs can re-route cooperatively with traffic signal again to minimise total travel time.

It can be observed from iteration 3 in Table 6.4 and Table 6.6 that when most of the green time assigned to λ (1,5), λ (12,6) and λ (10,11), CAVs re-routing cooperatively with traffic signal can further reduce total travel time from 1317.28 min to 1186.95.

Finally, as shown in Table 6.6, the system has been pushed to a point where total travel time cannot be improved by CAV re-routing cooperatively with traffic signals, meanwhile, HDVs' personal utility cannot be improved by changing their route independently. Compared with initial user equilibrium, the proposed model successfully reduce total travel time from 1506.13 min to 1151.23 min dynamically.

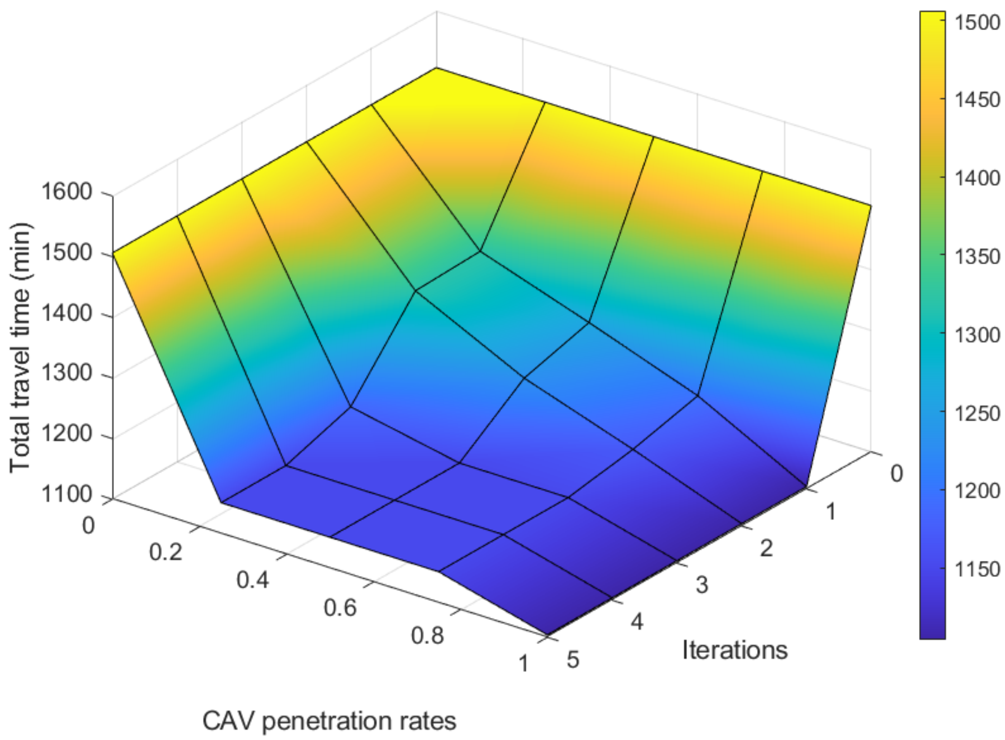

Figure 6.14 The performance of the proposed model under different CAV penetration rates

As system-level improvements can be achieved with a subset of the vehicles (the CAVs) behaving cooperatively with traffic signals when the user equilibrium is different from SO, to further investigate the performance of the proposed model under different CAV penetration rates. CAV penetration rate is varied from 0 to 1 and the results of the dynamic process are shown in Figure 6.14.

It can be observed from Figure 6.14 that when all the vehicles in the system are HDVs (0% CAV penetration rate), the total travel time remains at 1506.13 min, because there are no CAVs in the system to re-routing cooperatively with traffic signals to reduce total travel time. On the contrary, when all the vehicles in the system are CAVs (100% CAV penetration rate), a SO traffic distribution with 1103.96 min total travel time can be achieved with the cooperation between all CAVs and signals within one iteration.

In the mixed traffic condition, at a low penetration rate, a portion of the CAVs behaving cooperatively with traffic signal can gradually reduce total travel time dynamically. With the increase of CAVs penetration rate, it is easier to adjust travel cost on the network with CAVs and signal, meanwhile, total travel time can be reduced significantly with less iteration.

In summary, in this section, the proposed model is tested on a revised Nguyen-Dupuis network, where link travel cost $T_a(\boldsymbol{v})$ is calculated by the Bureau of Public Roads (BPR) function and the junction delay $D_a^{n^{(s)}}(\boldsymbol{v}, \boldsymbol{\psi})$ is calculated by two terms webster equation. The results of the case study demonstrate that the travel cost on the network can be adjusted by CAVs re-routing cooperatively with traffic signals. As HDVs' prefer to seek the shortest route to maximise personal utility, HDVs' routing behaviour can be influenced by CAVs and traffic signals. With the proposed model, though HDVs are not connected and prefer to seek the shortest route to maximise personal utility, system-level improvement can be achieved when only a portion of CAVs changing their route cooperatively with traffic signals.

6.4 Conclusion

In this chapter, the impacts of different driver information levels on routing and signal timing efficiency has been investigated and the question of whether travel efficiency can be improved with information from CAVs has been answered.

As link travel cost $C_a(\boldsymbol{v}, \boldsymbol{\psi})$ is influenced by link a, link flow $\boldsymbol{v}$ and signal setting $\boldsymbol{\psi}$, the information about traffic conditions has been divided into three categories, including information about the network, traffic flow and signal setting. Four existing routing and signal timing strategies under different levels of information and a proposed ORST control strategy for CAVs have been compared on the same simple road network. The results of the simulation and sensitivity analysis demonstrated that with the increase of information levels, total travel time can be reduced with proper routing and signal timing strategies.

The primary contributions of this research can be summarised as follows. Firstly, the impacts of information levels on routing and signal timing efficiency has been investigated quantitatively. The results demonstrate that different levels of information will lead the road traffic system to different equilibrium points. With more accurate information about the traffic conditions, total travel time can be reduced, which is also the reason why traffic guidance systems have been developed to reduce congestion.

Secondly, to reduce total travel time with information from CAVs, an ORST control strategy for CAVs has been proposed and tested in the simulation case study. Compared with UE, the ORST can further reduce the total travel time by approximately 10% . The proposed model has also been tested on a revised Nguyen-Dupuis network, where link travel cost is calculated by the Bureau of Public Roads (BPR) function and the junction delay is calculated by two terms webster equation. The results demonstrate that at 25% CAV penetration rates, the proposed model can successfully reduce about 23% of total travel time. The performance of the proposed model also evaluated under different CAV penetration rates. With the increase of CAVs, it is easier to adjust travel cost on the network with CAVs and signal, meanwhile, total travel time can be reduced significantly with less iteration.

Thirdly, the sensitivity analysis of ORST under different demands and CAVs penetration rates demonstrates that when only part of vehicles in the system can behave cooperatively, system efficiency can still be improved with ORST and the improvement is more significant at a high penetration rate and a mild congestion level (by approximately 13%).

Chapter 7 Conclusion and future work

7.1 Summary and contributions

In summary, the overall aim of this PhD research is to analyse the mixed flow of AVs and HDVs to help traffic managers and Local Authorities (LAs) to improve the performance of urban traffic systems by right-of-way re-allocation and dynamic traffic management. To achieve this aim, the PhD research has been divided into four Research Objectives (ROs):

- RO1: Explore the impact of heterogeneity between AVs and HDVs on road capacity and propose appropriate right-of-way reallocation strategies to improve road capacity.
- RO2: Develop driving strategies for CAVs to interact with HDVs and under mixed traffic conditions and explore whether CAVs can be used as mobile traffic controllers.
- RO3: Develop models to improve system travel efficiency with a few CAVs cooperatively changing their routing in mixed conditions.
- RO4: Explore whether additional travel efficiency can be achieved by jointly optimising routing and signal timing with information from CAVs.

In Chapter 3 (corresponding to RO1), the impacts of heterogeneity between AVs and HDVs on road capacity and whether road capacity can be increased with appropriate RoW reallocation strategies is investigated. Three Highlighted Contributions (HC) of this chapter are summarised as follows:

- Firstly, a theoretical model is proposed to calculate the maximum capacity of the heterogeneous traffic flow. According to the numerical analyses of the theoretical model, it has been shown that road capacity increases convexly with AV penetration rates. The properties of convex functions provide the theoretical basis for RoW reallocation.
- Secondly, crucial aspects of different RoW strategies on a two-lane road have been identified, which provides quantitative evidence for traffic managers and policymakers.

- Thirdly, the impacts of AVs behaviour changes caused by the development of technologies and users' personal settings on road capacity and RoW reallocation strategies have been investigated with sensitivity analysis, which found that even when the behaviour of AVs 'worsen' compared to HDVs, RoW strategies can still increase road capacity compared with a do-nothing policy.

In Chapter 4 (corresponding to RO2), whether CAVs can be used as mobile traffic controllers is investigated. Three highlighted contributions of this chapter are summarised as follows:

- Firstly, as most existing research only considered the CAV's influence on the speed of the following vehicle, but not the influences of CAVs' speed adjustment on HDV's routing behaviour, a theoretical model was proposed to explore this aspect.
- Secondly, according to the theoretical model and numerical analysis, it has been found that in some circumstances, system efficiency can be improved with CAVs acting as mobile controllers by adjusting their speed on a certain link. These factors include the cost-flow relationship, previous user equilibrium assignment, demand and characteristics of the network
- Thirdly, to take more realistic scenarios into account, TraCI is used to building up different control strategies for HDVs and CAVs under different scenarios in SUMO simulation. According to the simulation-based evaluation, when CAVs act as mobile traffic controllers to actively reduce speed on a link, total travel time was reduced by about 6.8% compared with the do nothing scenario and about 3.5% compared to CAVs not acting as controllers.

In Chapter 5 (corresponding to RO3), whether travel efficiency can be improved with only a part of the vehicular flow cooperatively changing its routing in the mixed condition are investigated. Three highlighted contributions of this chapter are summarised as follows:

- Firstly, an analytical model has been proposed to provide an insight into the dynamic process. By solving the optimisation problem, CAVs can know how many vehicles should re-route cooperatively to push the system towards system optimal distribution.

- Secondly, the numerical case study demonstrated that it is possible to influence HDVs' day-to-day routing using the CAVs and push the system towards system optimal distribution dynamically on a large network with multiple OD pairs.
- Thirdly the Optimal Routing and Signal Timing (ORST) control strategy is adopted for CAVs to take non-linear cost-flow relationship and signal timing into account. The results of the SUMO simulation cross-validate the results in the analytical model.

In Chapter 6 (corresponding to RO4), whether additional travel efficiency can be achieved by routing and signal timing with information from CAVs are investigated. Three highlighted contributions of this chapter are summarised as follows:

- Firstly, the impact of information levels on routing and signal timing efficiency has been investigated quantitatively. The results demonstrate that different levels of information will lead the road traffic system to different equilibrium points. With more accurate information about the traffic conditions, total travel time can be reduced, which is also the reason why traffic guidance systems have been developed to reduce congestion.
- Secondly, an ORST control strategy for CAVs has been tested in the simulation case study. Compared with UE, the ORST can further reduce the total travel time by approximately 10%. The proposed model has also been tested on a revised Nguyen-Dupuis network. The results demonstrate that at 25% CAV penetration rates, the proposed model can successfully reduce about 23% of total travel time
- Thirdly the sensitivity analysis of ORST under different demands and CAVs penetration rates demonstrates that when only part of vehicles in the system can behave cooperatively, system efficiency can still be improved with ORST and the improvement is more significant at a high penetration rate with medium congestion levels(by approximately 13%).

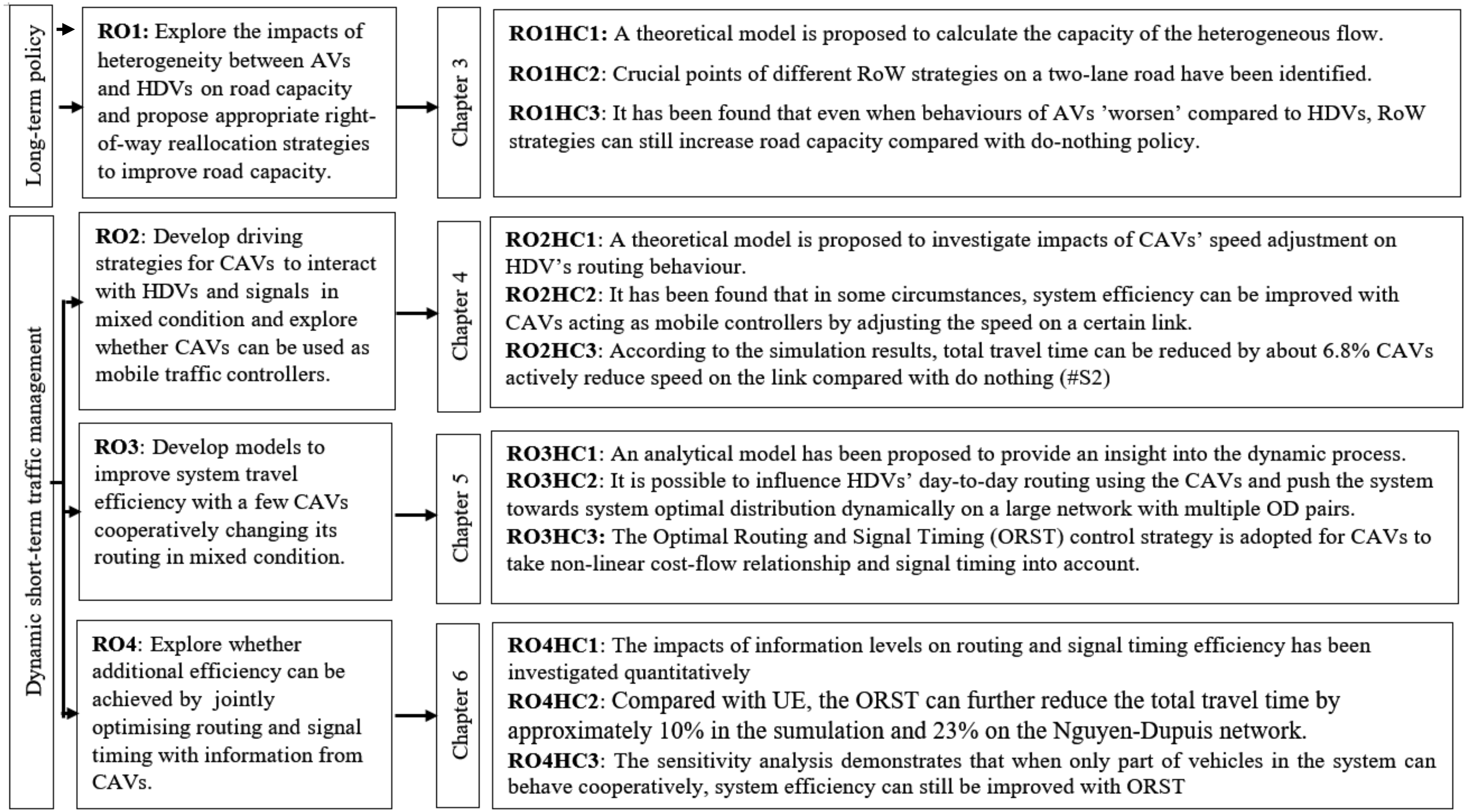

Figure 7.1 Summary of contributions

To sum up, the contribution of this PhD research has been discussed and summarised in Figure 7.1. To help traffic managers and LAs understand the characteristics of mixed traffic and make informed policy decisions. The impact of heterogeneity between AVs and HDVs on road capacity are first investigated in Chapter 3. Then, apart from long-term policy, the opportunities of dynamic short-term traffic management with the emergence of connected and automated technologies are investigated in chapter 4-6. Novel strategies that use CAVs to influence the behaviour of HDVs and manage mixed traffic flow have been proposed and tested by numerical analysis and simulation. In the next section, the potential practical applications of this PhD research will be discussed.

7.2 Potential practical applications

In chapters 3-6, the feasibility of the proposed strategies is first tested with macroscopic numerical analysis in theory. However, the macroscopic numerical analyses simplified the problem to some extent. To take more practical scenarios into account, in each chapter, microscopic SUMO simulations are used for case studies to cross-validate the results in numerical analyses.

Though microscopic simulations can take more practical scenarios into account, it is still an imitation of the operation of a real-world process or system over time. Achieving these strategies in the real world are challenging and might need further work. In Section 7.2, the potential practical applications based on the finding of this PhD research are discussed as follows:

- **Dynamic lane management system:** In Chapter 3, according to the theoretical model, it has been proved that road capacity increases convexly with AV penetration rates. The properties of convex functions provide the theoretical support for RoW reallocation. As different RoW reallocation strategies have different performances under different demands and AV penetration rates, a dynamic lane management system can be developed to adopt the most appropriate RoW reallocation strategy based on the traffic state to maximise road capacity.
- **CAVs acting as mobile traffic controllers for road traffic induction:** In Chapter 4, it has been found that system efficiency can be improved with CAVs acting as mobile controllers by adjusting the speed on a certain link. Currently,

road traffic induction systems rely on the reaction of human drivers to the guidance information. However, a crucial challenge is that some HDVs can ignore the guidance and make their own decision to maximise personal utility. By adjusting the speed on a certain link or road section, CAVs can become a part of the road traffic induction system to influence the routing behaviour of HDVs.

- **CAVs acting as mobile traffic controllers to push traffic system towards system optimal:** it also has been found that it is possible to influence HDVs' day-to-day routing using the CAVs and push the system towards system optimal distribution dynamically on a large network with multiple OD pairs. This opens up other possibilities, besides road pricing and vehicle guidance system, to improve system efficiency with proper routing and signal timing strategy for CAVs.

7.3 Future research

The potential future research works are identified as a part of this PhD research and summarised as follows:

1) **Mixed AVs and bus lanes**: With limited land and road space in the city, it might not be attractive to reallocate right-of-way for a few AVs at the early stage. However, the early stage's driving experience might be crucial to the development pathway of AVs. As most cities already have bus lanes, it is interesting to investigate the influence of allowing AVs to use these bus lanes.

2) **Model-free control with CAVs acting mobile traffic controller:** In this PhD research, whether system efficiency can be improved with CAVs acting as mobile controllers by adjusting the speed on a certain link was investigated. Given that the analysis in Chapter 4 is just a starting point. Reinforcement Learning can be used in the future research to formulate a model-free controller to find the best strategies to reduce speed.

3) **Measuring traffic state of junction/road sections with autonomous vehicles**: Equipped with sensors, AVs are able to perceive and collect data from the surrounding environments. Whether AVs can be used as mobile traffic sensors to replace conventional loop detectors or cameras is desired to be researched,

which can reduce the installation and maintenance cost of conventional sensors and bring a new source of data for traffic management.

4) **Stability of the dynamic process towards system optimal:** The case studies in this PhD research demonstrated that it is possible to influence HDVs' day-to-day routing using the CAVs and push the system towards system optimal distribution dynamically on a large network with multiple OD pairs. However, the stability of this dynamic process has not been fully studied, which will be further investigated in future works.

5) **Peer to Peer congestion charge with CAVs**: When using CAV as a mobile traffic controller or to pushing system towards system optimal, CAV might sacrifice some personal utility to maximise system efficiency during this process. In order to compensate for externality, a novel Peer to Peer congestion charge system can be developed to solve this problem.

In conclusion, as pointed out at the beginning of this PhD thesis, AVs are bringing revolutionary opportunities and challenges to urban transport systems. We, as a part of the transport community, has a role to play in shaping future transport systems to sustainably reduce congestion, energy consumption and hazardous pollution. As humans might overestimate what happens in the next five years but underestimate what happens in the next decade, the pathway through the transferring period to the future where all vehicles are potentially autonomous are derserved to be researched. In this PhD research, the characteristics of mixed traffic flow are analysed to help traffic managers and Local Authorities (LAs) to make informed policy decisions and identify novel traffic management strategies for the transition period. The long-term policy that increases road capacity with RoW reallocation and dynamic short-term traffic management strategies that use CAVs to influence the behaviour of HDVs and manage mixed traffic flow has been proposed and tested. Moreover, potential practical applications and future research directions are identified as a part of this PhD study. All of these provide an inspiration to the future where urban transport systems can sustainably have less congestion, pollution and energy consumption.

References

Ahmed, K. I. (1999) *Modeling drivers' acceleration and lane changing behavior.* PhD thesis. Massachusetts Institute of Technology.

Ahuja, R. K., Magnanti, T. L. & Orlin, J. B. (1988) *Network flows.*

Allsop, R. & Charlesworth, J. (1977) Traffic in a signal-controlled road network: An example of different signal timings including different routeing. *Traffic engineering & control.* 18, 262-264.

Allsop, R. E. (1974) Some possibilities for using traffic control to influence trip distribution and route choice. In: *Proceedings of the 6th International Symposium on Transportation and Traffic Theory.* pp. 345-373.

Amirgholy, M., Shahabi, M. & Oliver Gao, H. (2020) Traffic automation and lane management for communicant, autonomous, and human-driven vehicles. *Transportation Research Part C: Emerging Technologies.* 111, 477-495.

Andreas, S., Ina, S., Jan Becker, C. & Walter, S. (2000) Navigation and Control of an Autonomous Vehicle. *IFAC Proceedings Volumes.* 33 (9), 449-458.

Ararat, O., Kural, E. & Guvenc, B. A. (2006) Development of a Collision Warning System for Adaptive Cruise Control Vehicles Using a Comparison Analysis of Recent Algorithms. In: *2006 IEEE Intelligent Vehicles Symposium*. pp. 194-199.

Aron, M. (1988) Car following in an urban network: simulation and experiment. In: *Proceedings of Seminar D 16th Planning and Transport Research and Computation summer annual meeting*. pp. 27-39.

British Standards Institution (2016) BS ISO 19365:2016. *Passenger cars — Validation of vehicle dynamic simulation — Sine with dwell stability control testing*. London, British Standards Institution.

Bando, M., Hasebe, K., Nakayama, A., Shibata, A. & Sugiyama, Y. (1995) Dynamical model of traffic congestion and numerical simulation. *Physical review E.* 51 (2), 1035.

Beckmann, M., McGuire, C. B. & Winsten, C. B. (1956) *Studies in the Economics of Transportation.* Yale University Press.

Beji, L., Abichou, A. & Slim, R. (2003) Longitudinal and Steering Stabilization of an Autonomous Vehicle. *IFAC Proceedings Volumes.* 36 (17), 485-490.

Bella, F. & Russo, R. (2011) A Collision Warning System for rear-end collision: a driving simulator study. *Procedia - Social and Behavioral Sciences.* 20, 676-686.

Ben-Akiva, M. & Bierlaire, M. (1999) Discrete choice methods and their applications to short term travel decisions. In: *Handbook of transportation science*. pp. 5-33.

Bhujbal, P. N. & Narote, S. P. (2015) Lane departure warning system based on Hough transform and Euclidean distance. In: *Processings of 2015 Third International Conference on Image Information (ICIIP)*. pp. 370-373.

Bifulco, G. N., Cantarella, G. E., Simonelli, F. & Velonà, P. (2016) Advanced traveller information systems under recurrent traffic conditions: Network equilibrium and stability. *Transportation Research Part B: Methodological.* 92, 73-87.

Bohrer, S., Zielke, T. & Freiburg, V. (1995) An integrated obstacle detection framework for intelligent cruise control on motorways. In: *Proceedings of the Intelligent Vehicles '95. Symposium*. pp. 276-281.

Boyce, D. E. (1988) Route guidance systems for improving urban travel and location choices. *Transportation Research Part A: General.* 22 (4), 275-281.

Brackstone, M. & McDonald, M. (1999) Car-following: a historical review. *Transportation research part F: traffic psychology and behaviour.* 2 (4), 181-196.

Braess, D., Nagurney, A. & Wakolbinger, T. (2005) On a paradox of traffic planning. *Transportation Science.* 39 (4), 446-450.

Brownstone, D. & Small, K. A. (2005) Valuing time and reliability: assessing the evidence from road pricing demonstrations. *Transportation Research Part A: Policy and Practice.* 39 (4), 279-293.

Cacciola, S. J. (2007) *Fusion of laser range-finding and computer vision data for traffic detection by autonomous vehicles.* PhD thesis. Virginia Tech.

Cantarella, G. E., Improta, G. & Sforza, A. (1991) Iterative procedure for equilibrium network traffic signal setting. *Transportation Research Part A.* 25 (5), 241-249.

Cascetta, E., Russo, F., Viola, F. A. & Vitetta, A. (2002) A model of route perception in urban road networks. *Transportation Research Part B: Methodological.* 36 (7), 577-592.

Ceder, A. & May, A. D. (1976) Further evaluation of single-and two-regime traffic flow models. *Transportation Research Record.* 567, 1-15.

Ceylan, H. & Bell, M. G. (2004) Traffic signal timing optimisation based on genetic algorithm approach, including drivers' routing. *Transportation Research Part B: Methodological.* 38 (4), 329-342.

Chai, H., Zhang, H. M., Ghosal, D. & Chuah, C.-N. (2017) Dynamic traffic routing in a network with adaptive signal control. *Transportation Research Part C: Emerging Technologies.* 85, 64-85.

Chandler, R. E., Herman, R. & Montroll, E. W. (1958) Traffic dynamics: studies in car following. *Operations research.* 6 (2), 165-184.

Chang, T. H. & Lai, I. S. (1997) Analysis of characteristics of mixed traffic flow of autopilot vehicles and manual vehicles. *Transportation Research Part C: Emerging Technologies.* 5 (6), 333-348.

Chen, D., Ahn, S., Chitturi, M. & Noyce, D. A. (2017) Towards vehicle automation: Roadway capacity formulation for traffic mixed with regular and automated vehicles. *Transportation Research Part B: Methodological.* 100, 196-221.

Chen, O. J. (1998) *Integration of dynamic traffic control and assignment.* PhD thesis. Massachusetts Institute of Technology.

Chen, Z., Lin, X., Yin, Y. & Li, M. (2020) Path controlling of automated vehicles for system optimum on transportation networks with heterogeneous traffic stream. *Transportation Research Part C: Emerging Technologies.* 110, 312-329.

Chiabaut, N., Leclercq, L. & Buisson, C. (2010) From heterogeneous drivers to macroscopic patterns in congestion. *Transportation Research Part B: Methodological.* 44 (2), 299-308.

Chiou, S. W. (1999) Optimization of area traffic control for equilibrium network flows. *Transportation Science.* 33 (3), 279-289.

Chiou, S. W. (2003) TRANSYT derivatives for area traffic control optimisation with network equilibrium flows. *Transportation Research Part B: Methodological.* 37 (3), 263-290.

Coelingh, E., Eidehall, A. & Bengtsson, M. (2010) Collision Warning with Full Auto Brake and Pedestrian Detection - a practical example of Automatic Emergency Braking. In: *13th International IEEE Conference on Intelligent Transportation Systems*. pp. 155-160.

Coelingh, E., Lind, H., Birk, W., Distner, M. & Wetterberg, D. (2006) Collision warning with auto brake. In: *FISITA 2006 World Automotive Congress*.

Daganzo, C. F. & Sheffi, Y. (1977) On stochastic models of traffic assignment. *Transportation Science.* 11 (3), 253-274.

Dantzig, G. B. & Ramser, J. H. (1959) The truck dispatching problem. *Management science.* 6 (1), 80-91.

DARPA (2004) *The DARPA GRAND CHALLENGE 2004*. Available from: http://archive.darpa.mil/grandchallenge04/overview.htm [Accessed 23rd May 2018].

DARPA (2005) *The DARPA GRAND CHALLENGE 2005*. Available from: http://archive.darpa.mil/grandchallenge05/gcorg/index.html [Accessed 23rd May 2018].

Dawson, J. A. L. & Catling, I. (1986) Electronic road pricing in Hong Kong. *Transportation Research Part A: General.* 20 (2), 129-134.

Department for Transport (2016) *Research on the Impacts of Connected and Autonomous Vehicles (CAVs) on Traffic Flow : summary report*. Available from:

https://www.gov.uk/government/publications/driverless-vehicles-impacts-on-traffic-flow [Accessed 29th January 2019].

Dial, R. B. (1971) A probabilistic multipath traffic assignment model which obviates path enumeration. *Transportation Research.* 5 (2), 83-111.

Dijkstra, E. W. (1959) A note on two problems in connexion with graphs. *Numerische mathematik.* 1 (1), 269-271.

Eichelberger, A. H. & McCartt, A. T. (2014) Volvo Drivers' Experiences With Advanced Crash Avoidance and Related Technologies. *Traffic Injury Prevention.* 15 (2), 187-195.

Faro, A. & Giordano, D. (2016) Algorithms to find shortest and alternative paths in free flow and congested traffic regimes. *Transportation Research Part C: Emerging Technologies.* 73, 1-29.

Fisk, C. (1980) Some developments in equilibrium traffic assignment. *Transportation Research Part B: Methodological.* 14 (3), 243-255.

Flynn, M. R., Kasimov, A. R., Nave, J. C., Rosales, R. R. & Seibold, B. (2009) Self-sustained nonlinear waves in traffic flow. *Physical review E.* 79 (5), 056113.

Friesz, T. L., Bernstein, D., Mehta, N. J., Tobin, R. L. & Ganjalizadeh, S. (1994) Day-To-Day Dynamic Network Disequilibria and Idealized Traveler Information Systems. *Operations research.* 42 (6), 1120-1136.

Gaikwad, V. & Lokhande, S. (2015) Lane Departure Identification for Advanced Driver Assistance. *IEEE Transactions on Intelligent Transportation Systems.* 16 (2), 910-918.

Gazis, D. C., Herman, R. & Potts, R. B. (1959) Car-following theory of steady-state traffic flow. *Operations research.* 7 (4), 499-505.

Gazis, D. C., Herman, R. & Rothery, R. W. (1961) Nonlinear follow-the-leader models of traffic flow. *Operations research.* 9 (4), 545-567.

Geroliminis, N. & Levinson, D. M. (2009) Cordon Pricing Consistent with the Physics of Overcrowding. In: Lam, W.H.K., Wong, S.C. & Lo, H.K. (eds.) *Transportation and Traffic Theory 2009: Golden Jubilee.* pp. 219-240.

Ghiasi, A., Hussain, O., Qian, Z. & Li, X. (2017) A mixed traffic capacity analysis and lane management model for connected automated vehicles: A Markov chain method. *Transportation Research Part B: Methodological.* 106, 266-292.

Giammarino, V., Baldi, S., Frasca, P. & Delle Monache, M. L. (2020) Traffic flow on a ring with a single autonomous vehicle: An interconnected stability perspective. *IEEE Transactions on Intelligent Transportation Systems.* 22(8), 4998-5008.

Gipps, P. G. (1981) A behavioural car-following model for computer simulation. *Transportation Research Part B: Methodological.* 15 (2), 105-111.

Gipps, P. G. (1986a) A model for the structure of lane-changing decisions. *Transportation Research Part B: Methodological.* 20 (5), 403-414.

Gipps, P. G. (1986b) Multsim: a model for simulating vehicular traffic on multi-lane arterial roads. *Mathematics and Computers in Simulation.* 28 (4), 291-295.

Girault, A. (2004) A hybrid controller for autonomous vehicles driving on automated highways. *Transportation Research Part C: Emerging Technologies.* 12 (6), 421-452.

Girault, A. & Yovine, S. (1999) Stability analysis of a longitudinal control law for autonomous vehicles. In: *Proceedings of the 38th IEEE Conference on*. pp. 3728-3733.

Gollop, A. (2016) *Traffic Signals: An introduction to signalised junctions and crossing facilities in the UK.* CreateSpace Independent Publishing Platform.

Gong, S. & Du, L. (2018) Cooperative platoon control for a mixed traffic flow including human drive vehicles and connected and autonomous vehicles. *Transportation Research Part B: Methodological.* 116, 25-61.

Gordon, T., Sardar, H., Blower, D., Ljung Aust, M., Bareket, Z., Barnes, M., Blankespoor, A., Isaksson-Hellman, I., Ivarsson, J. & Juhas, B. (2010) *Advanced crash avoidance technologies (ACAT) program–Final report of the Volvo-Ford-*

UMTRI project: safety impact methodology for lane departure warning–Method development and estimation of benefits. National Highway Traffic Safety Administration.

Hajiahmadi, M., Knoop, V. L., Schutter, B. D. & Hellendoorn, H. (2013) Optimal dynamic route guidance: A model predictive approach using the macroscopic fundamental diagram. In: *16th International IEEE Conference on Intelligent Transportation Systems (ITSC 2013)*. pp. 1022-1028.

He, X., Guo, X. & Liu, H. X. (2010) A link-based day-to-day traffic assignment model. *Transportation Research Part B: Methodological.* 44 (4), 597-608.

Helly, W. (1959) Simulation of bottlenecks in single-lane traffic flow. In: *Proceedings of Symposium on Theory of Traffic Flow.* pp. 207-238.

Herman, R. & Potts, R. B. (1959) Single lane traffic theory and experiment. In: *Proceedings of Symposium on Theory of Traffic Flow.* pp. 120-146.

Heydecker, B. G. (1983) Some consequences of detailed junction modeling in road traffic assignment. *Transportation Science.* 17 (3), 263-281.

Heyes, M. & Ashworth, R. (1972) Further research on car-following models. *Transportation Research.* 6 (3), 287-291.

Heywood, P., Maddock, S., Bradley, R., Swain, D., Wright, I., Mawson, M., Fletcher, G., Guichard, R., Himlin, R. & Richmond, P. (2019) A data-parallel many-source shortest-path algorithm to accelerate macroscopic transport network assignment. *Transportation Research Part C: Emerging Technologies.* 104, 332-347.

Hu, X. & Sun, J. (2019) Trajectory optimization of connected and autonomous vehicles at a multilane freeway merging area. *Transportation Research Part C: Emerging Technologies.* 101, 111-125.

Huang, H.-J. & Lam, W. H. K. (2002) Modeling and solving the dynamic user equilibrium route and departure time choice problem in network with queues. *Transportation Research Part B: Methodological.* 36 (3), 253-273.

Ilgin Guler, S., Menendez, M. & Meier, L. (2014) Using connected vehicle technology to improve the efficiency of intersections. *Transportation Research Part C: Emerging Technologies.* 46, 121-131.

Jamson, A. H., Lai, F. C. H. & Carsten, O. M. J. (2008) Potential benefits of an adaptive forward collision warning system. *Transportation Research Part C: Emerging Technologies.* 16 (4), 471-484.

Kato, S. & Tsugawa, S. (2001) Cooperative driving of autonomous vehicles based on localization, inter-vehicle communications and vision systems. *JSAE Review.* 22 (4), 503-509.

Kelly, A. (1994) *Concept design of a scanning laser rangefinder for autonomous vehicles*. Carneige Mellon University.

Kennedy, J. & Eberhart, R. (1995) *Particle swarm optimization*. In: *Proceedings of ICNN'95-International Conference on Neural Networks*. pp. 1942-1948.

Kesting, A., Treiber, M. & Helbing, D. (2007) General lane-changing model MOBIL for car-following models. *Transportation Research Record.* 1999 (1), 86-94.

Kesting, A., Treiber, M., Schönhof, M. & Helbing, D. (2008) Adaptive cruise control design for active congestion avoidance. *Transportation Research Part C: Emerging Technologies.* 16 (6), 668-683.

Khattak, Z. H., Smith, B. L., Park, H. & Fontaine, M. D. (2020) Cooperative lane control application for fully connected and automated vehicles at multilane freeways. *Transportation Research Part C: Emerging Technologies.* 111, 294-317.

Kikuchi, S. & Chakroborty, P. (1992) Car-following model based on fuzzy inference system. *Transportation Research Record.* 1365, 82-82.

Kim, I., Kim, T. & Sohn, K. (2013) Identifying driver heterogeneity in car-following based on a random coefficient model. *Transportation Research Part C: Emerging Technologies.* 36, 35-44.

Krauss, S. (1998) *Microscopic modeling of traffic flow: investigation of collision free vehicle dynamics.* PhD thesis. Universität zu Köln.

Kreidieh, A. R., Wu, C. & Bayen, A. M. (2018) Dissipating stop-and-go waves in closed and open networks via deep reinforcement learning. In: *21st International Conference on Intelligent Transportation Systems (ITSC)*. pp. 1475-1480.

Laporte, G. (2009) Fifty Years of Vehicle Routing. *Transporation science.* 43 (4), 408-416.

Laval, J. A. & Daganzo, C. F. (2006) Lane-changing in traffic streams. *Transportation Research Part B: Methodological.* 40 (3), 251-264.

Le Vine, S., Kong, Y., Liu, X. & Polak, J. (2017) Vehicle automation and freeway 'pipeline' capacity in the context of legal standards of care. *Transportation.* 46(4), 1215-1244.

Le Vine, S., Liu, X., Zheng, F. & Polak, J. (2016) Automated cars: queue discharge at signalized intersections with 'Assured-Clear-Distance-Ahead' driving strategies. *Transportation Research Part C: Emerging Technologies.* 62, 35-54.

Le Vine, S., Zolfaghari, A. & Polak, J. (2015) Autonomous cars: the tension between occupant experience and intersection capacity. *Transportation Research Part C: Energing Technologies.* 52, 1-14.

Lentzakis, A. F., Ware, S. I., Su, R. & Wen, C. (2018) Region-based prescriptive route guidance for travelers of multiple classes. *Transportation Research Part C: Emerging Technologies.* 87, 138-158.

Lewis, R. & Johnston, A. (1977) A scanning laser rangefinder for a robotic vehicle. In: *Proceedings of the 5th International Joint Conference on Artificial Intelligence.* pp. 762-768.

Li, R., Liu, X. & Nie, Y. (2018) Managing partially automated network traffic flow: Efficiency vs. stability. *Transportation Research Part B: Methodological.* 114, 300-324.

Li, T., Guo, F., Krishnan, R., Sivakumar, A. & Polak, J. (2020) Right-of-way reallocation for mixed flow of autonomous vehicles and human driven vehicles. *Transportation Research Part C: Emerging Technologies.* 115, 102630.

Li, Z., Elefteriadou, L. & Ranka, S. (2014) Signal control optimization for automated vehicles at isolated signalized intersections. *Transportation Research Part C: Emerging Technologies.* 49, 1-18.

Likhachev, M. & Ferguson, D. (2009) Planning long dynamically feasible maneuvers for autonomous vehicles. *The International Journal of Robotics Research.* 28 (8), 933-945.

Liu, H., Kan, X. D., Shladover, S. E., Lu, X. Y. & Ferlis, R. E. (2018) Modeling impacts of cooperative adaptive cruise control on mixed traffic flow in multi-lane freeway facilities. *Transportation Research Part C: Emerging Technologies.* 95, 261-279.

Liu, L., Zhu, L. & Yang, D. (2016) Modeling and simulation of the car-truck heterogeneous traffic flow based on a nonlinear car-following model. *Applied Mathematics and Computation.* 273, 706-717.

Lo, C.W., Lin, S.H. & Wei, H.C. (2013). *Lane departure warning system.* U.S. Patents 8,587,649.

Lopez, P. A., Behrisch, M., Bieker-Walz, L., Erdmann, J., Flötteröd, Y., Hilbrich, R., Lücken, L., Rummel, J., Wagner, P. & WieBner, E. (2018) Microscopic Traffic Simulation using SUMO. In: *21st International Conference on Intelligent Transportation Systems (ITSC)*. pp. 2575-2582.

Maher, M. J., Zhang, X. & Vliet, D. V. (2001) A bi-level programming approach for trip matrix estimation and traffic control problems with stochastic user equilibrium link flows. *Transportation Research Part B: Methodological.* 35 (1), 23-40.

Mancini, S. (2017) The Hybrid Vehicle Routing Problem. *Transportation Research Part C: Emerging Technologies.* 78, 1-12.

May, A. & Keller, H. E. (1967) Non-integer car-following models. *Highway Research Record.* 199 (1), 19-32.

Mazzae, E. N., Barickman, F., Baldwin, G. & Ranney, T. (2008) *On-Road Study of Drivers' Use of Rearview Video Systems (ORSDURVS).* National Highway Traffic Safety Adminstration.

McDonald, M., Wu, J. & Brackstone, M. (1997) Development of a fuzzy logic based microscopic motorway simulation model. In: *Proceedings of Conference on Intelligent Transportation System*. pp. 82-87.

Meneguzzer, C. (1995) An equilibrium route choice model with explicit treatment of the effect of intersections. *Transportation Research Part B: Methodological.* 29 (5), 329-356.

Milanés, V. & Shladover, S. E. (2014) Modeling cooperative and autonomous adaptive cruise control dynamic responses using experimental data. *Transportation Research Part C: Emerging Technologies.* 48, 285-300.

Mirheli, A., Hajibabai, L. & Hajbabaie, A. (2018) Development of a signal-head-free intersection control logic in a fully connected and autonomous vehicle environment. *Transportation Research Part C: Emerging Technologies.* 92, 412-425.

Nagel, K. & Schreckenberg, M. (1992) A cellular automaton model for freeway traffic. *Journal de physique I.* 2 (12), 2221-2229.

Nagurney, A. & Zhang, D. (1997) Projected Dynamical Systems in the Formulation, Stability Analysis, and Computation of Fixed-Demand Traffic Network Equilibria. *Transportation Science.* 31 (2), 147-158.

Narote, S. P., Bhujbal, P. N., Narote, A. S. & Dhane, D. M. (2018) A review of recent advances in lane detection and departure warning system. *Pattern Recognition.* 73, 216-234.

Nazemi, A. & Omidi, F. (2013) An efficient dynamic model for solving the shortest path problem. *Transportation Research Part C: Emerging Technologies.* 26, 1-19.

Newell, G. F. (2002) A simplified car-following theory: a lower order model. *Transportation Research Part B: Methodological.* 36 (3), 195-205.

Nguyen, S. & Dupuis, C. (1984) An efficient method for computing traffic equilibria in networks with asymmetric transportation costs. *Transportation Science.* 18 (2), 185-202.

NHTSA (2009) *Federal Motor Vehicle Safety Standard; Rearview Mirrors*. National Highway Traffic Safety Administration. Available from: https://www.nhtsa.gov/sites/nhtsa.dot.gov/files/fmvss/Rear_Visibility_ANPRM_022509.pdf [Accessed 28th May 2018].

NHTSA (2013) *Preliminary Statement of Policy Concerning Automated Vehicles*. National Highway Traffic Safety Administration. Available from: https://www.transportation.gov/briefing-room/us-department-transportation-releases-policy-automated-vehicle-development [Accessed 28th May 2018].

Nowakowski, C., O'Connell, J., Shladover, S. E. & Cody, D. (2010) Cooperative adaptive cruise control: Driver acceptance of following gap settings less than one second. In: *Proceedings of the Human Factors and Ergonomics Society Annual Meeting*. pp. 2033-2037.

Olszewski, P. & Xie, L. (2005) Modelling the effects of road pricing on traffic in Singapore. *Transportation Research Part A: Policy and Practice.* 39 (7), 755-772.

Ouster (2018) *OS-2 Performance Lidar Sensor.* Available from: https://www.ouster.io/product-os2/ [Accessed 04th June 2018].

Ozaki, H. (1993) Reaction and anticipation in the car-following behavior. In: *Proceedings of International Symposium on Theory of Traffic Flow and Transportation.* pp. 349-366.

Peeta, S. & Yang, T. H. (2003) Stability issues for dynamic traffic assignment. *Automatica.* 39 (1), 21-34.

Pipes, L. A. (1953) An operational analysis of traffic dynamics. *Journal of applied physics.* 24 (3), 274-281.

Prashker, J. N. & Bekhor, S. (2000) Some observations on stochastic user equilibrium and system optimum of traffic assignment. *Transportation Research Part B: Methodological.* 34 (4), 277-291.

Rajamani, R. & Shladover, S. E. (2001) An experimental comparative study of autonomous and co-operative vehicle-follower control systems. *Transportation Research Part C: Emerging Technologies.* 9 (1), 15-31.

Ramming, M. S. (2001) *Network knowledge and route choice.* PhD thesis. Massachusetts Institute of Technology.

Reuschel, A. (1950) Vehicle movements in a platoon. *Oesterreichisches Ingenieur-Archir.* 4, 193-215.

Richardson, M. (1999) Adaptive cruise control: a product whose time has come. In: *Ninth Annual ITS America Conference.*

Robertson, D. I. (1969) TRANSYT method for area traffic control. *Traffic Engineering and Control.* 11, 276-281.

Robosense (2018a) *RS-LIDAR-16 Multi Beam Real Time LiDAR.* Available from: http://www.robosense.cn/rslidar/rs-lidar-16. [Accessed 04th June 2018].

Robosense (2018b) *RS-LiDAR-32 Multi Beam Real Time LiDAR.* Available from: http://www.robosense.cn/rslidar/rs-lidar-32 [Accessed 04th June 2018].

Rudin-Brown, C. M. & Parker, H. A. (2004) Behavioural adaptation to adaptive cruise control (ACC): implications for preventive strategies. *Transportation research part F: traffic psychology and behaviour.* 7 (2), 59-76.

Russell, M. E., Crain, A., Curran, A., Campbell, R. A., Drubin, C. A. & Miccioli, W. F. (1997) Millimeter-wave radar sensor for automotive intelligent cruise control (ICC). *IEEE Transactions on Microwave Theory and Techniques.* 45 (12), 2444-2453.

Sandholm, W. H. (2001) Potential Games with Continuous Player Sets. *Journal of Economic Theory.* 97 (1), 81-108.

Schermer, D., Moeini, M. & Wendt, O. (2019) A matheuristic for the vehicle routing problem with drones and its variants. *Transportation Research Part C: Emerging Technologies*. 106, 166-204.

Schifers, C. & Hans, G. (2000) *IEEE standard for communications-based train control (CBTC) performance and functional requirements*.

Schmidhuber, J. (2011) *Prof. Schmidhuber's highlights of robot car history*. Available from: https://people.idsia.ch/~juergen/robotcars.html [Accessed 14th October 2021]

Scholz, J., Willhoeft, V., Schulz, R. & Kluge, T. (2006) ALASCA User Manual. *Ibeo Automobile Sensor GmbH, Hamburg.* Available from: http://www.raginbot.com/wiki/images/d/d8/Manual_ALASCA.pdf [Accessed 14th October 2021]

Sentinel, T. M. (1926) *"Phantom Auto' will tour city*. The Milwaukee Sentinel. Available from: https://news.google.com/newspapers?id=unBQAAAAIBAJ&sjid=QQ8EAAAAIBAJ&pg=7304,3766749 [Accessed 23rd May 2018].

Smith, M. (2015) Traffic signal control and route choice: A new assignment and control model which designs signal timings. *Transportation Research Part C: Emerging Technologies.* 58, 451-473.

Smith, M. J. (1979a) The existence, uniqueness and stability of traffic equilibria. *Transportation Research Part B: Methodological.* 13 (4), 295-304.

Smith, M. J. (1979b) Traffic control and route-choice; a simple example. *Transportation Research Part B: Methodological.* 13 (4), 289-294.

Smith, M. J. (1981) The existence of an equilibrium solution to the traffic assignment problem when there are junction interactions. *Transportation Research Part B: Methodological.* 15 (6), 443-451.

Smith, M. J. (1983) The existence and calculation of traffic equilibria. *Transportation Research Part B: Methodological.* 17 (4), 291-303.

Smith, M. J. (1984) The stability of a dynamic model of traffic assignment—an application of a method of Lyapunov. *Transportation Science.* 18 (3), 245-252.

Smith, M. J. & Ghali, M. (1990) The dynamics of traffic assignment and traffic control: A theoretical study. *Transportation Research Part B: Methodological.* 24 (6), 409-422.

Smith, M. J. & Wisten, M. B. (1995) A continuous day-to-day traffic assignment model and the existence of a continuous dynamic user equilibrium. *Annals of Operations Research.* 60 (1), 59-79.

Spiess, H. & Florian, M. (1989) Optimal strategies: A new assignment model for transit networks. *Transportation Research Part B: Methodological.* 23 (2), 83-102.

Stern, R. E., Cui, S., Delle Monache, M. L., Bhadani, R., Bunting, M., Churchill, M., Hamilton, N., Pohlmann, H., Wu, F. & Piccoli, B. (2018) Dissipation of stop-and-go waves via control of autonomous vehicles: Field experiments. *Transportation Research Part C: Emerging Technologies.* 89, 205-221.

Sugiyama, Y., Fukui, M., Kikuchi, M., Hasebe, K., Nakayama, A., Nishinari, K., Tadaki, S.-i. & Yukawa, S. (2008) Traffic jams without bottlenecks—experimental evidence for the physical mechanism of the formation of a jam. *New journal of physics.* 10 (3), 033001.

Taale, H., van Kampen, J. & Hoogendoorn, S. (2015) Integrated Signal Control and Route Guidance based on Back-pressure Principles. *Transportation Research Procedia.* 10, 226-235.

Taale, H. & van Zuylen, H. J. (2001) The combined traffic assignment and control problem–an overview of 25 years of research. In: *9th World Conference on Transport Research.* pp. 22-27.

Tadaki, S.-i., Kikuchi, M., Fukui, M., Nakayama, A., Nishinari, K., Shibata, A., Sugiyama, Y., Yosida, T. & Yukawa, S. (2013) Phase transition in traffic jam experiment on a circuit. *New journal of physics.* 15 (10), 103034.

Taniguchi, E. & Shimamoto, H. (2004) Intelligent transportation system based dynamic vehicle routing and scheduling with variable travel times. *Transportation Research Part C: Emerging Technologies.* 12 (3), 235-250.

Taylor, J., Zhou, X., Rouphail, N. M. & Porter, R. J. (2015) Method for investigating intradriver heterogeneity using vehicle trajectory data: A Dynamic Time Warping approach. *Transportation Research Part B: Methodological.* 73, 59-80.

Teetor, R. R. (1950). *Speed control device for resisting operation of the accelerator.* U.S. Patent 2,519,859.

Teklu, F., Sumalee, A. & Watling, D. (2007) A genetic algorithm approach for optimizing traffic control signals considering routing. *Computer-Aided Civil and Infrastructure Engineering.* 22 (1), 31-43.

Treiber, M., Hennecke, A. & Helbing, D. (2000) Congested traffic states in empirical observations and microscopic simulations. *Physical review E.* 62 (2), 1805.

Treiterer, J. & Myers, J. (1974) The hysteresis phenomenon in traffic flow. *Transportation and traffic theory.* 6, 13-38.

Velogdyne (2018) *HDL-64E s3 High Definition Real Time 3D LiDAR.* Available from: http://velodynelidar.com/hdl-64e.html [Accessed 4th June 2018].

Wagner, P. (2012) Analyzing fluctuations in car-following. *Transportation Research Part B: Methodological.* 46 (10), 1384-1392.

Wagner, P. (2016) Traffic Control and Traffic Management in a Transportation System with Autonomous Vehicles. In: Maurer, M., Gerdes, J.C., Lenz, B. & Winner, H. (eds.) *Autonomous Driving: Technical, Legal and Social Aspects*. Berlin, Springer Berlin Heidelberg, pp. 301-316.

Wang, Y., Wei, L. & Chen, P. (2020) Trajectory reconstruction for freeway traffic mixed with human-driven vehicles and connected and automated vehicles. *Transportation Research Part C: Emerging Technologies.* 111, 135-155.

Wardrop, J. G. (1952) Some theoretical aspects of road traffic research, In: *Proceedings of the institution of civil engineers*. pp. 767-768.

Webster, F. V. (1958) *Traffic signal setting.* Road Research Technical Paper No. 39. London, H.M.S.O.

Wiedemann, R. & Reiter, U. (1992) *Microscopic traffic simulation: the simulation system MISSION, background and actual state*. Project ICARUS (V1052) Final Report.

Wilson, T. B., Butler, W., McGehee, D. V. & Dingus, T. A. (1997) Forward-looking collision warning system performance guidelines. *SAE transactions*. 701-725

Wolcott, R. W. & Eustice, R. M. (2014) Visual localization within LIDAR maps for automated urban driving. In: *2014 IEEE/RSJ International Conference on Intelligent Robots and Systems*. pp. 176-183.

Wongpiromsarn, T., Uthaicharoenpong, T., Wang, Y., Frazzoli, E. & Wang, D. (2012) Distributed traffic signal control for maximum network throughput. In: *15th International IEEE Conference on Intelligent Transportation Systems.* pp. 588-595.

Wu, M. C. & Shih, M. C. (2003) Simulated and experimental study of hydraulic anti-lock braking system using sliding-mode PWM control. *Mechatronics.* 13 (4), 331-351.

Xie, C., Wu, X. & Boyles, S. (2019) Traffic equilibrium with a continuously distributed bound on travel weights: The rise of range anxiety and mental account. *Annals of Operations Research.* 273 (1-2), 279-310.

Yang, D., Qiu, X., Yu, D., Sun, R. & Pu, Y. (2015) A cellular automata model for car–truck heterogeneous traffic flow considering the car–truck following combination effect. *Physica A: Statistical Mechanics and its Applications.* 424, 62-72.

Yang, F. (2005) *An evolutionary game theory approach to the day-to-day traffic dynamics.* PhD thesis. The University of Wisconsin-Madison.

Yang, H. (1999) System Optimum, Stochastic User Equilibrium, and Optimal Link Tolls. *Transportation science.* 33 (4), 354-360.

Yang, H. & Bell, M. G. H. (1997) Traffic restraint, road pricing and network equilibrium. *Transportation Research Part B: Methodological.* 31 (4), 303-314.

Yang, H. & Yagar, S. (1994) Traffic assignment and traffic control in general freeway-arterial corridor systems. *Transportation Research Part B: Methodological.* 28 (6), 463-486.

Yang, H. & Yagar, S. (1995) Traffic assignment and signal control in saturated road networks. *Transportation Research Part A: Policy and Practice.* 29 (2), 125-139.

Yang, K., Guler, S. I. & Menendez, M. (2016) Isolated intersection control for various levels of vehicle technology: Conventional, connected, and automated vehicles. *Transportation Research Part C: Emerging Technologies.* 72, 109-129.

Yang, Q. & Koutsopoulos, H. N. (1996) A microscopic traffic simulator for evaluation of dynamic traffic management systems. *Transportation Research-Part C Emerging Technologies.* 4 (3), 113-130.

Ye, L. & Yamamoto, T. (2018a) Impact of dedicated lanes for connected and autonomous vehicle on traffic flow throughput. *Physica A: Statistical Mechanics and its Applications.* 512, 588-597.

Ye, L. & Yamamoto, T. (2018b) Modeling connected and autonomous vehicles in heterogeneous traffic flow. *Physica A: Statistical Mechanics and its Applications.* 490, 269-277.

Yildirimoglu, M., Ramezani, M. & Geroliminis, N. (2015) Equilibrium Analysis and Route Guidance in Large-scale Networks with MFD Dynamics. *Transportation Research Procedia.* 9, 185-204.

Zaidi, A. A., Kulcsár, B. & Wymeersch, H. (2016) Back-Pressure Traffic Signal Control With Fixed and Adaptive Routing for Urban Vehicular Networks. *IEEE Transactions on Intelligent Transportation Systems.* 17 (8), 2134-2143.

Zanten, A. v., Erhardt, R. & Lutz, A. (1990) Measurement and Simulation of Transients in Longitudinal and Lateral Tire Forces. *SAE transactions.* 300-318.

Zhang, D. & Nagurney, A. (1996) On the local and global stability of a travel route choice adjustment process. *Transportation Research Part B: Methodological.* 30 (4), 245-262.

Zhao, J. & Kamel, A. E. L. (2009) Integrated Longitudinal and Lateral Control System Design for Autonomous Vehicles. *IFAC Proceedings Volumes.* 42 (19), 496-501.

Zheng, F., Jabari, S. E., Liu, H. X. & Lin, D. (2018) Traffic state estimation using stochastic Lagrangian dynamics. *Transportation Research Part B: Methodological.* 115, 143-165.

Zheng, N., Waraich, R. A., Axhausen, K. W. & Geroliminis, N. (2012) A dynamic cordon pricing scheme combining the Macroscopic Fundamental Diagram and an agent-based traffic model. *Transportation Research Part A: Policy and Practice.* 46 (8), 1291-1303.

Appendix 1: A algebraic analysis of the simple network in Subsection 5.3.1

Taking a simple network with two routes shown in Figure 5.1 as an example, assuming signal timing is given; demand from O to D is R; CAVs penetration rate is α; the cost-flow functions are $C(v_1) = av_1 + b$ on the upper route and $C(v_2) = cv_2 + d$ on the lower route

From any initial status, HDVs and CAVs can achieve user equilibrium by accumulating knowledge about the network via day-to-day routing without any cooperation. It can be solved that when $v_1 = \frac{cR-b+d}{a+c}$ and $v_2 = \frac{aR+b-d}{a+c}$, UE can be achieved. As CAVs penetration rate is α, CAVs flow on route 1 v_{1_CAVs} is $\alpha\frac{cR-b+d}{2a+c}$; CAVs flow on route 2 v_{2_CAVs} is $\alpha\frac{aR+b-d}{2a+c}$; HDVs flow on route 1 v_{1_HDVs} is $(1-\alpha)\frac{cR-b+d}{2a+c}$; HDVs flow on route 2 v_{2_CAVs} is $(1-\alpha)\frac{aR+b-d}{2a+c}$.

As CAVs can share information about traffic status and behave cooperatively, solving the optimisation problem $W(\boldsymbol{v})$ can help CAVs identify how many vehicles should re-route cooperatively on the next day to push the system towards SO distribution., when $v_1 = \frac{2cR-b+d}{2(a+c)}$ and $v_2 = \frac{2aR+b-d}{2(a+c)}$, SO can be achieved. Therefore, on the next day:

- when $\frac{cR-b+d}{a+c} - \frac{2cR-b+d}{2(a+c)} > 0$, $\frac{d-b}{2(a+c)}$ CAVs can actively shift from route 1 to route 2 to push the system towards system optimal distribution.
- when $\frac{cR-b+d}{a+c} - \frac{2cR-b+d}{2(a+c)} < 0$, $\frac{d-b}{2(a+c)}$ CAVs can actively shift from route 2 to route 1 to push the system towards system optimal distribution.

However, at the system optimal distribution point, the travel cost on the two routes are different, this travel cost difference will be experienced by HDVs and leads to the re-routing of HDVs:

- when $\frac{cR-b+d}{a+c} - \frac{2cR-b+d}{2(a+c)} > 0$, $\frac{d-b}{2(a+c)}$ HDVs will shift from route 2 to route 1 to push the system back to user equilibrium.

- when $\frac{cR-b+d}{a+c} - \frac{2cR-b+d}{2(a+c)} < 0$, $\frac{d-b}{2(a+c)}$ HDVs will shift from route 1 to route 2 to push the system back to user equilibrium.

These two processes will interact with each other dynamically on this simple network. When CAVs/HDVs can not push the system towards SO/UE, the system reaches a stable status:

- when $\frac{cR-b+d}{a+c} - \frac{2cR-b+d}{2(a+c)} > 0$; $\alpha\frac{cR-b+d}{2a+c} - (1-\alpha)\frac{aR+b-d}{2a+c} > \frac{d-b}{2(a+c)}$, SO will be reached.
- when $\frac{cR-b+d}{a+c} - \frac{2cR-b+d}{2(a+c)} > 0$; $0 < \alpha\frac{cR-b+d}{2a+c} - (1-\alpha)\frac{aR+b-d}{2a+c} < \frac{d-b}{2(a+c)}$, the system will approach SO.
- when $\frac{cR-b+d}{a+c} - \frac{2cR-b+d}{2(a+c)} > 0$; $0 > \alpha\frac{cR-b+d}{2a+c} - (1-\alpha)\frac{aR+b-d}{2a+c}$, UE will be reached.
- when $\frac{cR-b+d}{a+c} - \frac{2cR-b+d}{2(a+c)} < 0$; $\alpha\frac{aR+b-d}{2a+c} - (1-\alpha)\frac{cR-b+d}{2a+c} > \frac{b-d}{2(a+c)}$, SO will be reached.
- when $\frac{cR-b+d}{a+c} - \frac{2cR-b+d}{2(a+c)} < 0$; $0 < \alpha\frac{aR+b-d}{2a+c} - (1-\alpha)\frac{cR-b+d}{2a+c} < \frac{b-d}{2(a+c)}$, the system will approach SO.
- when $\frac{cR-b+d}{a+c} - \frac{2cR-b+d}{2(a+c)} < 0$; $0 > \alpha\frac{aR+b-d}{2a+c} - (1-\alpha)\frac{cR-b+d}{2a+c}$, UE will be reached.

Appendix 2: Permission document for reproduction

RightsLink®

Home | Help | Live Chat | Sign in | Create Account

Right-of-way reallocation for mixed flow of autonomous vehicles and human driven vehicles

Author: Tang Li,Fangce Guo,Rajesh Krishnan,Aruna Sivakumar,John Polak

Publication: Transportation Research Part C: Emerging Technologies

Publisher: Elsevier

Date: June 2020

Journal Author Rights

Please note that, as the author of this Elsevier article, you retain the right to include it in a thesis or dissertation, provided it is not published commercially. Permission is not required, but please ensure that you reference the journal as the original source. For more information on this and on your other retained rights, please visit: https://www.elsevier.com/about/our-business/policies/copyright#Author-rights

BACK | CLOSE WINDOW

Appendix 3: CRediT authorship contribution statement of Right-of-way reallocation for mixed flow of autonomous vehicles and human driven vehicles

Tang Li: Conceptualization, Methodology, Software, Investigation, Writing - original draft, Visualisation. Fangce Guo: Supervision, Writing - review & editing, Visualisation. Rajesh Krishnan: Supervision, Writing - review & editing. Aruna Sivakumar: Supervision, Writing - review & editing. John Polak: Supervision, Funding acquisition, Conceptualisation.

Appendix 4: A heuristic analysis of CAVs acting as mobile controllers in mixed traffic conditions by adjusting the speed on a certain link

A heuristic analysis is discussed here to investigate whether system travel efficiency can be increased when CAVs acting as mobile traffic controllers adjust the speed on a certain link. First of all, to take the influences of CAVs' speed adjustment on HDV's routing behaviour into account, HDV's behaviour is discussed. Then a theoretical model is proposed to improve system travel efficiency with CAVs acting as mobile traffic controllers adjusting the speed on a certain link.

1) HDVs' routing behaviour

To maximise personal utility, HDVs prefer to drive for a better driver environment. A typical behaviour to drive for a better driving environment is using the shortest route to the destination.

Ideally, when all the vehicles use the shortest route, a user equilibrium can be achieved based on Wardrop (1952) first principle, which can be described by the following Equation (A4.1)

$$\underset{\boldsymbol{v},\boldsymbol{r}}{\text{Minimise}}\, Z(\boldsymbol{v}) = \sum_{a \in L} \int_{v=0}^{v_a} C_a\,(v)dv \tag{A4.1}$$

Subject to

$$\left.\begin{aligned} r_p \geq 0 \quad \forall p \in P_{od} \\ \textstyle\sum_{p \in P_{od}} r_p = R_{od} \end{aligned}\right\} \quad \forall od$$

$$v_a = \sum_{od} \sum_{p \in P_{od}} r_p\, \delta_a^p \quad \forall\, a \epsilon L$$

Where od is an origin-destination pair; P_{od} is the set of all routes from an origin point to a destination point; p is a route in the set P_{od}; r_p is the flow assigned to route p; R_{od} is the sum of route flow via any route from the origin point to the destination point; v_a is the link flow on the link a; C_a is the travel cost on the link a.

However, in the mixed condition, the link flow v_a is consisted of HDVs flow v_{a_HDVs} and CAVs flow v_{a_CAVs}. When CAVs act as mobile traffic controllers adjusting the speed on a certain link, the link travel cost will change correspondingly. In this circumstance, whether system travel efficiency can be increased are further investigated.

2) Improving system efficiency with CAVs acting as mobile controllers by adjusting the speed on a certain link

When CAVs act as mobile traffic controllers actively adjusting the speed on a certain link, the link travel cost will change, which can be noted as Equation (A4.2)

$$C_{a,CAVAA}(v) = C_a(v) + \Delta_{CAV} \tag{A4.2}$$

In order to investigate whether system efficiency can be improved with CAVs acting as mobile traffic controllers actively adjusting the speed on a certain link, the total travel time $W(\boldsymbol{v})$ is used to measure system efficiency, which is noted as Equation (A4.3)

$$W(\boldsymbol{v}) = \sum_{a \in L} v_a \, C_a(\boldsymbol{v}) \tag{A4.3}$$

A bilevel programming problem can be formulated as Equation (A4.4),

$$\underset{\Delta_{CAV}}{\text{Minimise}}\, W(\boldsymbol{v}) = \sum_{a \in L} v_a \, C_{a,CAVAA}(v) = \sum_{a \in L} v_a \left(C_a(v) + \Delta_{a,CAV} \right) \tag{A4.4}$$

Subject to

$$\Delta_{CAV} \geq \Delta_{min}$$

$$\Delta_{CAV} \leq \Delta_{max}$$

$$\underset{\boldsymbol{v},\boldsymbol{r}}{\text{Minimise}}\, Z(\boldsymbol{v}) = \sum_{a \in L} \int_{v=0}^{v_a} C_a\,(v) dv$$

Subject to

$$\left. \begin{array}{l} r_p \geq 0 \quad \forall p \in P_{od} \\ \sum_{p \in P_{od}} r_p = R_{od} \end{array} \right\} \quad \forall od$$

$$v_a = \sum_{od} \sum_{p \in P_{od}} r_p \, \delta_a^p \quad \forall\, a \epsilon L$$

In Equation (A4.4), Δ_{CAV} is the control variable as CAVs are actively adjusting the speed on a certain link. To improve system efficiency, total travel time $W(\boldsymbol{v})$ should be minimised. Meanwhile, to take the influences of CAVs' speed adjustment on HDV's routing behaviour into account, the inner objection function should be satisfied, as HDVs prefer to drive for a better driver environment.

Without an expression of the function, it is hard to evaluate whether the optimisation problem is solvable or not. As the theoretical analysis provided an inspiration, in Section 4.2, a numerical analysis of CAVs acting as mobile traffic controllers will be conducted to demonstrate this possibility.

Appendix 5: Routing and signal timing strategies under different levels of information

1. The levels of information about traffic conditions

For an individual traveller, identifying the shortest route from the origin to the destination can significantly reduce individual travel time. To find the shortest route, travellers should have knowledge about the link travel cost $C_a(\boldsymbol{v}, \boldsymbol{\psi})$, which is related to the link a, link flow $\boldsymbol{v}$ and signal setting $\boldsymbol{\psi}$ (Bifulco et al., 2016; Chiou, 2003; Yang & Yagar, 1995). Against this, the information about traffic condition can also be divided into three categories.

The first category is information about the network, which is a fundamental level of information. For a network $G(N, L)$ with N nodes and L links, drivers should have information about the network topological structure. Apart from the topological structure, the length of the link and the numbers of lanes are also important for drivers to estimate travel cost, which can be easily got from maps.

The second category is information about traffic flow $\boldsymbol{v}$, which is an important level of information about traffic conditions. Based on the speed-flow-density relationship, drivers need to know the existing flow on the links to estimate link travel cost. However, in practice, human drivers only have partial knowledge about link flow, which can be acquired from their daily driving experience or navigation system, such as Advanced Traveller Information Systems (ATIS) (Bifulco et al., 2016). Without the help of sensors on CAVs and V2X communication technologies, it is hard for drivers to know accurate information about link flow.

The third category is information about the signal setting. As the delay at a signal-controlled junction $D_a^{(s)}(\boldsymbol{v}, \boldsymbol{\psi})$ can be adjusted by green time σ and cycle time ξ, the signal setting is another information required for drivers to estimate link travel cost. However, in practice, human drivers only have limited knowledge about the signal setting at junctions, which also leads to the fact that the signal setting has been ignored by some routing strategies.

In summary, the levels of information about traffic conditions can be divided into three categories. Based on the different levels of information, different routing and signal timing strategies have been proposed by existing literature. The emergence of connected and automated technologies also provides an opportunity to get additional information from CAVs, such as accurate link flow and signal timing. In the next section, four existing routing and signal timing strategies under different levels of information will be introduced. Then an optimal routing and signal timing control strategy for CAVs will be proposed.

2. Existing routing and signal timing strategies

Strategy 1: Shortest route and Dijkstra's algorithm

The most intuitive routing strategy for HDVs is to identify the shortest route based on the topological structure when the information about traffic flow and signal timing is not available or not reliable. To find the shortest route, Dijkstra's algorithm (Dijkstra, 1959) has been developed to seek the shortest route between nodes in a network. However, in Dijkstra's algorithm, the travel cost between nodes is a fixed value, which means the impacts of traffic flow and signal timing on travel cost have been ignored.

Strategy 2: Stochastic routing

To allow human drivers to have different levels of information about travel conditions, Daganzo and Sheffi (1977) proposed a revised behaviour principle that "no driver believes he can improve his travel time by unilaterally changing routes". This principle leads to the extension of the Beckmann's formulation shown as Equation (A5.1) (Beckmann et al., 1956) to Equation (A5.2) (Fisk, 1980).

$$\underset{\boldsymbol{v},\boldsymbol{r}}{\text{Minimise}}\, Z(\boldsymbol{v}) = \sum_{a\in L} \int_{v=0}^{v_a} C_a\,(v) dv \tag{A5.1}$$

Subject to

$$\left.\begin{array}{l} r_p > 0 \quad \forall p \in P_{od} \\ \sum_{p\in P_{od}} r_p = R_{od} \end{array}\right\} \quad \forall od$$

$$v_a = \sum_{od} \sum_{p\in P_{od}} r_p\, \delta_a^p \quad \forall\, a\epsilon L$$

$$\underset{\boldsymbol{v},\boldsymbol{r}}{\text{Minimise}}\, Z(\boldsymbol{v},\boldsymbol{r}) = \sum_{a\in L} \int_{v=0}^{v_a} C_a\,(v)dv \; + \frac{1}{\theta}\sum_{od} \sum_{p\in P_{od}} r_p(\log_e r_p - 1) \qquad \text{(A5.2)}$$

Subject to

$$\left.\begin{array}{l} r_p > 0 \quad \forall p \in P_{od} \\ \sum_{p\in P_{od}} r_p = R_{od} \end{array}\right\} \quad \forall od$$

$$v_a = \sum_{od} \sum_{p\in P_{od}} r_p\, \delta_a^p \quad \forall\, a\epsilon L$$

The Lagrangian of Equation (A5.2) can be rearranged as Equation (A5.3) to calculate assigned route flow (Dial, 1971; Fisk, 1980), which can satisfy the Logit mechanism to allow drivers having different levels of information about traffic conditions such as travel time.

$$r_p = \frac{e^{-\theta C_p}}{\sum_{p\in P_{od}} e^{-\theta C_q}} R_{od} \quad \forall\, p \in P_{od}\, \forall\, od \qquad \text{(A5.3)}$$

Strategy 3: Proportional-switch Adjustment Process (PAP)

As previously discussed in Section 1, though drivers might not have perfect information about traffic conditions, they can accumulate knowledge by day to day travelling. Smith (1979a) proposed that a driver might use the same routes tomorrow. However, if a driver changes the route, the new route must be a cheaper one. Based on this idea, He et al. (2010) proposed a Proportional-switch Adjustment Process (PAP).

Taking a simple network as shown in Figure 6.1 for example, on a specific day t, the travel cost via Route 1 $C_1(v_1(t))$ is lower than the travel cost using Route 2 $C_2(v_2(t))$. Assuming drivers have information about historical travel time, travellers will shift from Route 2 to Route 1 at day $t+1$, which is an increasing function of Route 2 flow $v_2(t)$ and the difference in travel cost between two routes.

Therefore, the flow vector $\boldsymbol{v(t)} = [v_1(t), v_2(t)]$; travel cost vector $\boldsymbol{C}\big(\boldsymbol{v(t)}\big) = [C_1\big(\boldsymbol{v}(t)\big), C_2\big(\boldsymbol{v}(t)\big)]$ and the changes $\Delta_1\big(\boldsymbol{v(t)}\big), \Delta_2\big(\boldsymbol{v(t)}\big)$ satisfy Equation (A5.4) and Equation (A5.5).

$$\Delta_1(\boldsymbol{v}(\boldsymbol{t})) = -wv_2(t)[C_2(\boldsymbol{v}(t)) - C_1(\boldsymbol{v}(t))] \quad \text{(A5.4)}$$

$$\Delta_2(\boldsymbol{v}(\boldsymbol{t})) = wv_2(t)[C_2(\boldsymbol{v}(t)) - C_1(\boldsymbol{v}(t))] \quad \text{(A5.5)}$$

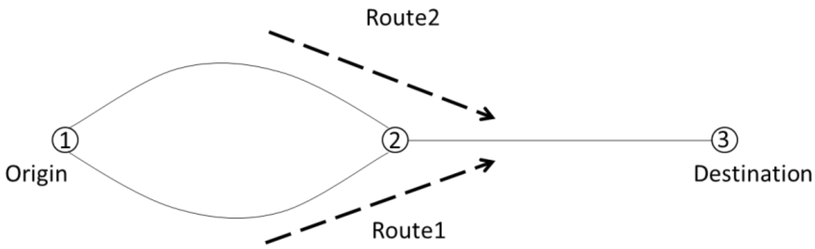

Figure A5.1 A simple network with two routes

Smith (2015) extended this process to a more general road network, shown in Equation (A5.6).

$$\Delta_{ODq}(\boldsymbol{v}) = \sum_{(r,s):r<s} w\{v_{qr}[C_{qr}(\boldsymbol{v}(t)) - C_{qs}(\boldsymbol{v}(t))]_+\Delta_{qrs} + v_{qs}[C_{qs}(\boldsymbol{v}(t)) - C_{qr}(\boldsymbol{v}(t))]_+\Delta_{qrs}\} \quad \text{(A5.6)}$$

where $x_+ = \max\{x, 0\}$; Δ_{qrs} is the swap vector from Route r to s for OD pair q.

Strategy 4: PAP and P0 policy

Taking signal timing into account, Smith (2015) further extended the proportional-switch adjustment process to embrace green time using P0 policy. For example, in the network of Figure 6.1 where Node 2 is a signal-controlled junction, the adjustment of green time will influence bottleneck delay on two routes. When the bottleneck delay b_1 multiplies the saturated flow s_1 on Route 1 higher than the one using Route 2, i.e. $s_1b_1 > s_2b_2$, green timing should be swapped from Route 2 to Route 1 to reduce delay at the junction. The change of green timing should satisfy Equation (A5.7) and Equation (A5.8).

$$\Delta G_1(\boldsymbol{t}) = wG_2(t)[s_1b_1(t) - s_2b_2(t)]_+ - wG_1(t)[s_2b_2(t) - s_1b_1(t)]_+ \quad \text{(A5.7)}$$

$$\Delta G_2(\boldsymbol{t}) = -wG_2(t)[s_1b_1(t) - s_2b_2(t)] + wG_1(t)[s_2b_2(t) - s_1b_1(t)]_+ \quad \text{(A5.8)}$$

where $G_i(t)$ is the green time on link i; $\Delta G_i(\boldsymbol{t})$ is the change of green time for the next iteration on link i; s_i is the saturation flow at the exit of link i; $b_i(t)$ is the bottleneck delay at the exit of link i and w is the weight of proportional-switch adjustment process. Based on the Lyapunov function, Smith proved that combining routing and signal timing dynamic system can converge to equilibrium.

3. Optimal Routing and Signal Timing (ORST) Control Strategy

As CAVs are able to communicate and interact with other CAVs and signal controllers, the interaction between routing and signal timing can be summarised in Figure 6.2. For a road traffic system, the total travel time $Z(\boldsymbol{v}, \boldsymbol{\psi}(\gamma, \boldsymbol{\lambda}))$ is a dependent variable controlled by the route choice r_p and the signal setting ψ_{a}. Given the information about travel flow v and signal setting $\boldsymbol{\psi}$, the route choice r_p is depended on the travel cost on the links $C_a(\boldsymbol{v}, \boldsymbol{\psi})$. Given the information about travel flow $\boldsymbol{v}$ and junction delay $D_a(\boldsymbol{v}, \boldsymbol{\psi})$, the signal setting can be adjusted correspondingly.

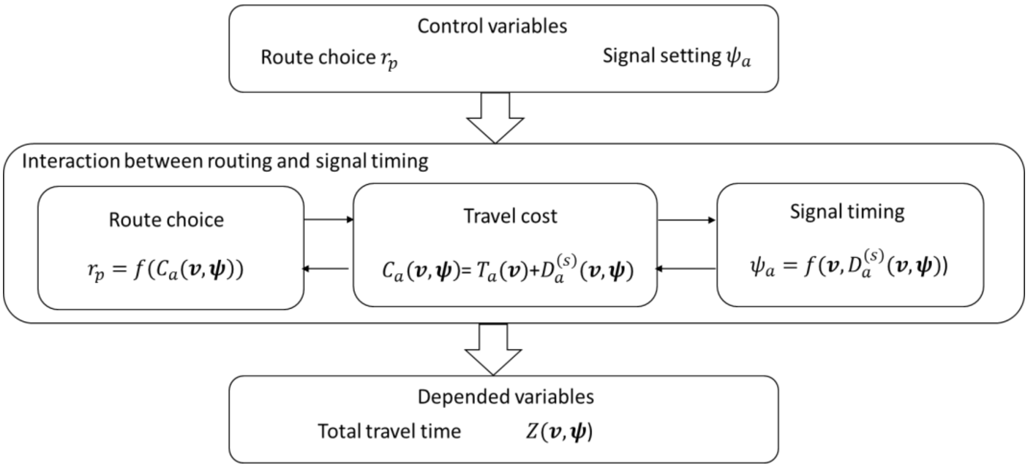

Figure A5.2 The interaction between routing and signal timing

A day to day dynamic system can be formulated, where route choice, travel cost and signal timing interact with each other. To improve system travel efficiency, total travel time should be minimised and therefore an optimisation problem can be formulated as in Equation (A5.9).

$$\underset{v,t,\boldsymbol{\psi}(\gamma,\boldsymbol{\lambda})}{\text{Minimise}}\, Z(\boldsymbol{v}, \boldsymbol{\psi}(\gamma, \boldsymbol{\lambda})) = \sum_{a\in L} v_a\, C_a(\boldsymbol{v}, \boldsymbol{\psi}) = \sum_{a\in L} v_a[T_a(\boldsymbol{v}) + \delta_a^{n^{(s)}} D_a^{n^{(s)}}(\boldsymbol{v}, \boldsymbol{\psi})] \quad \text{(A5.9)}$$

Subject to

$$\left.\begin{matrix} r_p > 0 \quad \forall p \in P_{od} \\ \sum_{p\in P_{od}} r_p = R_{od} \end{matrix}\right\} \quad \forall od \qquad (Demand\ constraint)$$

$$v_a = \sum_{od} \sum_{p\in P_{od}} r_p\, \delta_a^p \quad \forall\, a\epsilon L \qquad \text{(Link flow} - \text{route flow constraint)}$$

$$\sum_{a\in L} \sum_{s\in S} \lambda_a^{n^{(s)}} \delta_a^{n^{(s)}} = 1 \;\; \forall\, n\epsilon N^{(\boldsymbol{S})} \qquad \text{(signal timing constraint)}$$

$$\delta_a^{n^{(s)}} = \begin{cases} 1 & if\ link\ a\ is\ controlled\ by\ s^{th}\ phase\ at\ node\ n \\ 0 & otherwise \end{cases}$$

$$v_a \le \sum_{s\in S} \lambda_a^{n^{(s)}} Q_a \qquad \text{(Link capacity constraint)}$$

where demand constraint, link flow-route flow constraint, signal timing constraint and capacity constraint should be satisfied. For any route p, the flow on this route should be larger than zero and the sum of all routes from the origin to the destination should equal to demand of this OD pair. For any link a, the flow on this link should equal to the sum of route flows, using this link; meanwhile, the link flow a should not exceed the link capacity. For any signal-controlled nodes, the sum of proportional green time at different phases should equal to one.

Considering the lack of real-world data at this stage to calibrate the link travel cost function $C_a(\boldsymbol{v}, \boldsymbol{\psi})$ for CAVs, the $C_a(\boldsymbol{v}, \boldsymbol{\psi})$, including travel time and bottleneck delay, will be calculated by simulation, where CAVs are controlled by Cooperative Adaptive Cruising Control (CACC) (Milanés & Shladover, 2014). As the link travel cost function $C_a(\boldsymbol{v}, \boldsymbol{\psi})$ calculated by simulation is nonlinear, the Particle Swarm Optimisation (PSO) approach proposed by Kennedy and Eberhart (1995) to solve nonlinear optimisation problems, where particles are used to search for optimal solutions as a stylised representation of bird flocking or fish schooling movements, will be adopted.

Table A5.1 The summary of routing and signal timing strategies under different levels of information

Levels of information		Shortest route	Stochastic routing	PAP	PAP+P0	ORST
Network	topological structure	√	√	√	√	√
	link length	√	√	√	√	√
	numbers of lanes	√	√	√	√	√
Flow	partial knowledge		√			
	historical flow			√	√	√
	actual flow					√
Signal timing	green time				√	√

4. Summary

To sum up, the levels of information about traffic conditions can be divided into three categories. Based on the different levels of information, four existing routing and signal timing strategies under different levels of information and a proposed ORST control strategy for CAVs have been summarised in Table A5.1.